Studies on muscular dystrophy associated genes

Hadil Bakir

Studies on Muscular Dystrophy

Associated Genes

Hadil Bakir

A thesis submitted for the degree of Doctor of Philosophy

School of Biological and Biomedical sciences

University of Durham, UK

Submitted: March 2007

Declaration

I declare that the experiments described in this thesis were carried out by myself in the School of Biological and Biomedical Sciences, University of Durham. This thesis is a record of work that has not been submitted previously for a higher degree.

Hadil Bakir

Acknowledgments

Writing the acknowledgments for me was the best part of writing this thesis that is why I kept it to the end to mark the end of a truly life changing experience over the past four years. I would not have been able to complete this journey without the aid and support of countless people. I must first express my gratitude towards the best supervisor in the world, Dr. Nicholas Hole, a truly amazing person whom without his guidance, support and advice, completing this thesis was not possible.

Many thanks to Prof. Roy Quinlan and Prof. Christopher Hutchison for allowing me to use their facilities.

Many thanks to Christopher Thompson and John Gatehouse for their support and understanding during the difficult times.

A very special thank you to Marcel Van-Lith who was "the rescue" as I called him during messy scientific times and was patient enough to answer all my stupid questions!

Many thanks to Pam Ritchie, Christine Richardson, Anderi Smertenko, Ewa Markiewicz, Gareth Marlow.

Last but not least I want to thank my wonderful friend Sanjika, for her love and support through the difficult times by providing a continuous supply of tissue and laughter which made the bad times little bit more bearable. Marcel, Laura, Zainab, Preeti, Elke, and all my wonderful friends in the department and student accommodation, I really enjoyed every minute we spent together from birthdays, barbeques to goodbye parties and hope to stay friends for the years to come.

Abstract

Muscular dystrophy is a collective group of genetic disorder that results in progressive wasting of skeletal muscle. Dysferlin, the gene responsible for Limb Girdle Muscular Dystrophy type 2B (LGMD2B) and Miyoshi Myopathy (MM) was found to be a member of a newly identified protein family named the ferlins. Recent work has suggested that dysferlin is necessary for efficient calcium sensitive membrane resealing therefore is involved in membrane repair, a mechanism which if defective results in progressive muscle wasting. In this project, the involvement of other genes that could possibly be associated with muscular dystrophy is investigated.

Myoferlin, a member of the ferlin protein family is highly homologous to dysferlin and is also a plasma membrane protein with six C2 domains and a C-terminus transmembrane domain. To date no disease has been associated with mutations in the myoferlin gene but its high similarity to dysferlin means that it could be a potential muscular dystrophy associated gene.

Results obtained from this study strongly suggest that myoferlin like dysferlin is enriched at plasma membrane disruption sites and during myoblast differentiation, two processes which involve the fusion of two opposed bilayers, a process vital in membrane repair.

In addition, a fifth member of the ferlin protein family is reported in this project and the primary results obtained are consistent with it being a potential muscular dystrophy associated gene.

Finally, a group of MM affected families that were previously excluded for mutations in their dysferlin gene were analysed for muscular dystrophy associated genes other than dysferlin.

1 Chapter One, Introduction

1.1 Background

In 1925 it was first suggested that living cells are coated with a bilayer of phospholipids (Gorter & Grendel, 1925). The well known ability of phospholipids to reseal and fission into smaller membrane bound vesicles in aqueous solutions (following thermodynamic principles by removing hydrophobic domains from the aqueous environment therefore resulting in an energetically favoured molecule) (Tanford, 1973) suggested that the plasma membrane would have self-sealing characteristics (Parsegian et al., 1984), which meant that today's sophisticated mechanism of plasma membrane resealing following disruptions to its integrity was taken for granted and assumed to be a natural consequence of the phospholipids' interaction with water. However, we understand today that plasma membrane resealing is a complicated process, in which many simultaneous processes are needed for successful membrane resealing.

In 1930, Heilbrunn L.V. (Heilbrunn, 1930) described plasma membrane repair in sea urchin eggs as 'reactions of superficial precipitation' when large portions of the egg's surface were torn off and showed that egg survival depended on Ca^{2+} initiated events. Heilbrunn showed that this 'surface precipitation' does not occur in Ca^{2+}-free extracellular environment and termed this reaction as "Ca^{2+}-dependent response", in which it is absolutely dependent on near physiological levels of Ca^{2+} in echinoderm eggs (Heilbrunn, 1958).

Other evidence that plasma membrane resealing was a more complex process was seen in 1970 with experiments using *Physarum* (a plasmodial slime mold).

Sequential electron micrographs were the first to show rapid vesicle-vesicle fusion that served to seal plasma membrane lesions (Komnick et al., 1970). Evidence that plasma membrane repair was an active process and part of normal cell biology was seen in a series of experiments in the 1980 s for example the resealing ability for transacted neurons and skeletal muscle cells (Casademont et al., 1988,Yawo & Kuno, 1985).

This early work suggested that cell membrane repair was a widely observed phenomenon, suggesting that it was vital for normal cell physiological function. Scientists then turned their attention to what these functions may be.

1.2 Importance of Cell Membrane Repair

Cells of a mammalian body undergo cell membrane damage routinely as a result of exposure to mechanical forces. In order for cells to survive a plasma membrane disruption, developing a rapid resealing mechanism is vital, or otherwise small mammalian cells undergo apoptosis if not resealed within ~15 seconds (Miyake & McNeil, 1995,Steinhardt, 1994).

Cell death as a result of failing to reseal (Lemasters et al., 1987) is thought to be due to diffusion mediated Ca^{2+} entry down by a 10^4 concentration gradient (from the extracellular environment to the intracellular environment) that results in a rapid but transient increase in intracellular Ca^{2+} (McNeil et al., 1985) in addition to the escape of vital cell components. Skeletal muscle, cardiac muscle, epidermal cells, endothelial cells, and gut epithelial cells are all examples of cell types known to undergo cell wounding under normal physiological conditions (McNeil, 1993).

So far all cells with the exception of erythrocytes -which lack cytoplasmic organelles-, are thought to exhibit complex membrane repair mechanisms. Erythrocytes lack cytoplasmic organelles, as explained later in this chapter; this is the source of membrane repair. But the resealing in erythrocytes, like in a synthetic lipid bilayer is a simple thermodynamic principle, energy stability. The process of resealing removes the hydrophobic domains of the phospholipids molecules from the aqueous environment (Miyake & McNeil, 1995).

Cell wounding is thought to be the highest in muscle cells ranging between 5-30% in cardiac (Clarke et al., 1995) and skeletal muscle (McNeil & Khakee, 1992) cells respectively under normal physiological conditions, rising to approximately 80% in cardiac muscle cells when stimulated (Clarke et al., 1995).

Now that the importance of cell membrane repair has been clarified, in the next section the mechanisms suggested to be involved in membrane repair and the possible sources of resealing the membrane is investigated.

1.2.1 The Source of Membrane in Membrane Repair

The fact that stripped cytoplasm in Komnick's experiment (discussed earlier) (Komnick et al., 1970) managed to seal off from the external environment meant that the source of the new membrane was coming from inside the cells. But where these vesicles came from remained a question. Similar to the *Physarum* experiment, when naked cytoplasm of sea urchin eggs was injected to extracellular levels of Ca^{2+}, but still managed to form a cellular barrier, possessing cell membrane properties, merely from homotypic fusion events

suggested the reserve or yolk granule of the egg to be the key source in sea urchin eggs (Terasaki et al., 1997).

However, later experiments on other cells showed that once a plasma membrane disruption is resealed, normally distributed lipids and protein components of the plasma membrane are absent from plasma membrane disruption sites, indicating the involvement of internal membrane at these sites (McNeil et al., 2000).

As a matter of common sense the ability of the cells to repair the wound depends on the wound size. However, the resealing capacity is dependent on the local availability of the cytoplasmic vesicles which as explained later, are thought to patch with each other to reseal the plasma membrane which resulted in the patch hypothesis (McNeil et al., 2000).

Internal membrane or so called endomembrane is a vital substrate for resealing, such that red blood cells, which lack endomembrane, fail to reseal efficiently under physiological conditions in which nucleated cells readily reseal (McNeil et al., 2003). Now that the source of the resealing membrane has been clarified, how this membrane attempts to reseal the disruption is clarified in the next paragraph.

1.2.2 Patch Hypothesis

It is suggested that small membrane disruptions are sealed by exocytotic (vesicle-plasma membrane) fusion, but relatively large disruptions need homotypic (vesicle-vesicle) fusion to form a barrier (Terasaki et al., 1997) or a 'patch' of membrane be exocytotically joined to the plasma membrane. Later this idea was called the "patch hypothesis" (McNeil et al., 2000).

The Ca^{2+}-dependent surface precipitation of sea urchin eggs previously suggested, was shown to be true when organelles from echinoderm eggs expelled from a micro-needle into Ca^{2+}-depleted sea water, clustered or "tethered" to each other only to form a vesicular structure in the presence of Ca^{2+} (Terasaki et al., 1997).

It was concluded that echinoderm egg granules show Ca^{2+}-independent tethering prior to Ca^{2+}-dependent granule fusion *in vitro*, suggesting a role for membrane tethers in the production of the previously predicted 'patch' of membrane required for membrane resealing (McNeil, 2005).

The tethering factor is thought to be a multisubunit complex of at least seven high molecular weight proteins in which the depletion of the tethering factor complex *in vitro* inhibited tethering (McNeil, 2005).

However, once the patch of membrane is formed with the aid of tethering factors, how this patch of membrane is attached in a three dimensional model is the question. Very recently it has been suggested that a model developed to explain vacuole fusion in *Saccharomyces cervisiae* could be applicable to other cells too (Figure 1.1) (McNeil & Kirchhausen, 2005). The 'vertex fusion' model suggests that the patching membrane created from homotypic vesicle fusion is attached to the plasma membrane through several fusion pores or 'vertices'. These vertices are the curvilinear zones of outermost contact between two docked membranes where the protein machinery of fusion become concentrated. The lateral expansion of these fusion pores results in a continuous, sealed membrane. The residual plasma membrane is discarded to the extracellular space while the wound site is sealed using the lower part of the patch. The resulting concave patched domain is restored by cytoskeletal

Figure 1.1 This sketch demonstrates 'Vertex fusion' as a possible plasma membrane resealing mechanism in cells other than *Saccharomyces cervisiae*. (a) Calcium influx through a plasma-membrane disruption site. (b) A membrane patch is assembled through homotypic vesicle fusion. (c) Several fusion pores are designated between the membrane patch and the plasma membrane. (d) The fusion pores produce a continuous, resealed membrane via lateral expansion. (e) While the wound site is resealed using the lower part of the patch membrane resulting in a concave, the upper part is no longer needed and is discarded to the extracellular space. (f) The cell's normal architecture is restored by cytoskeletal remodelling (Figure taken from Mc Neil et al (McNeil & Kirchhausen, 2005).

Figure 1.1

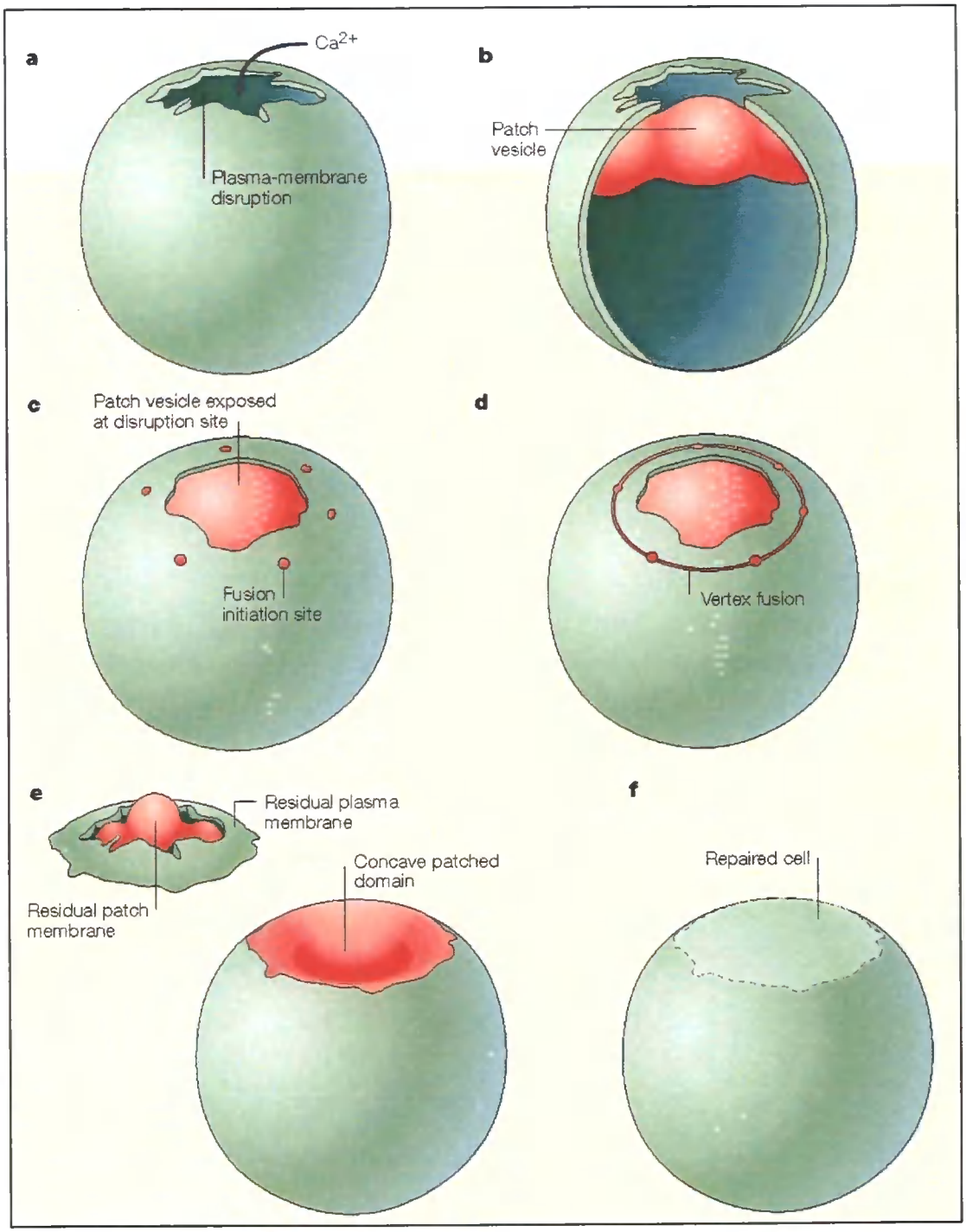
a
Ca^{2+}
Plasma-membrane disruption
b
Patch vesicle
c
Patch vesicle exposed at disruption site
Fusion initiation site
d
Vertex fusion
e
Residual plasma membrane
Concave patched domain
Residual patch membrane
f
Repaired cell

re-modelling (McNeil, 2005). The membrane needed for the patch hypothesis to be successful needs to be transported to the site of membrane disruption. One mechanism thought to be involved in transporting this membrane is exocytosis as explained in the next section.

1.2.3 Exocytosis Mechanism & Calcium

It is thought that membrane resealing by exocytosis follows a pattern similar to neurotransmitter release (Steinhardt, 1994). In this theory, quanta of neurotransmitters are released from presynaptic terminals as a result of electrical excitation which leads to opening voltage-gated calcium channels finally resulting in the exocytotic discharge of the neurotransmitters stored within synaptic vesicles (Augustine & Charlton, 1986). Synaptic vesicles within the interior of the presynaptic terminal are too far away from the plasma membrane to participate immediately in neurotransmitter release during an action potential. It has been proposed that these vesicles form a reserve pool that will be mobilised following the action potential to replenish vesicles that have undergone fusion (Pieribone et al., 1995). It is thought that activity-dependent mobilisation of vesicles from the reserve pool is controlled by phosphorylation of synapsin (a family of proteins that are peripherally associated with the synaptic vesicle membrane) by calcium-regulated kinases such as the type II calcium-calmodulin-dependent protein kinase. Once these vesicles are mobilised, they are docked to the presynaptic plasma membrane (Greengard et al., 1993) in a GTP-binding protein dependent manner (Ungermann et al., 1998). It has been suggested that docked vesicles undergo ATP-dependent priming reactions prior to exocytosis via dissociated complex SNARE proteins. These results are

supported by the finding that all SNAP (soluble NSF attachment protein) peptides that block Golgi vesicle fusion also inhibit neurotransmitter release. In addition injecting SNAP or SNF peptides cause an accumulation of synaptic vesicles that are apparently docked to the plasma membrane but can not fuse proving that SNARE complex dissociation is crucial for the step that follows vesicle docking preceding fusion with the plasma membrane (Augustine et al., 1999).

Calcium is thought to trigger exocytosis by catalysing vesicle fusion by binding to a presynaptic protein. One presynaptic calcium receptor is Synaptotagmin as detailed later (Sudhof & Rizo, 1996). It is not clear how vesicle fusion is triggered by calcium bound Synaptotagmin but it is thought that its interaction with SNARE proteins could be important (Jaiswal et al., 2004).

In adipocytes, the insulin stimulated trafficking of GLUT4 has several features in common with regulated exocytosis pathway of synaptic vesicles. GLUT4, a glucose transporter isoform, is highly expressed in adipose tissue and striated muscle, and is known to cycle between the plasma membrane and intracellular compartments, some of which overlap with the recycling endosome system (Pessin et al., 1999).

Since plasma membrane repair is thought to follow a pattern similar to neurotransmitter release, calcium is needed to initiate resealing by acting as a second messenger in response to alterations in Ca^{2+} level as low as 1μM (Andrews, 2005) and it is thought that there is a tight association between membrane integrity and the extinction of the signal leading to the resealing.

One mechanism in which internal membrane is transported to the external environment for resealing is exocytosis. Indeed, blocking fusion events using botulinium neurotoxins B and A, which are proteases that are thought to specifically target and thereby inactivate members of the SNARE family of proteins required for exocytotic events, inhibit wound resealing in both sea urchin eggs and fibroblasts proves the necessity of exocytosis for wound healing.

Membrane repair was also inhibited by the block of Ca^{2+}/calmodulin kinase. Ca^{2+}/calmodulin kinase regulates exocytotic vesicles during synapsis, and is also shown to be involved in the regulation of kinesin which is required for outward-directed transport of vesicles (Steinhardt, 1994).

Wound induced exocytosis was also demonstrated in bovine endothelial cells and 3T3 fibroblasts. Exocytosed vesicles were predicted to be endosome/lysosomes based on labelling by lipophilic fluorescent dye. These vesicles were abnormally abundant within seconds surrounding a wound site (Miyake & McNeil, 1995). This confirmed that plasma membrane disruptions are resealed by an exocytosis based mechanism, in which exocytosis was proportionate to the wound induced. In addition, those vesicles released from wounded cells in Ca^{2+}-free media were two times higher that that released from cells wounded in Ca^{2+}-medium, resulting in a proportionate cell death (Miyake & McNeil, 1995).

The dependency of successful membrane resealing on Ca^{2+} was also shown when sea urchin eggs were subjected to relatively large wounds in the presence of membrane impermeable dextran and Ca^{2+}, cells did not show any uptake of dextran indicating rapid wound healing (within seconds). In contrast when this

process was repeated in the absence of Ca^{2+} dextran was detected inside the cell in addition to continuous leakage of the cytoplasm indicating the failure to reseal in the absence of Ca^{2+} (Terasaki et al., 1997).

This proved that Ca^{2+} is needed for successful wound induced exocytosis. This also proves that wound healing involves Ca^{2+}-dependent formation of a membrane barrier rather than a dense precipitation of proteins and previously thought (Terasaki et al., 1997).

In fact, repeated membrane disruption shows long term potentiation of Ca^{2+}-regulated exocytosis, which is directly proportionate to faster membrane repair. In 3T3 fibroblasts, if a second wound is induced on the same location of a previously resealed wound, the second wound reseals more rapidly resulting in approximately twice as much exocytosis (Togo et al., 2003). This response is Ca^{2+} and PKC (protein kinase C) -dependent. PKC's kinase activity is necessary in Golgi vesicle formation, such that a PKC inhibitor (Ro 31-8220), results in the inhibition of vesicle formation in the Golgi apparatus. The PKC inhibitor, or the addition of BFA (Brefeldin A), a fungal metabolite that inhibits the formation of vesicles at the Golgi apparatus, did not disturb membrane repair in the first wound, but inhibited membrane repair at the second wound, suggesting the newly derived vesicles from the Golgi apparatus are used for the repair of multiple wound sites rather than endocytotic compartments (Togo et al., 1999).

This potentiation of exocytosis is shown to be PKA (protein kinase A) dependent as well, in the early stages post injury (few minutes) , leading to protein synthesis in the intermediate stage post injury (approximately 3 hours)

and depends on the activation of cAMP response element binding protein (CREB) in the 24 hours post injury (Togo et al., 2003).

One purpose of vesicle exocytosis during wound resealing is to reduce surface tension by the addition of new membrane. When chemicals known to reduce surface tension such as cytochalasin D were added to cells, membrane resealing was facilitated, although the amount of exocytosed vesicles was affected adversely in a slight manner, suggesting the compensation of reduced surface tension for exocytosis (Togo et al., 2000).

It was later shown that exocytosis precedes reduced membrane tension and that when cells are wounded twice; the rate of decrease in membrane tension at the second wound was approximately 2.3 times faster than that of the initial wound, a process inhibited by the induction of BFA. Furthermore, membrane tension did not decrease in low Ca^{2+} solution, thus inhibiting membrane repair (Togo et al., 2000).

1.2.4 Lysosomal Exocytosis

The theory of those exocytotic vesicles being endosomes/lysosomes predicted by Miyake et al. (Miyake & McNeil, 1995) was shown to be true in fibroblasts and epithelial cells during the protozoan parasite *Trypanosoma Cruzi* invasion. Lysosomes in the host cells were mobilised to the entry site to gradually allow fusion with the plasma membrane (Rodriguez et al., 1996). Further more, CHO cells with increased cell surface expression of rat lysosomal membrane glycoprotein Lamp-1 made them up to five times more susceptible to parasite invasion, but a mutation in critical residues in the lysosome-targeting motif of

Lamp-1 abolished the facilitated invasion of the parasite. In addition this facilitated invasion was microtubule dependent, such that pre-treatment of cells with microtubule destabilising agents such as nocodazole reduced the susceptibility to parasite invasion considerably (Kima et al., 2000).

This process is Ca^{2+}-dependent lysosomal exocytosis. It is Ca^{2+}-dependent since depleting the intracellular Ca^{2+} in the host cell blocks parasite entry. Lysosomal exocytosis was shown in several ways by 1) measuring the release of the lysosomal enzyme β- hexosaminidase, 2) lysosomal tracers released into the culture medium , 3) the release of the lysosomal marker Cathepsin D into the culture medium and 4) the surface appearance of Lamp-1 in cells with elevated intracellular Ca^{2+} induced by the use of ionomycin treatment and permeablisation using SLO (Streptolysin O) (Rodriguez et al., 1995). SLO permeablisation allows an intracellular and extracellular equilibrium of Ca^{2+} concentration enabling the determination of Ca^{2+} -induced exocytosis threshold. Later on this Ca^{2+}-dependent lysosomal exocytosis was shown to be true in other non-secretory cells such as NRK fibroblasts and muscle cells (Reddy et al., 2001) and is thought to be temperature and ATP dependent (Rodriguez et al., 1997). However, the Ca^{2+} induced exocytosis of Golgi, ER, early and late endosomal vesicles in response to a calcium ionophore has been ruled out (Jaiswal et al., 2002).

The process of exocytosis and endocytosis has to be in proportion in order for the cell to have a reasonably constant surface area. Since it is known for Ca^{2+} to be the control factor of exocytosis, it comes to no surprise that it is indeed

needed for endocytosis too (Gerasimenko et al., 1998) although its role is not yet fully understood.

Microinjection of NRK cells with Lamp-1 under normal intracellular Ca^{2+} , induced the formation of highly homogenous aggregates of individual lysosomes which retain their individual dimensions despite being highly compact, suggesting they cross-linked through the anti-Lamp-1 tail (Bakker et al., 1997).

However, when intracellular Ca^{2+} was elevated by Ca^{2+}-ionophore, ionomycin and thapsigargin, an inhibitor of the ER Ca^{2+} ATPase that triggers a rapid release of intracellularly stored Ca^{2+} into the cytoplasm, large Lamp-1-positive vesicles were detected, from the fusion of approximately 3-15 individual lysosomes (Bakker et al., 1997).

However, to what extent lysosomes are involved in membrane repair remains a question. A recent study suggested that lysosomes only undergo partial release of lumenal contents and none of the lysosomal membrane proteins diffuse into the plasma membrane and instead remain near the site of fusion. This process is dependent on the presence of Syt VII, as detailed in the next section (Jaiswal et al., 2004).

Another study showed that pre-treatment of cells with a new, unnamed drug that specifically blocked exocytosis of lysosomes did not affect wound healing (Meldolesi, 2003). This is supported by the fact that ionomycin induced lysosomal exocytosis takes approximately one minute or more, while plasma membrane repair takes seconds (Togo et al., 2003). In addition, a special clone

of PC12 cells that are deficient in lysosomal exocytosis can still reseal plasma membrane disruptions(Borgonovo et al., 2002).

Vacuolin-1 is a member of vacuolins, molecules known to induce homotypic fusion of endosomes and lysosomes to form vacuoles in different cells.

Cerny et al (Cerny et al., 2004) showed that the induction of vacuolin-1 halted the release of β-hexosaminidase and blocked the Ca^{2+}-dependent surface appearance of Lamp-1 in response to ionomycin treatment, while a more recent paper challenges these results and suggests that vacuolin-1 does not hinder lysosomal exocytosis despite morphological alteration in response to wounding or treatment with a calcium ionophore (Huynh & Andrews, 2005).

However, the inhibitory effect of vacuolin-1 on Ca^{2+}-dependent lysosomal exocytosis reported by Cerny et al (Cerny et al., 2004) did not affect the exocytosis of enlargosomes (novel vesicles expressing the protein AHNAK, see dysferlin associated proteins), or the resealing efficiency of those cells.

This data suggests the possible involvement of lysosomes in membrane repair and that they are not the only source of membrane during resealing, leaving the field open to other players such as novel vesicles named enlargosomes (as explained later).

Synaptotagmin VII, a member of the Synaptotagmin family is ubiquitously expressed and is localised on the membrane of lysosomes and is thought to have a role in lysosomal exocytosis as explained in the following section.

1.2.5 Synaptotagmins

Synaptotagmins (Syt) have at least 12 identified isoforms, characteristically sharing a unique NH2- terminal ecto domain and highly conserved cytosolic domain containing two Ca^{2+}-binding C2 domains , C2A and C2B (Schiavo et al., 1998)

Some synaptotagmins are expressed in neuronal tissue, they are found in the transmembrane protein of synaptic vesicles of the brain (Syt I & II & III) (Sugita et al., 1996) and secretory granules of pancreatic β-cells (Syt III) or ubiquitously expressed in several tissues (Syt VI, VII, VIII) (Craxton & Goedert, 1999,Li et al., 1995).

Syt VII in particular shows Ca^{2+}-dependent syntaxin binding in a relatively low micromolecular range (Li et al., 1995) making it a suitable candidate for involvement of lysosomal exocytosis. In NRK cells, Syt VII was found to be in mature lysosomes targeted to vesicles with the luminal domain of Lamp-1 at plasma membrane disruption sites. Functional exocytosis assay suggest that the C2A domain of Syt VII has a role in calcium regulated exocytosis (Martinez et al., 2000). This, in turn, suggests its involvement in plasma membrane repair since plasma membrane disruptions in fibroblasts or squid giant axons fail to reseal if cells are treated with competitive peptide fragments or neutralizing antibodies of Syt VII (Reddy et al., 2001).

In the presence of Syt VII during exocytosis, the opening of the lysosomal fusion pore is restricted geometrically and temporally and lysosomal membrane proteins do not diffuse into the plasma membrane; instead they remain near the fusion site. This is thought to aid in membrane resealing (Jaiswal et al., 2004).

In contrast, in the absence of Syt VII, cells from Syt VII knockout mice for example, lysosomes fuse completely and diffuse without restrictions into the plasma membrane leaving cells defective in lysosomal exocytosis, membrane resealing and less susceptible to T. Cruzi invasion (Chakrabarti et al., 2003).

These findings have led to the belief that Syt VII acts as a calcium sensor to regulate Ca^{2+}-dependent lysosomal exocytosis rather than a Ca^{2+}-dependent trigger (Jaiswal et al., 2004).

In the following section, the cytoskeleton and its role in plasma membrane repair as a possible transport network for resealing vesicles is investigated.

1.2.6 Cytoskeleton

The cytoskeleton is an extremely complex system. Studies carried out on microtubules, intermediate and actin filaments indicate that these filaments have a controlling role in cell shape, embryonic development and cell division, cell motility and most notably wound healing (Wakatsuki et al., 2001).

It is thought that the actin cytoskeleton, consisting of constant shifting G-actin and F-actin, help to distribute and support contractile stresses from inside or outside the cells (Gronewold et al., 1999). This has led to the believe that cytoskeletal elements are anchored to the plasma membrane in order to provide the necessary support needed (Wakatsuki et al., 2001) in addition to acting as rapid transport system needed for resealing (Miyake et al., 2001).

In resting cells, a layer of filamentous actin forming a cortical barrier is present underneath the plasma membrane. Once a cell is wounded, the calcium influx results in a local depolymerisation of actin to facilitate membrane fusion events

needed for resealing. However, once the membrane integrity is restored, actin polymerisation at the wound site is possibly needed for restitution and reconstruction of the plasma membrane. This theory was the result of a series of experiments carried out in which cells fixed within 15 seconds of inducing plasma membrane disruptions were observed to be depleted of F-actin staining at the wound site. However, cells fixed after plasma membrane repair (1<T<30 minutes) characteristically displayed a reproducible intense F-actin staining bordering the wound site. The addition of actin-depolymerising agent, DNase1, enhanced resealing, while the addition of actin stabilizing agents inhibited resealing (Miyake et al., 2001).

In addition to F-actin, kinesin and myosin are thought to be required for vesicle transport too. As expected the inhibition of kinesin and myosin inhibits membrane resealing by the lack of delivery of vesicles to the site of membrane disruption (Steinhardt, 1994). In sea urchin eggs, confocal studies have confirmed the involvement of kinesin and myosin motors in exocytotic-dependent membrane repair in a two step manner (Bi et al., 1997). Microtubules, another component of the cellular cytoskeleton, are also thought to have a significant role in overall cellular structure, mobility, vesicle trafficking and an involvement in ER and Golgi systems (Cole & Lippincott-Schwar, 1995).

Another anticipated role for the actin cytoskeleton is the active remodelling during the process of exocytosis events carried out in unwounded cells. GFP tagging of the F-actin showed that post-lysosomal vesicles stained by dextran chasing tend to be weakly associated with actin, and this association in itself does not initiate exocytosis. Once the vesicle is docked to the plasma

membrane, an actin polymerisation followed by fusion and release of the vesicle contents is initiated. This is followed by further polymerisation of actin, and a contraction of the actin cytoskeleton associated with the vesicle membrane. However, what happens to the vesicle membrane afterwards is still unclear. This data has strongly led to the belief that actin polymerisation starts as a pre-fusion event followed by post-fusion contraction and disassembly (Lee & Knecht, 2002).

This finding in fact supports the previous findings by Miyake et al (Miyake et al., 2001) indirectly. The post-resealing heavy F-actin polymerisation seen at the wound site in wounded cells (Miyake et al., 2001) is explained by the polymerisation seen once the vesicle contents have been released i.e. vesicle is firmly attached to the membrane therefore the wound has been resealed(Lee & Knecht, 2002). However, the F-actin depolymerisation seen by Miyake et al (Miyake et al., 2001) immediately before resealing might be explained as an emergency response to the induced wound in order to facilitate resealing.

1.3 Plasma Membrane Repair & Muscular Dystrophy

The emergence of fine details regarding plasma membrane repair and its complex mechanisms only highlights the importance of retaining plasma membrane integrity naturally and finding therapeutic methods to do so in diseases that fail to restore plasma membrane lesions. One disease falling under this category of particular interest is muscular dystrophy, to be more specific dysferlin deficient muscular dystrophy, MM and LGMD2B.

Skeletal muscle cells in mammals are large cells that are frequently subjected to plasma membrane disruptions as a result of the mechanical activity of the organism. Myogenesis, the process of new muscle formation consists of two stages; primary and secondary (as reviewed by (Ontell et al., 1988)). In studies of embryonic mouse development, newly formed myofibres were observed as early as 14 days post conception, followed by growth through fusion of newly formed myoblasts to existing myotubes. This is termed primary myogenesis followed by secondary myogenesis using previously formed myotubes as a back-bone (Ontell et al., 1988).

The maintenance of muscle after embryonic development exploits a different process. A pool of undifferentiated myogenic precursor cells named satellite cells located beneath the basal lamina that surrounds the myofibre are the progenitor cells in adult muscle which undergo asymmetrical division to produce myoblasts to proliferate following a muscle injury (Mauro, 1961,Schmalbruch & Lewis, 2000). This activation and proliferation of satellite cells is thought to be largely, if not entirely, responsible for the remarkable capacity for efficient repair and regeneration of damaged skeletal muscle, with the generation of large numbers of new myoblasts which then either undergo myoinitiation or myoaugmentation (the process of myoinitiation and myoaugmentation is explained in section 1.6.3) (Pena et al., 1995).

The terminal differentiation of mammalian muscle cells involves dramatic changes in sub-cellular architecture and cell morphology. One key change is microtubule reorganisation, resulting, in turn, in the reorganisation and redistribution of the Golgi complex and other cellular organelles (Bugnard et al., 2005).

The levels of cell wounding in skeletal muscle cells are the highest between the rest of the cells studied, for example the epithelial, endothelial, cardiac, etc reaching up to 30% under normal physiological conditions, correlating with the level of mechanical stress imposed on these cells (McNeil & Steinhardt, 1997). At this rate of plasma membrane disruptions replacing skeletal muscle cells as a result of injury as opposed to repairing them is not an option because simply it is too costly for the organism in terms of energy.

Cell wounding is defined as a survivable plasma membrane disruption, marked by uptake of a membrane impermeable substance (McNeil, 2002). There are some cases were the extent of damage to the cells is simply un-repairable and cell death is inevitable. An example of this case is seen in Duchenne muscular dystrophy (DMD). In this type of muscular dystrophy, as well as *mdx* mice (mdx mice are dystrophin deficient and is a model for DMD) , the muscle cells are fragile and easily injured by normal contractions of the muscle as a result of the lack of dystrophin protein (Hoffman & Kunkel, 1989) in the dystrophin-dystroglycan complex (DGC). Dystrophin is a mechanical stabiliser of the myofibre plasma membrane and regulator of intracellular calcium homeostasis (Clarke et al., 1993). Therefore cells lacking dystrophin have an unstable DGC. The role of DGC is to transmit forces generated inside the muscle cell by sub-sarcolemmal cytoskeleton to the collagen fibres of tendons i.e. the extracellular environment (Clarke et al., 1993). Upon failure to do so because of the unstable DGC, muscle cell loss outweighs cell repair and a vicious cycle of muscle wasting is seen (McNeil & Terasaki, 2001).

On the other hand, dysferlinopathic muscle seen in two distinct types of muscular dystrophy, Miyoshi myopathy (MM) and limb-girdle muscular

dystrophy 2B (LGMD2B) as a result of a mutation in the dysferlin gene possess a stable DGC suggesting a different mechanism to that of DMD/ *mdx* mice. In dysferlinopathic muscle it has been shown that muscle wasting is a result of defective membrane repair (Bansal et al., 2003). As detailed later in this chapter, dysferlin deficient muscle fibres are defective in calcium dependent sarcolemmal resealing, associated with sub-sarcolemmal accumulation of vesicles at the wound site when compared to wild type muscle fibres which reseal effectively in the presence of calcium and show dysferlin enriched membrane patches in response to injury as explained in details later in this chapter (Bansal et al., 2003). Therefore, defective membrane repair is another mechanism leading to muscle wasting i.e. muscular dystrophy.

1.4 Miyoshi Myopathy

1.4.1 Background

Miyoshi Myopathy (MM), a distal progressive muscular dystrophy inherited as an autosomal recessive disorder, was first described in Japan by Miyoshi et. al. (Miyoshi et al., 1986) and after that most cases were reported in Japan. But since then it has been found to be more frequent outside Japan than previously thought.

MM has an early adult onset between ages 15-25, (Barohn et al., 1991,Miyoshi et al., 1986) with the first prominent symptom of atrophy of the calf muscles resulting in patients unable to stand tip-toe, in addition to up to 150 times creatine kinase elevation above the normal level (Barohn et al., 1991).

Muscle biopsies from MM patients tend to show a wide range of abnormalities, such as changes in fibre size, nucleation, degeneration and regeneration, fibrosis and architectural change (Linssen et al., 1997).

MM was locus mapped to chromosome 2p12-14 (Bejaoui et al., 1998) at the same location to which the gene for a proximal limb-girdle muscular dystrophy termed LGMD2B (Passos-Bueno et al., 1995) and a distal myopathy with anterior tibial onset termed DMAT . MM, LGMD2B and DMAT share most symptoms except that MM affects the distal muscles, LGMD2B affects the proximal muscles and DMAT starts in the anterior tibial muscles and rapidly progresses to the proximal muscles (Illa et al., 2001,Liu et al., 1998).

In two large families both clinical phenotypes MM and LGMD2B occurred in siblings carrying the same haplotypes (Weiler et al., 1996). This was later shown to be true when native relatives of a Canadian family with the exact same missense mutation in dysferlin gene, which probably had the same origin, expressed both MM and LGMD2B, suggesting the involvement of modifier genes in the phenotypic expression of these two types of muscular dystrophy rather than an allelic diversity (Weiler et al., 1999).

The MM/ LGMD2B gene was cloned by constructing a 3Mb PAC (P1 derived Artificial Chromosome) contig spanning the entire candidate region (Liu et al., 1998) to which candidate genes were mapped prior to mutational analysis (Liu et al., 1998).

As a result, five skeletal muscle ESTs mapped to this narrowed down region corresponding with five candidate genes (Liu et al., 1998). Analysing one of the ESTs with a strong skeletal muscle signal on a Northern blot led to identifying

a 6.243 Kb ORF sequence corresponding to the dysferlin gene (Liu et al., 1998).

Further genetic analysis revealed that identical mutations in dysferlin in one family resulted in both the MM and LGMD2B phenotype (Liu et al., 1998). So far multiple mutations have been detected in the dysferlin gene and there appears to be no mutation hotspots in the gene nor genotype-phenotype correlations (Aoki et al., 2001).

Following the cloning of the dysferlin gene a study carried out by Linssen et al (Linssen et al., 1998) was conducted investigating the genetic heterogeneity of MM in four Dutch families displaying the MM phenotype and large enough to conduct linkage analysis. Haplotype analysis using microsatellite markers mapping to the dysferlin locus revealed no evidence of linkage in three of the four families to the dysferlin locus. Therefore a genome wide screen was undertaken in these families and in two of these families (F I and F II) showed a tentative linkage to the chromosome 10 marker, D10S2325. Additional chromosome 10 markers (D10S189, D10S1412, D10S172, D10S547, D10S570, D10S674, D10S191 and D10S1423) were used to confirm this result (giving lod scores of 2.578 at θ=0) (Linssen et al., 1998). This potential second locus for MM was designated MMD2 locus spanning a 23cM region on chromosome 10 (containing approximately 151 genes as estimated by NCBI Map viewer program). The fourth family appears not to be linked to either chromosome 2 or 10.

This genetic heterogeneity seems to coincide with the clinical heterogeneity seen in MM patients in general in terms of onset and muscular atrophy although non-dysferlin-linked MM shows identical clinical features as the dysferlin linked

MM such as predominant involvement of the distal musculature and high level of serum creatine kinase (Linssen et al., 1998).

However, these studies were carried out on unrelated families with only two affected subjects in each family in addition to the lack of samples from the deceased subjects which might have contributed to not obtaining very significant statistical scores. As a result the results obtained from this study needs to be further investigated.

1.4.2 Animal Models of Dysferlinopathy

SJL mice are known to be natural models for autoimmune diseases, inflammatory muscle disease in 100% of the population in addition to other abnormalities (Bernard & Carnegie, 1975,Rosenberg et al., 1987,Weller et al., 1997).

Further studies on SJL mice showed that they are natural models for progressive muscular dystrophy in which histopathological examinations showed muscle degeneration and regeneration accompanied by fibrosis, fat replacement and inflammation of the proximal muscle groups affected more severely than distal muscles. These symptoms turned into full-scale myopathy by 6-8 months of age and were inherited as an autosomal recessive trait (Bittner et al., 1999). Genetic studies confirmed the mutation of the SJL-dysferlin gene located on the mouse chromosome 6, the mouse homologue to the human dysferlin gene mutated in MM and LGMD2B (Bittner et al., 1999)

Genetic studies showed that in SJL mice, a 141bp deletion in the genomic sequence (Bittner et al., 1999) results in exon skipping, leaving the cDNA with a 171bp (57 amino acids) inframe RNA deletion, resulting in partial removal of the

fifth C2 domain (C2E) (Vafiadaki et al., 2001). The C2E domain is highly conserved in different ferlins suggesting its functional significance. Therefore, its deletion is thought to have a huge impact on the proteins' stability (Vafiadaki et al., 2001).

Like the human dysferlin gene, the mouse dysferlin also has six C2 domains, which share a high homology at the C2E (100% identical) and the C2F (96% identical) (Vafiadaki et al., 2001).

The SJL-dysferlin mutation was also confirmed by immunocytochemical studies, where dysferlin expression using NCL-Hamlet (explained later) antibody in SJL mice was reduced by approximately 85% compared to control mice and human samples (Bittner et al., 1999). SJL mice are reported to have up-regulated S100 Ca^{2+}-binding protein (Suzuki et al., 2005) and MHC-I expression (Kostek et al., 2002) and down-regulated intracellular protein traffic-associated proteins (Suzuki et al., 2005).

In a recent study, two additional mouse models of dysferlin muscular dystrophy were characterised. One mutant was generated by targeted gene inactivation at the C2E domain, and other mutant is a naturally occurring inbred strain, with a retrotransposon insertion in the fourth intron of the dysferlin gene, named A/J mice (Ho et al., 2004). A/J mice are natural models for lung cancers and different immunology-related diseases (Festing, 1969).

Despite differences in the dysferlin disruption, both strains of mice showed typical symptoms of dysferlin deficiency at histopathological level, in addition to phenotypic differences, elevated CK, loss of sarcolemmal integrity, thickening of basal lamina, sub-sarcolemmal vesicle accumulation similar to those seen in

human dysferlinopathic muscle. The most notable difference between A/J, dysferlin -/- and SJL mice was the lack of severe aggression observed in SJL mice (Ho et al., 2004).

As explained earlier, MM and LGMD2B is a result of mutations in the dysferlin gene. Dysferlin belongs to a newly identified protein named the ferlins. In the coming section, this protein family, its subgroups and few interacting proteins is studied in detail.

1.5 The Ferlins

The ferlin protein family is a new protein family that is still expanding with new members being added. The first member to be discovered was dysferlin (Bashir et al., 1998,Liu et al., 1998) and its *C-elegans* homologue fer-1 (Bashir et al., 1998), followed by otoferlin (Yasunaga et al., 1999), myoferlin (Britton et al., 2000,Davis et al., 2000), and fer1L4 (Doherty & McNally, 2003). Later on the discovery of a fifth ferlin protein named fer1L5 is reported.

All the ferlins characteristically share multiple C2 domains and a C-terminal transmembrane domain, which seems to be highly conserved (Figure 1.2) (Bansal & Campbell, 2004).

Proteins with C2 domains mostly are involved in signal transduction or membrane trafficking, since C2 domains are known to bind calcium and phospholipids. C2 domains consist of two four-stranded β-sheets, where 3 loops at the top and 4 loops at the bottom connect the 8 β-strands. Calcium binding is thought to occur at the top three loops depending on their ability to

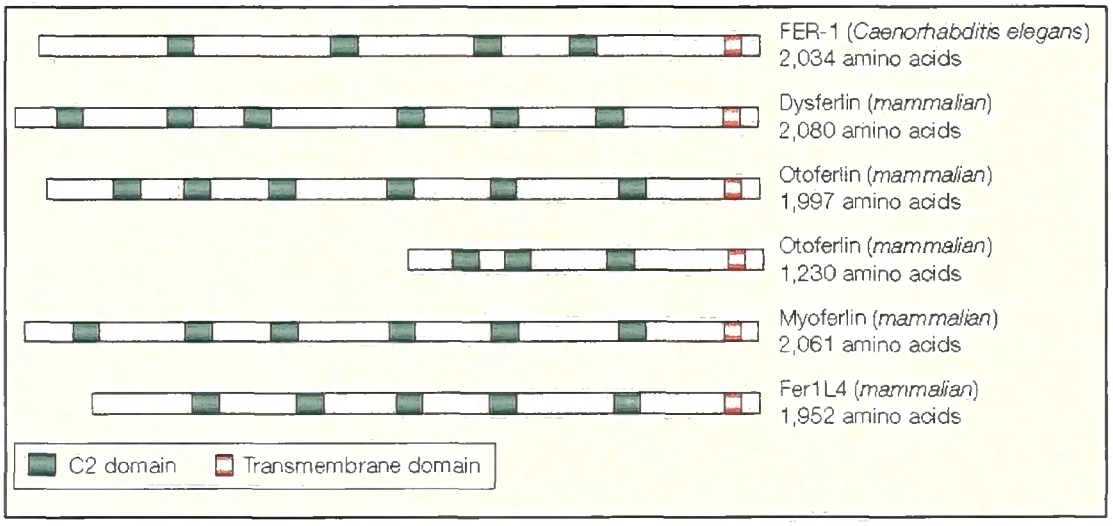

Figure 1.2 This figure shows the ferlin protein family alignment.

Figure taken from Mc Neil et al (McNeil & Kirchhausen, 2005)

act as electrostatic switches without needing major conformational changes. C2 domains exist in two topologies, with the major difference in the localisation of the C and N-termini, top or bottom. It is not clear why different topologies exist but it is thought that the topology affects the relative orientation of a C2 domain in respect to the neighbouring domains (Rizo & Sudhof, 1998).

The human and mouse dysferlin genes are 90% identical especially in the last two C2 domains (Britton et al., 2000). Dysferlin is 27% identical and 57% similar to the *C-elegans* fer-1 protein (Liu et al., 1998). In *C-elegans* spermatogenesis, the process of haploid spermatid maturation involves the fusion of the large vesicular membranous organelles with the spermatids plasma membrane to achieve directed surface membrane flow with the aid of extended pseudopodium. When the gene fer-1 is mutated, although mutant spermatids appear normal they are defective for membranous organelle fusion and fail to orient correctly at the plasma membrane, which led to the suggestion that dysferlin might have a role in plasma membrane fusion events (Achanzar & Ward, 1997).

1.6 The Ferlin sub-groups

Ponting et al (Ponting et al., 2001) used the *Prospero* algorithm to perform self-comparisons of all the predicted Drosophila melanogaster gene products to search for similarities across repetitive amino acid sequences. This resulted in discovering a domain of unknown function that was homologous to two domains in dysferlin. This domain was named the DysF domain. The two copies in dysferlin are not tandemly repeated but rather inserted within each other, a rare

evolutionary case which might reflect constraints on binding sites (Ponting et al., 2001). Consequently the DysF domain was divided into two parts: the N-terminal region, named DysF-N region and the C-terminal DysF-C region characterised by a stretch of arginine rich sections (NCBI).

The DysF domain is also present in fungal, worm and rodent genomes. One example is the Pex23p yeast protein (Brown et al., 2000).

According to the possession of the DysF domain, the ferlin protein family has been divided into two subcategories, the DysF ferlins consisting of dysferlin, myoferlin and FER1L5 and the non-DysF ferlins consisting of otoferlin and FER1L4 as detailed later.

1.6.1 Dysferlin

The dysferlin gene encodes a protein of 2080 amino acids producing in a 230 KDa protein consisting of six C2 domains.

The dysferlin gene has a single C-terminal transmembrane domain and is a type II transmembrane protein, in which the N-terminus end and most of the protein is located within the cytoplasm. This was later confirmed by immunogold cytochemistry that indeed 78% of the dysferlin antibody epitope located inside the cell (Anderson et al., 1999).

The dysferlin monoclonal antibody, NCL-Hamlet, was designed to an epitope near the C-terminal transmembrane domain (amino acids 1999-2016). It detects a signal on western blots from skeletal muscle of all mammals studied but not from birds (Anderson et al., 1999). Dysferlin tends to show ubiquitous

expression in different tissues and is reported in foetal tissue as early as 5-6 weeks gestation.

In wild type muscle fibres , dysferlin is localised in the sarcolemma and thought to be in cytoplasmic vesicles (Piccolo et al., 2000). Expression in the basal lamina, nuclear membrane and endoplasmic reticulum has not been detected (Anderson et al., 1999). A recent study has suggested dysferlin localisation in transverse tubule elements and the T-tubule system (Hernandez-Deviez, 2006). However, Immunoblotting of human muscle fractions detected distinct dysferlin bands in the microsomal, nuclear, mitochondrial and homogenate fractions. No signal was detected in the cytosolic fraction, all of which were clearly eliminated by immunoadsorption (Matsuda et al., 1999).

ER/SR's major function is folding, processing and exporting newly synthesised proteins. A disturbance in calcium homeostasis is one reason in functional disruption or so called stress of the ER/SR. As a response to this stress the ER is thought to derive pathological organelles named tubular aggregates (TAs) to help in maintaining intra-sarcoplasmic calcium homeostasis. Therefore cells possessing TAs are thought to be under stress.

In a recent study, dysferlin was shown to be expressed in all TAs without exception suggesting its localisation in the SR as well as the sarcolemma at least in pathological conditions (Ikezoe et al., 2003).

1.6.1.1 Dysferlin in Myopathies

As explained earlier, dysferlin deficiency leads to three distinct types of muscular dystrophy.

Western blot analysis of dysferlinopathy patients revealed a 95% reduction in dysferlin expression compared to control and non-dysferlinopathy patients. In addition, all control samples had multiple smaller bands below the 230 KDa marker, which are thought to be metabolic fragments of the dysferlin protein as a result of the long time taken to synthesis such a large protein (Anderson et al., 1999). These small bands were also missing from dysferlinopathy patients in addition to some cytoplasmic staining of dysferlin.

Dysferlin null mice start to show symptoms of muscular dystrophy as early as 2 months of age but by 8 months all the pathological characteristics of muscular dystrophy were observed such as split fibres and fat replacement. Based on experiments carried out on these mice it is suggested that injury and disease progression occur at single muscle fibre levels. In addition, in these muscle fibres sarcolemmal disruptions are associated with sub-sarcolemmal accumulation of dysferlin. Vesicular accumulation of dysferlin in the cytoplasm in MM patients and extreme reduction of dysferlin at the sarcolemma support these findings (Piccolo et al., 2000).

It has been shown that successful membrane repair requires the accumulation, followed by fusion of vesicles at the wound site (McNeil, 2002,Miyake & McNeil, 1995,Steinhardt, 1994). Wild type muscle fibres wounded in the presence of calcium showed membrane patches enriched with dysferlin at sites of plasma membrane disruption and resealed efficiently, while wild type muscle fibres wounded in the absence of calcium failed to reseal. Dysferlin null muscle fibres showed sub-sarcolemmal accumulation of vesicles at the site of plasma membrane disruption and failed to reseal in the presence or absence of calcium

(Bansal et al., 2003). The accumulation of vesicles in response to plasma membrane disruptions is also reported in fer-1 mutants of *C-elegans* (Bashir et al., 1998). All findings to date suggest that dysferlin is involved in membrane repair probably acting as a calcium-dependent sensor that facilitates the fusion of readily accumulated vesicles in response to plasma membrane disruption to the sarcolemma (Bansal et al., 2003).

In addition to its similarity to fer-1 and dysferlin's C2 domains being highly homologous to the C2A domain of rat synaptotagmin III (Britton et al., 2000), these findings lead to the hypothesis that dysferlin is involved in membrane repair (Bansal et al., 2003).

Muscle microarray profiling of dysferlinopathies showed an over-expression of genes involved in myogenisis, proteolysis and intracellular protein trafficking, a sign of active cycles of regeneration and degradation (Campanaro et al., 2002). It has been suggested that patients with dysferlinopathy show an increased expression of MHC class I , increased counts of macrophages and T lymphocytes tightly adhered to the sarcolemma, which in turn with the basal lamina are unusually multilayered and thick, in addition to numerous electron dense aggregates of small vesicles thought to be derived from the Golgi apparatus (Cenacchi et al., 2005).

1.6.1.2 Dysferlin Associated Proteins

In order to understand dysferlin's cellular function, and that of myoferlin-since they are highly similar- studying associated or interacting protein can be a useful tool. In the next section, some of the proteins known to interact with dysferlin in one way or another are detailed.

Calpain3

Calpain3 is the muscle specific member of the Ca^{2+}-activated proteases, and it appears to control the expression of muscle specific transcription factors (Prelle et al., 2003).

Dysferlin has been associated with calpain3 in LGMD2A (Cohn & Campbell, 2000). However, calpain3 expression in addition to other DGC proteins like the α, β, γ, δ, and ε- sarcoglycans and dystrophin are thought to be expressed at normal levels in dysferlin-deficient muscle suggesting the integrity of the DGC (Bansal et al., 2003,Matsuda et al., 1999) and confirming that dysferlin is not an integral component of the DGC as suggested in the early days of dysferlin (Piccolo et al., 2000). However, in some cases a secondary calpain3 reduction has been reported in association with dysferlinopathy (Anderson et al., 2000).

Caveolin 3

Caveolins are membrane proteins present in caveolae which are components of lipid rafts (Razani & Lisanti, 2001). Lipid rafts are membrane domains rich in cholesterol and saturated polar lipids (usually sphingolipids) in a liquid ordered state (Megha & London, 2004). Caveolae are named so due to their resemblance to 'little caves' on TEM microscopes as a result of their electron density (Razani & Lisanti, 2001). Caveolin 3 is a component of caveolae and is characteristically expressed in sarcolemma of muscle cells of all types. Caveolin 3 expression is elevated during myoblast fusion (Tang et al., 1996). Caveolin 3 is also concentrated in the T-tubule system of developing muscle but expressed at lower levels in the T-tubules of mature muscle (Parton et al., 1997). Caveolin 3 is thought to function as a scaffolding protein in the formation

of caveolae membranes by interacting and organising lipid and protein components of caveolae (Tang et al., 1996). Caveolin 3 null mice are deficient in sarcolemmal caveolae but do not show evident clinical symptoms of LGMD1C even at old age as seen in humans as a result of Caveolin 3 mutation, but they reveal variably sized muscle fibres, necrotic fibres and myopathic changes, indicating that Caveolin 3 is needed in skeletal muscle cells for caveolar biogenesis (Razani & Lisanti, 2001). Caveolin 3 mutation causes an autosomal dominant form of Limb Girdle muscular dystrophy, LGMD1C (Minetti et al., 1998). This mutation acts in a dominant negative way, by forcing both wild type and mutant caveolin 3 proteins to aggregate in the Golgi apparatus (Galbiati et al., 1999). In addition, caveolin 3 expression is normal in dysferlinopathy but caveolin 3 deficiency results in the secondary reduction of dysferlin (Matsuda et al., 2001). One explanation for this result might be that caveolin 3 is well attached to the plasma membrane, therefore not affected by dysferlin deficiency, while vice versa is not true for dysferlin (Matsuda et al., 2001).

A very recent study has shown that dysferlin and caveolin 3 are both targeted to the sarcolemma in mature muscle fibres, although they do not completely co-associate and in C2C12 myotubes dysferlin and Caveolin3 seem to partially colocalise (Hernandez-Deviez, 2006). It was also observed that caveolin 3 or caveolin 1 mutants result in the retention of dysferlin in the Golgi complex of muscle and non-muscle cells or more dramatically the absence of caveolin 3/1 impairs plasma membrane targeting of dysferlin. This suggests a vital role for Caveolins in post-Golgi trafficking of dysferlin (Hernandez-Deviez, 2006).

Annexins

Dysferlin also interacts in a Ca^{2+} dependent fashion with annexins A1 and A2 whose genes are located on chromosome 9q21.3 and 4q31.3 respectively. Annexins in general are calcium and phospholipid binding proteins, predicted to have a role in fusion and aggregation of intracellular vesicles in response to plasma membrane disruptions, a role in membrane trafficking and transmembrane channel activity. But annexin A1 and A2 have been shown to act as calcium dependent lipid-raft and vesicle aggulators (Lennon et al., 2003). Dysferlin was shown to colocalise with both annexins at the sarcolemma in wild type muscle fibres by immunohistochemistry but this association was not observed in dysferlinopathic muscle. While dysferlin is associated with annexin A1 in uninjured cells but not in injured ones, annexin A2 seems to be associated in both wounded and unwounded cells (Lennon et al., 2003). Annexins A1 and A2 are strong candidates for non-dysferlin linked muscular dystrophy (Lennon et al., 2003).

Affixin

Affixin is also named as β-parvin and is a focal adhesion protein that was identified through a search for proteins that interact with integrin-linked kinase (ILK). The integrin-linked kinase (ILK) is a multi-domain focal adhesion protein. It is thought to be involved in regulating cellular signalling, fibronectin matrix assembly, survival, and differentiation (Khyrul et al., 2004). Affixin is ubiquitously expressed but is especially upregulated in heart and skeletal muscles (Matsuda et al., 2005). In normal skeletal muscle, affixin is expressed in the cytoplasm and sarcolemma, but co-localises with ILK only at the

sarcolemma. A secondary affixin reduction is reported at the sarcolemma of dysferlinopathic muscle in humans suggesting close association. But the overall protein content was not changed. It is thought that a part of affixin localises to the sarcolemma through binding to dysferlin. The C-terminal intracellular region of amino acids 1977-1988 (EKKILAGKLEMT) on the dysferlin molecule is thought to be the affixin-binding site. However, a change in the overall distribution of affixin in some non-dysferlinopathic, dystrophic muscle has been reported (Matsuda et al., 2005).

AHNAK

Another protein recently raising interest in connection with dysferlin is AHNAK. AHNAK was first co-purified with desomosomal component of keratinocytes during bovine muzzle epidermis fractionation and was also named desmoyokin (Hieda & Tsukita, 1989). Later studies showed that AHNAK is not associated with desmosomes (Gentil et al., 2003,Masunaga et al., 1995) and its human counterpart is located on the human chromosome 11q12. AHNAK is a large protein of approximately 700 KDa composed of a single exon (Shtivelman et al., 1992). It is composed of a short N-terminus and a nuclear localisation phosphorylation site for PKC/PKB and an export signal on its C-terminus (Hashimoto et al., 1995,Nie et al., 2000,Shtivelman et al., 1992,Sussman et al., 2001).

The intracellular distribution of AHNAK is unique and does not overlap with known vesicles. AHNAK's function is not fully understood despite its expression in different tissues. It was suggested that in resting cells, AHNAK is localised to

the lumen of specific vesicles. These novel vesicles were named enlargosomes (Borgonovo et al., 2002).

AHNAK lacks a transmembrane domain, therefore its long exposure at the cell surface in response to elevated intracellular calcium, differentially induced expression and slow post-exocytosis recycling seems to suggest that it is dependent on specific interactions with other vesicle components and their involvement in cell surface enlargement (Borgonovo et al., 2002) and the structural support of the plasma membrane (Gentil et al., 2003) although its function is not clearly understood.

AHNAK can be localised to the nucleus or to the plasma membrane depending on extracellular Ca^{2+} concentration (Hashimoto et al., 1995,Nie et al., 2000).

AHNAK was found to be predominantly expressed in muscle and cells with contractile properties in addition to some epithelial cells, but absent from epithelial cells with secretory or absorptive function (Gentil et al., 2003).

In adult mouse tissue (e.g. muscle and epithelial cells), AHNAK is mainly localised to the plasma membrane. Adult mouse tissue AHNAK expressing cells are terminally differentiated and do not go through proliferation, indicating that AHNAK is anchored to the plasma membrane and might be involved in growth arrest of epithelial cells and that membrane targeting of AHNAK is regulated by cell density and the formation of cell to cell contacts (Sussman et al., 2001) which explains the down regulation of AHNAK in neuroblastoma cells and few other tumours (Shtivelman et al., 1992). In cardiomyocytes AHNAK is thought to be involved in the regulation of ion-channel activity (Hohaus et al., 2002). AHNAK binds S100B (an EF-hand Ca^{2+}-binding protein) in a strictly Ca^{2+}-

dependent manner, suggesting a regulatory role in Ca^{2+} homeostasis (Gentil et al., 2001).

AHNAK null mice and ES cells showed no difference to wild type mice and cells, leading to the conclusion that AHNAK by itself had minimal or no affect on cell adhesion, tumorigenisis, proliferation and differentiation or overall mouse development leaving the possibility for a compensatory protein with a similar function (Kouno et al., 2004).

AHNAK in epithelial cells in vivo is targeted to the plasma membrane in a Ca^{2+} dependent fashion. This process is reversible and the disruption of E-cadherin – mediated cell to cell contacts by low extracellular Ca^{2+} results in the dissociation of AHNAK from plasma membrane. However, if Ca^{2+} levels are increased AHNAK is targeted again to newly formed cell-cell contact points (Benaud et al., 2004). AHNAK interacts with annexin2/S100A10 complex at the C-terminus domain of AHNAK in epithelial cells. Annexin 2 is thought to play a role in the organisation of cholesterol rich membrane microdomains, the connection of lipid rafts and actin cytoskeleton and cholesterol mediated adherent junctions form S100A10 mediates interaction between AHNAK and annexin 2. The AHNAK/annexin2/S100A10 complex is thought to be involved in the regulation of the actin cytoskeleton organisation (Benaud et al., 2004).

Very recently Komuro et al (Komuro et al., 2004) found another similar protein to AHNAK expressed in AHNAK-null mice, named AHNAK 2, which needs to be investigated further.

1.6.2 Otoferlin

Otoferlin was the second of the ferlin protein family to be identified through cDNA derived from total human foetal RNA (Yasunaga et al., 1999). Northern blot analysis revealed a signal in heart, placenta, liver, pancreas, skeletal muscle, kidney and two variable length transcripts in the brain (Yasunaga et al., 1999). Otoferlin is thought to exist as two isoforms, long and short. The long isoform has six C2 domains with 1997 amino acids producing a 227 KDa protein and is expressed in human brain and inner ear hair cells in which a mutation causes some cases of an autosomal recessive form of prelingual sensorineural deafness, DFNB9 (Yasunaga et al., 1999). The short isoform is expressed exclusively in humans with only three C2 domains, as a result of alternative splicing and its mutation causes most cases of DFNB9 (Yasunaga et al., 1999). Shorter truncated forms of dysferlin and myoferlin have also been reported (Davis et al., 2000).

1.6.3 Myoferlin

Two years after the discovery of dysferlin, the third member of the ferlin protein family was identified, named myoferlin (Davis et al., 2000) or FER1L3 (Britton et al., 2000). It was named myoferlin due to its high homology to dysferlin (68% similar and 58% identical) and its high expression in cardiac and skeletal muscle detected by a specific antibody to myoferlin although low expression was also detected in the lung, kidney, placenta and the brain (Davis et al., 2000). Myoferlin, a 230 KDa protein, maps to chromosome 10q23.3 and also contains six C2 domains at amino acid positions 1-85 (C2A), 200-281(C2B), 359-458(C2C), 1113-1218(C2D), 1525-1625(C2E) and 1777-1890(C2F) in

addition to one hydrophobic C-terminus transmembrane domain (Britton et al., 2000). All except one Ca^{2+} binding residue in the C2D and C2E domain in dysferlin and myoferlin are identical (Britton et al., 2000). In addition myoferlin has an SH3 domain that is thought to mediate interactions with other proteins. This domain is not found in dysferlin (Davis et al., 2000).

The role of myoferlin is unknown. But myoferlin's expression was found to be upregulated up to 274% in *mdx* mice. *mdx* mice are dystrophin deficient, therefore possess an unstable DGC. This suggests a role for myoferlin in membrane regeneration or repair or a compensatory role (Davis et al., 2000).

A recently generated breed of myoferlin null mice showed defects in myogenesis, greatly reduced area of individual muscle fibres, resulting in overall reduction in cross-sectional area of the whole muscle. In addition these mice had reduced muscle mass, resulting in smaller sized mice compared to control mice, meaning that myoferlin–null mice are less efficient in myoblast-myotube fusion or so called 'myoaugmentation'. Myoaugmentation has been described by Doherty et al (Doherty et al., 2005) as the second stage of myoblast fusion in which myoblasts fuse with existing myotubes. Myoaugmentation is preceded by 'myoinitiation' where individual myoblasts start to fuse with each other. Impaired skeletal muscle regeneration after cardiotoxin injury, in addition to disorganised muscle architecture with fat replacement in post injury muscle, is also seen in myoferlin null mice (Doherty et al., 2005). Dysferlin expression did not change in injured, control, wild type or myoferlin null muscle.

During the first 24 hours of differentiation, dysferlin expression is equivalent in myoferlin null cells when compared to wild type. Then, it is up-regulated by X1.6 in myoferlin-null cells after 4 days of differentiation. However, dysferlin is not

upregulated in adult muscle fibres (when all of the fusion events have been completed) in response to myoferlin deficiency. This might be due to the fact that myoferlin is already expressed at low levels in healthy adult mouse tissue (Doherty et al., 2005).

This finding suggests that dysferlin or other ferlins might be able to compensate for the loss of myoferlin in the early stages of fusion.

The fact that loss of myoferlin hinders myogenisis rather than completely blocking it and that myoferlin is present in low levels of healthy adult muscle in addition to the belated upregulation of dysferlin in maturing myotubes suggests that myoferlin through its Ca^{2+}-sensitive phospholipid binding may have a role in myoblast-myotube fusion. Both muscle membrane resealing and myoblast fusion involve the use of specialised vesicles suggesting the involvement of ferlins in muscle fusion events (Doherty et al., 2005).

1.6.3.1 Myoferlin Cell Biology

Immunocytochemical studies using the myoferlin antibody, Myof1 showed that similar to dysferlin, myoferlin is also localised to the plasma membrane in muscle fibres, in addition nuclear localisation is also detected. This unique expression might explain the need for two highly similar proteins in the same tissues (Davis et al., 2000). Although Matsuda et al. (Matsuda et al., 1999) have reported a nuclear and mitochondrial signal in muscle cell fractions by western blots using a polyclonal antibody against dysferlin.

A difference in the level of protein expression and mRNA expression between skeletal and heart muscle was detected using Myof1 antibody. This may indicate that mRNA expression is not directly proportionate to protein

expression and/or that post–translational regulation of myoferlin protein may happen (Davis et al., 2000).

Cell fractionation of skeletal muscle cells into nuclei, light microsomes and heavy microsomes revealed that myoferlin was preferentially found in the nuclear fraction. Further fractionation showed that myoferlin is heavily associated with nuclear membrane and has been associated with plasma membranes too (Davis et al., 2000). Later on, Davis et al (Davis et al., 2002) reported a vesicular staining in the perinuclear region in addition to general cytoplasmic staining.

Very recently it was shown that myoblasts cultured *in vitro* show increased expression of myoferlin prior and during myoblast fusions in which myoferlin is concentrated at cell to cell contact points. In addition, myoferlin is highly up-regulated after muscle fibres were injured using cardiotoxin (polypeptides that cause the depolarisation and degradation of the plasma membrane (Doherty et al., 2005).

In conclusion: 1) myoferlin is highly similar to dysferlin (Davis et al., 2000), and dysferlin in known to be a crucial component in membrane repair (Bansal et al., 2003), 2) myoferlin is highly similar to the *C-elegans* protein FER-1 (Davis et al., 2000), and FER-1 is required for the fusion of specialised vesicles, called membranous organelles, with the sperm plasma membrane during *C-elegans* spermatogenesis (Washington & Ward, 2006), 3) myoferlin possess a SH3 domain, thought to be involved in mediating interactions with other proteins (Davis et al., 2000), 4) myoferlin is up-regulated in dystrophin deficient mice (Davis et al., 2000), 5) myoferlin's C2A domain is highly homologous to the C2A

domain of rat synaptotagmin III (Britton et al., 2000) and Synaptotagmins are known to be calcium sensors (Jaiswal et al., 2004), 6) a point mutation to the C2A domain of myoferlin disrupts calcium induced phospholipid binding (Doherty et al., 2005), 7) myoferlin is upregulated in differentiating myoblasts (Doherty et al., 2005), and finally 8) myoferlin null muscle is defective in muscle regeneration following an injury (Doherty et al., 2005).

So far, nothing more is known about myoferlin, especially its function, but following this evidence presented here leads to the suggestion that myoferlin has a role in calcium dependent membrane fusion.

1.6.4 FER1L4

Fer1L4 is the newest member of the ferlin protein family (Doherty & McNally, 2003) (although its sequence has not been published yet) . It maps to human chromosome 20q11.22 (NCBI). It is thought to consist of 1953 amino acids, five C2 domains and a C-terminus transmembrane domain. Initial studies show that it is widely expressed and subjected to alternative splicing which as a result might produce multiple isoforms. So far its function is unknown (Doherty & McNally, 2003).

1.6.5 FER1L5

The characterisation of a fifth member of the ferlin protein family assigned by Dr. Bashir's laboratory as FER1L5 is reported here later in the thesis. *FER1L5* maps to the human chromosome 2q11.2. It is thought to consist of six C2 domains in addition to the conserved C-terminus transmembrane domain and shares the highest homology to myoferlin as discussed in chapter 3.

1.7 Hypothesis

As explained earlier in this chapter, Dysferlin, myoferlin and FER1L5 are members of the DysF subgroup of a moderately new protein family named the Ferlins. The ferlins are characterised by their homology to the C-elegans sperm vesicle fusion protein FER-1.

Myoferlin is one of the least well studied proteins of this protein family compared to dysferlin. It has not been linked with any human disease yet and not much is known about its function.

The fact that 1) myoferlin and dysferlin are 68% similar and 58% identical (Davis et al., 2000), 2) myoferlin is upregulated in dystrophin-deficient *mdx* mice (Davis et al., 2000), 3) dysferlin is upregulated in mature myotubes of myoferlin-deficient cells (Doherty et al., 2005), and 4) dysferlin is involved in membrane repair (Bansal et al., 2003), leads to the hypothesis that **1) the study of myoferlin and related proteins would provide a better understanding of the cell and molecular biology of myopathy, 2) myoferlin might have a role as a modifier gene in dysferlinopathies, 3) myoferlin might act as a compensatory protein in dysferlin deficiencies, 4) myoferlin will have a very similar response pattern to plasma membrane disruptions to that of dysferlin, 5) myoferlin might have a role in vesicle fusion similar to that of dysferlin, and might therefore be essential in membrane repair and other cellular functions of muscle cells such as differentiation.**

In addition, ferlins are a highly conserved, expanding protein family mostly with unknown functions. This leads to believe in the **existence of other un-identified ferlin proteins.**

Finally, the genetic heterogeneity of MM and the identification of several MM families not linked to the chromosome 2 locus lead to the hypothesis that **there is at least one more gene responsible for non-chromosome 2-linked MM**.

2 Chapter Two, Materials and Methods

2.1 Tissue Culture

2.1.1 Cell Culture

All tissue culture products were purchased from GIBCO, Invitrogen and all procedures were carried out at room temperature unless otherwise indicated.

C2C12 cells (mouse C3H muscle myoblast, (Yaffe and Saxel 1977)) and HDF (Human Dermal Fibroblasts, (Markiewicz, Dechat et al. 2002)) cell line were a generous gift from Prof. C.J. Hutchinson (School of Biological Sciences, University of Durham). The NRK (Normal Rat Kidney Fibroblasts, (Duc-Nguyen 1966) cell line was a kind gift from GlaxoSmithKline. All cells were cultured in DMEM (Dulbecco's Modified Eagles Medium, 1x liquid, with 4500 mg/L D-glucose, 110 mg/L sodium pyruvate, glutaMAX 1 (L- Alanyl-L-Glutamine 862 mg/L)) supplemented with 10% v/v heat inactivated FBS (Foetal Bovine Serum) and 1% v/v 5000 u/ml penicillin/ streptomycin and usually cultured in 75 cm^2 filter capped flasks (Griener) unless stated otherwise at 37°C in a humidified 5% CO_2 incubator.

The cells were passaged when 80% confluent by washing twice in 10 ml PBS for 1 minute then incubating with trypsin-EDTA (Ethylenediaminetetraacetic acid ,1x liquid, 0.05% v/v Trypsin, 0.53 mM EDTA) for 45 seconds at 37°C. Cells were passaged at 1:5 ratios.

SJL/J myoblasts (passage 1) and the controls, Fw+10j (passage 3 mouse myoblasts, extracted from 10 days old female wild type mice) were a kind gift from Genethon III, Gene Therapies Research and Applications Centre, France.

These cells were cultured in 80.1% v/v F-10 nutrient mixture (Ham) media (1x liquid, with L-glutamine), 8.9% v/v DMEM supplemented with 10% v/v heat inactivated FBS and 1% v/v 5000 u/ml penicillin/ streptomycin in 25 cm^2 filter cap flasks (Greiner) at 37°C in a humidified 5% CO_2 incubator.

All cells needed for immunolabelling were cultured overnight on heat sterilised 13 mm glass coverslips (SLS) in 12 well plates (Griener) at an average density of $4x10^4$ cells per coverslip in 1 ml of culture media.

2.1.2 Myoblast differentiation

C2C12 Cells were passaged at a 1:3 ratio and allowed to grow overnight on 13 mm glass coverslips (SLS) in 12 well plates (Griener) in 1 ml of culture media.

The next day, cells were gently rinsed once with differentiation media (D-MEM supplemented with 2% v/v horse serum, 1% v/v 5000 u/ml penicillin/ streptomycin) to remove any traces of FBS, then incubated with 1 ml of differentiation media as normal. The cultures were thereafter maintained up to 14 days by changing the media every 48 hours.

2.2 Cell Membrane Wounding Assays

2.2.1 Cell Membrane Wounding

C2C12 cells were injured using either a needle or glass beads. These methods are standard for wounding cells in published papers and injured cells are recognised by their dextran intake (McNeil and Steinhardt 1997). Under normal circumstances dextran is membrane impermeable and would only enter the

cytosol via endocytosis. When the integrity of the membrane is disturbed i.e. wounded, fluorescein dextran uptake is visible under UV light. Therefore dextran uptake is an indicator of cell wounding.

C2C12 cells grown to 80% confluence on coverslips were rinsed once in 3 ml PBS for 10 seconds and wounded in the presence or absence of fluorescein dextran, using the tip of a 25 Gauge needle (5/8 , VWR) in a grid like pattern (Figure 2.1).

The excess impermeablised dextran was removed by aspiration and cells were fixed (see below). Two different fluorescent dextrans were used depending on the nature of the subsequent secondary antibody to be used. Cells were always wounded in the presence of 5 mg/ml fluorescent Oregon green dextran (10 KDa, lysine fixable, Molecular Probes, Invitrogen) if cells were to be immunolabelled with fluorophore labelled Goat anti rabbit Alexa 546 as a secondary antibody, or in the presence of 5 mg/ml fluorescent Texas red dextran (10 KDa, lysine fixable, Molecular Probes, Invitrogen) if the cells were to be immunolabelled with fluorophore labelled Goat anti mouse Alexa 488 as a secondary antibody.

All secondary antibodies were purchased from Molecular Probes, Invitrogen.

An alternative method of inducing injury was treating the cells with acid washed glass beads (425-600 µm, sigma). C2C12 cells on coverslips were rinsed once in 3 ml PBS for 10 seconds. 500 µl of 5 mg/ml of fluorescent dextran in 1.0 mM Ca^{2+} PBS was then overlaid on them. Approximately 100 mg (400 beads) of acid washed glass beads were evenly sprinkled from an Eppendorf tube held 2 cm above the cells. The dish was gently rocked four times to roll the beads on the cells. The cells were then washed with PBS to remove glass beads and

Figure 2.1 Induced cell wounding using a needle

The sketch shows the needle wounding method used to induce injury in this study. Cells were scratched using a 25 Gauge needle in cross sections in the presence of fluorescein dextran or simply PBS.

Figure 2.1

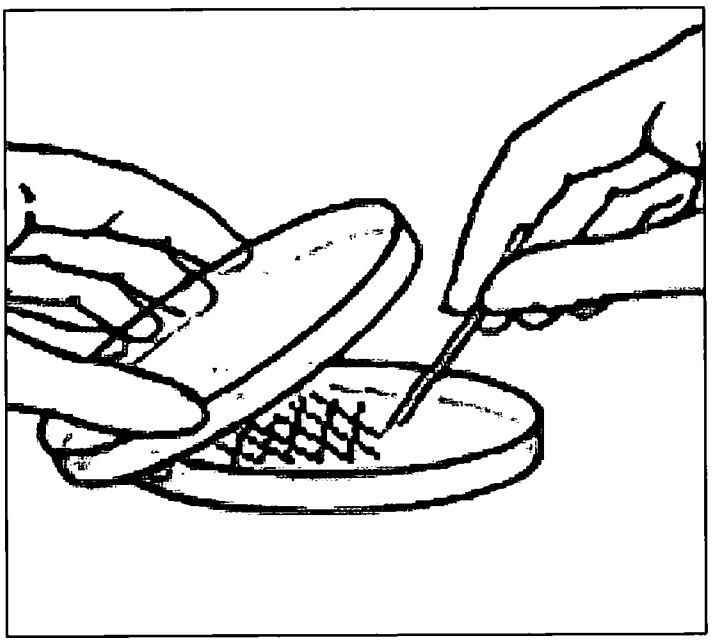

dextran, followed by formaldehyde fixation, washing, immunolabelling and confocal analysis.

2.2.2 Myotube Wounding

Differentiating myoblasts at the phase of interest were wounded using the tip of a 25 Gauge needle (5/8 , VWR) in a grid like pattern in the presence of membrane impermeable dextran.

2.2.3 Cell Membrane Resealing Assay

C2C12 cells were wounded with glass beads as described above in the presence of Oregon green dextran except that after injury the cells were rapidly washed with 37°C PBS three times (<1 min) and transferred to 37°C cell culture media to allow recovery for 5 minutes at 37°C in 5% CO_2. After 5 minutes the recovery media was removed and cells were incubated for a further 2 minutes in media containing 5 mg/ml fluorescent Cascade Blue dextran (lysine fixable, 10 KDa, Molecular Probes, Invitrogen) followed by formaldehyde fixation. Alternatively some cells were not allowed to recover and were exposed to the second dextran immediately (1<T<15 sec) before fixation. Using confocal microscopy the percentage of cells that had taken up the first dextran and those showing the uptake of the second dextran were calculated at 0 and 5 minutes in 15 microscopic fields (x40 oil lens) where at least 40% of the cells in each field were along the injury line. The exclusion of the second dextran reflected wound healing (Cerny, Feng et al. 2004). This experiment was repeated twice and the average was displayed as a percentage.

2.2.4 Ionomycin Induced Exocytosis

A rabbit polyclonal antibody was developed against the KIS epitope (CKISMPDVDLHLKGPK) of AHNAK (Gentil, Delphin et al. 2003).

C2C12 cells grown on coverslips were transferred to HMEM at 37°C then treated or not with 5 µM ionomycin (free acid, *streptomyces conglobatus*, Calbiochem) in HMEM (HEPES-buffered minimal essential medium) for 5 minutes at 37°C in 5% CO_2 followed by formaldehyde fixation as explained previously. Permeablised or non-permeablised cells were then immunolabelled with myoferlin and AHNAK antibodies and analysed by confocal microscopy.

2.3 Immunocytochemistry & Confocal Microscopy

For Immunocytochemistry, after the desired treatment cells were fixed using 2% v/v formaldehyde in PBS, pH 7.4 for 10 minutes, followed by three; two minute washes in 3 ml PBS then permeablised in 0.2% v/v Triton x-100 (sigma) in PBS for 5 minutes at 4°C, followed by three, five minute washes in PBS. Alternatively, cells were fixed in ice-cold (-20°C) neat methanol (VWR) for 10 minutes followed by three fifteen minute washes in 3 ml PBS. Cells fixed using methanol were not permeablised.

To block non-specific binding, cells were then incubated in blocking buffer (10% v/v FBS in PBS) for one hour. Blocking buffer was used for washes, as well as diluting primary (if necessary) and secondary antibodies in subsequent steps. After one hour incubation in the desired concentration of primary antibody, cells were washed for three, fifteen minute washes and finally incubated for one hour in the suitable secondary antibody followed by another three, fifteen minute

washes. Coverslips were then inverted and mounted on microscope slides (Sigma) using Mowial (appendix 1) containing 2 mg/ml DAPI (4', 6-Diamidino-2-phenylindole Dihydrochloride, Sigma) and allowed to set at 4°C overnight before confocal analysis and imaging. All confocal imaging was carried out using a Zeiss 510 confocal scanning microscope x60 oil immersion lens and its analysis using Zeiss Meta 510 with scale bar of 20 μm unless otherwise stated. Each immunocytochemistry experiment was repeated three times and cells were selected for imaging randomly.

2.4 Gene Expression Assays

2.4.1 mRNA Extraction

C2C12 cells were grown on nine 25 cm^2 filter capped flasks. The first three flasks were harvested the following day at 80% confluence and treated as explained later in this section. The remaining six flasks were induced to differentiate by withdrawing growth media and replacing it with differentiation media. After 24hrs in the differentiation media three flasks were harvested and treated (D1 samples) while the remaining three continued to differentiate for five days before harvesting (D5 samples). For each sample the media was removed from the flasks and cells were lysed following the recommended procedure for attached cell cultures in GenElute Mammalian Total RNA Kit from Sigma.

In brief, the culture media was completely removed and cells were lysed by incubating the cells for two minutes at RT with 500 μl lysis solution (provided) supplemented with 1:100 added 2-mercaptoethanol (2-ME) with two intervals of shaking. The collected lysates were then filtered using the GenElute filtration

column provided and centrifuged at 15000g in Eppendorf 5415R centrifuge for 2 minutes. 500 µl of 70% (v/v) ethanol was added to the filtered lysate, briefly vortexed and loaded to GenElute binding column, centrifuged at 15000g in Eppendorf 5415R centrifuge for 15 seconds. The bound RNA was then washed with 500 µl of wash solution 1, centrifuged for 15 seconds at 15000g in Eppendorf 5415R centrifuge, then washed with solution 2 and centrifuged for 15 seconds at 15000g in Eppendorf 5415R centrifuge followed by a second wash in solution 2 and centrifuged for 2 minutes at 15000g in Eppendorf 5415R centrifuge. 50 µl of Elution buffer was used to elute the bound RNA and centrifuged for 1 minute at maximum speed. The last step was repeated twice and the concentration of the total RNA was determined using a spectrophotometer.

mRNA was isolated following the recommended procedure for GenElute mRNA Miniprep Kit from Sigma. In brief, 40 µl of DEPC- treated water, 250 µl 2X Binding Solution was added to 500 µg of total RNA and vortexed. Then 15 µl of oligo (dT) beads were added to the tube and heated for 3 minutes at 70°C, then left at RT for 10 minutes and centrifuged at maximum speed for 2 minutes. The pellet is then washed in 500 µl of wash solution and transferred to GenElute spin filter collection tube and centrifuged at 15000g in Eppendorf 5415R centrifuge for 2 minutes. A second wash was performed in the same manner. 50 µl of pre-heated (70°C) Elution solution is added to the spin filter in a clean collection tube and allowed to stand at 70°C for 5 minutes followed by centrifugation at 15000g in Eppendorf 5415R centrifuge for one minute. This step was repeated one more time. The mRNA was then used for RT-PCR reactions as explained in the next section.

2.4.2 cDNA Generation

Single stranded cDNA was synthesised from mRNA using Promega Reverse Transcription System Kit. For each of the three stages investigated (D0, D1, D5), two random primer and two oligo (dT) primer reactions were generated. The final concentration of each reaction component was; 1X Reverse Transcription buffer with $MgCl_2$, 1 mM each dNTP, 1 U/µl Recombinant Rnasin Ribonuclease Inhibitor, 15 U/µg AMV Reverse Transcriptase, 0.5 µg primer (Oligo(dT) or random) per µg RNA, 50 ng/µl mRNA, made up to a total of 20 µl in DEPC-treated water. The oligo (dT) primer reactions were incubated at 42°C for 15 minutes, followed by 95°C for 5 minutes and finally at 4°C for 5 minutes. While the random primer reactions were incubated at RT for 10 minutes preceding the reverse transcription reaction. The product cDNA was normalised using primers designed to amplify the mouse glyceraldehyde-3-phosphate dehydrogenase (GAPDH) gene. cDNA used in dysferlin, myoferlin, and otoferlin expression profiling were provided and normalised using primers designed to amplify the mouse glyceraldehyde-3-phosphate dehydrogenase (GAPDH) gene by G. Marlow from Dr. R. Bashir's group (University of Durham, UK).

2.4.3 Primer Design

The Primer 3 programme (Whitehead Institute for Biomedical Research, USA) which combines a primer design algorithm with a web-based interface for analysis was used to generate primers for mouse genes and primers were supplied by MWG Oligonucleotides. The FER1L5 primers were designed within the EST sequence while the dysferlin, myoferlin and otoferlin primers were designed to the 3 UTR region of the genes. A complete list of primers to

dysferlin, myoferlin, otoferlin and FER1L5 is stated in appendix 2. These primers were used for subsequent PCR amplifications of these genes.

2.4.4 PCR and Agarose Gel Electrophoresis

PCR mix was set up containing 100 ng of DNA (or cDNA), 1X Reaction Buffer, 1.5/1.8 mM $MgCl_2$, 200 µM of dNTP mixture, 0.25 µM of both forward and reverse primers and 0.5 units of Taq polymerase made up to 30 µl in dH_2O. All reagents were supplied by Promega. The PCR reactions were carried out using the Hybaid Omn-E thermal cycler using the following programme: 94°C for 4 minutes for 1 cycle followed by 35 cycles of 94°C for 30 seconds, 48-50°C for 1 minute, 72°C for 1 minute and finally at 72°C for 10 minutes for 1 cycle.

PCR reactions were then analysed by agarose gel electrophoresis. A 1.5% w/v agarose powder (Bioline) was dissolved in hot 1X TAE buffer and allowed to cool. At 60-55°C, 1 µg/ml ethidium bromide was added and thoroughly mixed. The gel was poured in a Biorad pre-cast gel trays with a comb and allowed to set at room temperature for 30-45 minutes. The gels were then submerged in 1X TAE buffer. 10 µl of the desired sample (or 5 µl of the 100 bp or 1 Kb DNA ladder (Promega)) was mixed with 5 µl loading buffer (appendix 1) and loaded into each well. The gel was run at 65 volts (constant power) for approximately 30 minutes and the DNA was visualized using BioRad Gel-Doc Ultra Violet Transilluminator. Samples which demonstrated successful PCR amplification were stored at 4°C for subsequent SSCP analysis.

2.5 Protein Expression Assays

2.5.1 Sub-cellular Fractionation

C2C12 cells for sucrose gradient fractionation were grown to 80% confluence (approximately 1 x 10^6 cells per dish) in five 10 cm^2 round Petri dishes (Griener). Culture media was aspired and each dish was rinsed once in 5 ml of PBS, then the cells in the first plate were scraped using a cell scraper (Greiner) in the presence of 5ml of HES buffer (appendix 1) supplemented with freshly added Complete Mini Protease Inhibitors (1 tablet per 10 ml, Roche Molecular Biochemicals) and then added to the next plate. After all five plates were scraped the cells were transferred to a homogeniser (Borosilicate glass tube, stainless steel pestle shaft, VWR) and homogenised by hand by 15 turns of the pestle. The homogenate was centrifuged at 19,000g for 20 minutes at 4°C (12,500 rpm) in a Beckman centrifuge JA-20 rotor. The pellet obtained from this centrifugation (P1) was retained on ice for the preparation of a plasma membrane fraction while the supernatant was used to prepare intracellular fractions by centrifugation at 40,000g (18.25 rpm) for 20 minutes at 4°C in the Beckman JA-20 rotor. This yields a pellet of high density microsomes (HDM), while the supernatant was centrifuged again at 180,000g (33,000 rpm) for 75 minutes at 4°C in a Beckman Ultracentrifuge in a SW-41 rotor to isolate the low density microsomes (LDM). The pellet from the first centrifugation (P1) is re-suspended in 0.8 ml HES buffer and layered on to 10 ml of 1.12 M sucrose in HES buffer and centrifuged at 100,000g (26,000 rpm) for 60 minutes at 4°C in the SW-41 rotor. The pellet from this centrifugation spin yielded the endoplasmic reticulum and nuclear (ERN) fraction, while the plasma membrane fraction was recovered from the interface between the sucrose layers of the

supernatant and washed with 25 ml of HES buffer by centrifugation at 40,000 g (18,250 rpm) for 20 minutes at 4°C in a Beckman JA-20 rotor. This pellet is the plasma membrane (PL). All membrane fractions were re-suspended in 100 µl of HES buffer and snap frozen in liquid nitrogen (Method adapted from (Howland 1973)).

2.5.2 Protein Extractions

For western blots differentiation of myoblasts was carried out in 75 cm^2 filter capped flasks for larger samples. Cells were harvested at time points of interest, D0, D1, D3, D5, D7 and D14 as follows. Media was removed from the cells and rinsed 3 times with ice-cold PBS. 500 µl of RIPA (RadioImmunoPrecipitation Assay, appendix 1) buffer supplemented with freshly added Complete Mini Protease Inhibitors (1 tablet per 10 ml, Roche Molecular Biochemicals) was added to the flask and cells were scraped using a cell scraper (Griener), transferred to a centrifuge tube and allowed to stand on ice for 20 min with occasional shaking. The samples were then centrifuged for 10 min at 13,000 rpm (16,000g) in Eppendorf 5415R centrifuge at 4°C. The supernatant was then transferred to a clean tube and protein concentration was determined using the Bio-rad assay.

2.5.3 Protein Quantification

The protein concentration in each sample was determined using Bradford assay as described (Bradford 1976) using BSA (stock solution 0.1 mg/ml) as standard.

In brief, 1.5 µl of each sample of unknown concentration was mixed with 798.5 µl dH_2O, 200 µl Bradford reagent (Sigma) and incubated at room temperature for 20 minutes. The samples were then transferred to polystyrene cuvettes (2 ml capacity, light path 10 mm, VWR) and readings were taken using an Eppendorf Biophotometer spectrophotometer set at 595 nm (A595). Protein concentrations of each fraction were determined and then normalised.

2.5.4 Western Blotting

The desired samples were mixed with 5x sample buffer (appendix 1) in the ratio of 1:4 v/v and heated at 95°C for 5 minutes. A final concentration of 15 µg of protein from the sub-cellular fractionation and 100 µg of protein from the myoblast differentiation profile was loaded into slots of a 6% discontinuous SDS-PAGE gel.

A discontinuous SDS-PAGE (sodium dodecyl sulfate polyacrylamide gel electrophoresis) gel formed in a mini-Protean 3 gel system (Biorad). Biorad pre-stained protein size markers were used as standards. The concentration of the resolving gel depended on the size of the protein of interest. For analysis of myoferlin and FER1L5, a 6% resolving gel (50% polyacrylamide, Prosieve 50 gel, Cambrex) was used while all other proteins were run on 12% resolving gel (50% polyacrylamide, Prosieve 50 gel, Cambrex). A 5% stacking gel (50% polyacrylamide) was used throughout (Table 2.1).

Gels were then immersed in 1x tank buffer (appendix 1) then loaded and run with a Biorad power pak 300 at 80V (constant power) for one hour followed by 100V (constant power) for another hour. The gels were removed from the plates

and stained with Coomassie Blue stain (Sigma) by immersing in water for 3 times, five minutes each then stained with Coomassie blue stain for one hour at room temperature and de-stained in water for one hour at room temperature. Alternatively the gels were removed from plates and rinsed in transfer buffer (appendix 1) for 15 minutes with the nitrocellulose membrane (Protran pore size 0.45 µm, Schleicher and Schuell Bioscience) and placed into a Biorad Mini Trans-Blot Electrophoretic Transfer Cell. A sandwich was formed from the cathode in the following order: 1 fibre pad, 2 Whatman 3MM filter paper, gel, nitrocellulose membrane, 2 Whatman 3MM filter paper, 1 fibre pad. The transfer was carried out at 50V (constant power) for two hours in transfer buffer and ice pack. After transfer, blots were blocked overnight at 4°C in blocking buffer (appendix 1). The next day blots were incubated for one hour in 6 ml of the appropriate concentration of the primary antibody (neat or diluted in wash buffer, appendix 1). The wash buffer was used for subsequent washes and secondary antibody dilution (Table 2.2).

After washing two times for 5 minutes, one time for 15 minutes, and one time for 5 minutes, the blots were incubated in the appropriate concentration of the secondary antibody, followed by another two 5 minute washes, one 15 minute wash and one 5 minute wash.

For immunoblotting of FER1L5, gel electrophoresis and transfer were carried out as described previously with the following changes. The blots were blocked for one hour at RT in blocking buffer composed of 5% (w/v) skimmed MP (milk powder) in TBS at pH8. These blots were then washed three times in TBS for 5 min each and were incubated overnight at 4°C in 6 ml of the FER1L5 D84 serum, 1:500 diluted in 3% (w/v) MP TBS. The next day blots were rinsed three

times in TBS for 5 min each and incubated in 6 ml HRP (Horse Redish Peroxidase) conjugated Donkey anti-rabbit, IgG diluted 1:5000 in 3% (w/v) MP, 0.1% (v/v) Tween20 and TBS for one hour at RT and finally rinsed three times for 5 min each in TBS.

The blots were then treated with mixed equal volumes (2 ml of each) of ECL (Enhanced Chemiluminescence) western blot detection reagent (Amersham Biosciences) for 10 seconds, and exposed to Amersham Hyperfilm ECL autoradiography films (18 x 24 cm, Amersham). The length of exposure was empirically determined for each blot but 1 minute exposure was commonly used. The films were then hand developed for 30 seconds and fixed for four minutes using GBX hand developing kit (Sigma), washed with water and allowed to air dry.

Table 2.1 SDS-PAGE gel recipes

This table shows the different components of SDS-PAGE gels. 6% resolving gel was used for high molecular weight proteins, e.g. dysferlin, myoferlin while the 12% resolving gel was proteins with lower molecular weights. In all gels a 5% stacking gel was used.

Table 2.1

Components	6% resolving gel	12% resolving gel	5% stacking gel
Deionised water	6.1 ml	4.9 ml	3.75 ml
Prosieve 50 gel	1.2 ml	2.4 ml	0.5 ml
1.5 M Tris-HCl, pH 8.8	2.5 ml	2.5 ml	-
1.0 M Tris-HCl, pH 6.8	-	-	0.65 ml
10% SDS	100 µl	100 µl	50µl
10% APS	100 µl	100 µl	50µl
TEMED	4 µl	4 µl	5µl

Table 2.2 Antibodies used in this study

A) A brief summary of the primary antibodies used in this study. (B) A brief summary of the secondary antibodies used and their working concentration.

Target	Antibody	Species/ clonality	Assay	Dilution	Source
Myoferlin	FER1L3	Mouse monoclonal	Immunocytochemistry Immunoblotting	Neat Neat	Dr L. Anderson (University of Newcastle upon Tyne,UK)
Myoferlin	Myof2	Rabbit polyclonal	Immunocytochemistry	1:300	Dr L. Anderson(University of Newcastle upon Tyne,UK)
Myoferlin	Myof1	Rabbit polyclonal	Immunocytochemistry	1:300	Dr L. Anderson(University of Newcastle upon Tyne,UK)
Caveolin3	Cav3	Rabbit polyclonal	Immunocytochemistry Immunoblotting	1:300 1:300	BD Biosciences
ER	PDI	Rabbit polyclonal	Immunocytochemistry Immunoblotting	1:750	A kind gift from Dr A. Benham (School of Biology, University of Durham, UK)
AHNAK	KIS	Rabbit polyclonal	Immunocytochemistry	1:15	A kind gift from Dr. H Haase, Max-Delbruck-Center for Molecular Medicine, Berlin, Germany
Lysosomes	Lamp-1/ 1D4B	Mouse monoclonal	Immunocytochemistry	1:300	Hybridoma Collection, University of Iowa, USA
F-actin	Anti-actin (C4)	Mouse monoclonal	Immunocytochemistry	1:30	Dr. A. Smertenko (University of Durham, UK)

Tubulin	Anti-α-tubulin	Rat monoclonal	Immunocytochemistry	1:100	A kind gift from Dr. A Smertenko
Dysferlin	NCL-Hamlet	Mouse monoclonal	Immunoblotting	1:250	Novocastra
TGN	TGN38	Sheep/Goat polyclonal	Immunocytochemistry	1:100	Serotec

B)

Antibody	Assay	Dilution	source
Alexa 488 goat-anti-mouse	immunocytochemistry	1:500	Molecular probes
Alexa 546 goat-anti-rabbit	immunocytochemistry	1:500	Molecular probes
FITC goat-anti-rat	immunocytochemistry	1:100	Dr. A. Smertenko
Donkey-anti-mouse HRP	Immunoblotting	1:5000	Jackson Immunoresearch
Donkey-anti-rabbit HRP	Immunoblotting	1:5000	Jackson Immunoresearch

2.5.5 FER1L3 Antibody Immunoadsorption

The gel electrophoresis and blot transfer were carried out as explained previously. 200µl of the 1 mg/ml FER1L3 peptide (C-GDEPPPERRDRDNDSDDVE, Dr. L Anderson, University of Newcastle Upon Tyne) was added to 2 ml FER1L3 antibody diluted in blocking buffer (1:50 dilution) to bind overnight at 4°C. The antibody / peptide solution (or antibody alone in the case of control) was then added to the membrane for one hour at RT, followed by secondary antibody and exposure as explained previously. This experiment was carried out by Dr. M. Hill (University of Durham, UK).

2.5.6 FER1L5 Assembly & Analysis

The locus XM_937145 (GeneID: 90342) maps to the human chromosome 2q11.2. Using the web based programme SMART (Simple Modular Architecture Research Tool, http://smart.embl-heidelberg.de) this protein is predicted to have six C2 domains (C2A: 1-98, C2B: 168-264, C2C: 326-423, C2D: 1236-1397, C2E: 1717-1816, C2F: 1952-2081 and a C-terminal transmembrane domain: 2192-2211) in addition to a nested DysF domain (DysFN: 913-963, DysFC: 1040-1078 & 1103-1135). Using the BLAST program, FER1L5 was found to be 37.5% identical and 55% similar to myoferlin and 37.5% identical and 53% similar to dysferlin.

The mouse FER1L5 gene is thought to be located on chromosome 1, locus XM_136730. It is predicted to have five C2 domains (C2A: 208-327, C2B: 397-493, C2C: 554-651, C2D: 1828-1927, C2E: 2000-2192), a transmembrane

domain (a. a 2305-2327) and a nested DysF domain using the SMART programme.

2.5.7 FER1L5 Antibody Immunoadsorption

The FER1L5 antibody was raised to peptides TRIEKHQNRQKYGLC and LAPLPRPCMSIDFRD (derived from human FER1L5 sequence) in rabbits supplemented by a sepharose beads column that had adsorbed 5mg of the FER1L5 peptides by CovalAb, UK.

The FER1L5 affinity purified antibody did not work by immunocytochemistry, and gave a very dirty background when used for immunoblotting. As an alternative the Day 84 serum was tested for peptide specificity by immunoadsorption and used for immunoblotting.

Day 84 serum was diluted 1:100 in PBS and left in the sepharose beads-peptide bound column 1 hour at 37°C followed by overnight incubation at 4°C. The unbound serum was used for peptide blocking analysis.

RIPA lysed C2C12 cells were loaded into a 6% discontinuous SDS-PAGE gel in the following order: lanes 1 & 4 (23 µg), 2 & 5 (35 µg) and 3 & 6 (57 µg). Gel electrophoresis, blot transfer and blocking were carried out as explained previously. For primary antibody incubation lanes 1, 2 and 3 were incubated with day 84 FER1L5 serum (1:100) while lanes 4, 5 and 6 were incubated with unbound FER1L5 serum (1:100) from the incubation in sepharose beads-peptide bound column followed by incubation in 6 ml HRP (Horse Redish Peroxidase) conjugated Donkey anti-rabbit, IgG diluted 1:5000 in 3% (w/v) MP, 0.1% (v/v) Tween20 and PBS for one hour at RT and finally rinsed three times

for 5 min each in PBS. This entire experiment was carried out by Dr. K. Saleki (University of Durham, UK).

2.6 Sub-cellular Localisation Studies

2.6.1 Latrunculin B Treatment

C2C12 cells were cultured at a 1:3 ratio and allowed to grow overnight on 13 mm glass coverslips (SLS) in 12 well plates (Griener) in 1 ml of culture media.

Latrunculin B (LA-B) was a generous gift from Dr. Anderi Smertenko (University of Durham, UK). A working stock solution of LA-B was made to 1 µM diluted in culture media. C2C12 cells were then incubated with a wide range of LA-B concentrations and time points using concentrations from published data as a guideline (Gronewold, Sasse et al. 1999; Wakatsuki, Schwab et al. 2001).

Cells were incubated with 0 nM, 50 nM, 100 nM, 150 nM, 200 nM and 250 nM of LA-B diluted in culture media for 2 hours at 37°C. Treated and control cells were then fixed by neat methanol at -20°C for 10 minutes and re-hydrated as explained previously. Treated and control cells were then immunolabelled with F-actin antibody (1:30) or Myof2 antibody (1:300) and analysed by confocal microscopy.

2.6.2 Nocodazole Treatment

1 mg of Nocodazole (Sigma) was solubilised in 1 ml of DMSO. A working stock concentration of 1 µg/ml diluted in culture media was used for experiments. C2C12 cells were then treated with 0 ng/ml, 15 ng/ml, 25 ng/ml, 35 ng/ml, 50 ng/ml of nocodazole for 15 minutes at 37°C. The treated cells were then fixed with neat methanol as explained previously, immunolabelled with tubulin antibody (1:100) and Myof2 antibody (1:300) and examined by confocal microscopy.

2.6.3 ATP Depletion

C2C12 cells cultured overnight on 13 mm glass coverslips (SLS) in 12 well plates (Griener) in 1 ml of culture media were treated for ATP depletion as follows. Cells were treated with a mixture of 0.025%-0.2% (w/v) sodium azide (NaN_3) and 25 µM-200 µM 2-deoxyglucose (2-DG) for 30 minutes (Reits, Benham et al. 1997). NaN_3 and 2-DG were both kind gifts from Dr. A. Benham (University of Durham, UK).

To study which concentration of NaN_3 and 2-DG successfully depleted the cells from ATP therefore inhibited endocytosis, Oregon green dextran (5 mg/ml) (Wubbolts, Fernandez-Borja et al. 1996; Reits, Benham et al. 1997) was added to the NaN_3 / 2-DG media for 30 minutes followed by rapid washing and fixing by methanol. Although dextran was used previously as an indicator of induced plasma membrane disruptions when exposed to cells for seconds (during injury) it is used here as an endocytosis marker when exposed to cells for longer time

i.e. minutes. The lowest effective dose to inhibit endocytosis for C2C12 cells was 0.1% NaN_3 and 100 μM 2-DG, where no endocytosis was detected.

Control C2C12 cells or cells treated with 0.1% NaN_3 (w/v) and 100 μM 2-DG for 30 minutes at 37°C were then wounded using a needle in the presence of dextran as explained previously. These cells were then fixed by methanol, and immunolabelled with Myof2 antibody for confocal analysis.

2.7 Single-Strand Conformation Polymorphism (SSCP) Analysis

2.7.1 Gene analysis & Primer design

The two Dutch families (I & II) from the genetic heterogeneity in Miyoshi myopathy study by Linssen et al (Linssen, de Visser et al. 1998) that were excluded for dysferlin-linked MM based on genetic analysis in addition to showing provisional linkage to a 23cM region on chromosome 10 (Linssen, de Visser et al. 1998) were used in this study. Genomic DNA extracted from leukocytes of patients' blood samples was provided by Dr. R. Bashir's lab.

These two families (FI & FII) were genotyped with several chromosome 10 microsatellite markers, their order and segregation of alleles investigated by Dr. Bashir's group. From each of these two families, two affected individuals and one carrier (affected: Ib, Ig, IIb and IIh; carrier: Id and IIe) was chosen for SSCP analysis in six genes that lay in the 23cM region on chromosome 10 in addition to one sample from a healthy donor used as a control sample.

Figure 2.2 Pedigrees of the two families selected for SSCP screening.

These two families have been excluded for dysferlin-linked MM. Open symbols: unaffected subjects, solid symbols: affected subjects, half-solid symbols: carrier subjects, slashed symbols: deceased subjects.

Family I

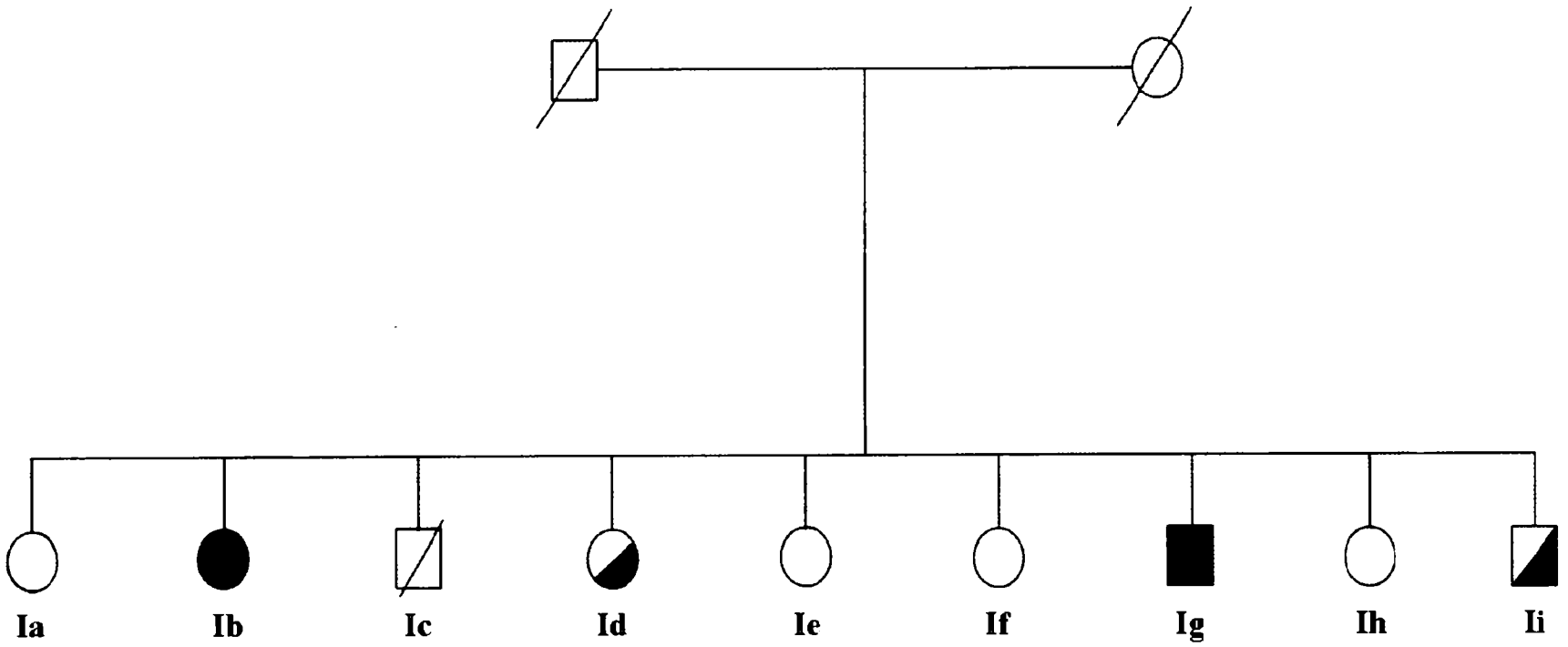

Family II

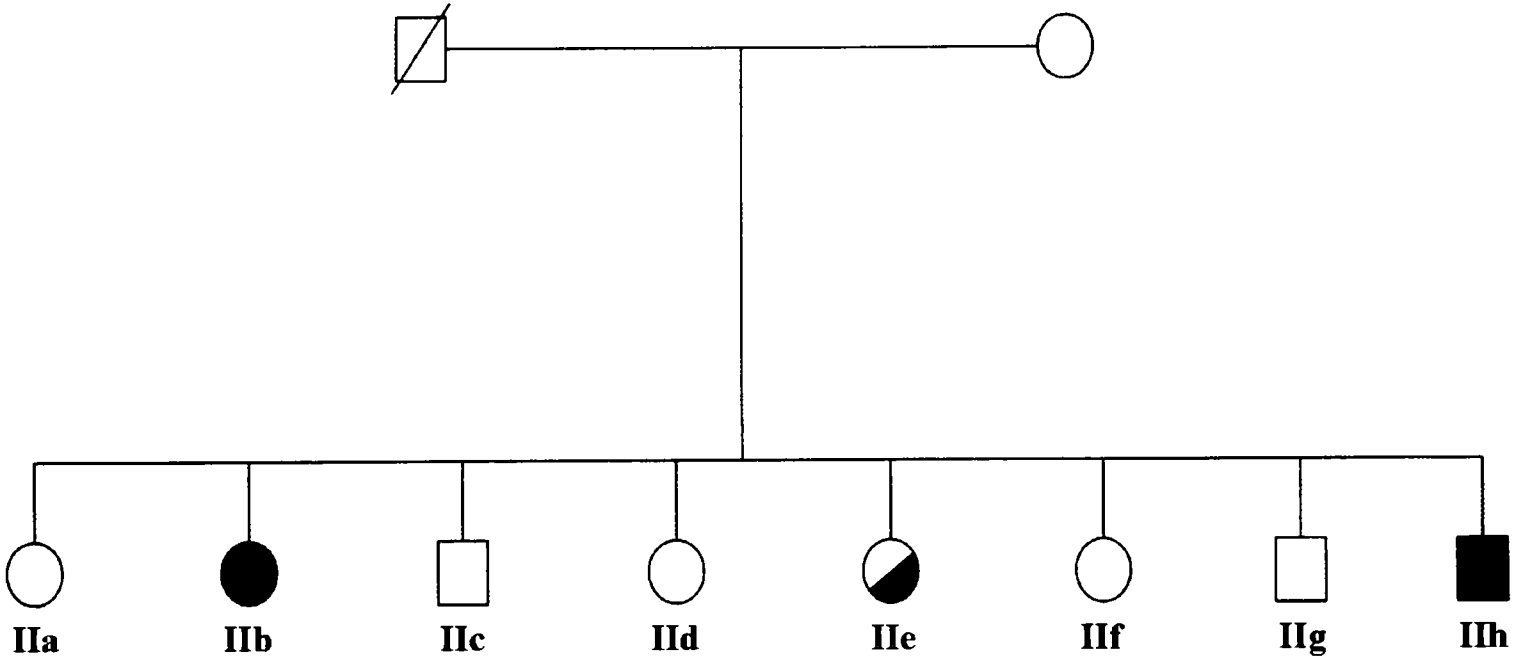

The primers were designed using Primer 3 programme and were supplied by MWG Oligonucleotides. The list of all the primers is detailed in appendix 3.

Caveolin 3 was also screened on a panel of 19 MM patients that were previously excluded by Dr. R. Bashir's group for mutations on chromosomes 2 and 10.

2.7.2 SSCP Gel Electrophoresis

The SSCP gels (30 ml Hydrolink-MDE (AT Biochem, USA), 3.6 ml 10x TBE, 6 ml 50% glycerol, 360 µl 10% APS, 55 µl TEMED, 20.4 ml H_2O) were cast in PROTEAN II xi system (Bio-Rad) and allowed to set for one hour at room temperature. 7.5 µl of PCR samples were then aliquoted out and mixed with 7.5 µl of SSCP loading buffer (95% v/v formaldehyde, 5% v/v 20 mM EDTA, 0.05% xylene, 0.05% bromophenol blue) and denatured at 94°C for 4 minutes and transferred immediately to ice. The set gels were then transferred into the electrophoresis tank and immersed in 0.6x TBE (appendix 1). The wells were thoroughly washed and the PCR-loading buffer mixture was loaded into each well. The system was connected to cold water supply for cooling and samples were allowed to run overnight at 80V (Biorad power pac 300 at constant power). The next day the 1mm thick gels were removed from gel plates and carefully transferred into a plastic tray. The gel was fixed by incubating in SSCP solution 1 (appendix 1) for 3 minutes with gentle shaking. After 3 minutes the solution was discarded and gels re-incubated in SSCP solution1 for a further 3 minutes. The gels were then incubated in SSCP solution 2 (appendix 1) for 15 minutes with gentle shaking followed by two 15 second washes in distilled water. Finally

gels were incubated in SSCP solution 3 (appendix 1) for 20 minutes with gentle shaking. Gels were then rinsed with distilled water and scanned for further analysis.

3 Chapter Three, Subcellular Localisation of Myoferlin

3.1 Introduction

The aims of this chapter were to confirm the specificity of an uncharacterised myoferlin monoclonal antibody, FER1L3 by studying the subcellular localisation of myoferlin in wild type muscle cells, dysferlin deficient muscle cells and two other cell lines.

Once the subcellular localisation of myoferlin using the FER1L3 antibody was confirmed, myoferlin localisation in response to plasma membrane disruptions was investigated to study whether myoferlin is enriched at plasma membrane disruption sites following cell membrane wounding.

For these studies C2C12 myoblasts were primarily used. This cell line is the most common cell line used for muscle research since it can be induced to undergo differentiation from mononucleate myoblasts to multinucleate myotubes upon the withdrawal of serum from the growth media.

The first step was to characterise the specificity of FER1L3 antibody to confirm that it was reactive with myoferlin and not other, similar ferlin family members. Then, the localisation and mobilisation of myoferlin was also investigated during cell wounding and membrane resealing.

Cell membrane wounding was induced by standard techniques used for membrane repair research such as scratching using a fine needle or glass bead wounding (McNeil & Warder, 1987,Swanson, 1987). However, how efficient

these methods were in inducing injury at the conditions used in this thesis was investigated. Since most vesicles needed for plasma membrane repair post wounding are not pre-docked at the wound site, it is necessary for successful plasma membrane repair to remove any physical barrier sitting between vesicles needed for repair and the injured membrane. One such barrier is the filamentous actin (F-actin) docked below the plasma membrane. Its temporary depolymerisation in the seconds preceding membrane repair is an absolute necessity. However, its polymerisation post resealing is reported (Miyake et al., 2001) and can be used as a good indicator of wounded cells or the wound site in particular.

Myoferlin trafficking was also investigated following elevations of intracellular calcium using calcium ionophore. Calcium ionophore is a valuable tool in establishing the link between the concentration of calcium and the rate of exocytosis. Enlargosomes, like lysosomes, undergo a calcium-dependent exocytotic fusion with the plasma membrane (Borgonovo et al., 2002). Therefore wounding cells physically or treating with ionomycin, induced Ca^{2+}-dependent exocytosis. This method is used to test whether myoferlin enrichment at the wound site in Ca^{2+}-dependent or not.

3.2 Results

3.2.1 Specificity of FER1L3 Antibody

3.2.1.1 Peptide Blocking Results

To ensure the specificity of the FER1L3 antibody, western blots of C2C12 cells were probed with the antibody. As seen in Figure 3.1, a band of correct molecular weight was identified. This interaction was proved to be antigen specific by the complete abrogation of antibody binding. This experiment was carried out by Dr. M. Hill (University of Durham, UK) and provided supporting evidence that experiments using the FER1L3 antibody would characterise the presence or absence of myoferlin.

3.2.1.2 Myoferlin Distribution by Immunoblotting

To further clarify the intracellular localisation of myoferlin, C2C12 cells were fractioned to light and dense microsomes, ER-nuclei and plasma membrane fraction as described in materials and methods chapter. An antibody to the nuclear membrane protein Lamin A tail, Jol4 (Dyer et al., 1997) was used to determine the purity of the fractions and the degree of nuclear contamination in the high density and low density microsomes and the plasma membrane fraction. Only the nuclear fraction could be recognised by the antibody even at very long exposure times (Figure 3.2C) indicating that there was no detectable contamination of the other fractions with the nuclear components. Immunoblotting of these fractions with FER1L3 antibody showed that myoferlin is preferentially in the ER-nuclear fraction and the weak signal in the light and dense microsomes in addition to the plasma membrane has been reported

using Myof1/2. Myoferlin was clearly absent from the cytosol fraction (Figure 3.2B) (Davis et al., 2000).

These fractions were also probed with dysferlin antibody. Although dysferlin is not associated with the nuclear membrane fraction, this fractionation technique does not separate the nuclei from the endoplasmic reticulum. Therefore, although dysferlin is not associated with the nuclear membrane fraction but dysferlin's presence in this fraction could indicate its presence in the ER not nuclei. Similar to myoferlin, dysferlin was also clearly absent from the cytosol (Figure 3.2A). Given the structural similarity between dysferlin and myoferlin, there is a formal possibility that antibodies to myoferlin could cross-react with dysferlin. Western blots are unable to discriminate between the two as the molecular weights of these two proteins are very similar, i.e. 230 KDa (2080 amino acids for dysferlin and 2061 amino acids for myoferlin). In order to address this, the expression of these gene products in normal and dysferlin deficient cells was examined.

3.2.1.3 Reactivity to Dysferlin Deficient Cells

SJL/J cells are deficient in dysferlin (Bittner et al., 1999), but to date no mutations in their myoferlin gene is reported.

Since the pattern of staining of dysferlin in immunoflorescence has been characterised previously (Matsuda et al., 2001), the reactivity of FER1L3 was assessed in SJL/J and control cells (Fw+10j) by confocal microscopy. The pattern of immunoflorescence was very similar when compared between the control and dysferlin deficient cells (Figure 3.3), a result consistent with FER1L3 antibody being specific for myoferlin. To support this, the nuclear membrane

and peri-nuclear region staining seen in Figure 3.3 is characteristic of myoferlin (Davis et al., 2000). In order to examine this further, the colocalisation of immunoflorescence of FER1L3 antibody with another antibody to myoferlin, Myof1, was examined.

3.2.1.4 Colocalisation with Myof1 Antibody

Myof1, is a polyclonal antibody specific for myoferlin, and was the first antibody developed to myoferlin peptide SEDGSRIRYGGRDYSLD (amino acids 1692-1708). Cross reactivity with dysferlin has been reported as being undetectable (Davis et al., 2000). In order to confirm that the new FER1L3 antibody demonstrated similar patterns of reactivity compared to Myof1, C2C12 cells were double labelled for Myof1 and FER1L3 antibodies and subjected to confocal analysis. As can be seen from Figure 3.4 , the pattern of staining of the two antibodies was indistinguishable from one another, confirming that FER1L3 was at least as good as Myof1 as a confocal tool, and supporting the evidence that FER1L3 was specific for myoferlin.

Having determined the suitability and specificity of the antibody, the expression pattern of myoferlin in normal and wounded cells was assessed by confocal microscopy.

In addition to Myof1, a second polyclonal antibody named Myof2 that was developed to myoferlin peptide TEFTDEVYQNESRYPGGD (amino acids 928-945) by Davis et al (Davis et al., 2000) was also used in experiments of this project.

Figure 3.1 FER1L3 antibody binding is blocked by the cognate antigenic peptide

Western blots of C2C12 myoblasts were probed with FER1L3 antibody in the presence or absence of the specific peptide. Lanes 1 and 3 shows the control (unblocked signal) while lanes 2 and 4 clearly show that the peptide has resulted in the total abolishment of signal. The molecular weight is indicated (KDa). This procedure was performed by M. Hill (School of Biological Sciences, University of Durham, UK).

Figure 3.1

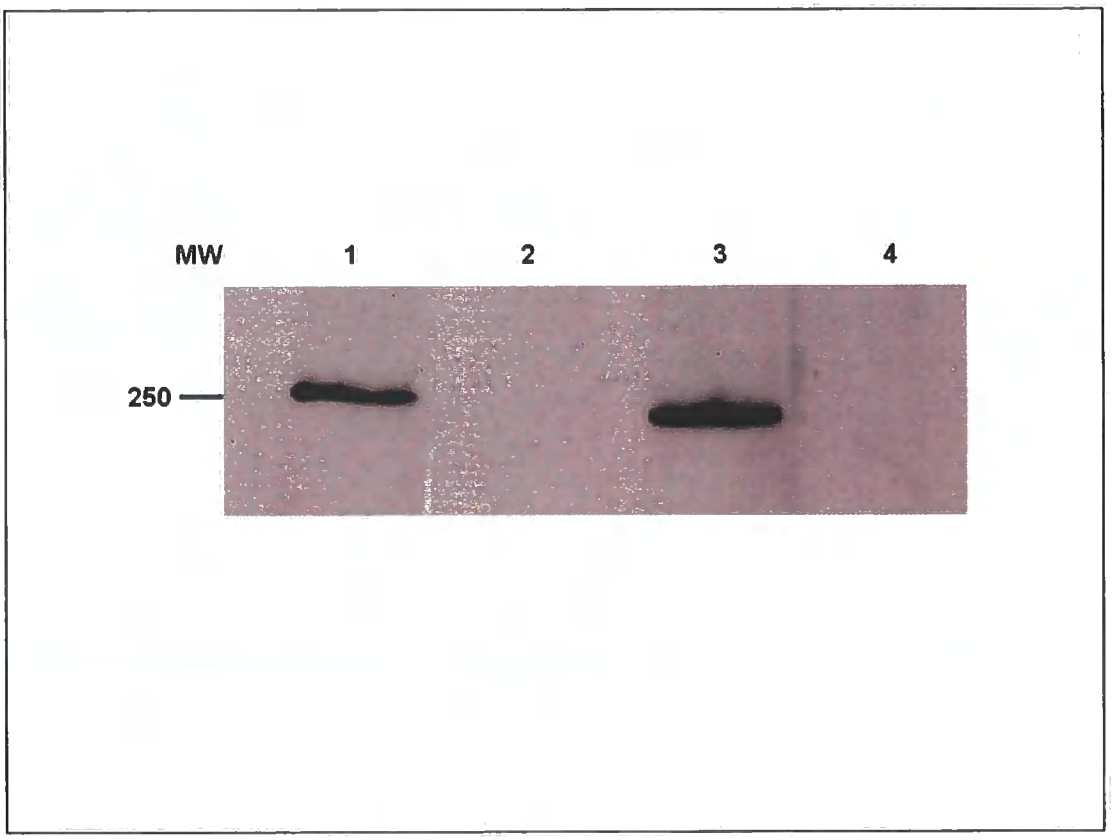

Figure 3.2 Expression of dysferlin, myoferlin and Lamin A in cell fractions of C2C12 cells.

C2C12 cells were subjected to differential centrifugation and the membrane fractions analysed by western blot. Lane1; High density microsomes (HDM), Lane2; Low density microsomes (LDM), Lane 3; ER-nuclear fraction (ERN), Lane 4; Plasma membrane (PL), Lane 5; cytosol. A) anti-Dysferlin, B) anti-Myoferlin, C) anti-Lamin A. Molecular weight marker in KDa. Protein stained gels confirmed equal loading of samples (data not shown).

Figure 3.2

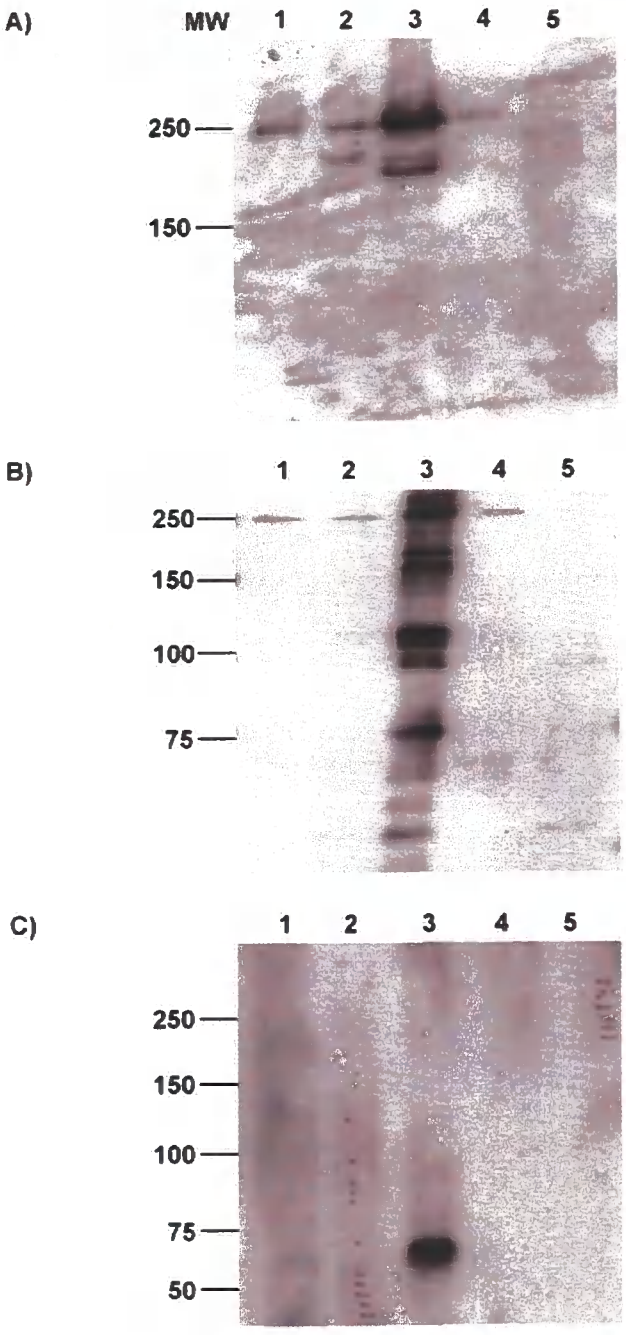
A)
MW
1
2
3
4
5
250
150
B)
1
2
3
4
5
250
150
100
75
C)
1
2
3
4
5
250
150
100
75
50

Figure 3.3 FER1L3 reactivity to dysferlin deficient cells

Confocal images of SJL cells (Lane 1) and control cells, Fw+10j (Lane 2) stained by immunocytochemistry using FER1L3 antibody. Both groups showed very similar staining pattern when analysed and imaged by confocal microscopy.

Figure 3.3

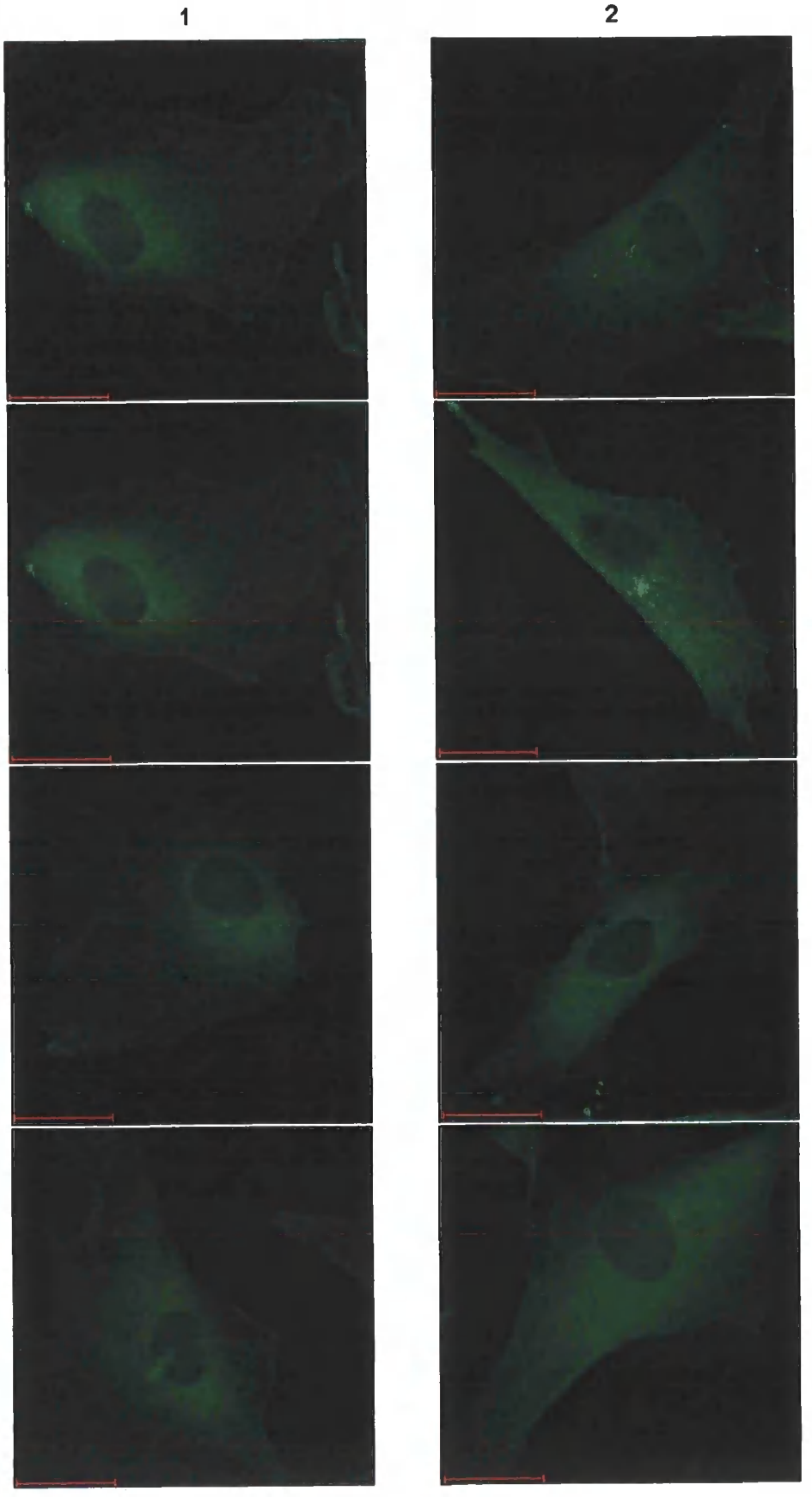

Figure 3.4 FER1L3/ Myof1 colocalisation

C2C12 cells were double labelled by immunocytochemistry with FER1L3 and Myof1 antibodies to investigate their colocalisation. A) Myof1 staining, B) FER1L3 staining, C) merged images. The first set of images shows a group of cells while the second set of images shows a close-up of individual cells.

Figure 3.4

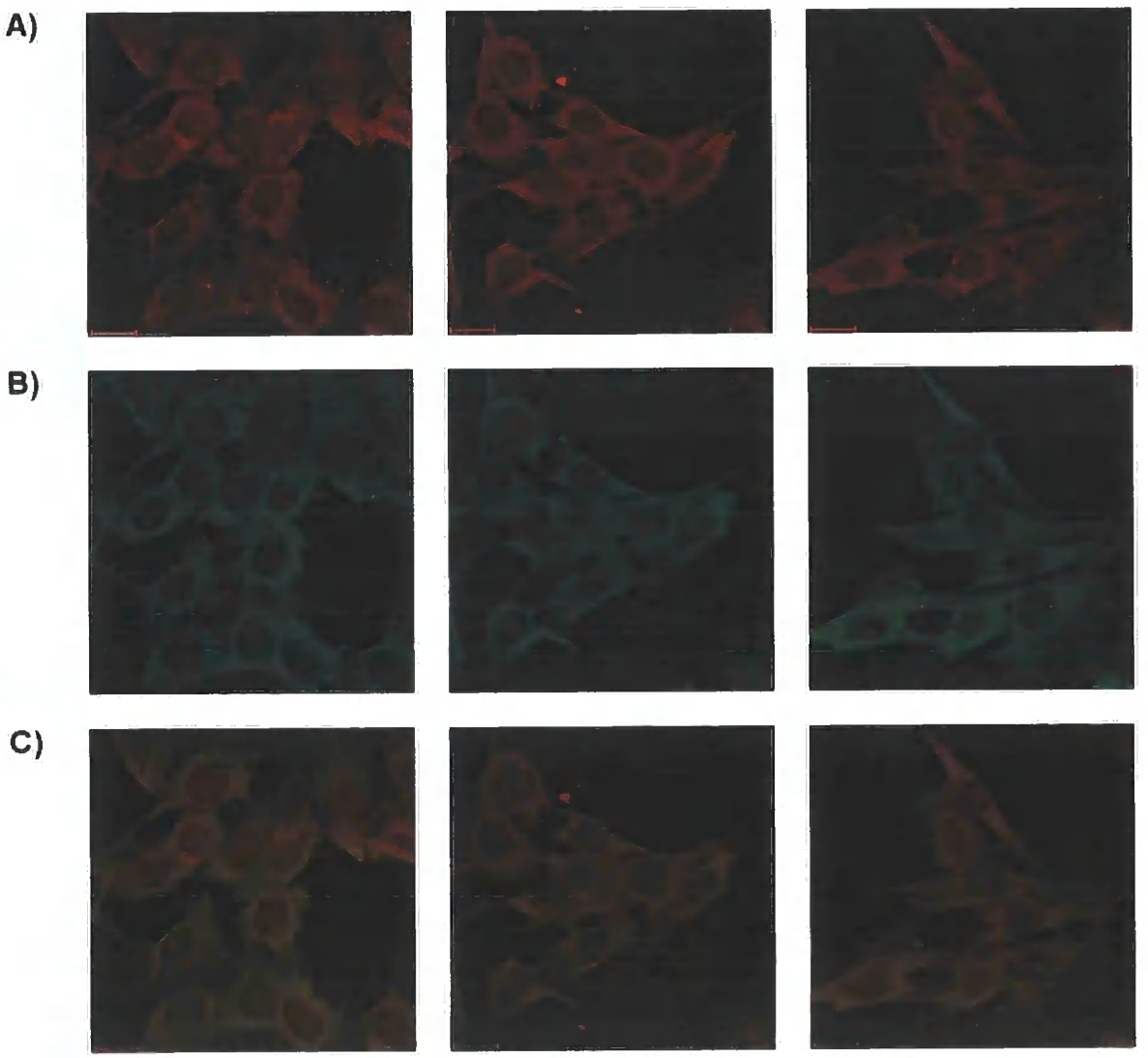

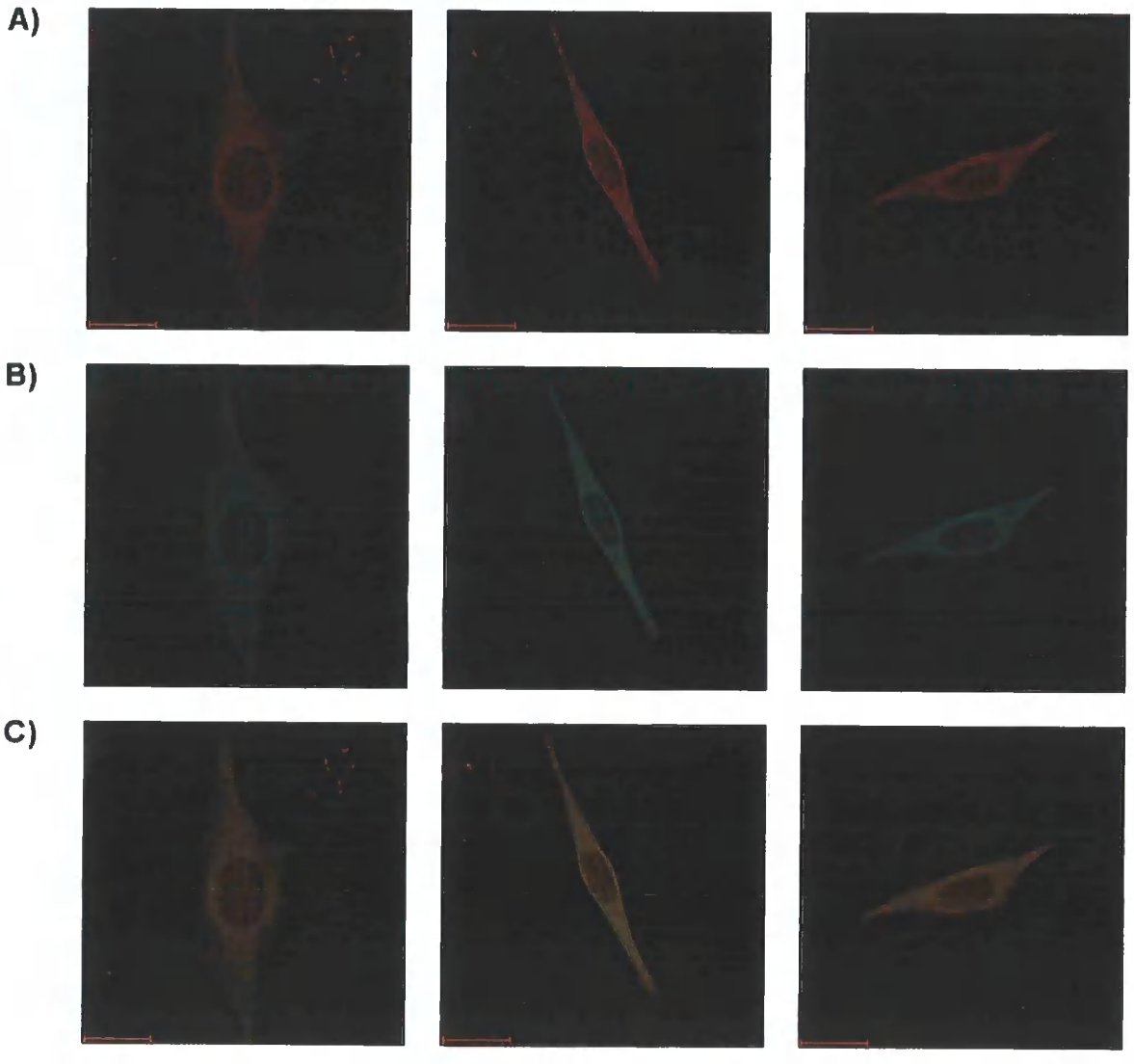
A)
B)
C)

3.2.2 Myoferlin Localisation

3.2.2.1 Myoferlin Localisation in Normal Cells

As explained earlier myoferlin staining has been previously described using Myof2 antibody. It was reported that myoferlin shows a nuclear and plasma membrane expression in addition to high vesicular expression in the peri-nuclear region (Davis et al., 2002).

C2C12 cells stained with FER1L3 were compared to C2C12 cells stained with Myof2 (Figure 3.5A). In both cases the staining pattern seems to be very similar. This experiment was repeated on HDF and NRK cells.

In HDF cells the peri-nuclear staining was less prominent (Figure 3.5B), while in NRK cells the overall expression was very similar to C2C12 (Figure 3.5C).

3.2.2.2 Myoferlin Localisation in Wounded Cells

C2C12 cells wounded in the presence of Texas red dextran, and immunolabelled with FER1L3 showed an enrichment of myoferlin in wounded cells identified by dextran uptake (Figure 3.6A & B). Enrichment of dysferlin in injured muscle fibres has been reported previously (Bansal et al., 2003). These results were consistent when repeated with Myof2 antibody (Figure 3.6 C & D). Using both antibodies, no cells that had taken up dextran failed to show myoferlin enrichment and the opposite is true.

F-actin (Filamentous actin) polymerisation at the wound site was used as a wound site indicator. F-actin rapidly goes through repeated cycles of polymerisation and de-polymerisation inside the cell but in general a cortical barrier consisting in part of F-actin is present in normal cells. Once the cell is injured, Ca^{2+} influx from the extracellular environment induces F-actin de-

polymerisation locally at the wound site. Depolymerised F-actin facilitates vesicle-vesicle and vesicle-plasma membrane fusion required for wound healing. Shortly after membrane resealing (T>1 min) a thick layer of polymerised F-actin is formed lining the injury site which is thought to be required for repair of the monolayer injury (Miyake et al., 2001). Therefore F-actin polymerisation is an indicator of the injury site. C2C12 cells wounded in the presence of Cascade blue dextran and double labelled for myoferlin and F-actin show enrichment of myoferlin at the wound site confirmed by F-actin polymerisation and dextran uptake (Figure 3.7).

As a control and to prove that increased levels of myoferlin at the wound site is specific and not artefacts as a result of injury or a fluorescence channel spill over, C2C12 cells were injured in the presence of Oregon green dextran and immunolabelled with caveolin 3 antibody. All injured cells that had taken up the dextran did not show any enrichment or increased levels of caveolin 3 at the wound site (Figure 3.8). In addition, the possibility of myoferlin enrichment seen in wounded cells being a fluorescence channel spill over from dextran was eliminated by analysing and imaging cells immunolabelled for myoferlin and wounded in the absence of dextran or wounding cells in the presence of dextran not immunolabelled for myoferlin. In both cases, no fluorescence spill over was detectable.

3.2.2.3 Myoferlin Localisation Post Membrane Resealing

As detailed in materials and methods chapter, the number of cells that had taken up the first and second dextran at 0 and 5 minutes were counted in 15 microscopic fields where at least 40% of the cells were wounded in each field

Figure 3.5 Myoferlin expression in different cells

Confocal images of A) C2C12, B) HDF, C) NRK cells stained with Myof2 and FER1L3 antibody by immunocytochemistry. In general cells stained with theses two antibodies show a very similar staining pattern with slightly intense staining around the nuclear membrane and some cytoplasmic staining.

Figure 3.5 (A)

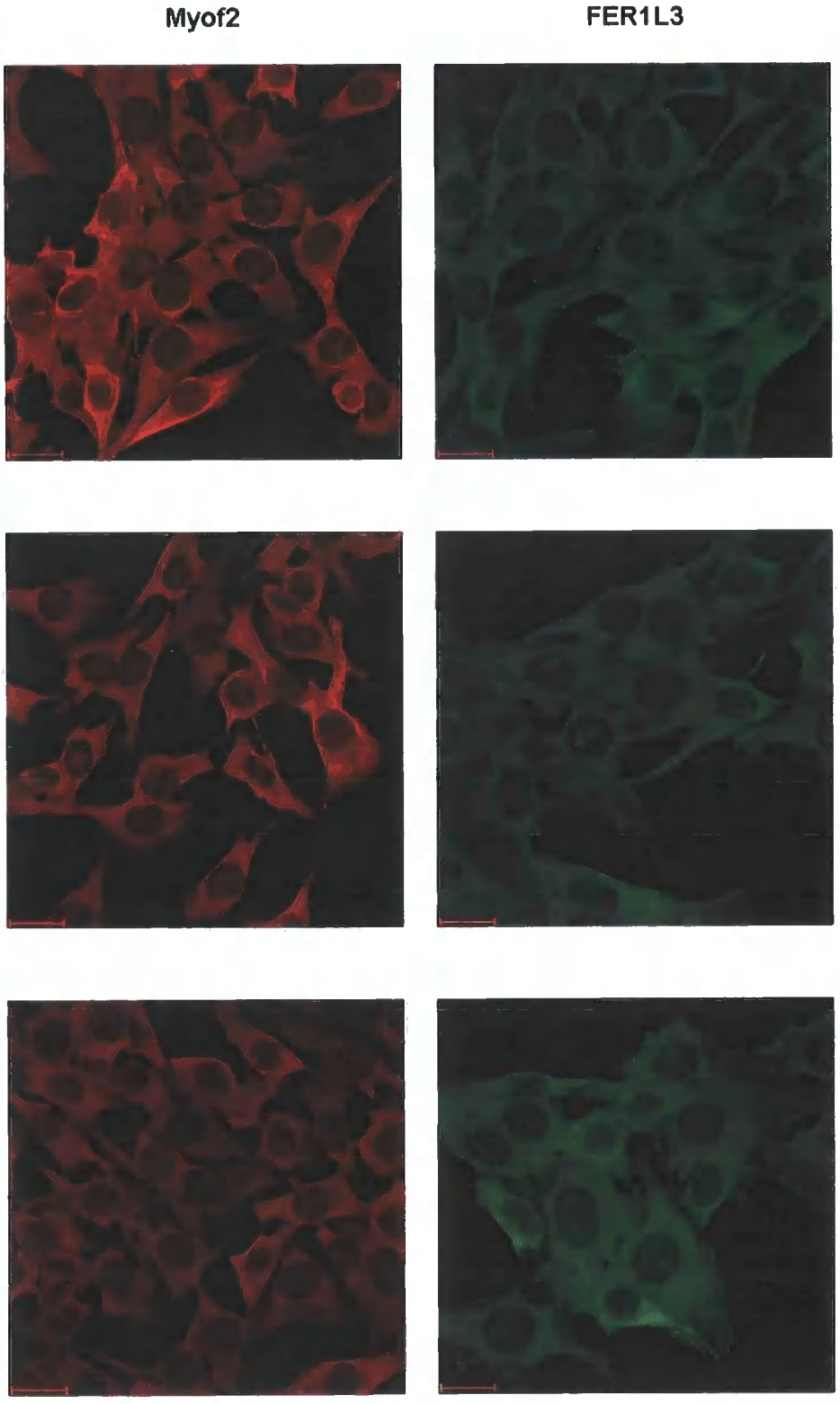

Figure 3.5 (B)

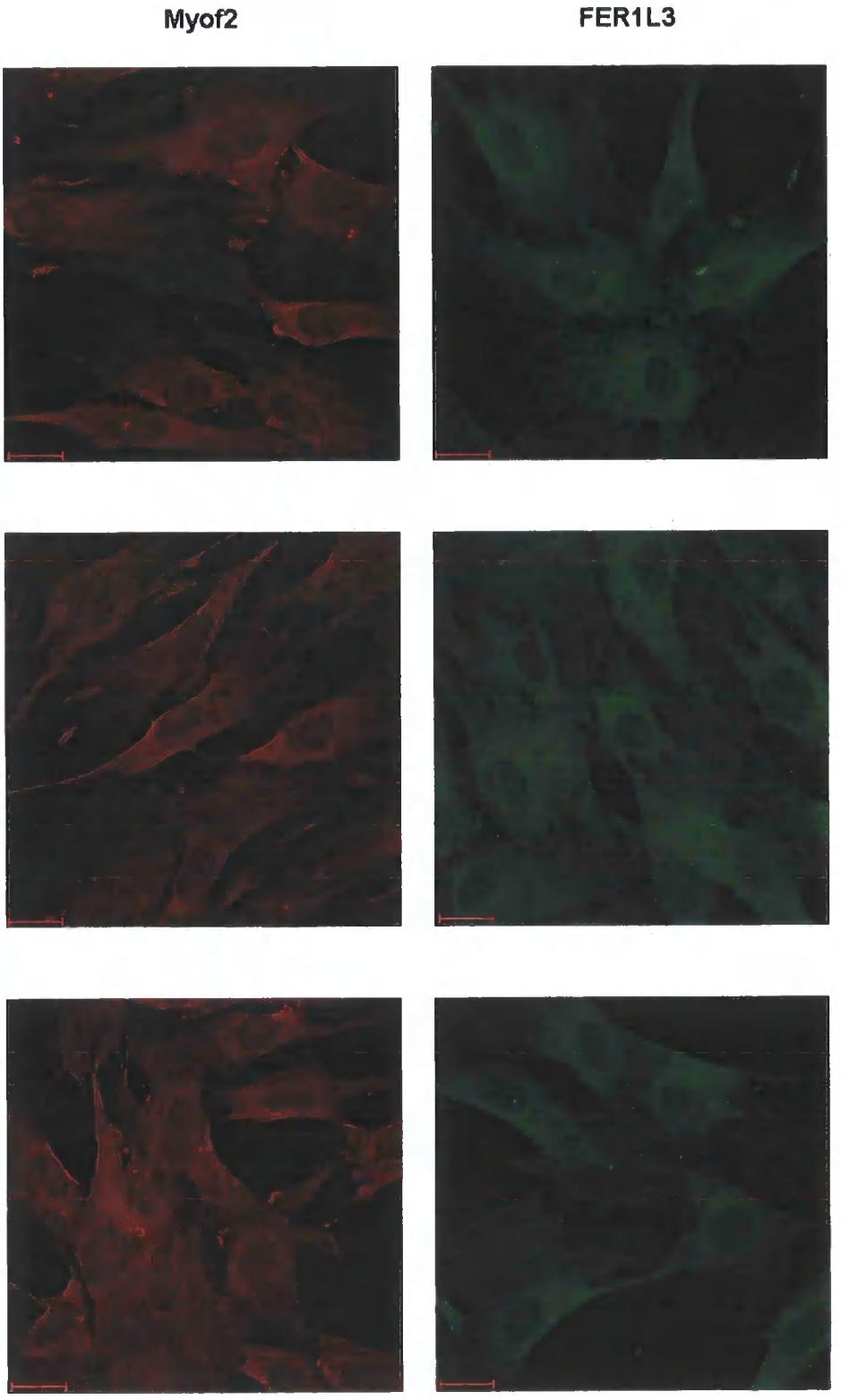

Figure 3.5 (C)

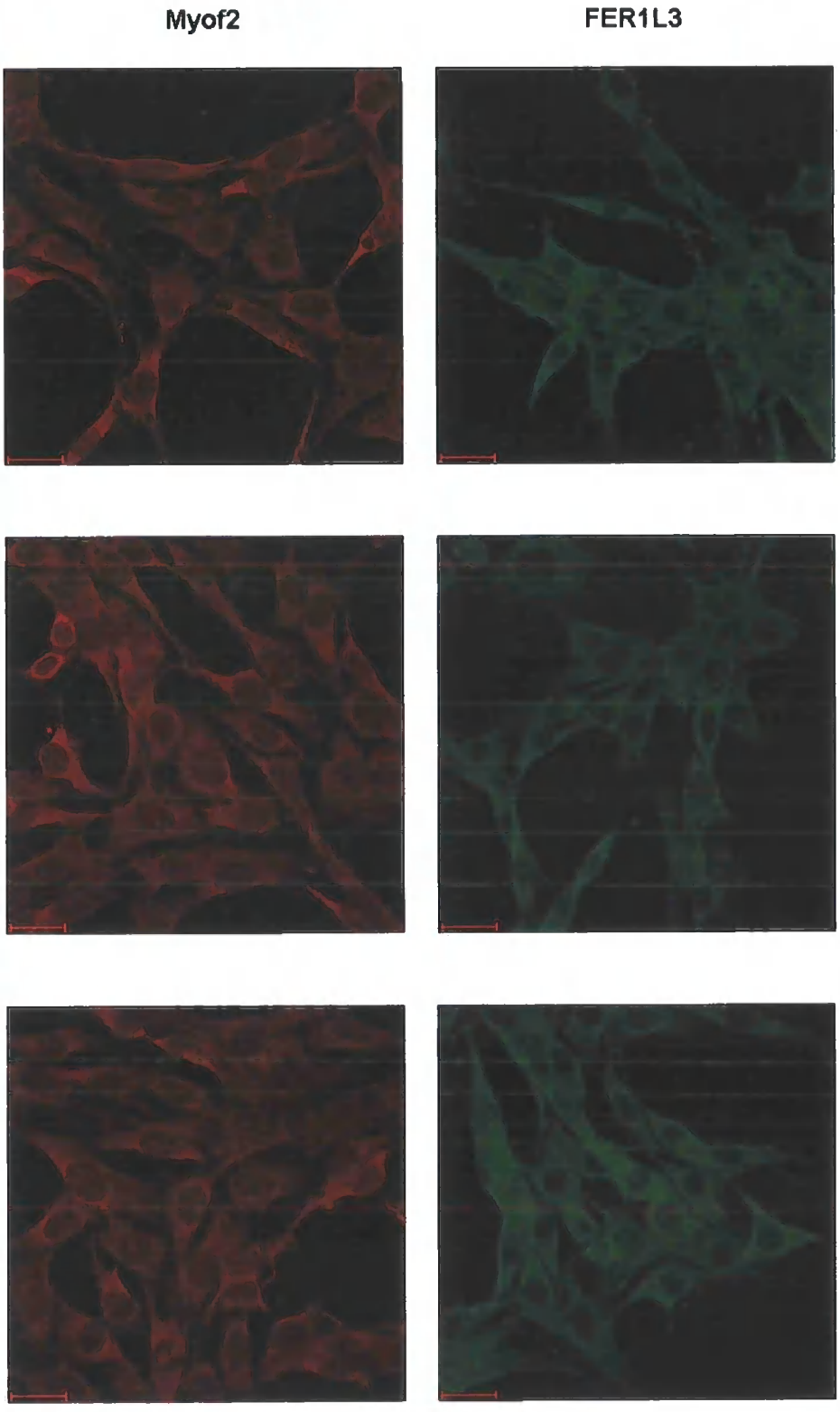

Figure 3.6 Myoferlin expression in wounded cells

C2C12 cells wounded in the presence of dextran and labelled by immunocytochemistry for myoferlin. A) Group of cells wounded in the presence of Texas red dextran and stained with FER1L3 antibody. B) A close-up image of wounded FER1L3 stained cells. C) Group of cells wounded in the presence of Oregon green dextran and stained with Myof2 antibody. D) A close-up image of wounded Myof2 stained cells. Wounded cells are characterised by myoferlin enrichment at the wound site confirmed by dextran uptake compared to control (uninjured) cells in the background.

Figure 3.6 (A)

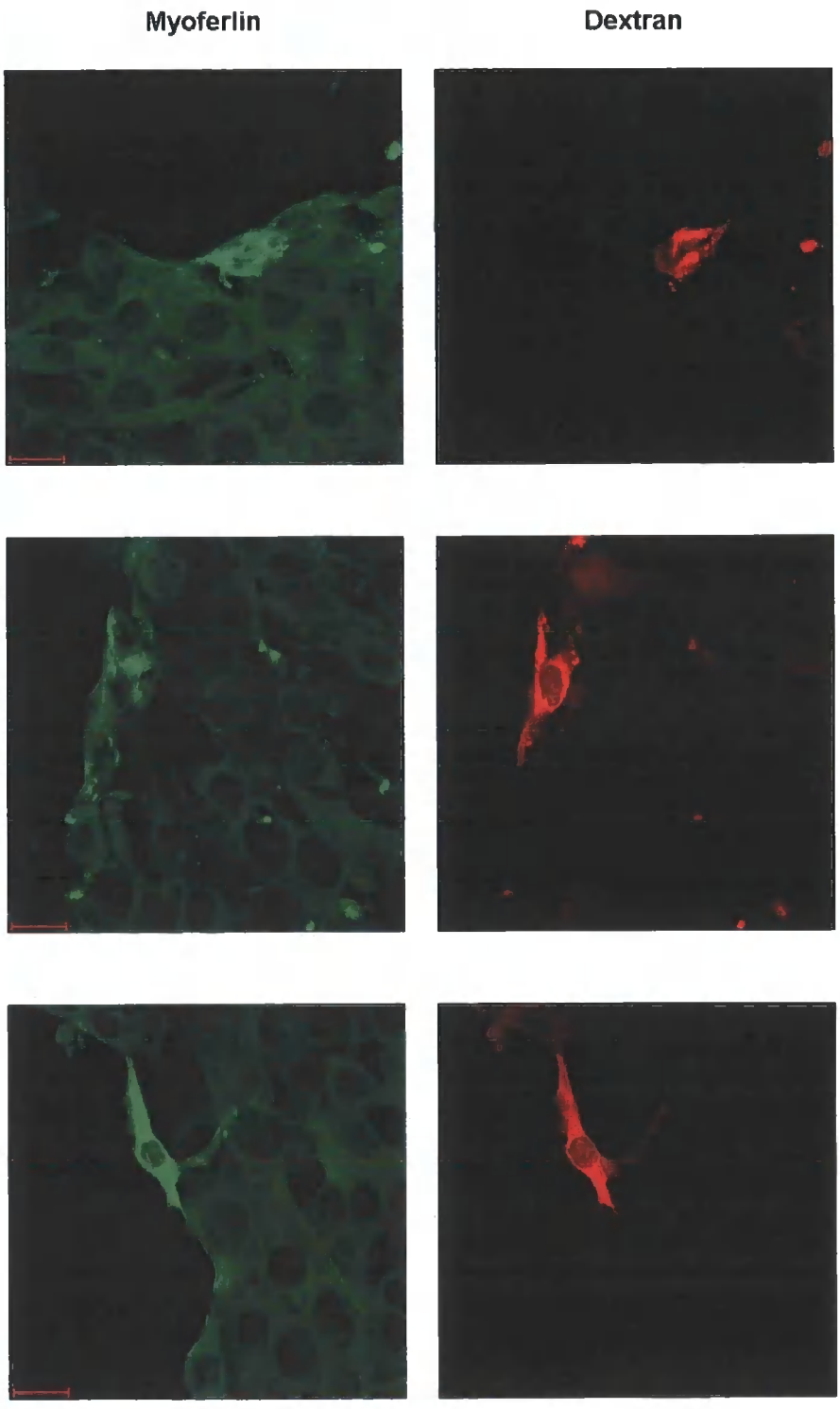

Figure 3.6 (B)

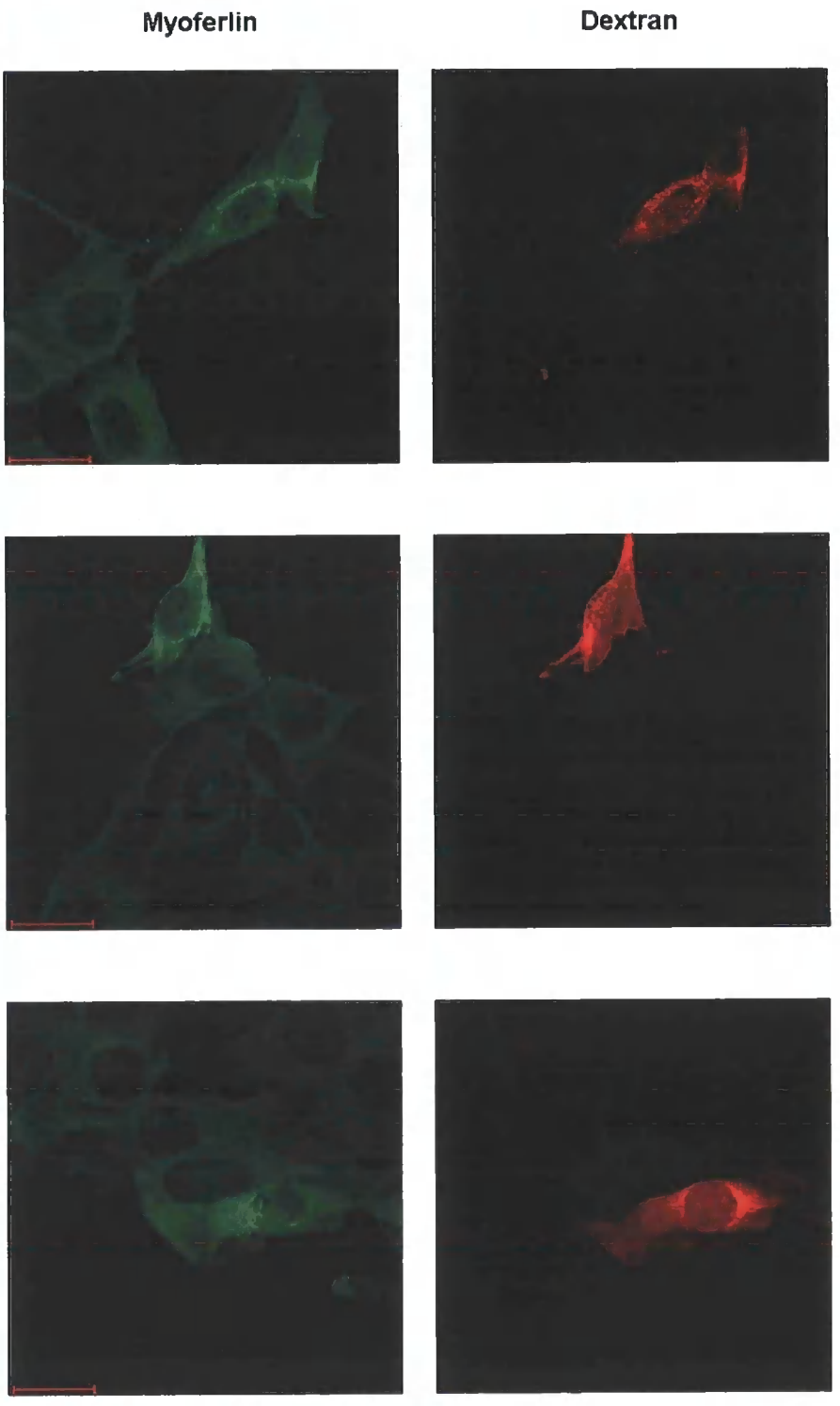

Figure 3.6 (C)

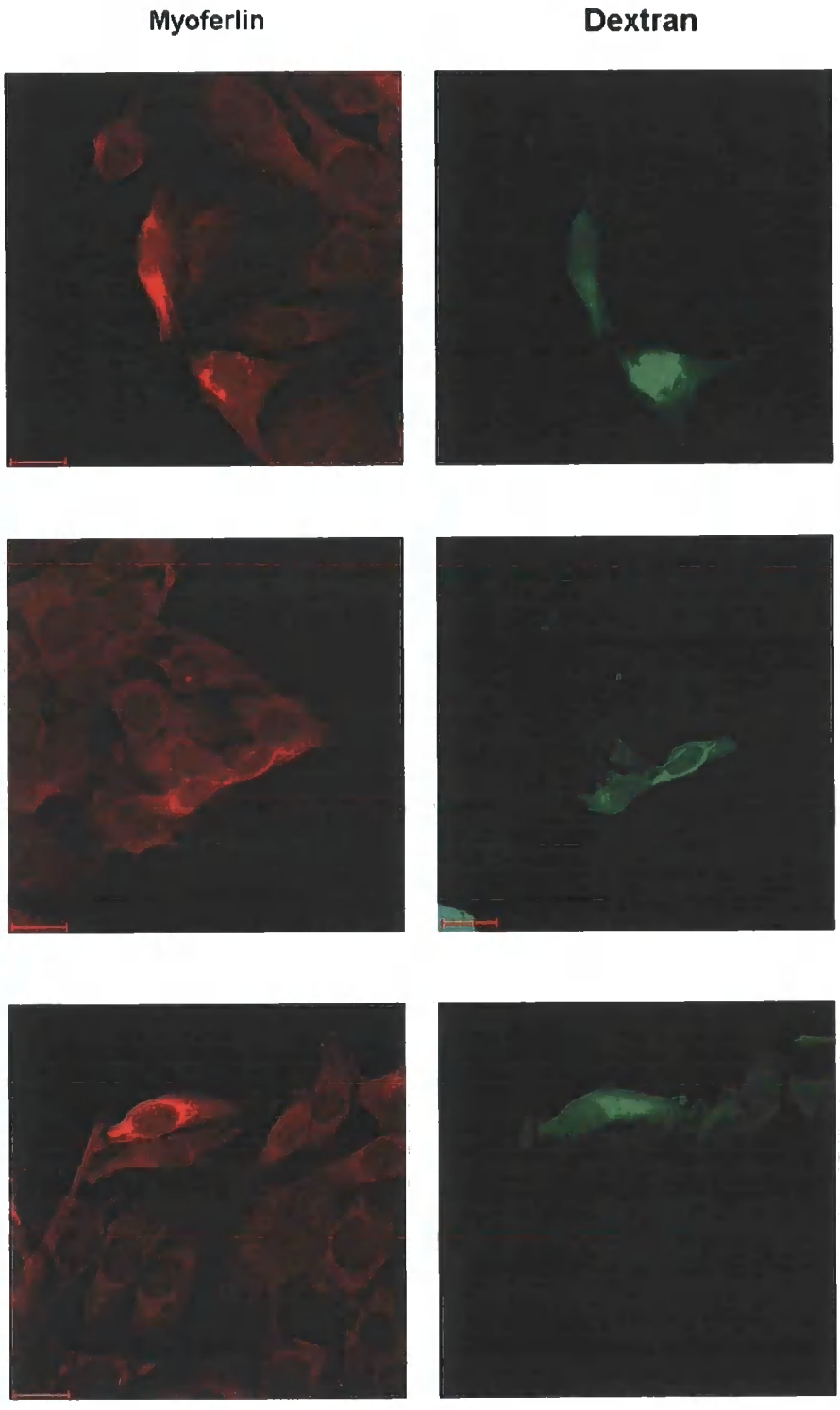

Figure 3.6 (D)

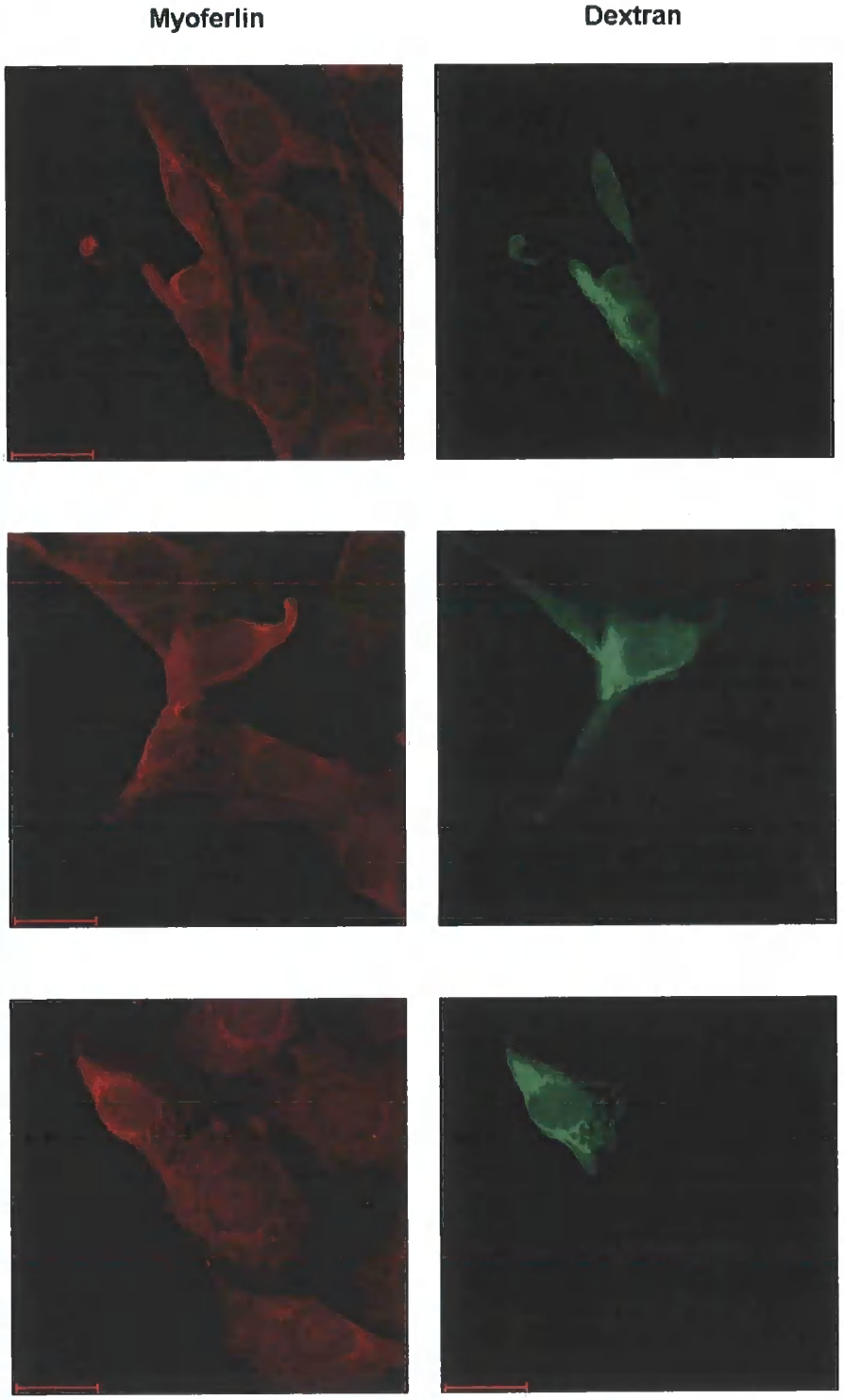

Figure 3.7 Wound site indication by F-actin polymerisation

C2C12 cells wounded in the presence of cascade blue dextran were double labelled for myoferlin and F-actin using Myof2 and anti-actin antibodies respectively. Myoferlin enrichment is noted in wounded cells confirmed by dextran uptake. While actin polymerisation in wounded cells also acts as an indication of cell injury.

Figure 3.7

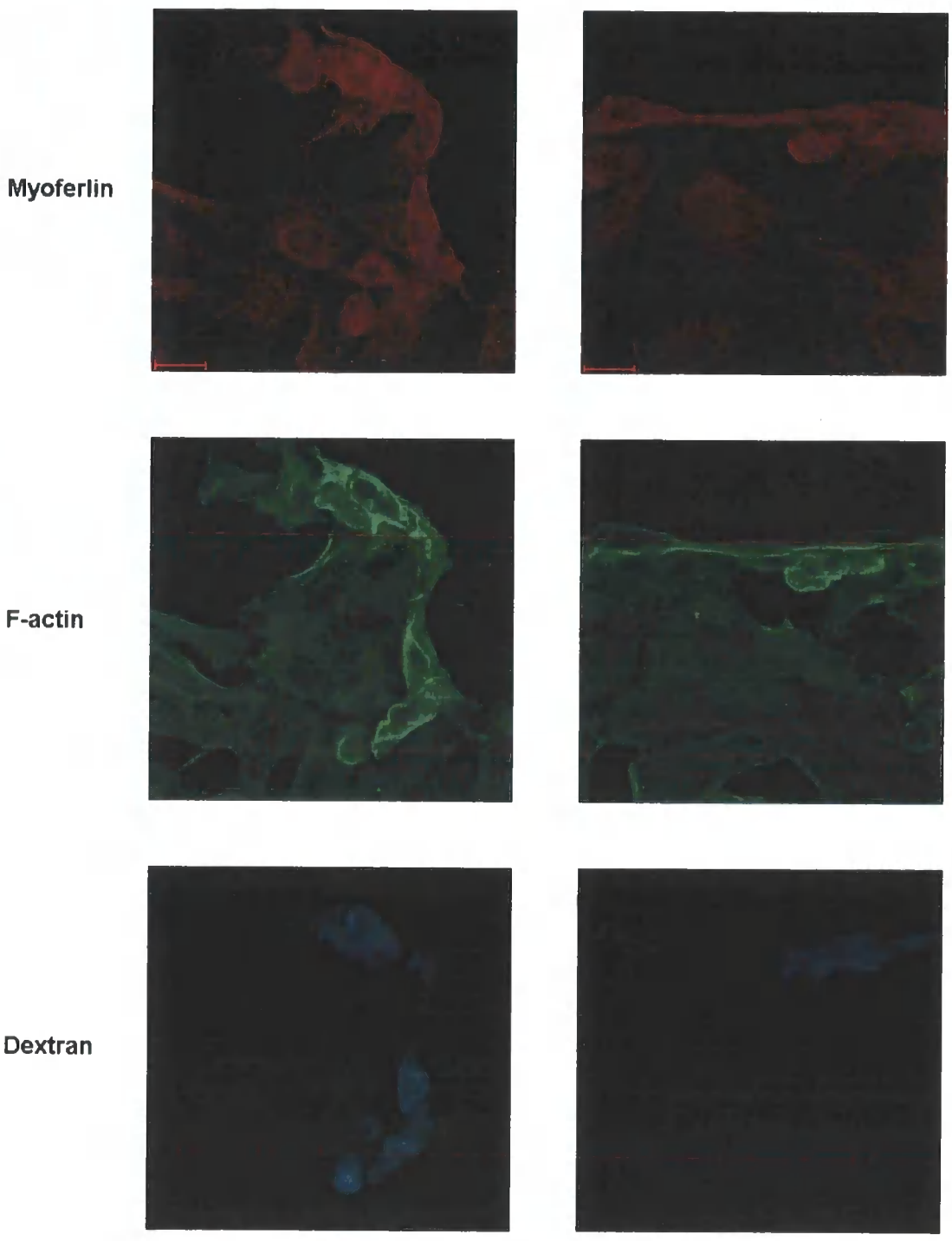

Figure 3.8 Control experiments to myoferlin enrichment at plasma membrane disruption sites

Caveolin 3 expression was investigated by immunolabelling of C2C12 cells with caveolin 3 antibody. A) Un-injured C2C12 caveolin stained cells imaged by confocal microscopy in a group of cells and a close-up. B) Cells wounded in the presence of Oregon green dextran and immunolabelled with caveolin 3 (group and close-up) show no enrichment of caveolin neither at the wound site nor in wounded cells in contrast to myoferlin. C) The possibility of myoferlin enrichment seen in wounded cells being a fluorescence channel spill over from dextran was eliminated by analysing and imaging cells immunolabelled for myoferlin and wounded in the absence of dextran or wounding cells in the presence of dextran not immunolabelled for myoferlin. In both cases, no fluorescence spill over was detectable.

Figure 3.8 (A)

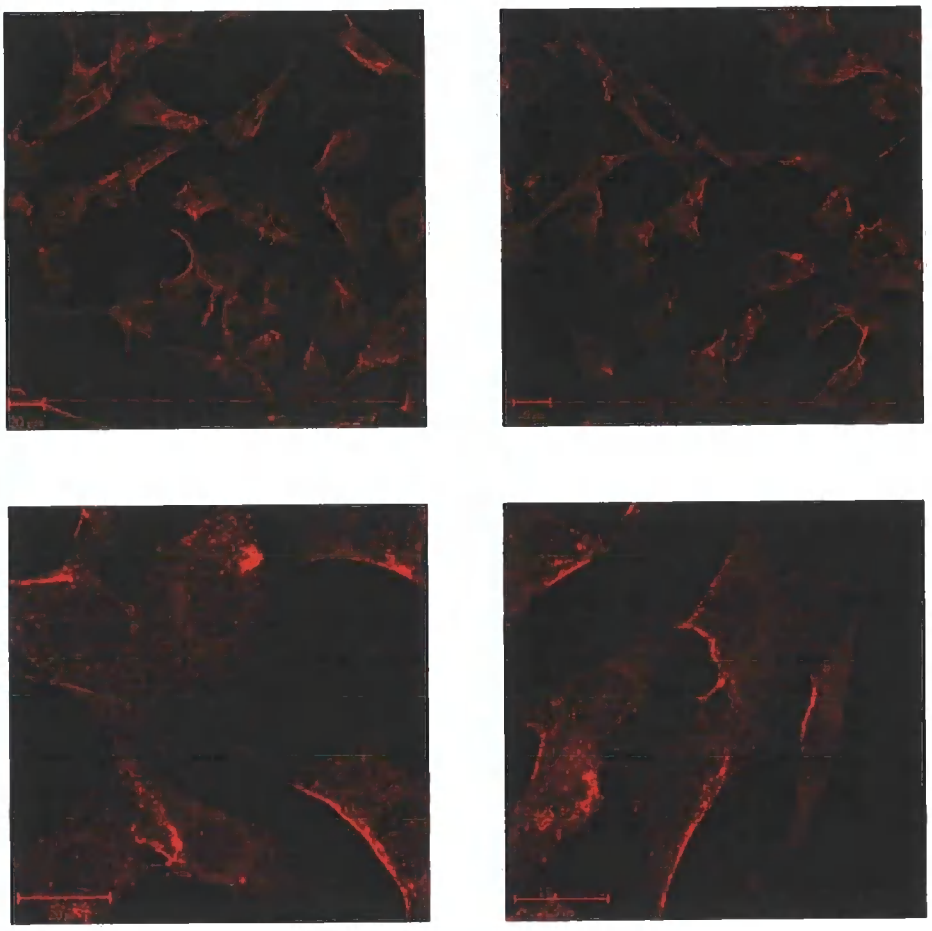

Figure 3.8 (B)

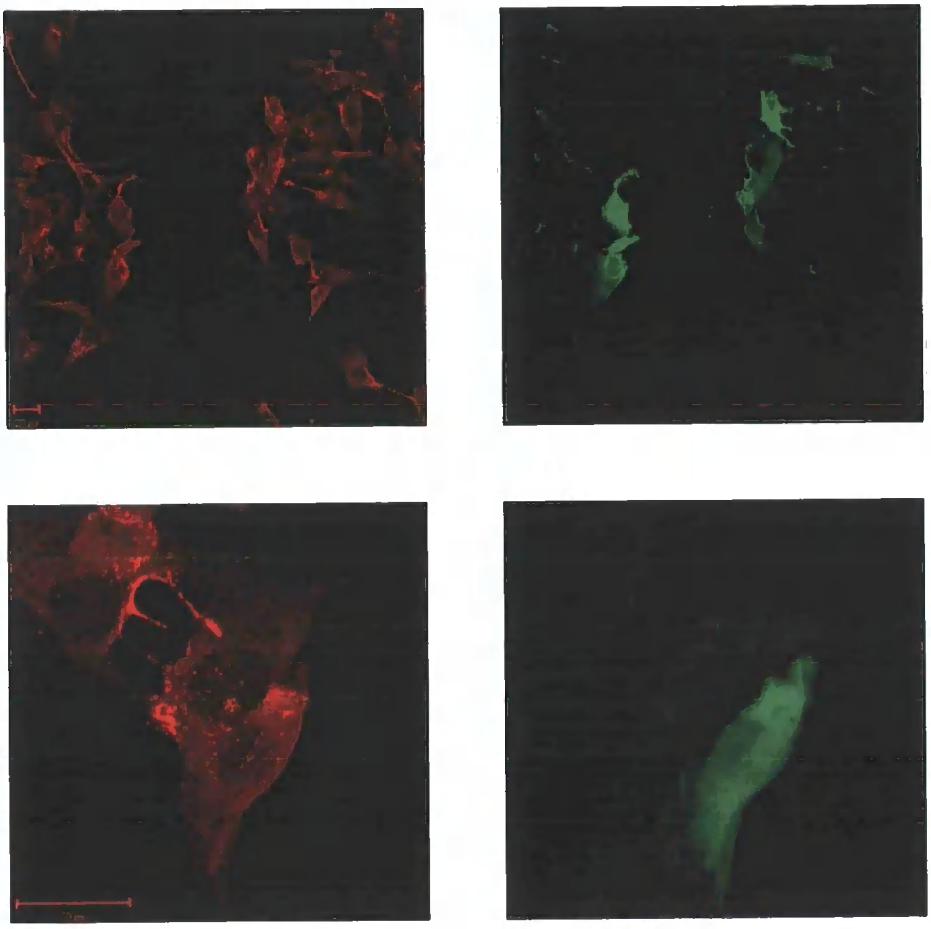

Figure 3.8 (C)

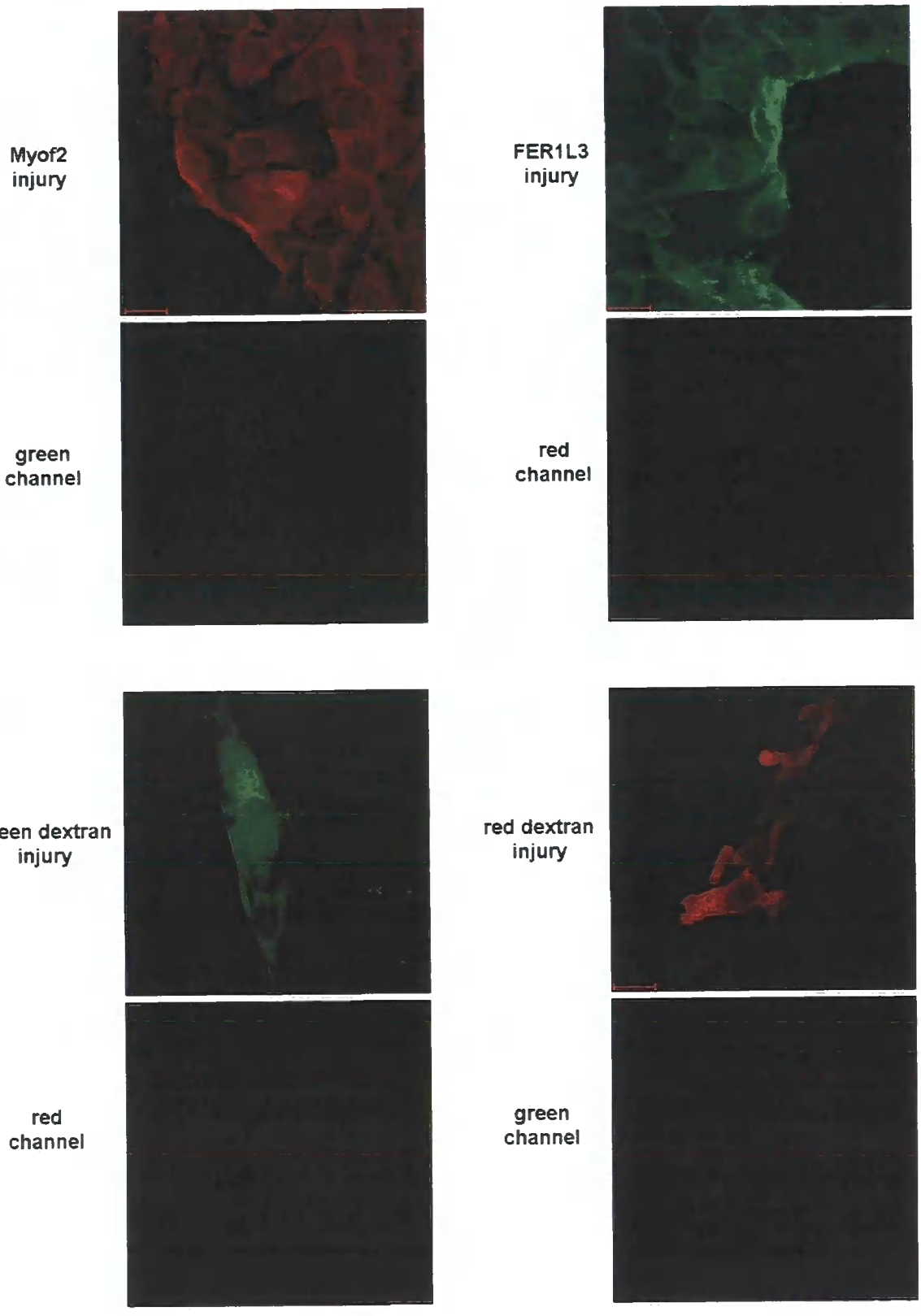
Myof2 injury
FER1L3 injury
green channel
red channel
green dextran injury
red dextran injury
red channel
green channel

Figure 3.9 Myoferlin expression post membrane resealing

C2C12 cells injured in the presence of Oregon green dextran were allowed to recover for 5 minutes then incubated in Cascade blue dextran for a further 2 minutes (A). Alternatively another group was not allowed to recover and transferred to blue dextran immediately and incubated for 2 minutes (B). All cells were then immunolabelled with Myof2 antibody and analysed by confocal microscopy.

In 15 (x40 oil lens) microscopic fields where at least 40% of cells were along the injury line, the number of cells that had increased myoferlin staining was counted. In the same field the number of these cells that had taken up the first and second dextran was counted at 0 and 5 minutes post recovery. This experiment was repeated twice and the average of the readings was converted to a percentage. As seen from section C of this figure, when cells were not allowed to recover (i.e. T=0) the percentage of cells along the injury line with enriched myoferlin is relatively close to the percentage of cells that had taken up the first and second dextran. While, when cells were allowed to recover for 5 minutes, cells that had taken up the first dextran during the wounding process healed and failed to uptake the second dextran which reflected successful wound healing, however myoferlin enrichment was still visible.

Figure 3.9 (A)

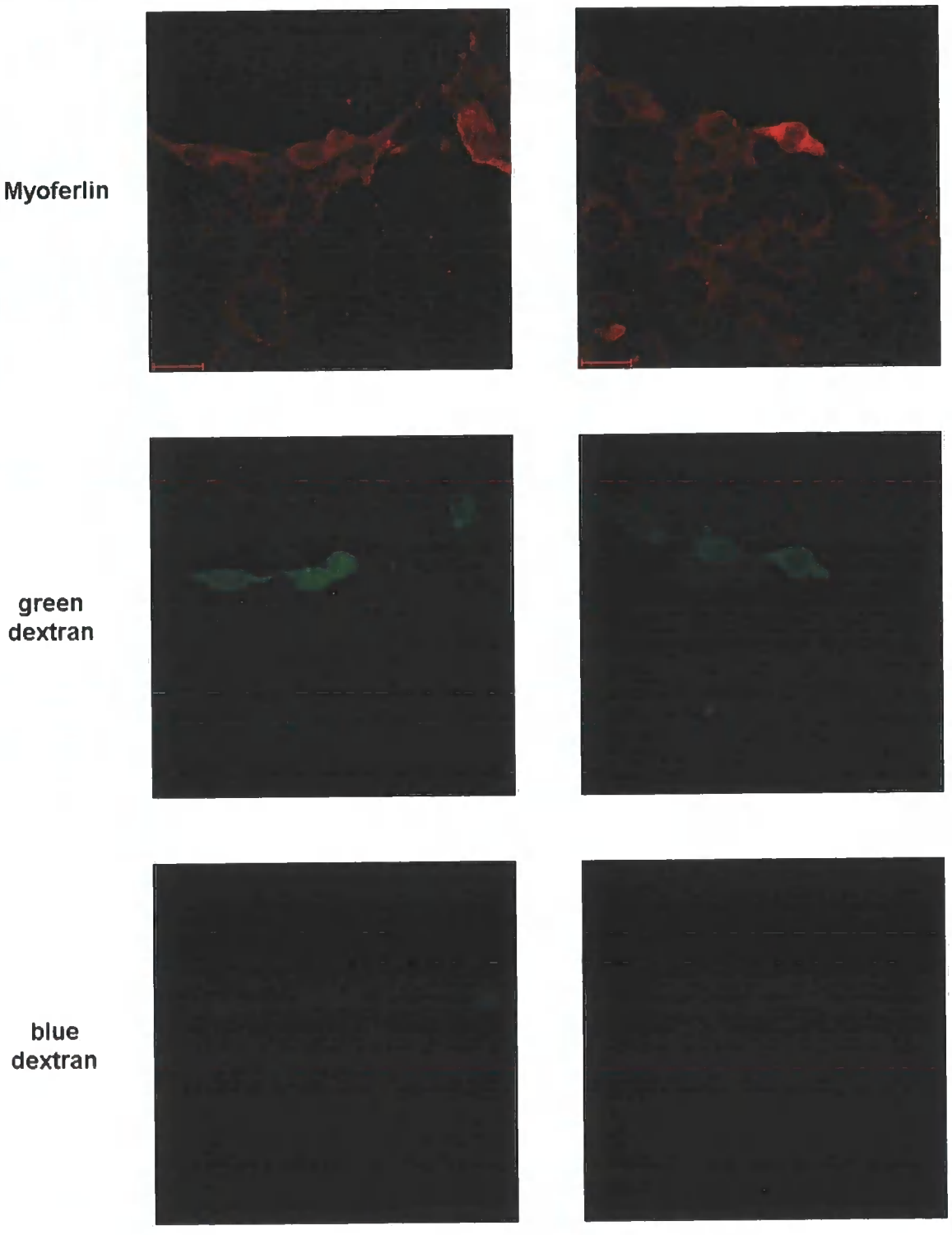

Figure 3.9 (B)

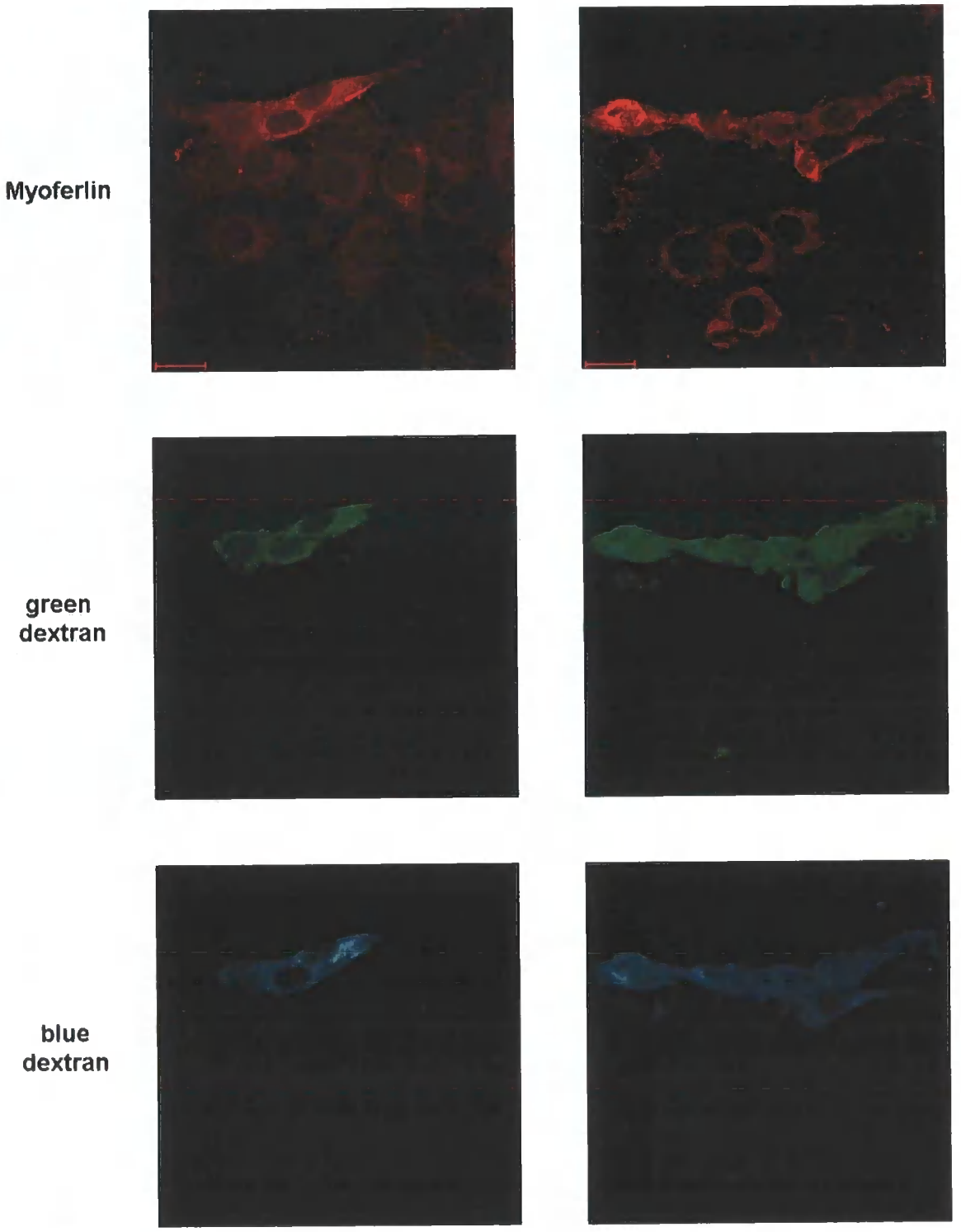

Figure 3.9 (C)

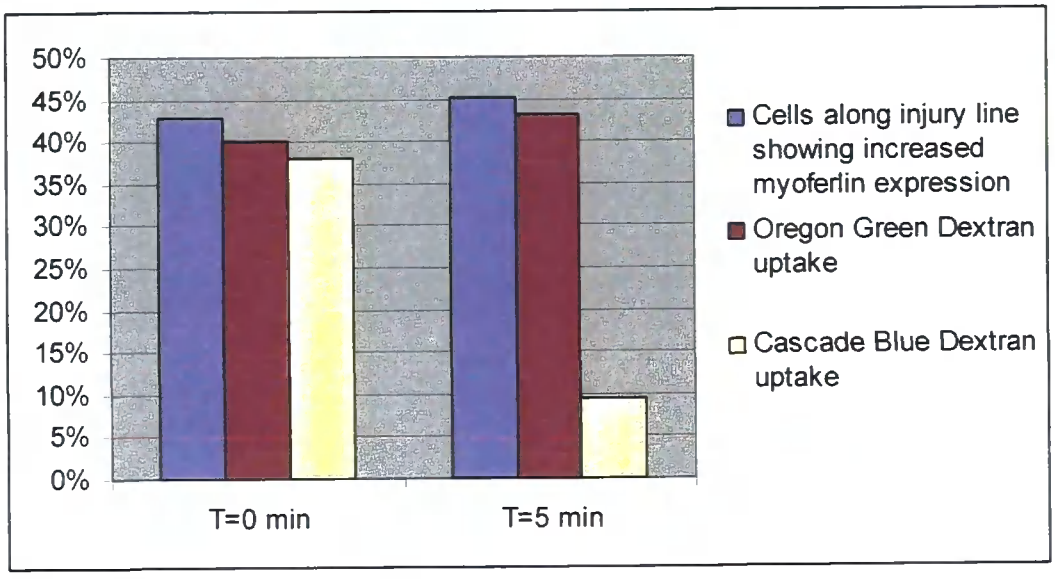
50%
45%
40%
35%
30%
25%
20%
15%
10%
5%
0%
T=0 min
T=5 min
Cells along injury line showing increased myoferlin expression
Oregon Green Dextran uptake
Cascade Blue Dextran uptake

(Figure 3.9). When analysed and imaged by confocal microscopy, myoferlin enrichment in the injured cells was visible. After 5 minutes recovery most of the cells that had taken up the first dextran were excluded for the second dextran uptake, a result consistent with membrane resealing. However, although the plasma membrane may have successfully resealed, elevated levels of myoferlin at the wound site was still clearly detected. These results suggest that myoferlin's high levels induced by a plasma membrane disruption do not return to normal levels immediately or until few minutes after membrane resealing (Figure 3.9).

3.2.2.4 Myoferlin Localisation Post Ionomycin Induced Exocytosis

As explained earlier, in order to confirm myoferlin mobilisation to the surface in response to the Ca^{2+} increase inside the cell, ionomycin, a calcium ionophore that has been shown to trigger intracellular calcium increase has been used. The mobilisation of enlargosomes detected by AHNAK antibody to the cell surface in response to this concentration of ionomycin has been reported previously (Cerny et al., 2004).

C2C12 cells treated with ionomycin were checked for viability by trypan blue uptake and no toxic effect as a result of ionomycin treatment was detected on these cells.

Next, C2C12 cells were treated with ionomycin and immunolabelled for total and surface expression of myoferlin and enlargosomes inside the cells. In resting cells, no expression of enlargosomes was detected at the cell periphery, while some intracellular expression was detected. After treatment with ionomycin (5 µM, 5 min), the enlargosomes' marker AHNAK shifts towards the

cell periphery and appears at the surface, reflecting the Ca^{2+}-regulated exocytosis. This pattern of expression has been reported previously (Cerny et al., 2004). Alternatively when resting C2C12 cells were surface stained with Myof2 no myoferlin was detected at cell surface when compared to total myoferlin staining. After ionomycin treatment the surface staining of myoferlin was strongly detectable at the peri-nuclear region, in both total and surface staining. When compared to AHNAK, this shows calcium induced exocytosis of myoferlin in response to elevated calcium a similar pattern to that observed in wounded cells in response to plasma membrane disruptions (Figure 3.10).

3.2.2.5 Myoferlin Co-localisation with Lysosomes & Enlargosomes

Lysosomes are known to be important membrane providing vesicle populations during the process of wound healing. When WT and injured C2C12 cells were double labelled for myoferlin and an antigen associated with lysosomes, Lamp-I, myoferlin did not appear to be substantially associated with lysosomes. However, in injured cells both myoferlin and lysosomes could be seen at the injury site but in an independent manner, not co-localising (Figure 3.11). This was not true for Enlargosomes, another vesicle population known to mobilise to the cell surface in response to elevated calcium levels (Borgonovo et al., 2002) (e.g. plasma membrane disruption). The function of enlargosomes is still not properly understood but they are thought to have a role in cyto-architecture. In normal cells myoferlin and AHNAK have a distinct and different expression pattern. However, in injured cells both myoferlin and AHNAK seem to mobilise to the injury site and do show some partial co-localisation (Figure 3.12).

Figure 3.10 Enlargosomes and myoferlin response to induced exocytosis

In impermeablised resting cells, AHNAK was not detected at the cell surface. In permeablised resting cells both AHNAK was expressed in its normal expression pattern. When treated with ionomycin, the enlargosomes' marker AHNAK shifts towards the cell periphery and appear at the surface, reflecting the Ca^{2+}-regulated exocytosis (A).

Myoferlin surface staining of resting cells was nil while myoferlin total staining of resting cells reflected the normal expression pattern shown previously. After ionomycin treatment myoferlin was strongly detectable at the peri-nuclear region, in both total and surface staining (B) compared to resting cells.

Figure 3.10 (A)

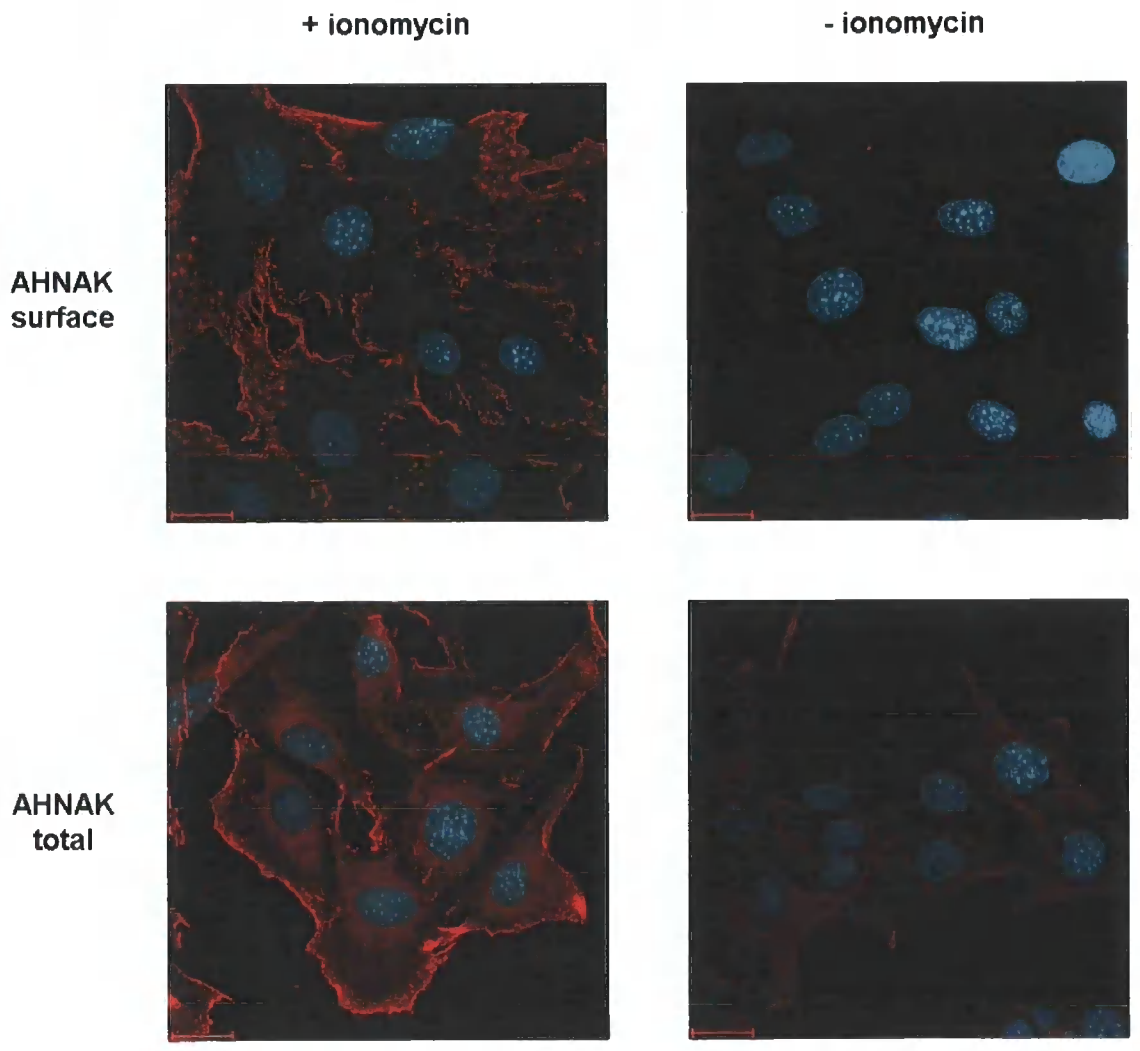

Figure 3.10 (B)

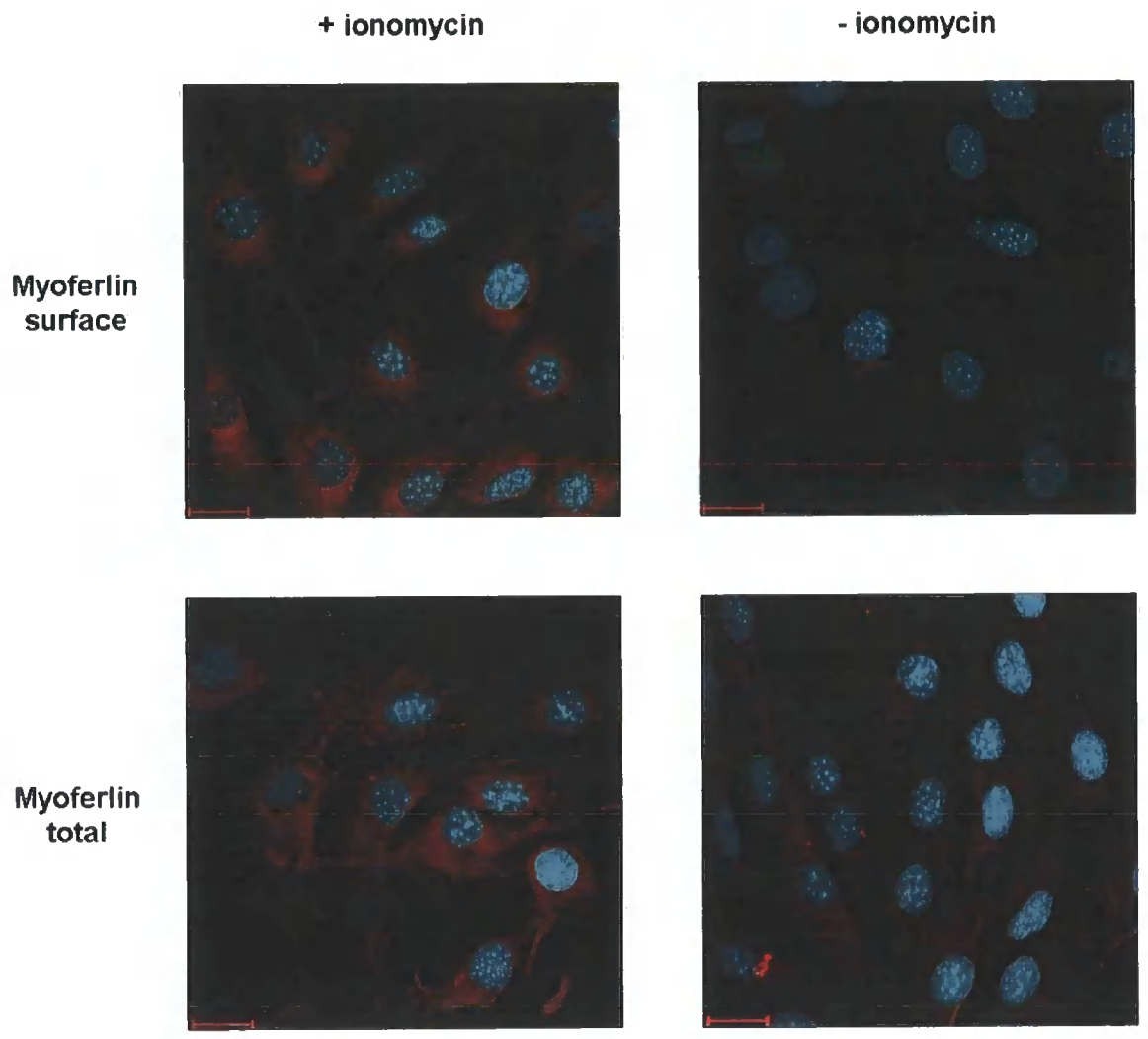

Figure 3.11 Myoferlin colocalisation with lysosomes

C2C12 cells were double labelled for myoferlin (Myof2) and lysosomes (Lamp-1) and imaged. In uninjured cells myoferlin and lysosomes clearly sustain a distinguished and different cellular localisation (A). Wounded cells show the enrichment of myoferlin and the mobilisation of lysosomes to the wound site (B). However, they do not colocalise at any stage.

Figure 3.11 (A)

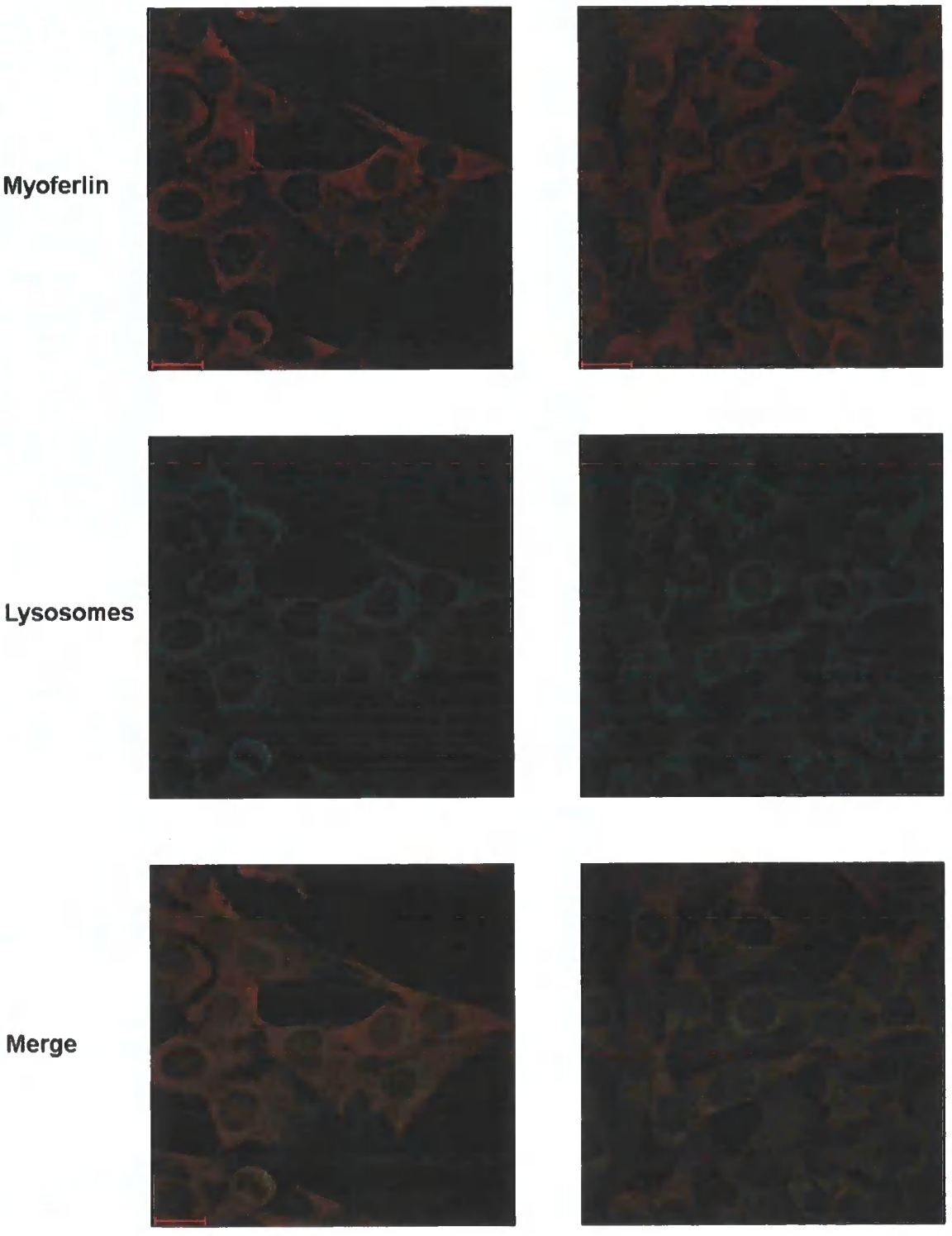

Figure 3.11 (B)

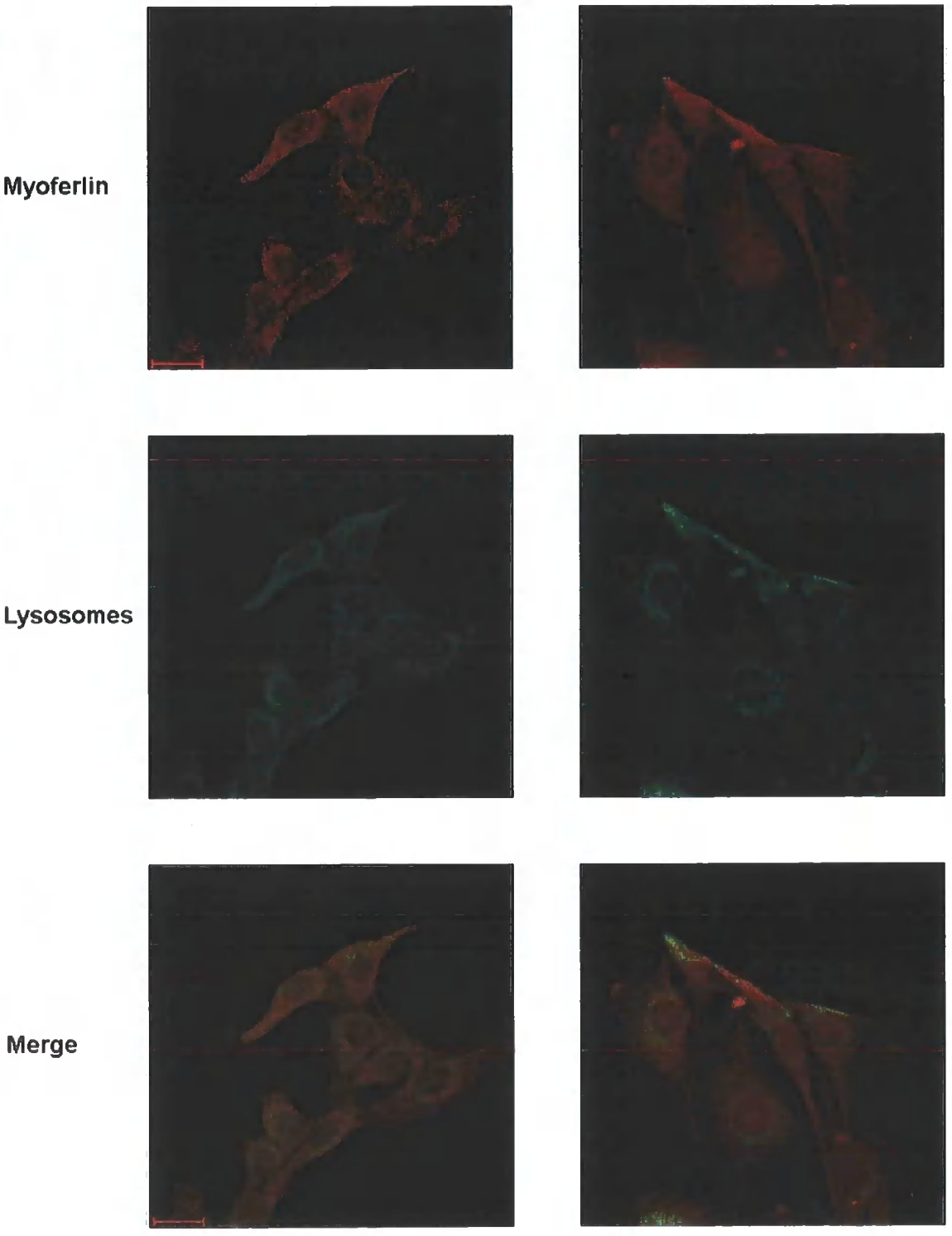

Figure 3.12 Myoferlin colocalisation with enlargosomes

C2C12 cells double labelled with myoferlin (FER1L3) and enlargosomes (AHNAK) imaged show distinct and different expression in control cells (A). However, contrary to lysosomes, myoferlin and AHNAK show some colocalisation (B), indicated by yellow staining at plasma membrane disruption sites.

Figure 3.12 (A)

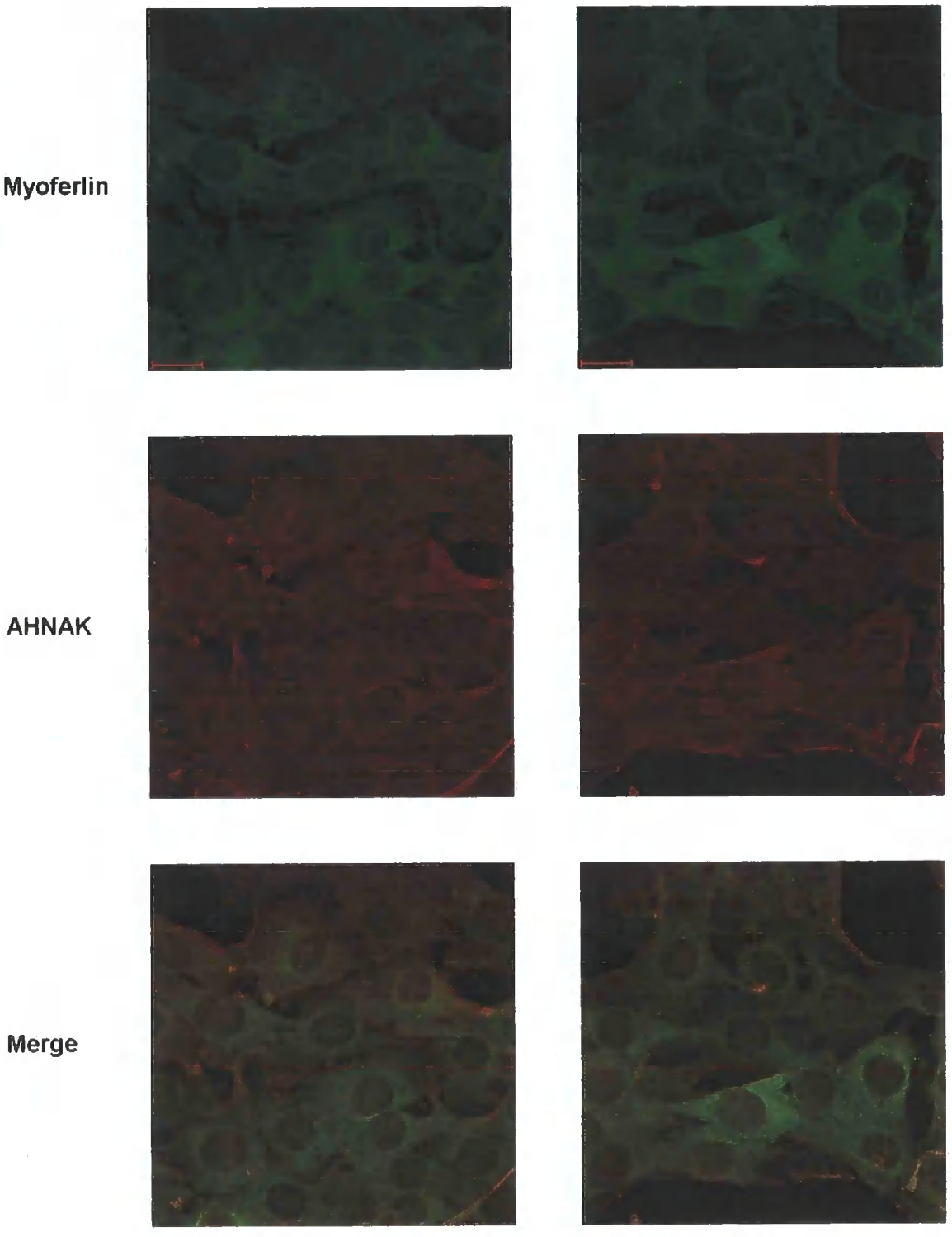

Figure 3.12 (B)

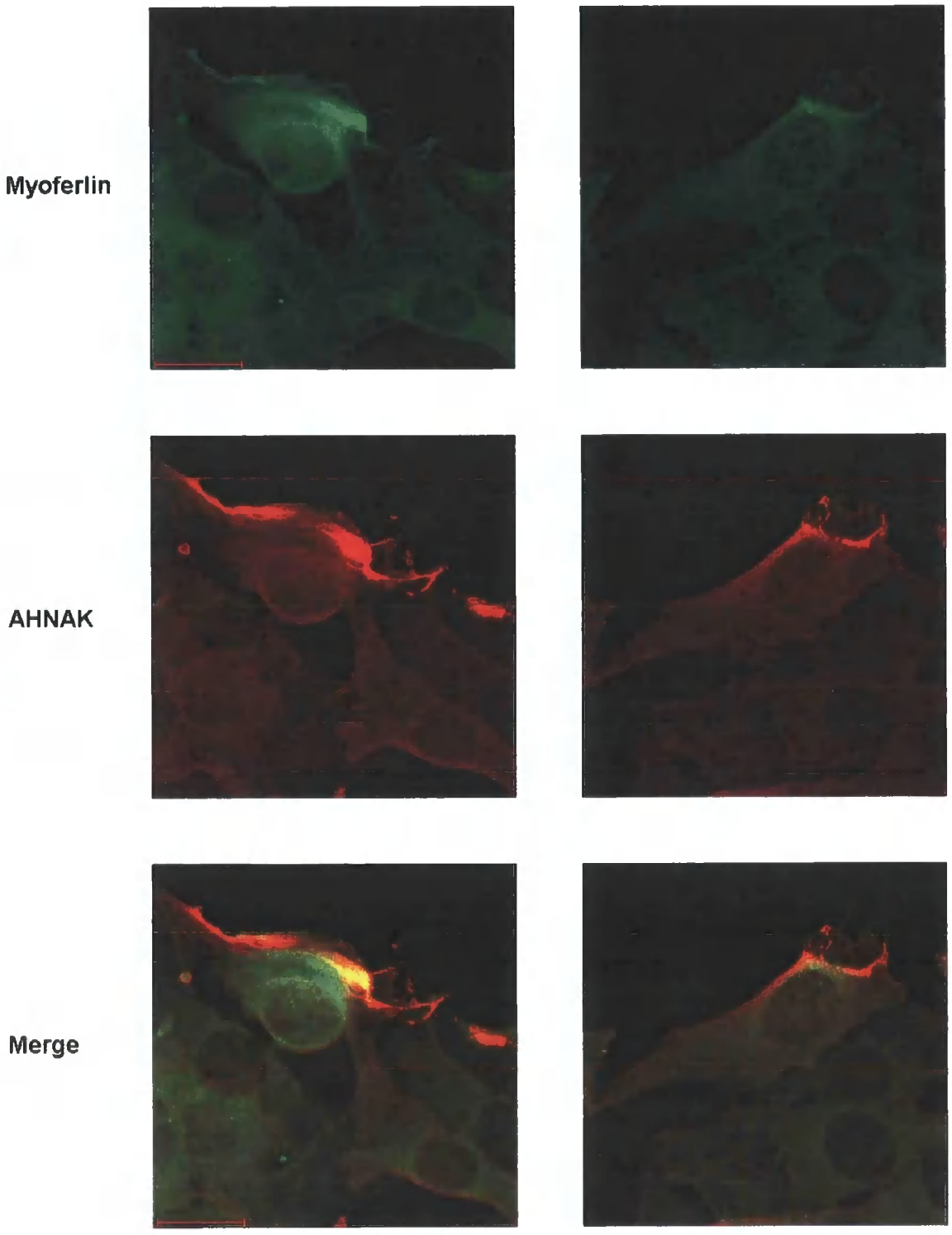

3.3 Summary

In this chapter the specificity of a new monoclonal antibody, FER1L3 to myoferlin was investigated. This was achieved by 1) a peptide block experiment performed by a colleague, 2) studying the subcellular localisation of myoferlin using the FER1L3 antibody on fractionated cell membranes by western blots and comparing it to the subcellular localisation of dysferlin 3) studying FER1L3 reactivity in dysferlin deficient cells and comparing it to control cells 4) studying the colocalisation of FER1L3 antibody with another known myoferlin antibody, Myof1.

The signal from the FER1L3 antibody was completely abolished by the peptide, confirming that the signal is specific to the peptide while Western blots performed on subcellular membrane fractions of C2C12 cells, labelled with FER1L3 did specifically label the band at 230 KDa in most fractions and not the other bands seen on the protein blot (data not shown).

More bands were labelled in the ER and nuclear fraction when probed with FER1L3 antibody but this pattern has been reported previously in dysferlin which were thought to be metabolic fragments of the dysferlin protein as a result of the long time taken to synthesis such a large protein (Anderson et al., 1999). In addition, the subcellular localisation of myoferlin labelled by FER1L3 was very similar to that of dysferlin. The labelling of fractions by lamin A antibody confirms the identity of the nuclear fraction. Given the structural similarity between dysferlin and myoferlin, there is a formal possibility that antibodies to myoferlin could cross-react with dysferlin. Western blots are unable to discriminate between the two as the molecular weights of these two proteins are very similar, i.e. 230 KDa (2080 amino acids for dysferlin and 2061 amino acids

for myoferlin). In order to address this, the staining pattern of FER1L3 antibody in normal and dysferlin deficient cells was examined.

Immunolabelling of dysferlin deficient cells with FER1L3 strongly suggests the specificity of this antibody to myoferlin since the staining pattern observed in dysferlin deficient cells is highly similar to that of the control cells expressing dysferlin.

In addition, results obtained from Myof1 and FER1L3 immunocytochemistry yielded a very similar staining pattern. In conclusion, these experiments strongly suggest that FER1L3 is a myoferlin specific antibody and was therefore used in subsequent experiments.

In the next section of this chapter the subcellular distribution of myoferlin was investigated. Myoferlin staining pattern by immunolabelling has been published in C2C12 cells using Myof2 antibody (Davis et al., 2002) therefore its subcellular localisation was investigated in two other cell lines (NRK, HDF) using Myof2 and FER1L3 antibodies. Since myoferlin is 68% similar and 58% identical to dysferlin (Davis et al., 2000), and dysferlin is known to be enriched at plasma membrane disruption sites, myoferlin's response to plasma membrane disruption was investigated.

Results obtained from this set of data strongly suggested that myoferlin like dysferlin is enriched at plasma membrane disruption sites. Control experiments such as caveolin 3 expression in response to plasma membrane disruption and fluorescence channel spill were performed and results were consistent with myoferlin's specific response to plasma membrane disruptions.

In order to study the relationship between myoferlin enrichment at plasma membrane disruption sites and calcium influx from the extracellular environment as a result of plasma membrane disruption, an intracellular calcium increase was induced using ionomycin and compared to other vesicles known to exocytose in response to an increase in intracellular calcium levels.

Lysosomes are known to travel to plasma membrane disruption sites in response to calcium influx (Jaiswal et al., 2002). C2C12 cells double labelled for myoferlin and lysosomes showed no colocalisation in uninjured cells, with each showing their distinctive staining patterns. However, when cells were wounded, myoferlin localised to the same region as the lysosomes i.e. plasma membrane disruption site but did not colocalise. This result strongly suggests that myoferlin is localised to plasma membrane disruption sites in response to calcium influx from a wound site.

In addition, as explained in chapter 1, AHNAK is also known to undergo calcium induced exocytosis (Borgonovo et al., 2002,Hashimoto et al., 1995). Therefore, when the same experiment was repeated with AHNAK and myoferlin each showed distinctive staining patterns in uninjured cells but partially colocalising at plasma membrane disruption sites.

In summary, experiments performed in this chapter strongly suggest that FER1L3 is a myoferlin specific antibody and that myoferlin shows calcium induced enrichment in response to plasma membrane disruption.

4 Chapter Four, Myoferlin & FER1L5 Expression During Differentiation

4.1 Introduction

At the time this work was conducted, it had been shown that *in vitro*, the C2A domain of dysferlin has a role in Ca^{2+}-dependant phospholipid binding (Davis et al., 2002) and that dysferlin deficient muscle fibres are defective in Ca^{2+}-dependant membrane resealing (Bansal et al., 2003). All this and other indications as discussed in chapter 1 pointed to the involvement of dysferlin in muscle membrane fusion. Myoferlin –previously found to be in vesicles (Davis et al., 2002)- and FER1L5's high similarity to dysferlin suggested that they might have a similar role in aiding membrane repair.

In addition, evidence from chapter 3 suggested that myoferlin is also enriched at plasma membrane disruption sites. Myoferlin may have a role in membrane repair since both myogenesis and membrane repair involve the fusion of two adjacent lipid bilayers; therefore studying myoferlin expression during differentiation and in wounded myotubes might provide extra clues to myoferlin's function.

4.2 Results

4.2.1 FER1L5 Analysis & Antibody Immunoadsorption

In order to prove that the assembled FER1L5 sequence is not a pseudogene, one pair of primers were designed within an EST sequence (BY715517 RIKEN full-length enriched, adult male testis Mus musculus cDNA clone 4930533D13-5', mRNA sequence) which mapped to amino acids 5561 to 6182 on the XM_136730 locus. The primers were designed to amino acids 5833-5852 (mFER1L5 _forward) and 5969-5989 (mFER1L5 _reverse) with a product size of 157 bp.

These primers were used for PCR on cDNA extracted from three stages of differentiating myoblasts. PCR results suggested a differential expression throughout the different stages when compared to a house keeping gene (GAPDH) as detailed later in this chapter.

As for immunoadsorption of FER1L5 serum, samples incubated with immunoadsorbed serum showed a complete abolishment of signal (lanes 4, 5 and 6) when compared to samples incubated with the serum (lanes 1, 2 and 3) suggesting the specificity of day 84 FER1L5 serum to the peptides it was designed to (Figure 4.1). This experiment was carried out by Dr. K. Saleki (University of Durham, UK).

4.2.2 DysF-Ferlins Expression During Differentiation

Evidence from chapters 1 and 3 suggested that two out of three (dysferlin and myoferlin) DysF ferlins have upregulated expression during repair of damaged

Figure 4.1 Immunoadsorption of FER1L5 antibody.

RIPA lysed C2C12 cells were loaded into a 6% discontinuous SDS-PAGE gel in the following order: lanes 1 & 4 (23 µg), 2 & 5 (35 µg) and 3 & 6 (57 µg). Lanes 1, 2 and 3 were incubated with day 84 FER1L5 serum (1:100) while lanes 4, 5 and 6 were incubated with unbound FER1L5 serum (1:100) from the incubation in sepharose beads-peptide bound column. Lanes 4, 5 and 6 show a complete abolishment of the FER1L5 antibody. This entire experiment was carried out by Dr. K. Saleki (University of Durham, UK).

Figure 4.1

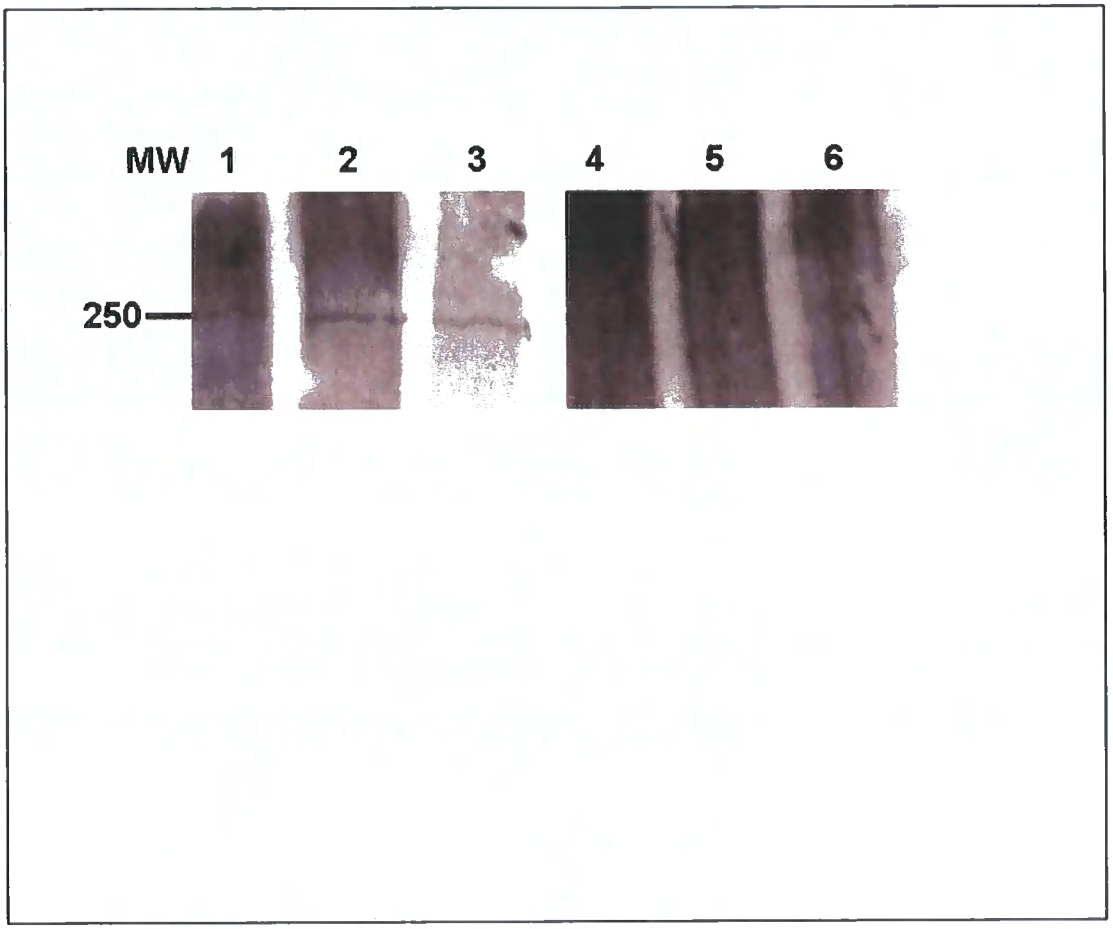

cells. In order to investigate whether a similar process was occurring during myotube neogenesis, the level of protein expression and mRNA in all three DysF ferlins was investigated using immunoblotting and RT-PCR respectively.

Myoblasts were successfully differentiated into myotubes by serum withdrawal as explained in the materials and methods chapter. Evidence of differentiation as suggested by previously published data (Doherty et al., 2005,Salani et al., 2004) is the formation of multinucleate myotubes by day 3 of differentiation and reaching maximum differentiation (indicated by the proportion of myotubes to myoblasts) by day 5 (Figure 4.2). After 5 days of differentiation the number of formed myotubes reached a plateau and this stage of myotubes were used for immunocytochemistry analysis while two additional stages (day 7 and day 14) of myotubes were used for immunoblotting analysis (Salani et al., 2004) in addition to D0 myoblasts as control cells, D1 myoblasts as early differentiating cells, D3 cultures as the start of multinucleate myotube formation (Doherty et al., 2005,Salani et al., 2004).

4.2.3 Dysferlin

Primers designed to the 3' UTR region of dysferlin were used to study dysferlin transcript levels during differentiation by PCR on cDNA extracted from D0, D1 and D5 of differentiating myoblasts. Results from this set of data suggested a low but detectable level of dysferlin in control cells after which an increase in dysferlin transcripts is seen throughout differentiation (Figure 4.3).

Levels of mRNA as determined by PCR may not reflect changes in protein expression. In order to demonstrate effects at the protein level, a series of western blots was carried out.

Results obtained from immunoblotting analysis of dysferlin during differentiation suggest the low expression of this protein in control cells (D0) followed by a constant elevated expression (i.e. during D1 and D3) until the myotube formation reaches its maximum (i.e. D5), after that which the level of dysferlin expression seems to remain relatively constant at D7 and D14 (Figure 4.4). These results suggest that dysferlin expression correlates with the number of forming/formed myotubes in the culture and is consistent with the results obtained from the PCR.

Dysferlin's expression during differentiation by immunoblotting has been reported previously with similar results. Salani et al. (Salani et al., 2004) reported a relatively significant dysferlin expression at D0, and reported the proteins expression as constant at D7, D14 and D21. While Doherty et al (Doherty et al., 2005) reported almost nil dysferlin expression until later in the differentiation when most myotubes were forming or already formed (D5), and after that the expression level was reported to be constantly high.

4.2.4 Myoferlin

Similar to that of dysferlin, primers designed to the 3' UTR region of myoferlin were used to study myoferlin transcript levels during differentiation by PCR on cDNA extracted from D0, D1 and D5 of differentiating myoblasts. Results strongly suggested a low but detectable level of myoferlin (but relatively higher

than that of dysferlin) in control cells after which a constant increase in myoferlin transcripts is seen at the remaining two stages studied (D1 and D5) (Figure 4.3).

As levels of mRNA determined by PCR may not reflect changes in protein expression these results were to be confirmed by western blots.

Western blot analysis suggested that myoferlin was present already in myoblasts (D0). At D1 the start of myoinitiation correlated with an increase in myoferlin level and the protein expression continued to rise until most myotubes were formed (D5). However, the expression levels did not seem to change after 7 days (D7) and 14 days (D14) of switching to differentiation media (Figure 4.4) also correlating with the number of forming/formed myotubes in the culture and is consistent with the results obtained from PCR.

Changes in levels of message and protein may however reflect global changes in transcription/translation, or may be a result of changes in a subpopulation of cells. In order to identify those cells which are responsible for the changes, and to characterise the subcellular expression in these cells, confocal microscopy analysis was carried out using myoferlin antibodies Myof2 and FER1L3.

Myoferlin expression was found to be notably high in single nucleated myoblasts initiating cell to cell fusion (D1) compared to control myoblasts (D0 C2C12). After that myoferlin expression seems to increase until D5 where the majority of the myoblasts have differentiated into myotubes i.e. completion of myoinitiation (Figure 4.5).

4.2.4.1 Myoferlin Expression During Myotube Injury

Myotubes wounded in the presence of Oregon green dextran were labelled with Myof2 antibody, while myotubes wounded in Texas red dextran were labelled with FER1L3 antibody.

Results obtained from this set of experiments strongly suggest that myotubes tend to show enrichment of myoferlin at the wound site (Figure 4.6). These results are consistent with results obtained from chapter 3 where an enrichment of myoferlin was detected at plasma membrane disruption sites of C2C12 cells.

4.2.5 FER1L5

Primers designed to an EST of the assembled FER1L5 gene were used to compare FER1L5 transcript levels during differentiation on the cDNA previously extracted from D0, D1 and D5 of differentiating myoblasts by PCR. Results from this set of data suggested the presence of a very low level of FER1L5 transcripts in control cells. However, this level seemed to increase dramatically during differentiation at the time points studied, D1 and D5 (Figure 4.3).

In order to investigate if the levels of FER1L5 mRNA detected by PCR correlate to changes in FER1L5 protein expression western blot analysis was conducted. Results obtained from immunoblotting analysis of FER1L5 during differentiation suggest the low expression of this protein in control cells (D0) although relatively higher than that of dysferlin and myoferlin. Expression of FER1L5 in early stages of differentiation (i.e. D1) is elevated compared to that of control cells. However, FER1L5 protein expression seems not to be as high in

differentiated myotubes (i.e. D5, D7, and D14) compared to dysferlin and myoferlin (Figure 4.4).

Figure 4.2 Phase-contrast image of differentiating myoblasts

C2C12 cells are derived to differentiate by withdrawing growth media and replacing it with D-MEM supplemented with 2% (v/v) horse serum. This figure shows three stages of myoblast differentiation, Day 0 control myoblasts (A), Day1 (B) and Day 5 (C) post differentiation.

Figure 4.2

A)

B)

C)

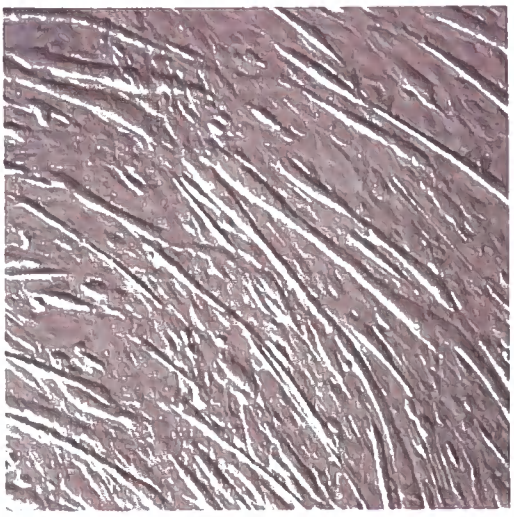

Figure 4.3 Ferlins mRNA profile by RT-PCR during myoblast differentiation

PCR of dysferlin, myoferlin, FER1L5, Otoferlin and GAPDH with cDNA extracted from three stages of C2C12 differentiation (control, D0; pre-fusion, D1; myotubes, D5). (A) Dysferlin- 150 bp product. (B) Myoferlin- 200 bp product. (C) FER1L5 - 157 bp product. (D) Otoferlin - 130 bp product. (E) GAPDH - 190 bp product.

Figure 4.3

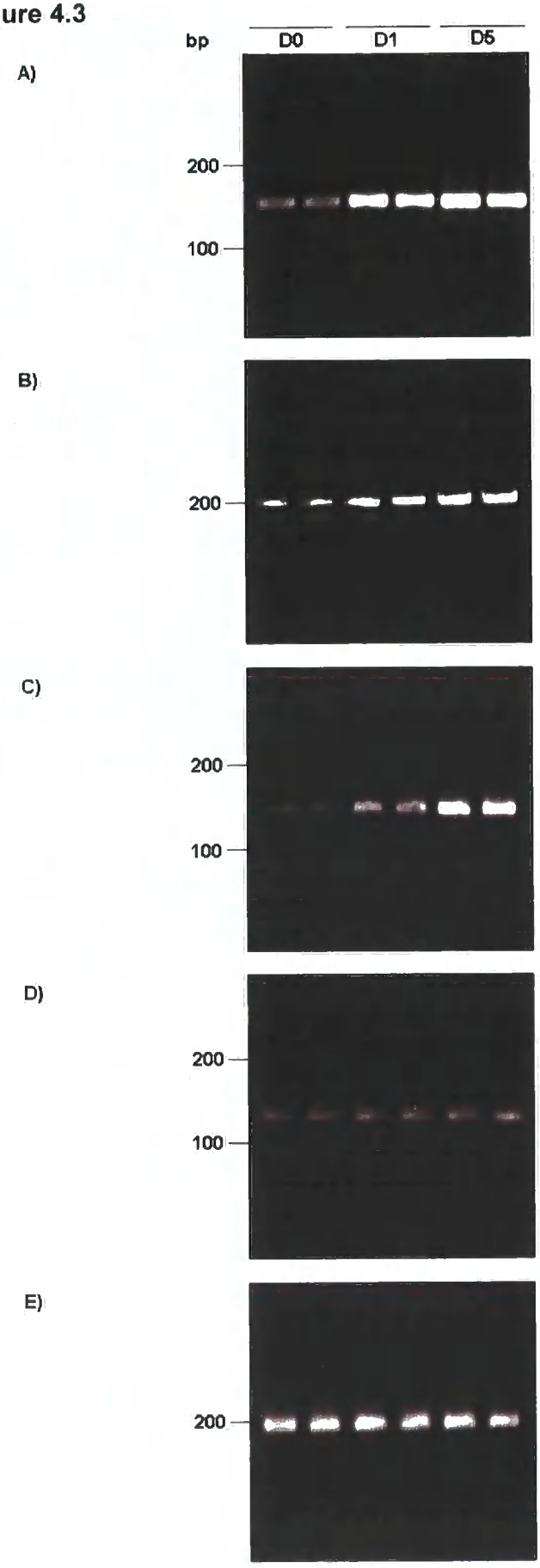

Figure 4.4 dysF-ferlins expression profile by immunoblotting during myoblast differentiation

Comparison of dysferlin expression (A), myoferlin (B) and FER1L5 (C) in control myoblasts (D0, lane1), pre-fusion (D1, lane2), and during progressive time points in myotube formation (D3, lane 3; D5, lane 4; D7, lane 5; D14, lane 6). Protein extracts were prepared from differentiating myoblasts. 100µg of total protein per lane was resolved on 6% SDS-PAGE, transferred to a membrane and immunoblotted with monoclonal antibody HCL-Hamlet (1:250) for dysferlin, with monoclonal antibody FER1L3 (neat) for myoferlin and polyclonal D84 serum (1:500) for FER1L5. Molecular weight markers are in KDa. Coomassie blue stained protein gels were used to confirm equal loading and no global changes in protein expression (data not shown).

Negative control blots ((D) HRP conjugated Donkey anti-rabbit, IgG; (E) HRP conjugated Donkey anti-mouse) blotted against the same samples from six stages of differentiating myoblasts.

Figure 4.4

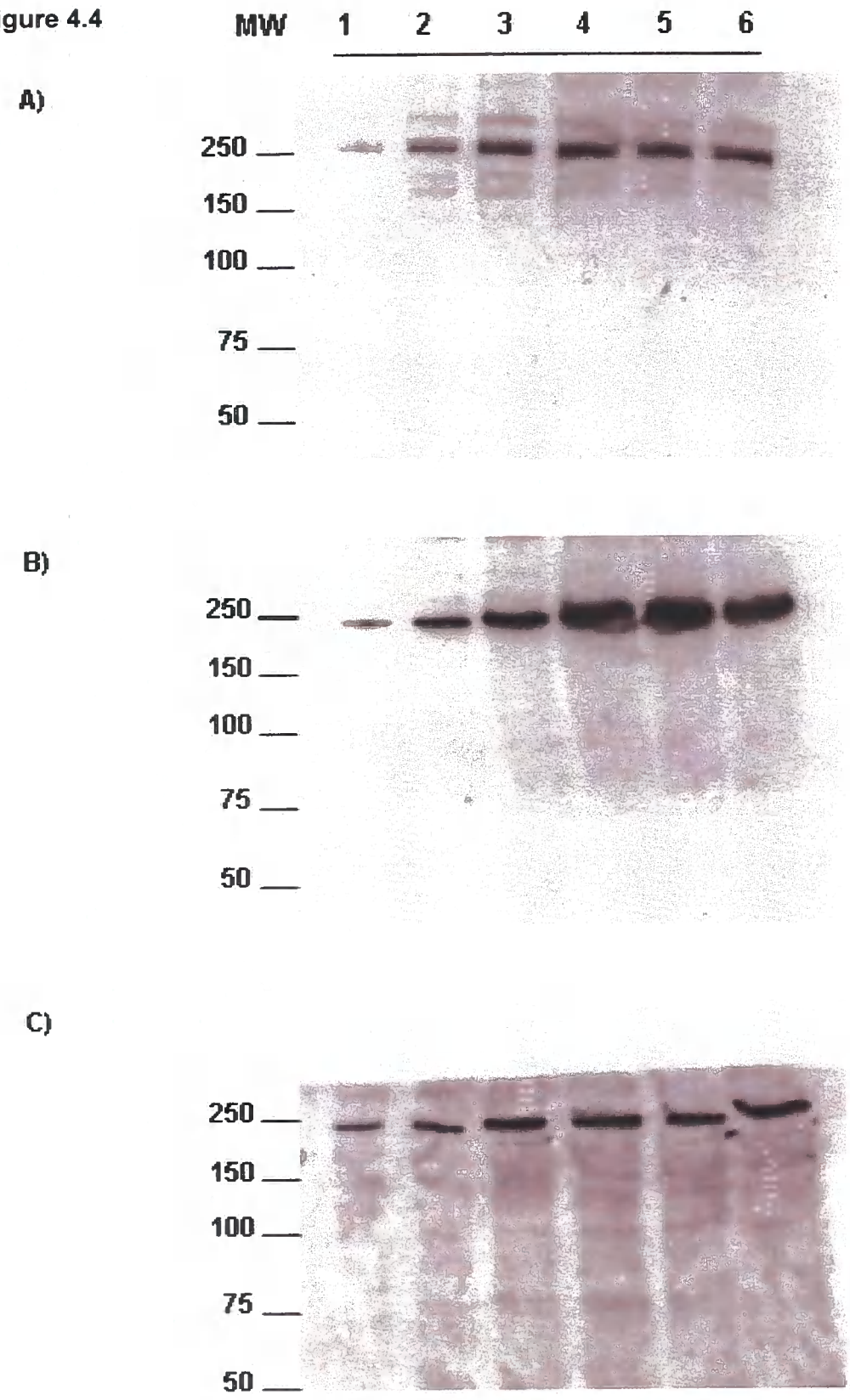
MW
1
2
3
4
5
6
A)
250
150
100
75
50
B)
250
150
100
75
50
C)
250
150
100
75
50

D)

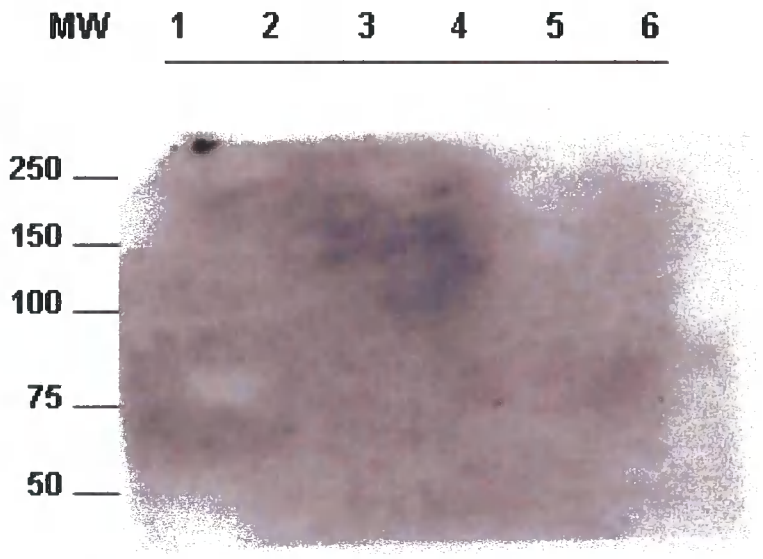

E)

Figure 4.5 Myoferlin expression during myoblast differentiation by immunoflorescence

Differentiating myoblasts were analysed by immunoflorescence using Myof2 (A) and FER1L3 (B) antibodies during different stages of differentiation (D0, D1, D3, and D5) and imaged by confocal microscopy. Results strongly suggest that myoferlin expression increases throughout differentiation with the highest levels detected in myotubes.

Figure 4.5 (A)

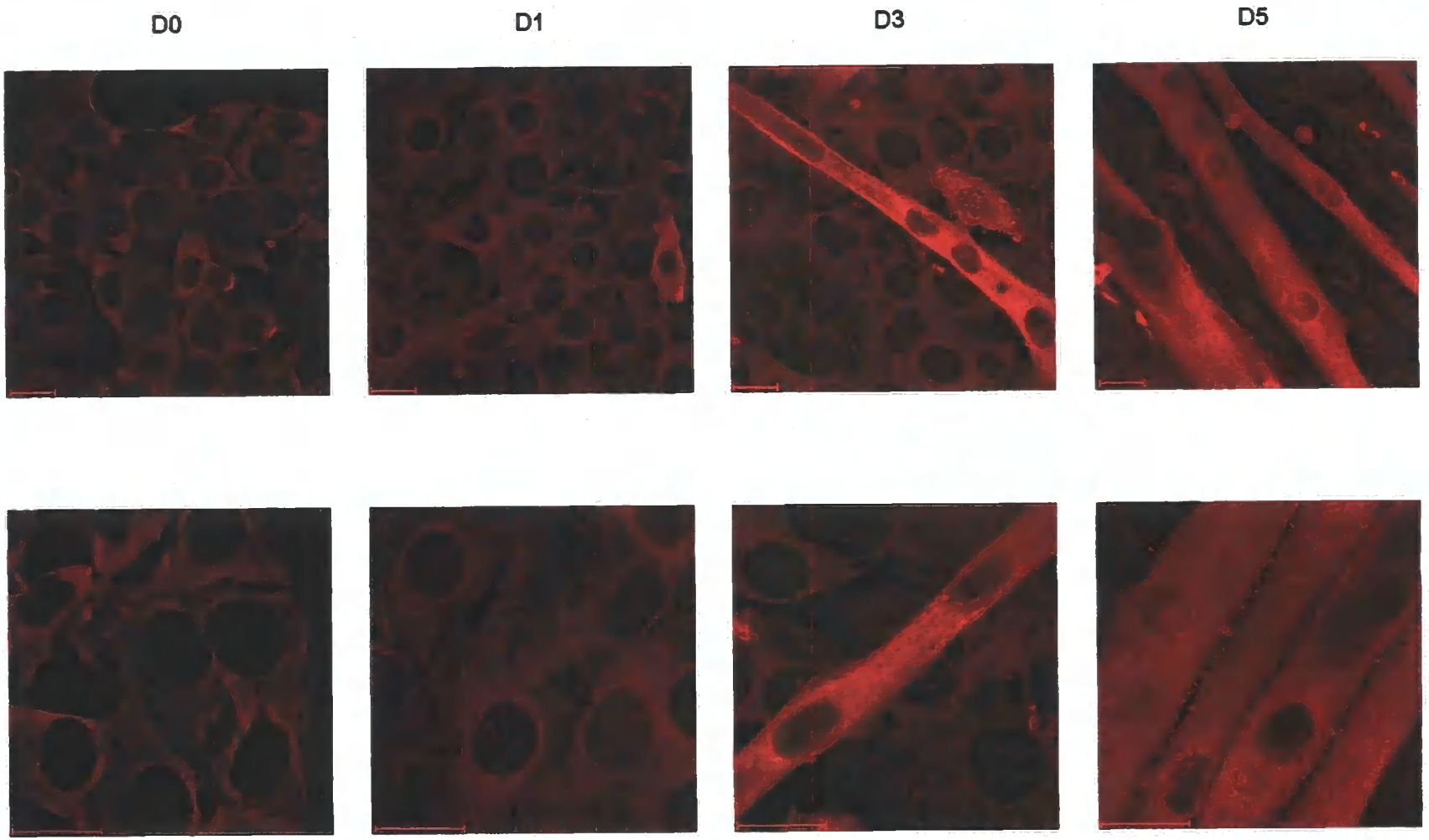

Figure 4.5 (B)

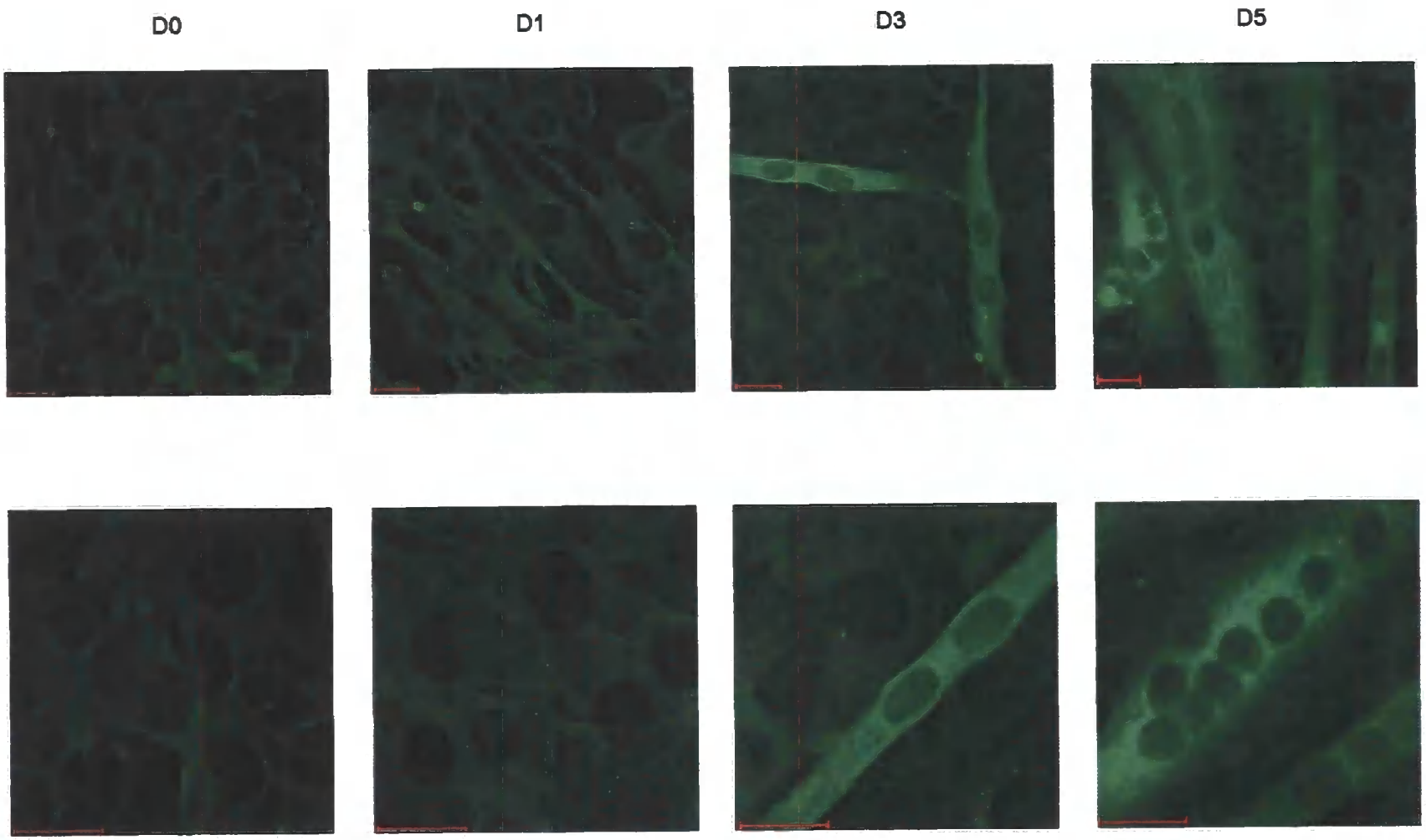

Figure 4.6 Myoferlin expression in wounded myoblasts during differentiation

Differentiating myoblasts wounded in the presence of dextran (Myof2 (A) and FER1L3 (B)) show enrichment of myoferlin at the wound site similar to that seen in C2C12 cells, although the enrichment due to wounding is not as obvious as in control cells due to the fact that differentiated cells already show an increased myoferlin expression.

Figure 4.6 (A)

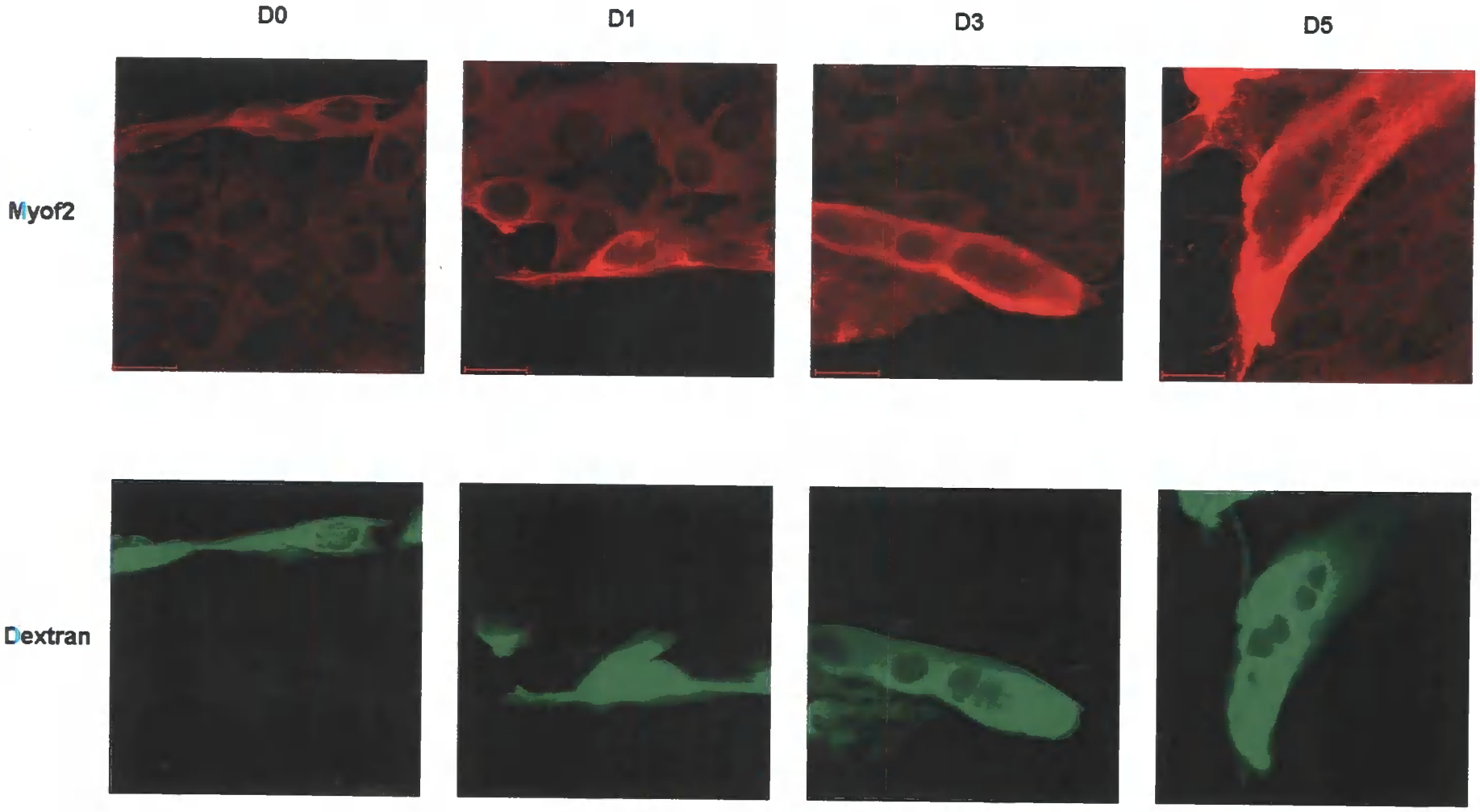

Figure 4.6 (B)

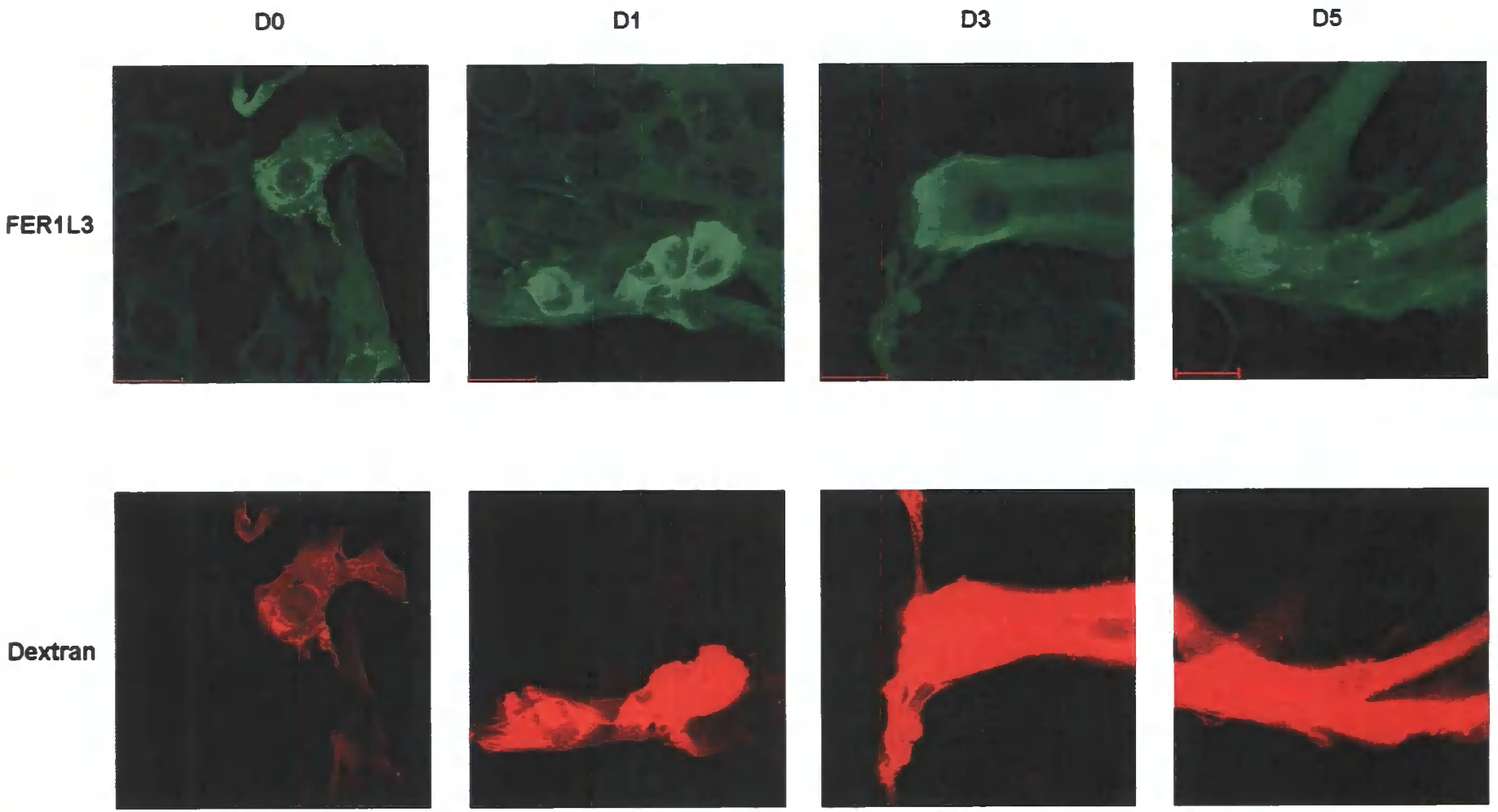

4.3 Summary

In this chapter the expression of DysF ferlins during myoblast differentiation was investigated. Dysferlin and myoferlin (i.e. DysF ferlins) mRNA levels were analysed by RT-PCR during three stages of differentiation and compared to that of otoferlin (i.e. non-DysF ferlins) and a house keeping gene, GAPDH. Results suggested that DysF ferlins have elevated mRNA levels during differentiation. These results were followed by western blot analysis which confirmed protein expression levels of DysF ferlins are higher in later stages of differentiation coincided with proportions of myotubes to myoblasts in the studied cultures.

In addition, myoferlin's expression during differentiation was also analysed by immunoflorescence, and results strongly suggested that myoferlin's expression was the highest in myotubes confirming the results obtained by PCR and immunoblotting.

Myoferlin's increased expression during differentiation is very significant because the process of differentiation involves the fusion of two membranes together, similar to that seen in membrane repair following a plasma membrane disruption. This supports the hypothesis that myoferlin like dysferlin is involved in membrane repair.

Indeed, after the completion of this project, a recently published study (Doherty et al., 2005) used a similar method in understanding myoferlin cellular function. In addition, the group generated myoferlin-null mice through homologous recombination by inducing a point mutation in the C2A domain of myoferlin, which blocked Ca^{2+}-sensitive phospholipid binding (Doherty et al., 2005) similar to that seen in dysferlin (Davis et al., 2002).

The myoferlin null mice were used to study myoferlin's significance in cells. Myoferlin deficient myoblasts were reported to be defective in myoaugmentation but not myoinitiation resulting in smaller muscle area in vivo, in addition to defective muscle regeneration post injury associated with upregulation of myoferlin (Doherty et al., 2005).

Also in this chapter the addition of a new member of the ferlin protein family is reported. FER1L5 shares the highest homology with dysferlin and myoferlin, in addition to possessing a DysF domain which places it in the DysF ferlins subgroup. Using SMART analysis, the human FER1L5 is thought to consist of 6 C2 domains and a C-terminal transmembrane domain.

In order to prove that FER1L5 is not a pseudogene, one set of primers were designed to an EST region of mouse FER1L5 and its expression analysed by PCR on cDNA extracted from three stages of myoblast differentiation. The resulting expression pattern was compared, to the expression pattern of dysferlin, myoferlin, otoferlin and GAPDH.

As mentioned earlier, dysferlin, myoferlin, and FER1L5 (i.e. DysF ferlins), showed an increase in mRNA levels throughout differentiation with the highest levels detected in myotubes, while otoferlin (a non-DysF ferlin) and GAPDH showed a constant level throughout the studied stages of differentiation.

Since the increase in mRNA levels detected does not necessarily reflect the increase in these protein's expression western blot analysis was conducted to investigate whether increased FER1L5 mRNA levels reflect increased levels of FER1L5 protein.

Western blot analysis was conducted on extracts from the same three stages of differentiation used in PCRs (D0, D1, D5) in addition to three more stages (D3,

D7, D14) of differentiation and results obtained from western blot analysis were consistent with those results obtained from PCR suggesting an elevated expression of FER1L5 in myotubes compared to control myoblasts.

5 Chapter Five, Myoferlin sub-cellular colocalisation

5.1 Introduction

The experiments carried out in previous sections of this project may help us in a better understanding to myoferlin's expression, localisation and mobilisation of myoferlin in C2C12 cells in undisturbed conditions or during significant events of a muscle cell's life cycle such as plasma membrane disruptions and differentiation. Although myoferlin was suggested to be found in vesicles (Davis et al., 2002) of some kind, to date the exact nature of these vesicles is ambiguous. We still do not have a clear map of myoferlin's passage in the cell once it has left the nucleus post transcription, whether this protein is found inside a vesicle or simply attached to it and if so, is this a vesicle of known structure and function or a novel vesicle and how this vesicle mobilises inside the cell and if the cellular cytoskeleton and cellular ATP levels are involved in one way or another in this process and whether myoferlin or its vesicle are subjected to conformational changes during myoferlin's mobilisation or not . All these questions remain to be answered in order for us to fully understand myoferlin's function to use this information further and possibly a therapeutic purpose.

The experiments carried out in this chapter aim at answering some of these questions by investigating the possible colocalisation of myoferlin with any other cellular structure. Myoferlin's colocalisation with lysosomes and enlargosomes was shown in chapter 3. However, since most proteins pass through the TGN network at one stage of their cycle or another and ER is known to be

responsible for folding of proteins, both the TGN and the ER were investigated for a possible colocalisation with myoferlin. Co-immunolabelling of the structures of interest with myoferlin followed by confocal imaging was performed.

Next, myoferlin's possible colocalisation with the cytoskeleton or possible dependency on the cytoskeleton in its cellular localisation in normal cells and how drug induced re-organisation or disruption of the cellular cytoskeleton affect this localisation or mobilisation was investigated. Latrunculin B (LA-B) was used in this study to investigate the affects of actin re-organisation and disruption on myoferlin cellular expression while Nocodazole, a benzimidazole derivative was used to study how myoferlin is affected by microtubule re-organisation.

In the last section of this chapter, myoferlin's possible dependency on ATP in cellular mobilisation and localisation in normal and wounded cells was examined by drug-induced ATP depletion of the cells.

5.2 Results

5.2.1 Myoferlin Colocalisation with TGN and ER

TGN38 is a type 1 membrane protein that cycles between the TGN and the cell surface by endosomal intermediates (Ponnambalam et al., 1994). A unique motif on the protein's cytosolic domain is responsible for the internalisation from the plasma membrane to the TGN through endosomes (Humphrey et al., 1993), while its movement back to the cell surface is through exocytotic vesicles (Jones et al., 1993). Cells studied for myoferlin colocalisation with TGN were double labelled with TGN38 antibody (1:100, serotec) diluted in FER1L3 antibody (neat). Alexa 488 and Alexa 546 were used as fluorophores.

In addition, myoferlin localisation relative to the ER was investigated by labelling the ER with the antibody for Protein Disulfide Isomerase (PDI). PDI is a 55 KDa ER protein (Brockway et al., 1980). In cells, whether *in vivo* or *in vitro*, side reactions during folding may lead to inactive protein especially in proteins involving disulfide bonds (Buchner & Rudolph, 1991,Hurtley & Helenius, 1989). Therefore cells have developed a set of helper proteins like folding catalysts and chaperones to guide the polypeptides to a correct structural folding. In this context, PDI influences the formation of disulfide bonds in the ER such that PDI depleted microsomes *in vitro* have been shown to accumulate mis-folded polypeptides at the translation and translocation of secretory proteins. This strongly suggests the role of PDI to be a disulfide bond formation facilitator (Bulleid & Freedman, 1988).

To examine colocalisation of myoferlin with ER vesicles, cells were labelled with PDI antibody (1:750, a kind gift from Dr. A Benham) diluted in FER1L3 antibody

(neat), and treated with Alexa 488 and 546 as fluorophores. Negative control experiments confirmed no cross binding (data not shown).

TGN38 staining on C2C12 cells resulted in a prominent vesicular staining in proximity to the nucleus as reported previously (Roquemore & Banting, 1998), while FER1L3 staining was not as vesicular but still present at higher levels near the nucleus than the remainder of the cell. Overall, myoferlin staining did not substantially colocalise with that of TGN38 (Figure 5.1). Although this strongly suggests that myoferlin is not found in or on TGN38 vesicles at the time point studied, this study does not rule out other TGN vesicles or the possibility of myoferlin being present at a very specific and short time period.

PDI expression in C2C12 cells was very similar to expression patterns reported previously in other cells (Mezghrani et al., 2000). PDI expression, as expected from ER distribution in cells, is clustered around the nucleus forming a fine network. When images obtained by confocal microscopy of cells double labelled with PDI and myoferlin were merged a partial colocalisation of myoferlin and PDI was observed in the area surrounding the nucleus. No colocalisation was visible in the rest of the cell (Figure 5.2). These results indicate the presence of myoferlin in the ER at one point; however, immunocytochemistry is not an accurate enough tool to indicate at which time point of myoferlin's cell cycle this protein passes through the ER and how long it resides there.

Figure 5.1 Myoferlin colocalisation with TGN38

C2C12 cells immunolabelled with FER1L3 (neat) and TGN38 (1:100) antibodies and imaged by confocal microscopy suggest no substantial colocalisation. White arrowheads show TGN38 vesicles which propose no colocalisation when merged with that of myoferlin staining.

Figure 5.1

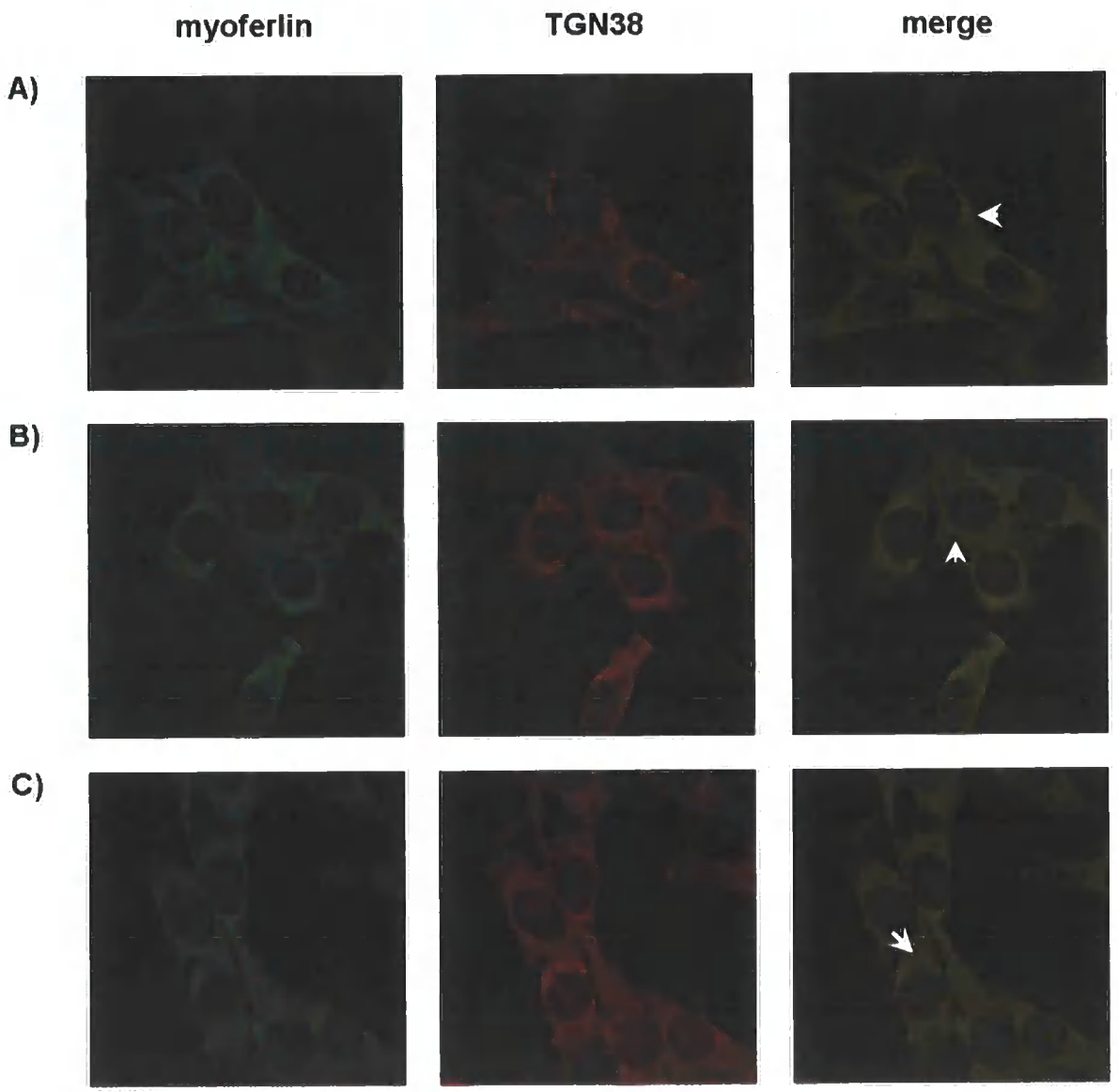

Figure 5.2 Myoferlin colocalisation with PDI

C2C12 cells immunolabelled with FER1L3 (neat) and PDI (1:750). Merged confocal images strongly suggest a partial colocalisation at the peri-nuclear region (orange colour).

Figure 5.2

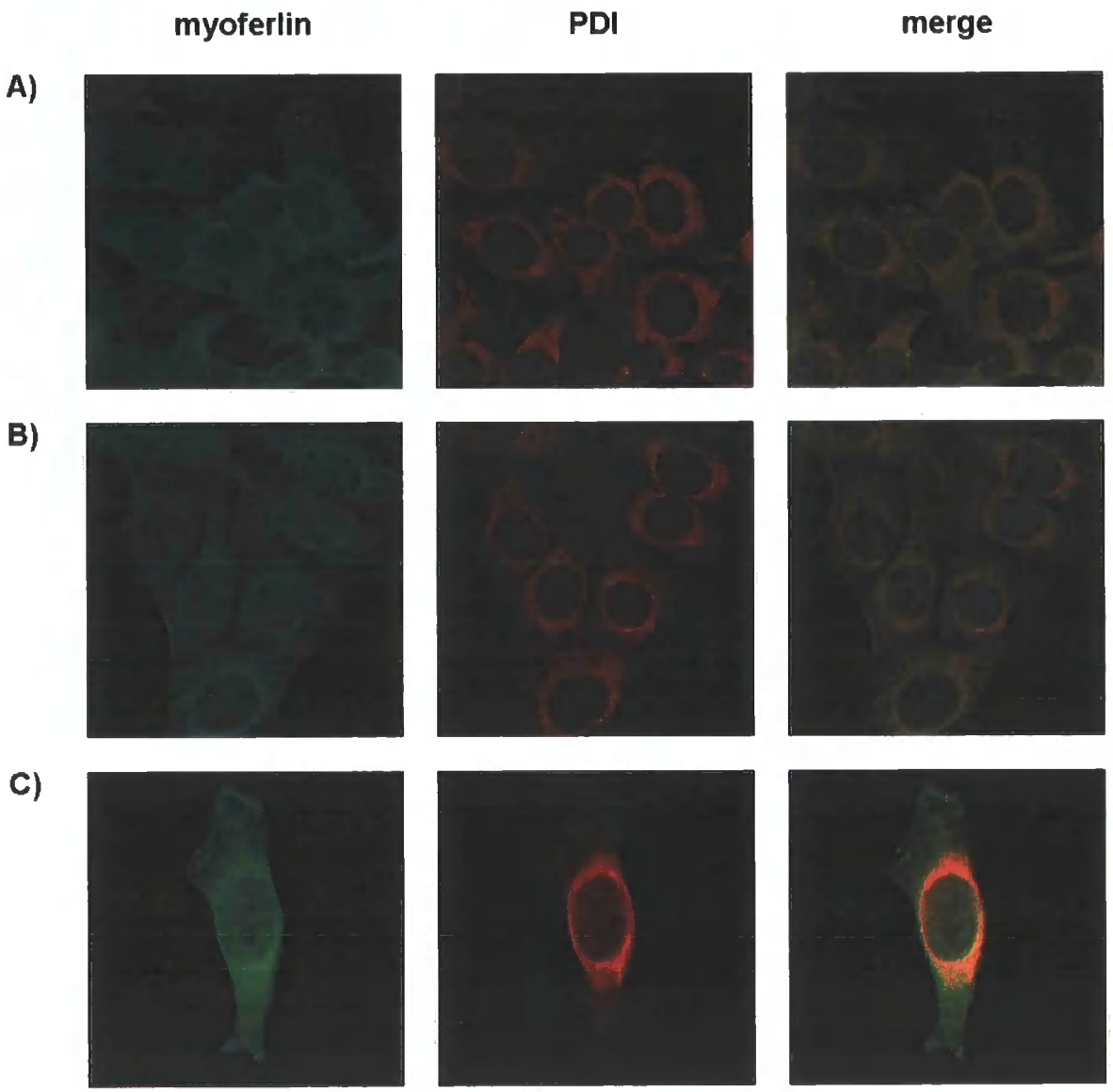

5.2.2 Effect of LA-B on Cellular Localisation of Myoferlin

LA-B is a marine powerful toxin known to inhibit actin polymerisation by forming complexes with actin monomers (Spector et al., 1989) therefore resulting in the reorganisation of the actin cytoskeleton. Its effects can be seen almost immediately after drug application by the disappearance of stress fibres and radiating actin fibres. Shortly afterwards, a cloudy, unstructured body thought to be short scattered F-actin is reported in treated cells. LA-B is also reported to induce a shift of F-actin to G-actin shortly after the introduction of the drug (Gronewold et al., 1999).

Actin destabilising drugs like LA-B are known to result in the production of runner-like extensions in addition to resulting in cells losing their mobility and polarity at high doses. Although cells stop to divide at this stage, cell growth is not affected resulting in large multinucleate cells (Gronewold et al., 1999).

The tubulin cytoskeleton is thought not to be affected or destroyed by LA-B but rather re-organised at high doses when the cell shape is affected (Gronewold et al., 1999).

In vitro, a narrow range of the toxin (20 nM-200 nM) has been shown to disrupt actin filaments resulting in focal aggregates of F-actin (Wakatsuki et al., 2001). In this experiment visible changes to the actin cytoskeleton, including focal aggregates, were only visible at 150 nM of LA-B or more.

At 200 nM LA-B, where most but not all of the cellular actin had been disintegrated and the appearance of few focal aggregates was visible, myoferlin's localisation inside the cell was showing a slightly different pattern to that of control cells. At the next higher dose, 250 nM, most cellular actin had been broken down and the changes to myoferlin's localisation could be examined.

Myoferlin appeared to be randomly scattered inside the cell and had lost its distinct pattern of perinuclear subcellular distribution. The subcellular distribution of myoferlin also appeared as small aggregates and was grainy in texture compared to control cells (Figure 5.3). However, at doses higher than 250 nM the cells collapsed and the appearance of runner-like extensions was visible.

As a control to myoferlin, Caveolin 3 expression was also investigated in cells treated with LA-B. In contrast to myoferlin, Caveolin 3 localisation inside the cell did not seem to be affected by the breakdown in the actin cytoskeleton and continued to show the regular pattern when compared to control cells.

Finally, in an attempt to investigate the affect of the actin cytoskeleton breakdown on myoferlin enrichment in response to injury in wounded cells, C2C12 cells treated with LA-B were wounded in the presence of dextran. Unfortunately, despite repeated attempts this experiment was not successful and each time treated cells floated off the coverslips once injured. A possible explanation might be that LA-B had resulted in the disintegration of the actin cytoskeleton, which in turn resulted in loosening the cell's attachment to the growth surface (i.e. coverslip) or that inducing a wound to a cell lacking a cytoskeleton might be too much of a stress therefore cells undergo apoptosis.

5.2.3 Effect of Nocodazole on Cellular Localisation of Myoferlin

Microtubules are linear protein polymers characterised by their dynamic instability (Cassimeris, 1993) and are thought to have a significant role in vesicle trafficking (Cole & Lippincott-Schwar, 1995) among other roles. This instability is divided into two phases: 1) Catastrophe, which is the switch from

elongation to shortening and 2) Rescue, the switch from shortening to elongation (Walker et al., 1988).

Nocodazole was originally developed as a probable anticancer drug, and has been shown to induce mitotic arrest in cells and to interfere with dynamic instability of microtubules by increasing the time microtubules spend in a paused state (Vasquez et al., 1997).

Visible effects to the tubulin network were slightly noticeable at 25 ng/ml where slight aggregates were starting to form. At 50 ng/ml most of the tubulin network had broken down and few disoriented tubulin fibres were left. At 60 ng/ml most cells had collapsed and rounded up. However, at all the tested doses (≤ 50 ng/ml) were cell shape was not affected, myoferlin localisation did not appear to be different to that of control cells and continued to show the regular staining pattern observed previously (Figure 5.4).

As a control, similar to that of LA-B experiment, Caveolin 3 localisation was investigated in nocodazole treated cells. Caveolin 3 expression did not seem to change at the highest doses where cells retained their shape and structure when compared to that of control cells.

5.2.4 Effect of ATP Depletion on Cellular Localisation of Myoferlin

ATP is known to be involved in several steps of the calcium-dependant exocytotic secretion pathway by undergoing hydrolysis to act as a source of energy for motor proteins that transport vesicles from the TGN to plasma membrane (Martin & Kowalchyk, 1997). Cells were treated with the lowest effective dose of ATP depleting reagents (0.1% NaN_3/ 100 μM 2-DG) confirmed

by the failure to endocytose dextran (Figure 5.5). Unwounded ATP depleted cells suggested no evident re-organisation of myoferlin in these cells when compared to control cells. However, when ATP depleted cells had plasma membrane disruptions induced the confocal images obtained from these cells suggested a slight reduction in myoferlin staining in wounded cells when compared to control cells and imaged at the same confocal settings (Figure 5.6). This suggests a possible minor dependency of myoferlin on ATP in its mobilisation to sites of plasma membrane disruption.

Figure 5.3 Myoferlin expression in LA-B treated cells

C2C12 cells treated with 0 nM, 150 nM, 200 nM, 250 nM of LA-B were immunolabelled with F-actin (1:30) or Myof2 (1:300) or Cav3 (1:300) antibodies. At 0 nM i.e. control cells, each of F-actin, myoferlin and Caveolin 3 show normal expression patterns. At 150 nM the first visible changes to F-actin is observed with the appearance of stress fibres (arrow heads) while myoferlin dramatically loses its distinct peri-nuclear staining. At 200 nM more stress fibres are prominent in F-actin stained cells and few focal aggregates start to form while myoferlin appears grainier in texture. At 250 nM, the highest dose where cells retain their shape, focal aggregates (white circles) dominate the cell and very few stress fibres remain while myoferlin looses its usual cellular localisation pattern and is uniformly distributed. At all four doses Caveolin 3 expression seems to be unchanged.

Figure 5.3

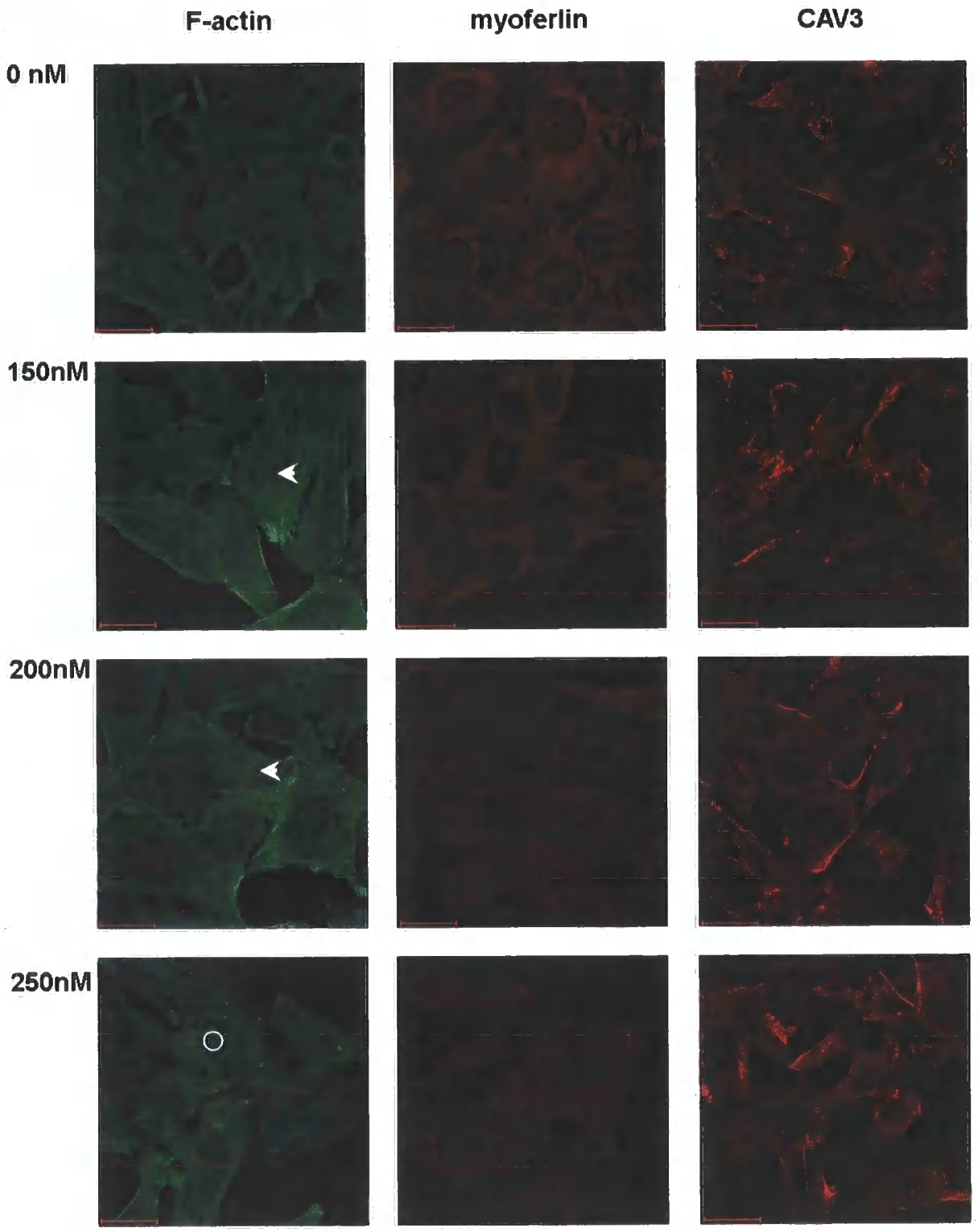

Figure 5.4 Myoferlin expression in nocodazole treated cells

C2C12 cells treated with 0 ng/ml, 25 ng/ml, 35 ng/ml, 50 ng/ml of nocodazole were immunolabelled with tubulin (1:100) or Myof2 (1:300) or Cav3 (1:300) antibodies. At 0 ng/ml i.e. control cells, tubulin, myoferlin and Caveolin 3 show their normal expression patterns. At 25 ng/ml the first visible changes to tubulin is seen when tubulin starts to loose its rather spectacular finely weaved structure and tubulin appears as short, disorganised strands while no visible change in myoferlin and Caveolin 3 expression is observed. At 35 ng/ml the first focal aggregates (white circles) start to appear and tubulin starts to breakdown while myoferlin and Caveolin 3 seem unchanged. At 50 ng/ml, the highest dose where cells retain their shape, very little cellular tubulin remains and tubulin focal aggregates dominate the cell. Even at this dose myoferlin and Caveolin 3 expression seem to be unchanged.

Figure 5.4

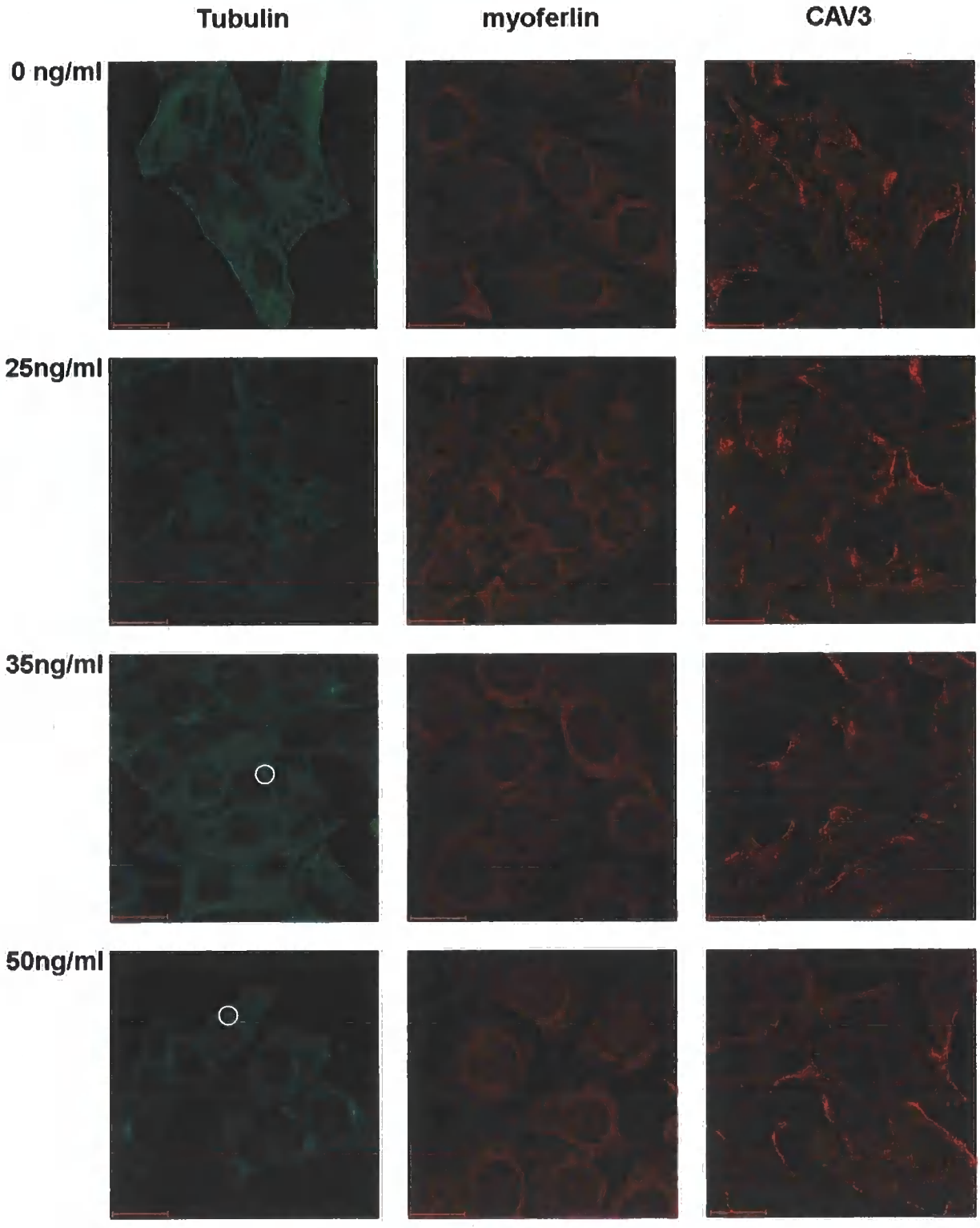

Figure 5.5 Endocytosis in ATP depleted cells

C2C12 cells treated with 0.025%-0.2% (w/v) sodium azide (NaN_3) and 25 μM-200 μM 2-deoxyglucose (2-DG) for 30 minutes were incubated with 5 mg/ml Oregon green dextran for a further 30 minutes to study the lowest effective dose to inhibit endocytosis here used as an indicator of successful ATP depletion. A) Control cells not treated with ATP depleting reagents, B) cells treated with 0.1% NaN_3/ 100 μM 2-DG fail to endocytose dextran.

Figure 5.5

A)

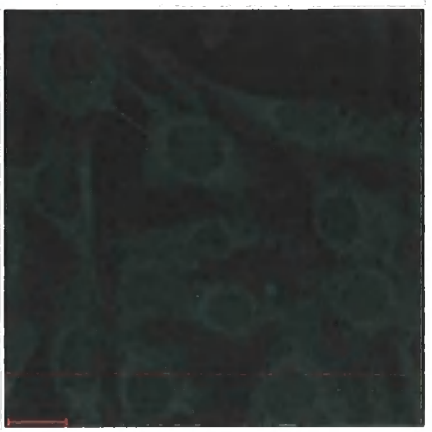

B)

Figure 5.6 Cell membrane wounding in ATP depleted cells

A) Cells treated with 0.1% NaN_3/ 100 μM 2-DG and wounded in the presence of dextran (here used as an indicator to plasma membrane disruption) show a relatively normal enrichment at plasma membrane disruption sites when compared to non-ATP depleted and wounded cells (B).

Figure 5.6 (A)

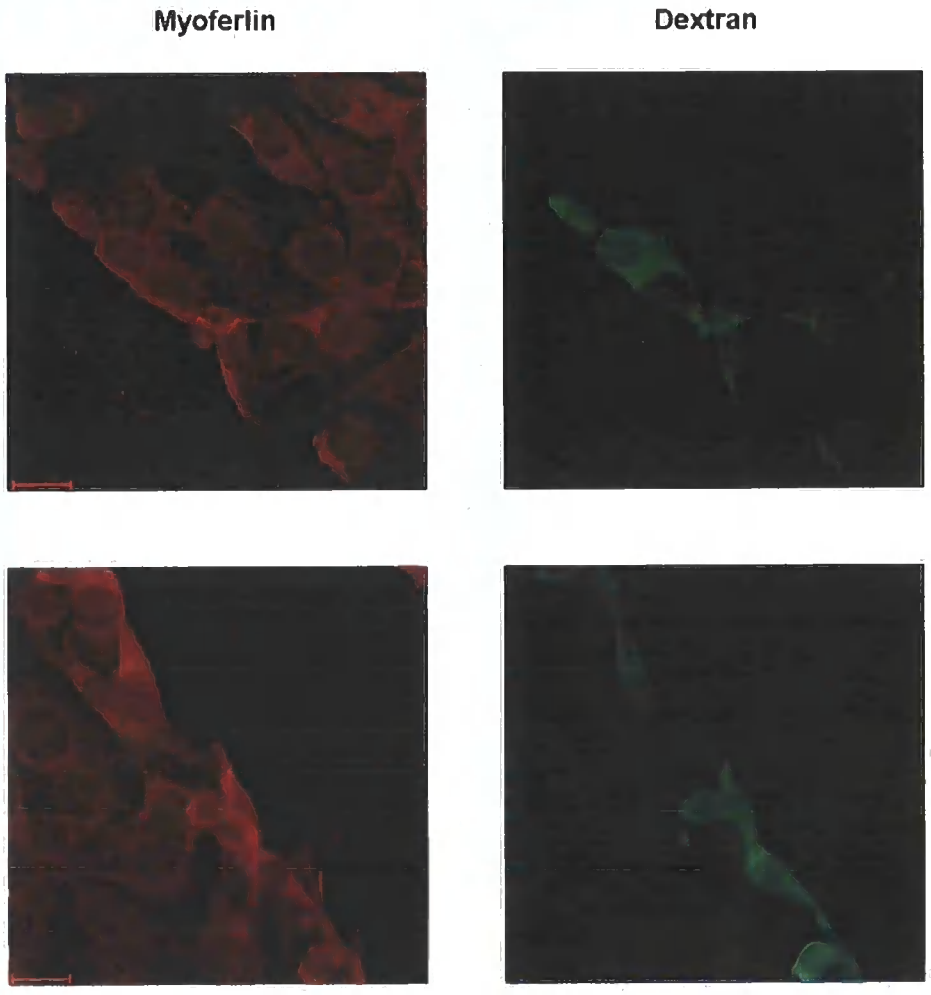

Figure 5.6 (B)

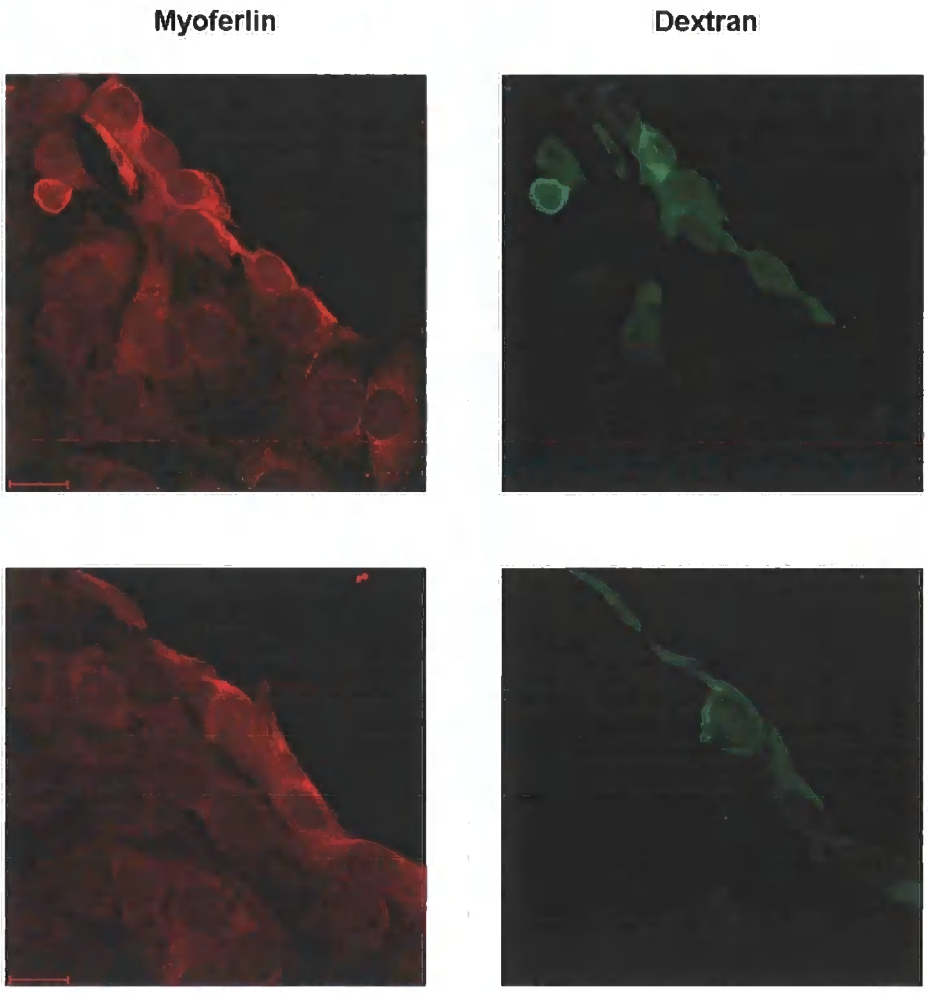

5.3 Summary

To summarise this chapter, myoferlin's possible colocalisation with some known cytoplasmic vesicles or the cellular cytoskeleton was investigated. Myoferlin was analysed for colocalisation with vesicles from the TGN and ER by immunocytochemistry using TGN38 and PDI antibodies respectively. TGN38 and myoferlin did not substantially colocalise with each other giving a distinct staining pattern and localisation inside the cell when analysed by immunoflorescence and confocal microscopy suggesting that myoferlin is not found in or on TGN38 vesicles under the circumstances investigated. However, these results do not conclude in any way that myoferlin is not found in the TGN at all. Further future experiments can be conducted (see chapter 7) in order for myoferlin's presence or absence from the TGN can be concluded.

ER staining by PDI gave its known distinct pattern in the area adjacent to the nucleus as expected from known ER distribution inside the cell and as detailed in chapter 3 of this thesis myoferlin also possesses a unique peri-nuclear staining in addition to some cytoplasmic staining. Cells double labelled for PDI and myoferlin imaged by confocal microscopy showed an overlapping staining in the area surrounding the nucleus. This observation suggests that myoferlin expressing vesicles do pass through the ER at one stage or another.

In chapter 3 of this thesis, myoferlin was also shown to partially colocalise with AHNAK expressing vesicles at sites of plasma membrane disruption while suggesting an independent expression pattern in undisturbed cells. However, this was not the case for lysosomes where lysosomes and myoferlin did not

seem to colocalise in wild type or wounded cells although both showing an increased mobilisation at sites of plasma membrane disruption.

Although immunocytochemistry is an important tool in investigating the first steps of cellular localisation and mobilisation of a protein, it is not the most accurate of methods. Deploying more sophisticated methods combined with more time and resources can be used to confirm the results observed regarding myoferlin possible colocalisation with other cellular vesicles and give better details of this process.

In the second section of this chapter, myoferlin's dependency on two main components of the cellular cytoskeleton (actin filaments and microtubules) for its intracellular distribution and localisation was investigated. Results obtained from this study strongly suggested that dissociated tubulin network did not seem to have any affect on myoferlin's distribution, while in contrast, a dissociated actin network seemed to result in the re-distribution of myoferlin inside the cell. This was observed as the loss of myoferlin's unique peri-nuclear staining and instead a rather uniformly distributed grainy myoferlin staining was seen. These results strongly suggest that myoferlin is dependant on actin cytoskeleton for its normal cellular distribution.

Both actin and tubulin cytoskeleton disassembly did not seem to affect the cellular localisation of Caveolin 3, which was used as a control in these experiments.

In the last section of this chapter, cells depleted of ATP and wounded were used to study whether ATP is a contributing factor to myoferlin's enrichment at plasma membrane disruption sites. Although a very slight reduction was

observed in cells depleted of their ATP and wounded when compared to control cells, these results lack any scientific quantification but most importantly of all it is not clear whether the lowest effective dose to inhibit endocytosis has any affect on the actin cytoskeleton or not. It is very possible that no noticeable difference in myoferlin enrichment at the wound site in ATP depleted cells was observed because the lowest effective dose to inhibit endocytosis was not high enough to inhibit actins' routine polymerisation and depolymerisation in which myoferlin was shown in the previous section of this chapter to be dependant on for normal cellular distribution. Further future experiments can be performed to confirm these results.

The work involved in the last three chapters focused on myoferlin and FER1L5 as possible muscular dystrophy associated genes and their possible role in membrane resealing post wounding. However, in the next chapter a fresh examination of the previously suggested chromosome 10-linked muscular dystrophy associated genes is undertaken.

6 Chapter Six, Non-dysferlin linked MM

6.1 Introduction

In previous chapters, immunoblotting and immunocytochemistry combined with confocal microscopy and analysis were used to investigate the distribution and expression of myoferlin following membrane injury repair at a cellular level which could ultimately give a clue to its possible involvement in muscular dystrophy. This approach combined with genetic analysis, resulted in the description of a new ferlin protein family member, FER1L5, as reported in previous chapters. These two proteins (myoferlin and FER1L5) are closely related and their extent of interaction with each other or involvement in muscular dystrophy or possibly MM is not fully understood.

This raises the question of how many more genes are still unidentified that might be involved in phenotype variation of muscular dystrophy such of that seen in LGMD2B and MM patients or genes that play a role in disease progression or genetic modification or even be responsible for non-chromosome 2-linked MM (i.e. non-dysferlin-linked MM) such as that previously reported by Linssen et al (Linssen et al., 1998).

The number of genes present in the 23cM region that segregated with the MMD2 region described in Linssen et al (Linssen et al., 1998) is too many to analyse all of them for SSCP, and thus a more rational approach was adopted. All of the genes within that region whose known structure or function made them strong candidates for analysis were studied. Six genes were selected: ARHGAP21, PRKCQ, PTPLA, RAB18, ANKRD26, FLJ14813 and caveolin 3.

6.2 Results

6.2.1 ARHGAP21

ARHGAP21 gene was identified by Basseres et al (Basseres et al., 2002). The gene consists of 26 exons and is located on the human chromosome 10p12.32. Its function is not fully understood but it has been shown to be upregulated in brain, muscle and differentiating HL-60 cells and since it belongs to the Rho-GTPase activating proteins it is thought to have a role as a negative regulator of Rho-GTPase signaling pathway related to actin cytoskeleton dynamics, cell proliferation, and cell differentiation (Basseres et al., 2002) which makes it a strong candidate for SSCP analysis.

38 out of 40 PCR reactions for this gene were successfully amplified and analysed by SSCP (exon 1 and 9d PCR amplifications were not successful). Exons 5, 11, 15, 19, need to be repeated since the number of samples that resulted in a clear banding pattern was small compared to the total number of samples. For reasons of time and resources, it was only possible that only one set of analysis were carried out for each SSCP test. The banding pattern in general obtained at the level of analysis adopted seem to be consistent with affected and carrier subjects suggesting no polymorphism.

Figure 6.1 SSCP gel analysis of ARHGAP21 gene

Exons 1 and 9d could not be amplified by PCR. However, gel scans of the rest of the exons are shown in this figure. From left to right of each gel are two affected individuals from family I (Ib and Ig) alongside one carrier from family one (Id), followed by two affected individuals from family II (IIb and IIh) alongside one carrier from the same family (IIe). In some exons a control sample was added. As explained previously both families have been excluded from chromosome 2-linked- MM.

ARHGAP21

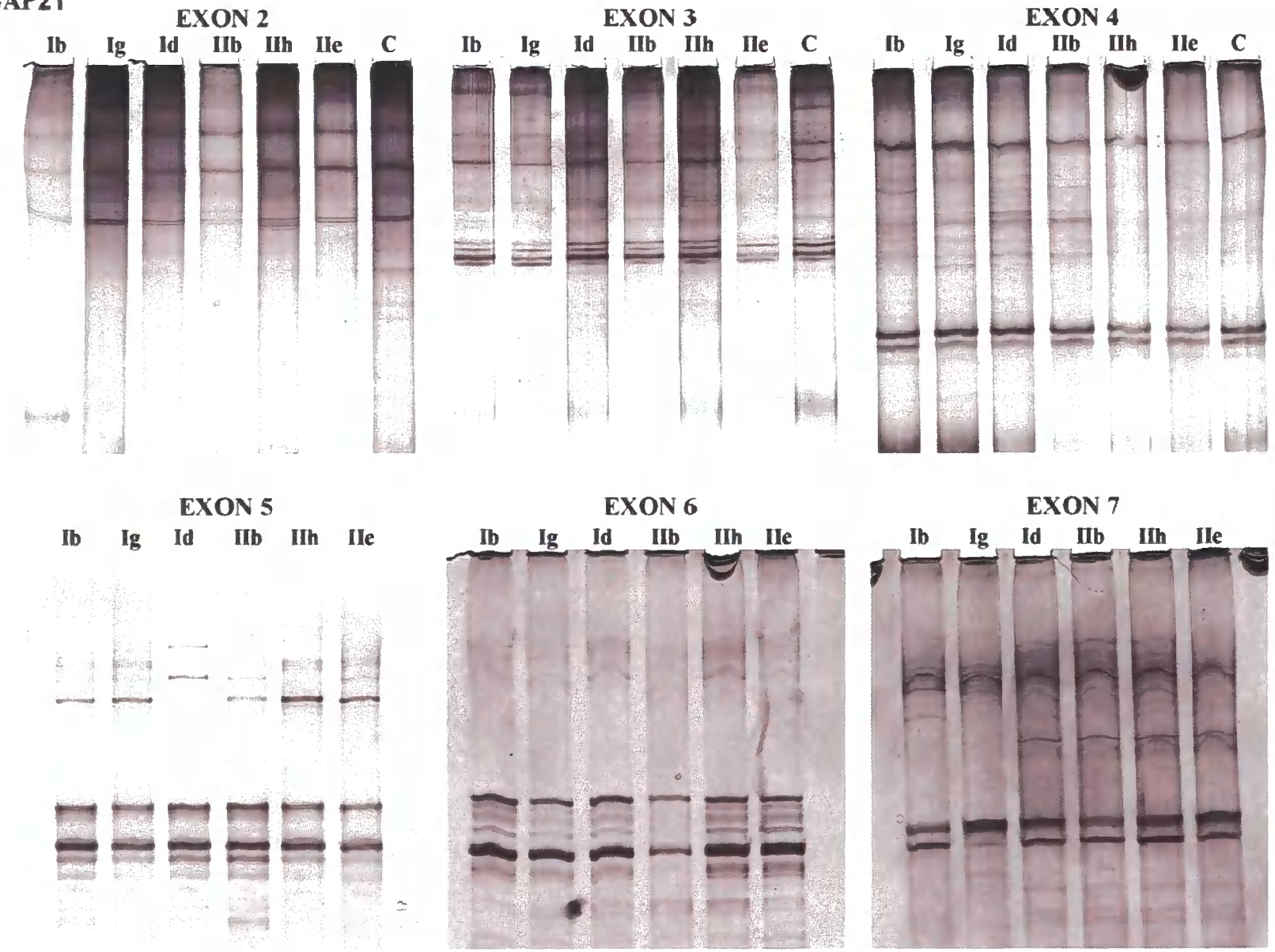
EXON 2
Ib Ig Id IIb IIh IIe C
EXON 3
Ib Ig Id IIb IIh IIe C
EXON 4
Ib Ig Id IIb IIh IIe C
EXON 5
Ib Ig Id IIb IIh IIe
EXON 6
Ib Ig Id IIb IIh IIe
EXON 7
Ib Ig Id IIb IIh IIe

ARHGAP21

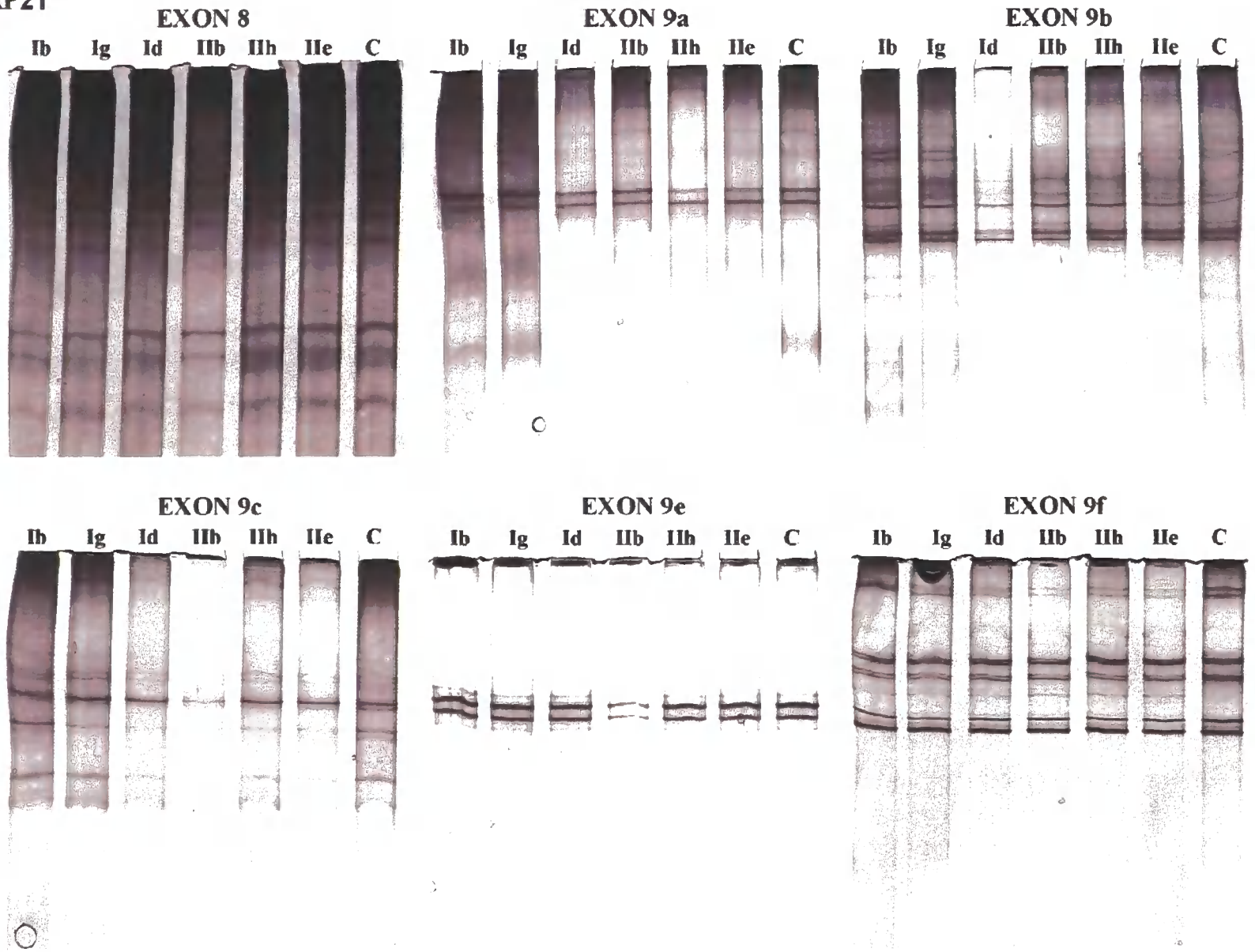
EXON 8
Ib Ig Id IIb IIh IIe C
EXON 9a
Ib Ig Id IIb IIh IIe C
EXON 9b
Ib Ig Id IIb IIh IIe C
EXON 9c
Ib Ig Id IIb IIh IIe C
EXON 9e
Ib Ig Id IIb IIh IIe C
EXON 9f
Ib Ig Id IIb IIh IIe C

ARHGAP21

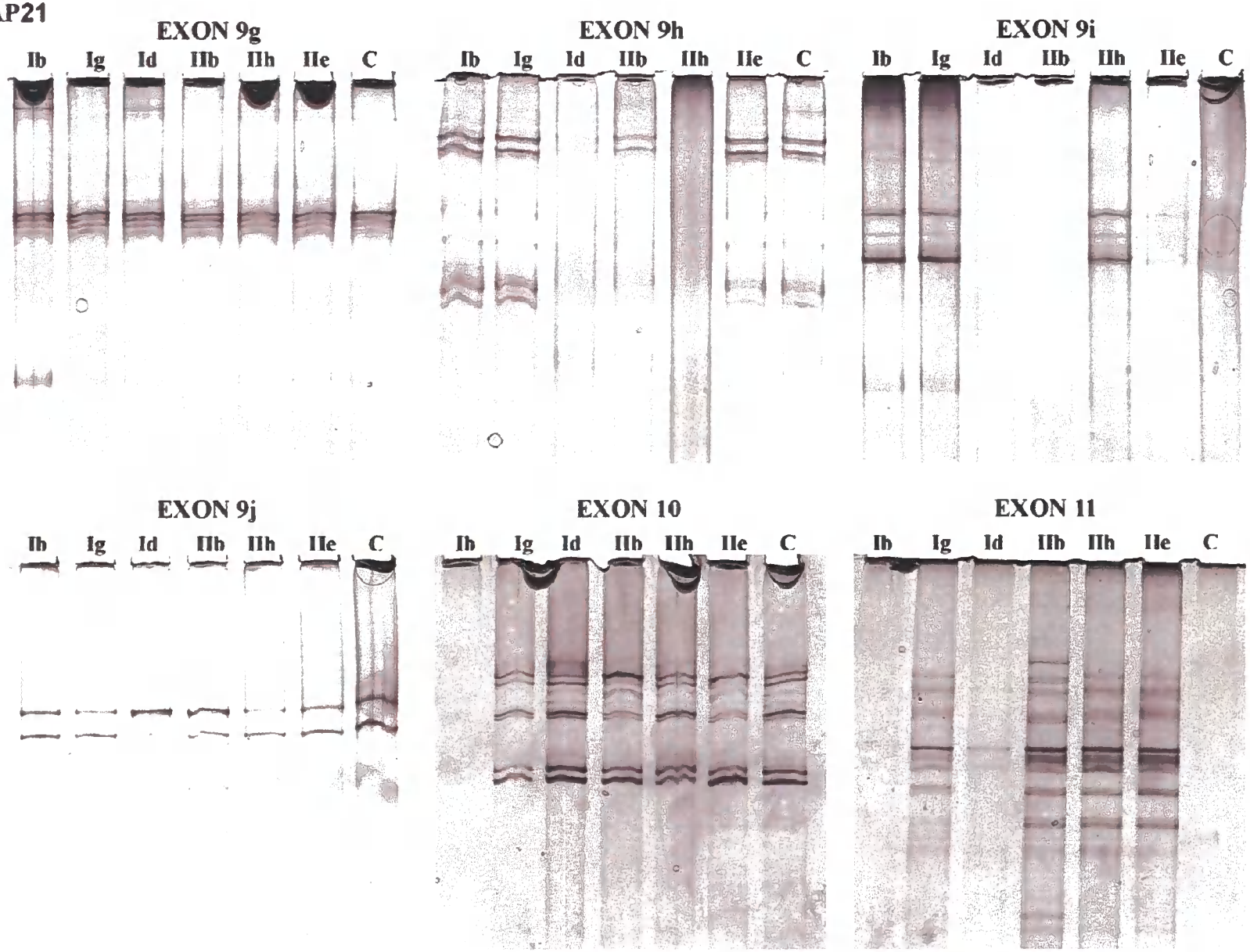
EXON 9g
Ib Ig Id IIb IIh IIe C
EXON 9h
Ib Ig Id IIb IIh IIe C
EXON 9i
Ib Ig Id IIb IIh IIe C
EXON 9j
Ib Ig Id IIb IIh IIe C
EXON 10
Ib Ig Id IIb IIh IIe C
EXON 11
Ib Ig Id IIb IIh IIe C

ARHGAP21

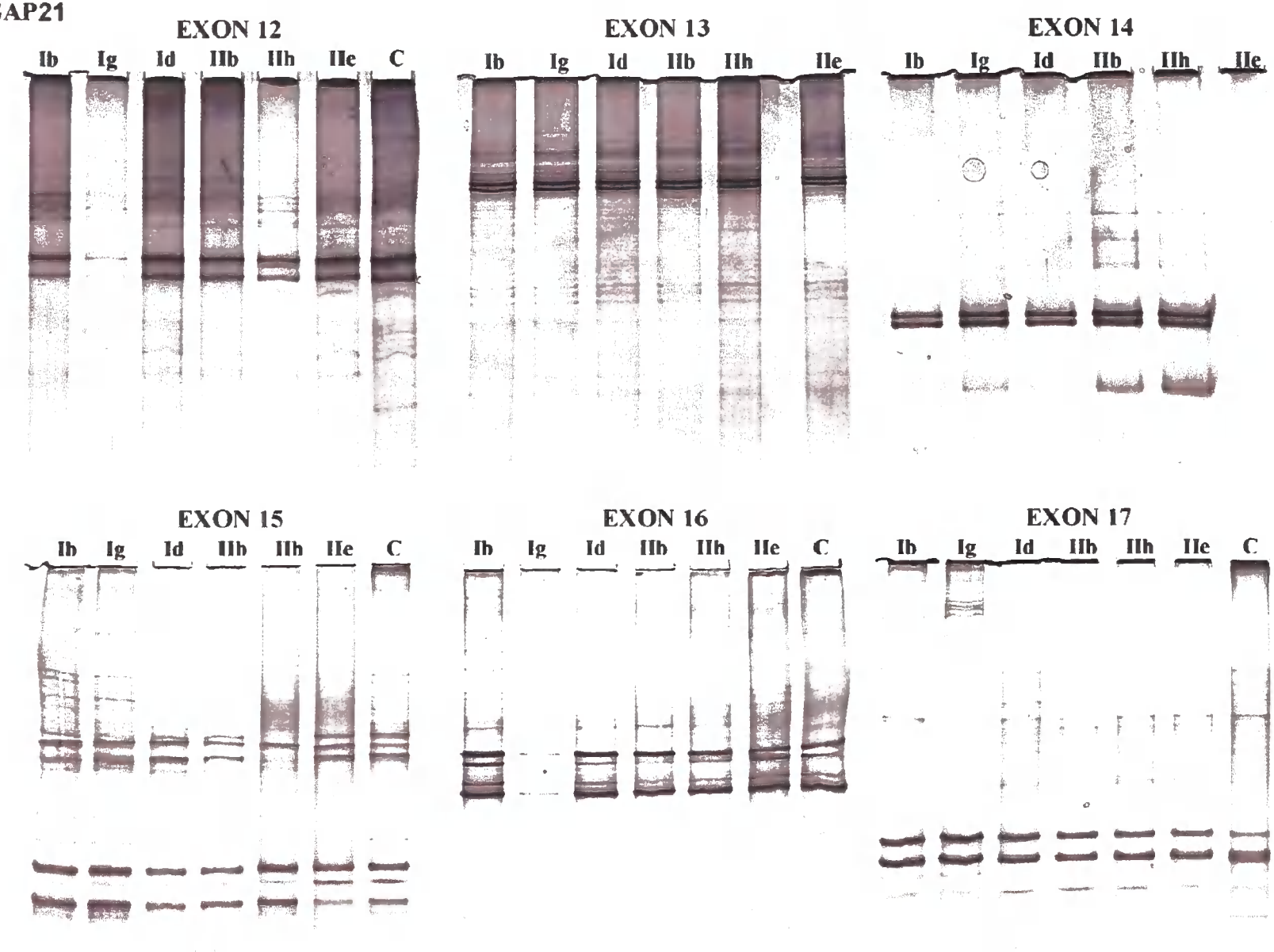
EXON 12
Ib Ig Id IIb IIh IIe C
EXON 13
Ib Ig Id IIb IIh IIe
EXON 14
Ib Ig Id IIb IIh IIe
EXON 15
Ib Ig Id IIb IIh IIe C
EXON 16
Ib Ig Id IIb IIh IIe C
EXON 17
Ib Ig Id IIb IIh IIe C

ARHGAP21

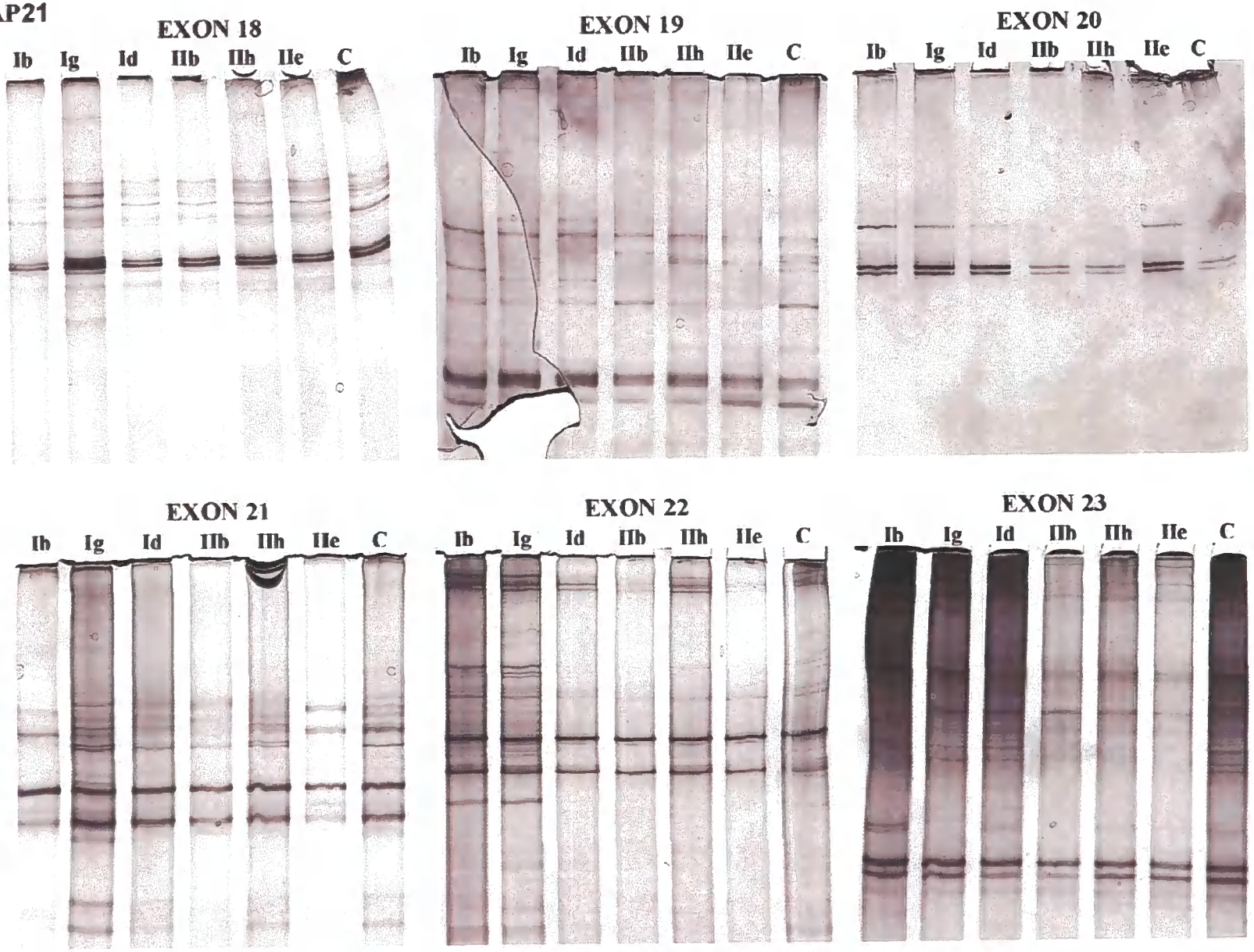
EXON 18
Ib Ig Id IIb IIh IIe C
EXON 19
Ib Ig Id IIb IIh IIe C
EXON 20
Ib Ig Id IIb IIh IIe C
EXON 21
Ib Ig Id IIb IIh IIe C
EXON 22
Ib Ig Id IIb IIh IIe C
EXON 23
Ib Ig Id IIb IIh IIe C

ARHGAP21

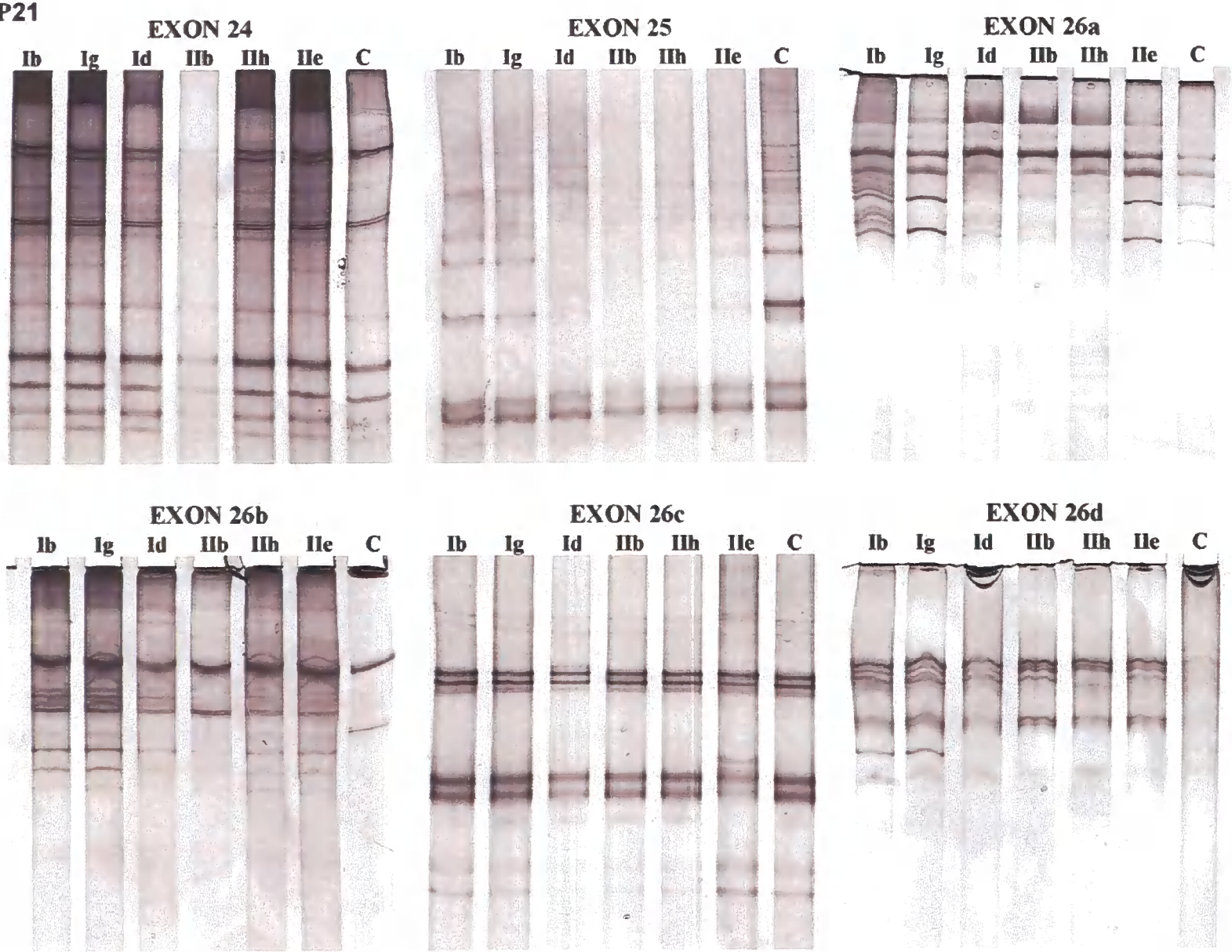
EXON 24
Ib Ig Id IIb IIh IIe C
EXON 25
Ib Ig Id IIb IIh IIe C
EXON 26a
Ib Ig Id IIb IIh IIe C
EXON 26b
Ib Ig Id IIb IIh IIe C
EXON 26c
Ib Ig Id IIb IIh IIe C
EXON 26d
Ib Ig Id IIb IIh IIe C

ARHGAP21

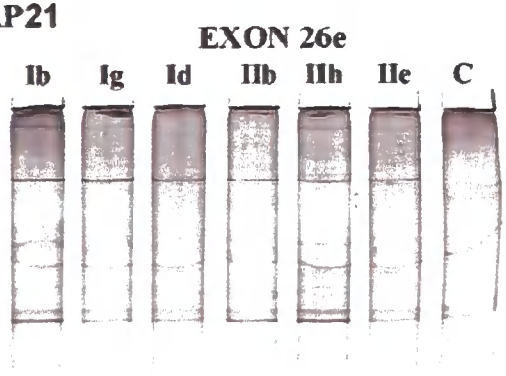
EXON 26e
Ib
Ig
Id
IIb
IIh
IIe
C

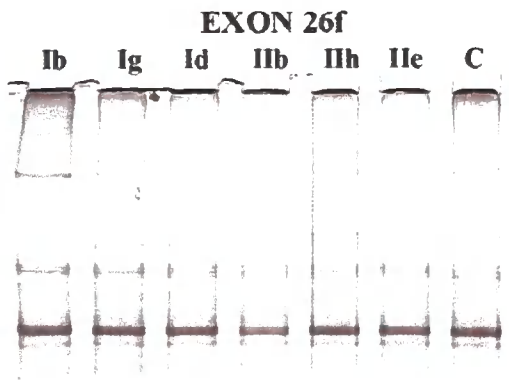
EXON 26f
Ib
Ig
Id
IIb
IIh
IIe
C

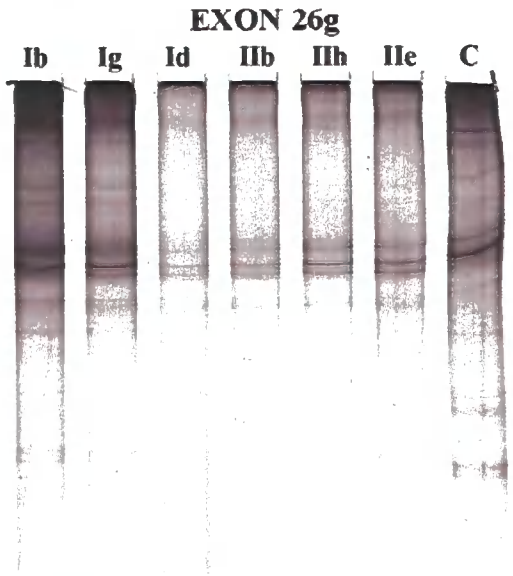
EXON 26g
Ib
Ig
Id
IIb
IIh
IIe
C

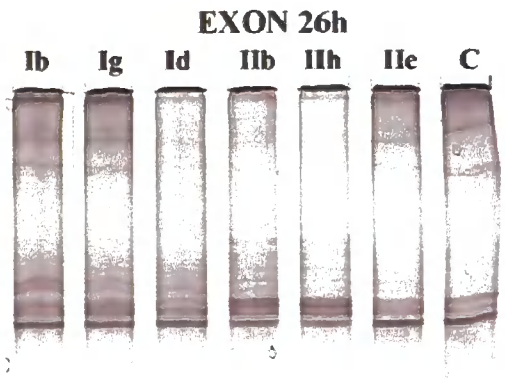
EXON 26h
Ib
Ig
Id
IIb
IIh
IIe
C

6.2.2 PRKCQ

The human PRKCQ gene that encodes PKC-θ (protein kinase C theta) was identified by Kofler et al (Kofler et al., 1998). It is located on the human chromosome 10p15 and consists of 18 exons.

The PRKCQ predominant isotype is expressed in skeletal muscle cells (Osada et al., 1992) and was shown to have increased expression in differentiating human muscle cells (Chalfant et al., 2000). Its expression in muscle cells and elevated expression during differentiation made this gene a strong candidate for SSCP screening.

PRKCQ is also expressed in haematopoietic tissues, platelets and testis (Osada et al., 1992) and was shown to have a role in T-cell activation and regulation of gene expression (Kofler et al., 1998).

16 out of 17 PCR reactions for this gene were amplified successfully and analysed by SSCP (exon 13 PCR amplifications were not successful).

SSCP analysis of exons 4 and 9 need to be repeated since the exon 4 banding pattern was not clear and exon 9 showed some banding inconsistency within the panel of samples. In exon 15, the two affected individuals, IIb and IIh show a different banding pattern compared to the carrier, IIe, from the same family. Repeating this exon in addition to DNA sequencing would clarify if this is a polymorphism or not.

Figure 6.2 SSCP gel analysis of PRKCQ gene

Exons 13 could not be amplified by PCR. However, gel scans of the rest of the exons are shown in this figure. From left to right of each gel are two affected individuals from family I (Ib and Ig) alongside one carrier from family one (Id), followed by two affected individuals from family II (IIb and IIh) alongside one carrier from the same family (IIe). In some exons a control sample was added. As explained previously both families have been excluded from chromosome 2-linked- MM.

PRKCQ

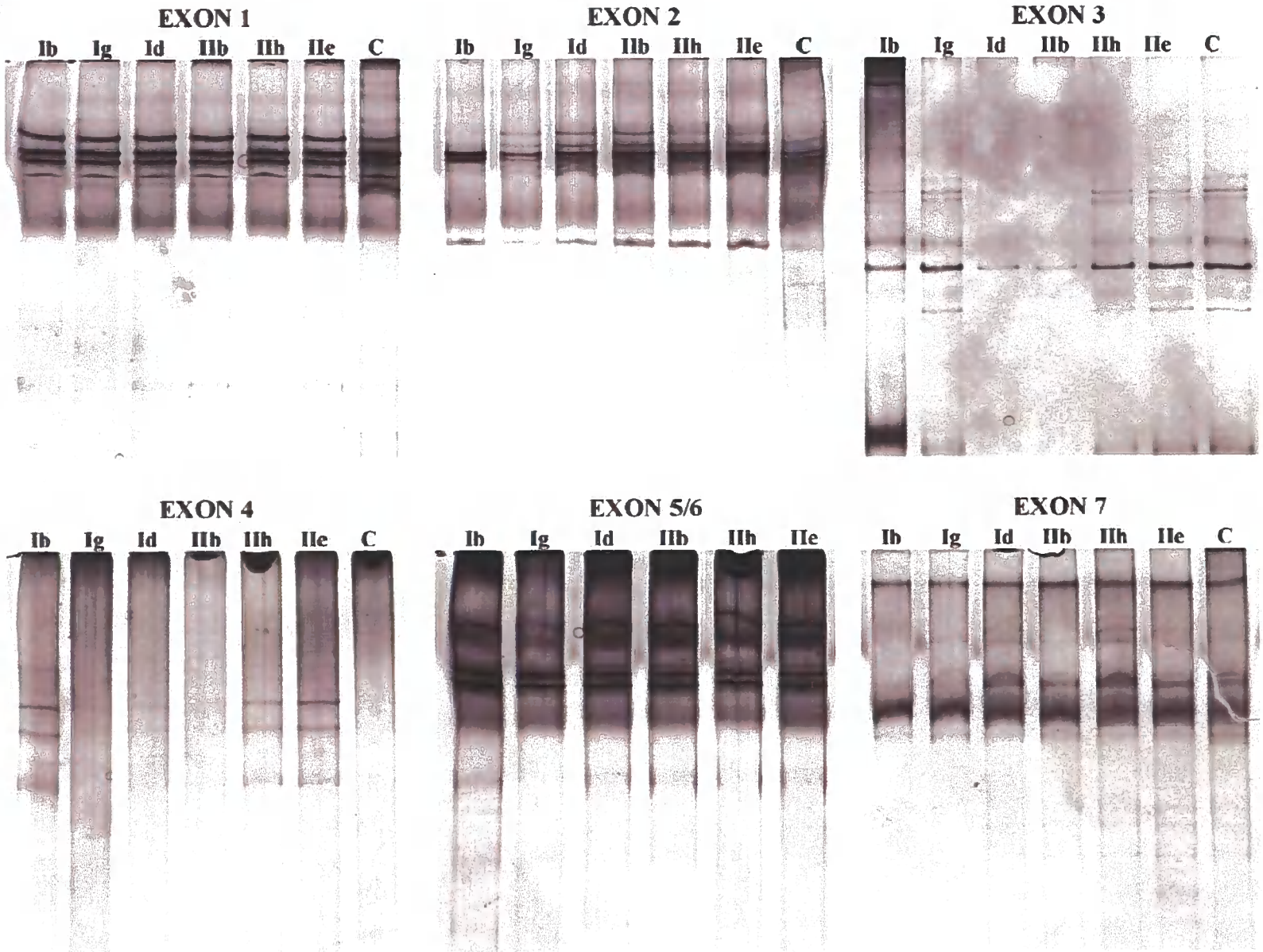
EXON 1
Ib Ig Id IIb IIh IIe C
EXON 2
Ib Ig Id IIb IIh IIe C
EXON 3
Ib Ig Id IIb IIh IIe C
EXON 4
Ib Ig Id IIb IIh IIe C
EXON 5/6
Ib Ig Id IIb IIh IIe
EXON 7
Ib Ig Id IIb IIh IIe C

PRKCQ

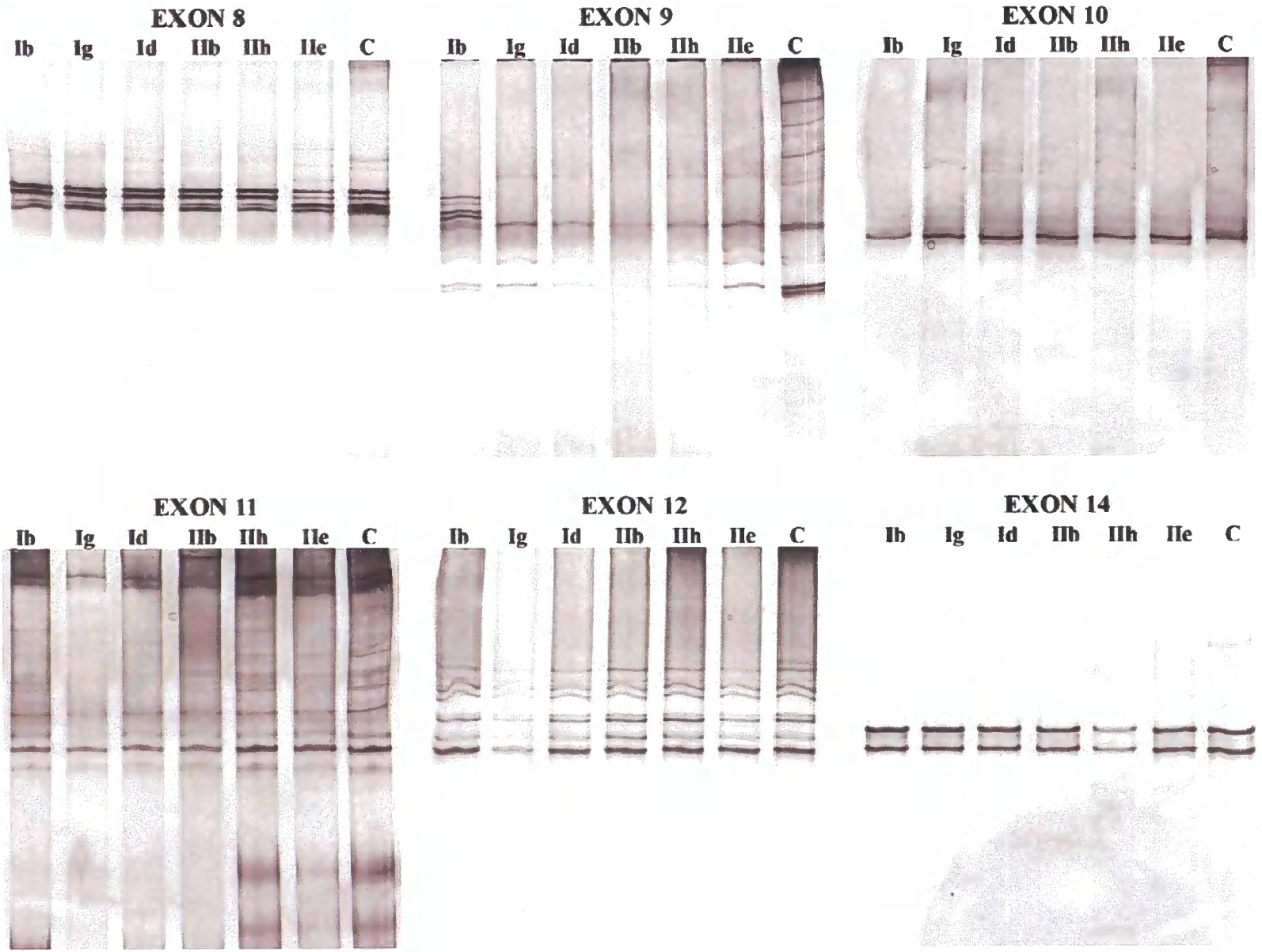
EXON 8
Ib Ig Id IIb IIh IIe C
EXON 9
Ib Ig Id IIb IIh IIe C
EXON 10
Ib Ig Id IIb IIh IIe C
EXON 11
Ib Ig Id IIb IIh IIe C
EXON 12
Ib Ig Id IIb IIh IIe C
EXON 14
Ib Ig Id IIb IIh IIe C

PRKCQ

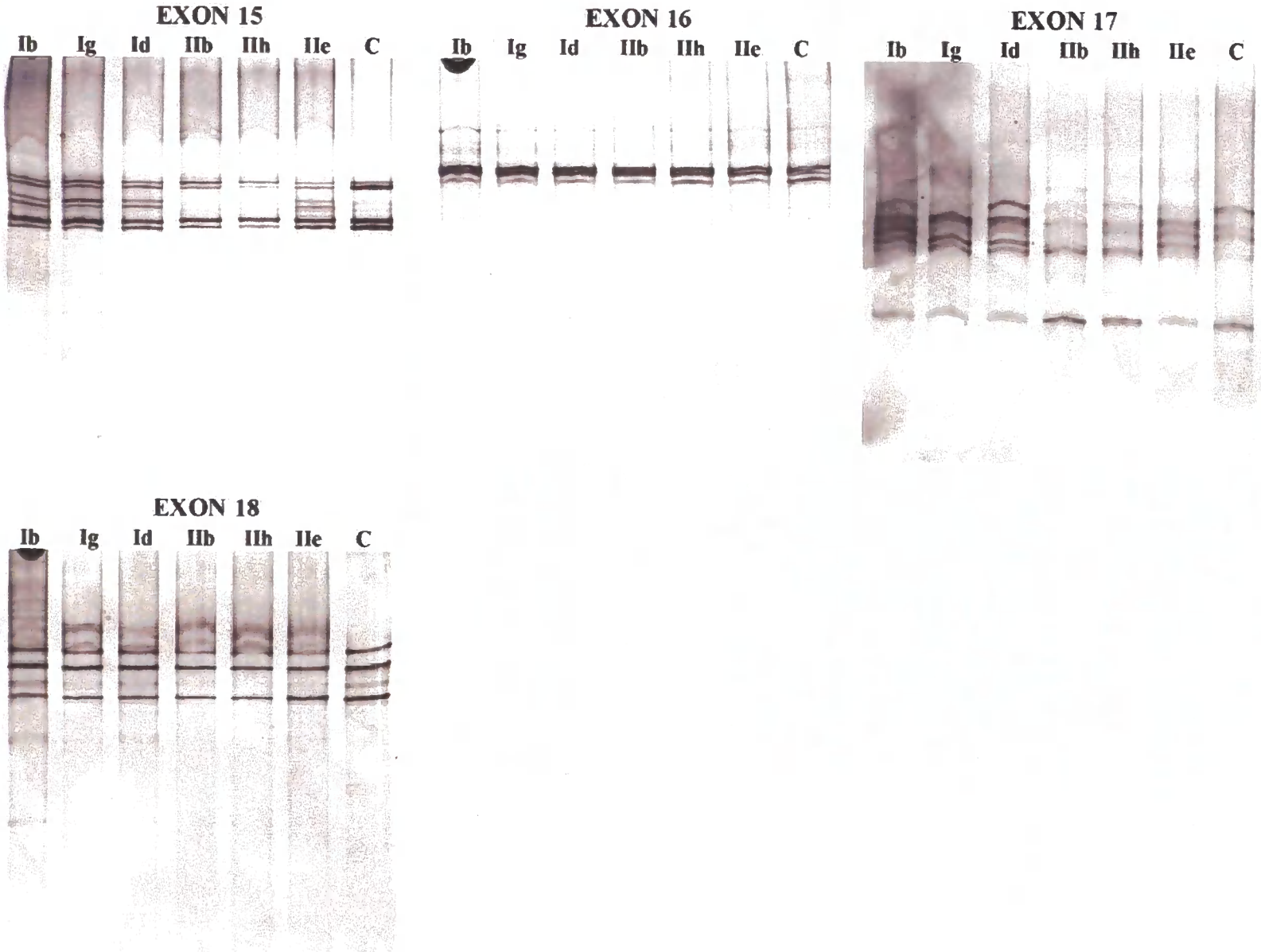
EXON 15
Ib Ig Id IIb IIh IIe C
EXON 16
Ib Ig Id IIb IIh IIe C
EXON 17
Ib Ig Id IIb IIh IIe C
EXON 18
Ib Ig Id IIb IIh IIe C

6.2.3 PTPLA

PTPLA (protein tyrosine phosphatase-like; proline instead of catalytic arginine, member A) was first identified by Uwanogho et al (Uwanogho et al., 1999). It maps to human chromosome 10p13-p14 and consists of 7 exons.

PTPs (Protein tyrosine phosphatises) has three members and are thought to mediate the dephosphorylation of phosphotyrosine, to be involved in signal transduction, cell growth, differentiation, and oncogenic transformation.

PTPLA is expressed in the developing and adult cells of the heart, skeletal muscle, liver and lungs. The early expression pattern of this gene and its continual expression in adult tissues suggest that it may have an important role in the development, differentiation, and maintenance of a number of different tissue types (Uwanogho et al., 1999) which made it a strong candidate for SSCP screening.

5 out of 6 PCR reactions for this gene were successfully amplified while exon 1 PCR amplifications were not possible. Exons 2, 3/4 and 7 need to be repeated since some samples show a variable banding pattern while exons 5 and 6 tend to show a consistent banding suggesting no polymorphism.

Figure 6.3 SSCP gel analysis of PTPLA gene

Exons 1 could not be amplified by PCR. However, gel scans of the rest of the exons are shown in this figure. From left to right of each gel are two affected individuals from family I (Ib and Ig) alongside one carrier from family one (Id), followed by two affected individuals from family II (IIb and IIh) alongside one carrier from the same family (IIe). In some exons a control sample was added. As explained previously both families have been excluded from chromosome 2-linked- MM.

PTPLA

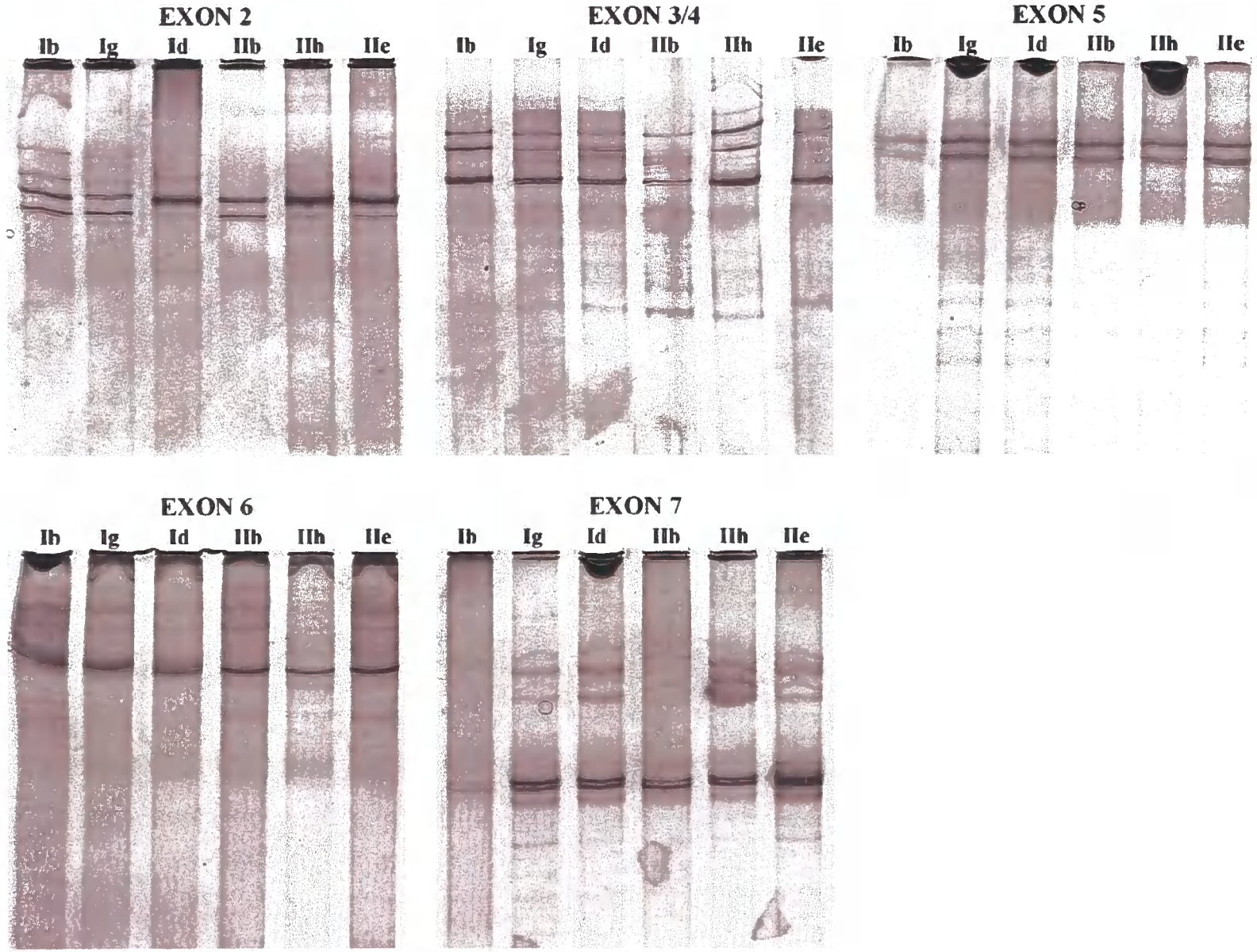
EXON 2
Ib Ig Id IIb IIh IIe
EXON 3/4
Ib Ig Id IIb IIh IIe
EXON 5
Ib Ig Id IIb IIh IIe
EXON 6
Ib Ig Id IIb IIh IIe
EXON 7
Ib Ig Id IIb IIh IIe

6.2.4 RAB18

RAB18 was first identified in humans by Schafer et al (Schafer et al., 2000). It localises to chromosome 10p12.1 and consists of 7 exons. It is a member of a family of Ras-related GTPases that regulate membrane trafficking in organelles and transport vesicles.

Rab18 is thought to be a component of Lipid droplets (LDs). Lipid droplets (LDs) are organelles that store neutral lipids, but their regulatory mechanism is not well understood. The function of RAB18 is still not properly understood but it is thought that it might have a role in regulating LD-associated membrane formation, that are involved in mobilizing lipid esters stored in LDs (Ozeki et al., 2005) or may relate to inflammation and some kinds of tumour (Dou et al., 2005).

All PCR amplifications for this gene were successful and were subjected to SSCP analysis. Out of the 7 exons, two need to be repeated (exon 3 and 6) but overall the general banding pattern obtained from these 5 exons indicates no evident polymorphism.

Figure 6.4 SSCP gel analysis of RAB18 gene

Gel scans of RAB18 exons analysed by SSCP are shown in this figure. From left to right of each gel are two affected individuals from family I (Ib and Ig) alongside one carrier from family one (Id), followed by two affected individuals from family II (IIb and IIh) alongside one carrier from the same family (IIe). In some exons a control sample was added. As explained previously both families have been excluded from chromosome 2-linked- MM.

RAB18

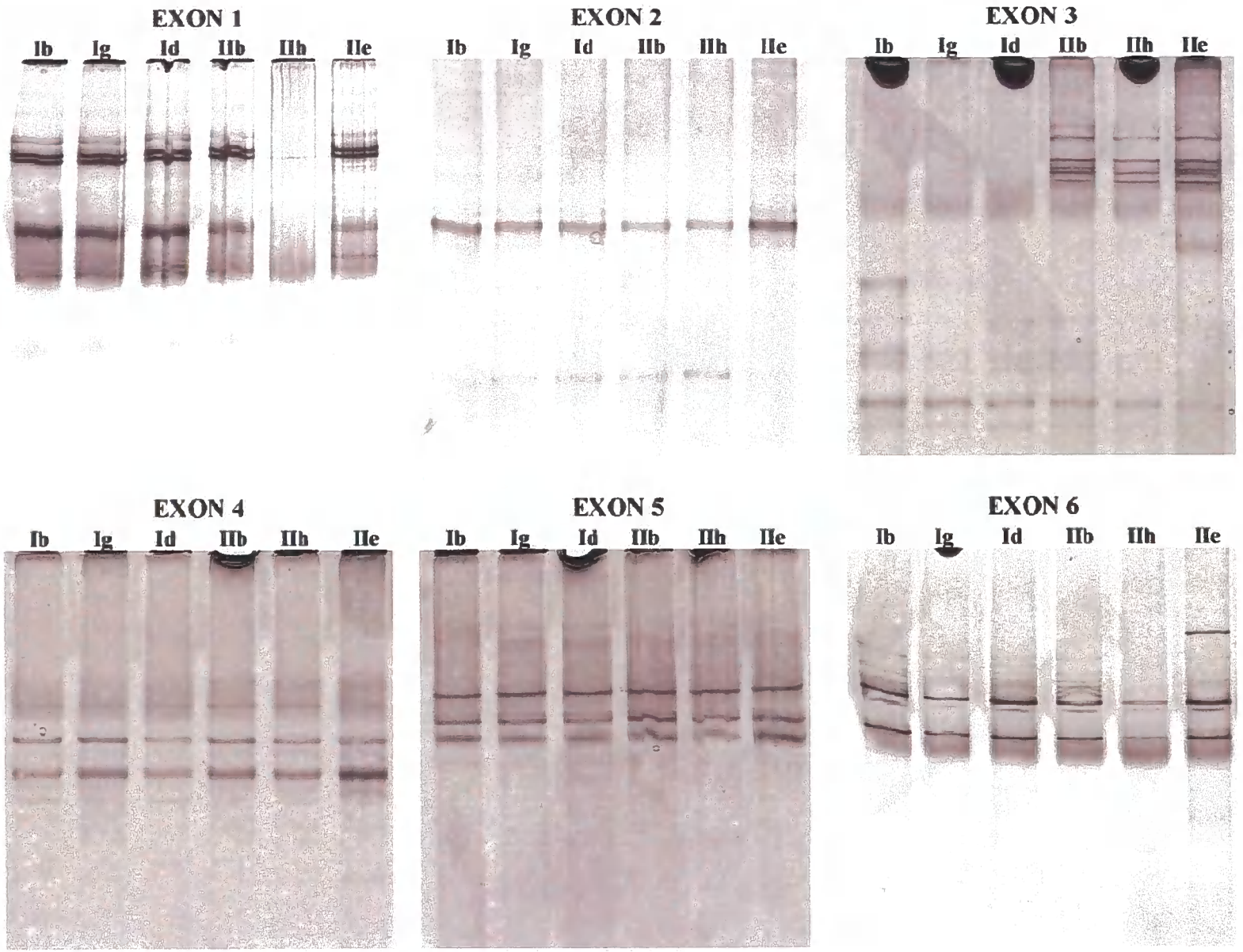
EXON 1
Ib
Ig
Id
IIb
IIh
IIe
EXON 2
Ib
Ig
Id
IIb
IIh
IIe
EXON 3
Ib
Ig
Id
IIb
IIh
IIe
EXON 4
Ib
Ig
Id
IIb
IIh
IIe
EXON 5
Ib
Ig
Id
IIb
IIh
IIe
EXON 6
Ib
Ig
Id
IIb
IIh
IIe

RAB18

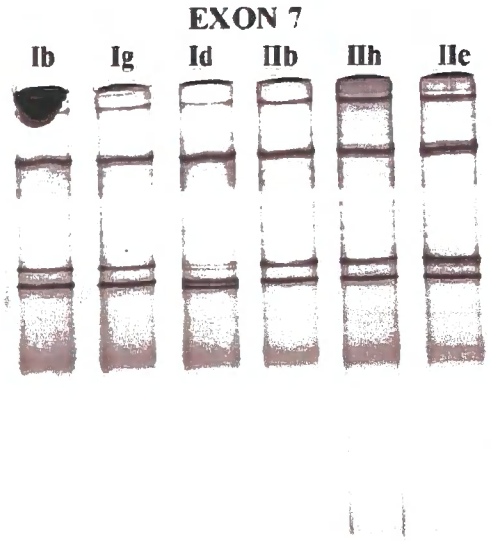

6.2.5 ANKRD26

Ankyrin repeat domain 26 (ANKRD26) or otherwise referred to as KIAA1074 is a protein of unknown function. It localises to the human chromosome 10pter-q22.1 and has 34 exons. It consists of several ankyrin repeat domains, in addition to a myosin tail domain.

Ankyrin repeats are protein-protein interaction motifs composed of tandemly repeated modules of amino acids and are mainly found in eukaryotic proteins with diverse functions such as transcriptional initiators, cell-cycle regulators, cytoskeletal, ion transporters and signal transducers (Bork, 1993). A group of muscle ankyrin repeat proteins are thought to be involved in muscle stress response pathways (Miller et al., 2003). In addition the ANKRD26 gene is thought to contain sequences similar to those found in the myosin tail domain and since myosin fibres are basic components of a muscle contractile unit, this gene was a strong candidate for the SSCP screening.

PCR amplifications of exons 11, 12, 13, 14, 15, 18, 19, 20, 30, 31, 32, 33, 34 of this gene were not possible but all the rest of the exons were successfully amplified and subjected to SSCP analysis. Few exons such as 1,2, 3, 16, 22, 24a, 26 and 27 need to be repeated to obtain and clear banding profile for these exons. Exon 2 in particular shows a different banding pattern for the carrier Id, therefore repeating this exons' SSCP analysis along with a control sample followed by genetic sequencing can clarify if this is a polymorphism or not. Interestingly exon 7 showed variable SSCP banding between the two families although within each family there is no evident polymorphism between affected and carrier subjects.

Figure 6.5 SSCP gel analysis of ANKRD26 gene

Exons 11, 12, 13, 14, 15, 18, 19, 20 could not be amplified by PCR. However, gel scans of the rest of the exons are shown in this figure. From left to right of each gel are two affected individuals from family I (Ib and Ig) alongside one carrier from family one (Id), followed by two affected individuals from family II (IIb and IIh) alongside one carrier from the same family (IIe). In some exons a control sample was added. As explained previously both families have been excluded from chromosome 2-linked- MM.

ANKRD26

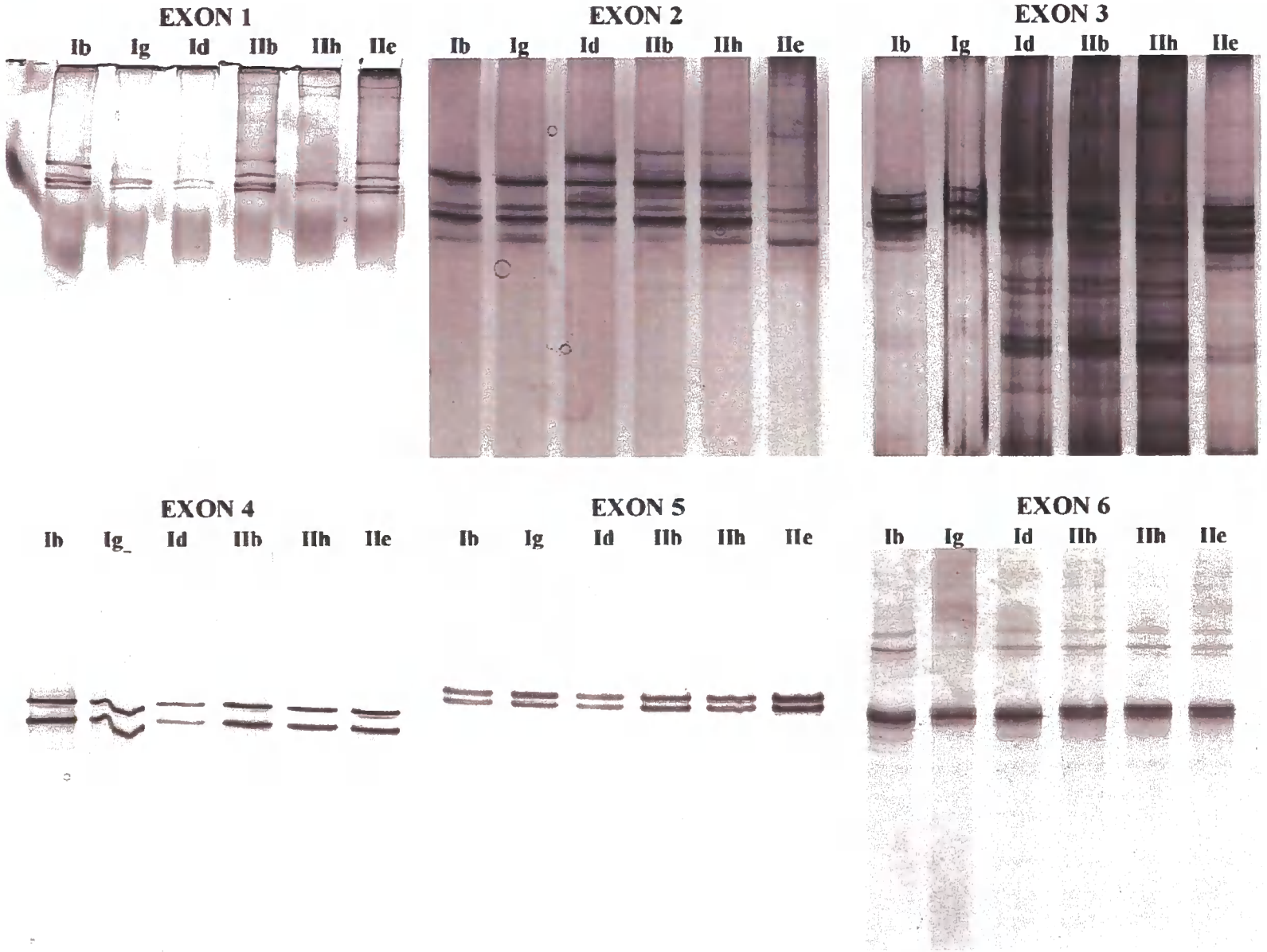
EXON 1
Ib Ig Id IIb IIh IIe
EXON 2
Ib Ig Id IIb IIh IIe
EXON 3
Ib Ig Id IIb IIh IIe
EXON 4
Ib Ig Id IIb IIh IIe
EXON 5
Ib Ig Id IIb IIh IIe
EXON 6
Ib Ig Id IIb IIh IIe

ANKRD26

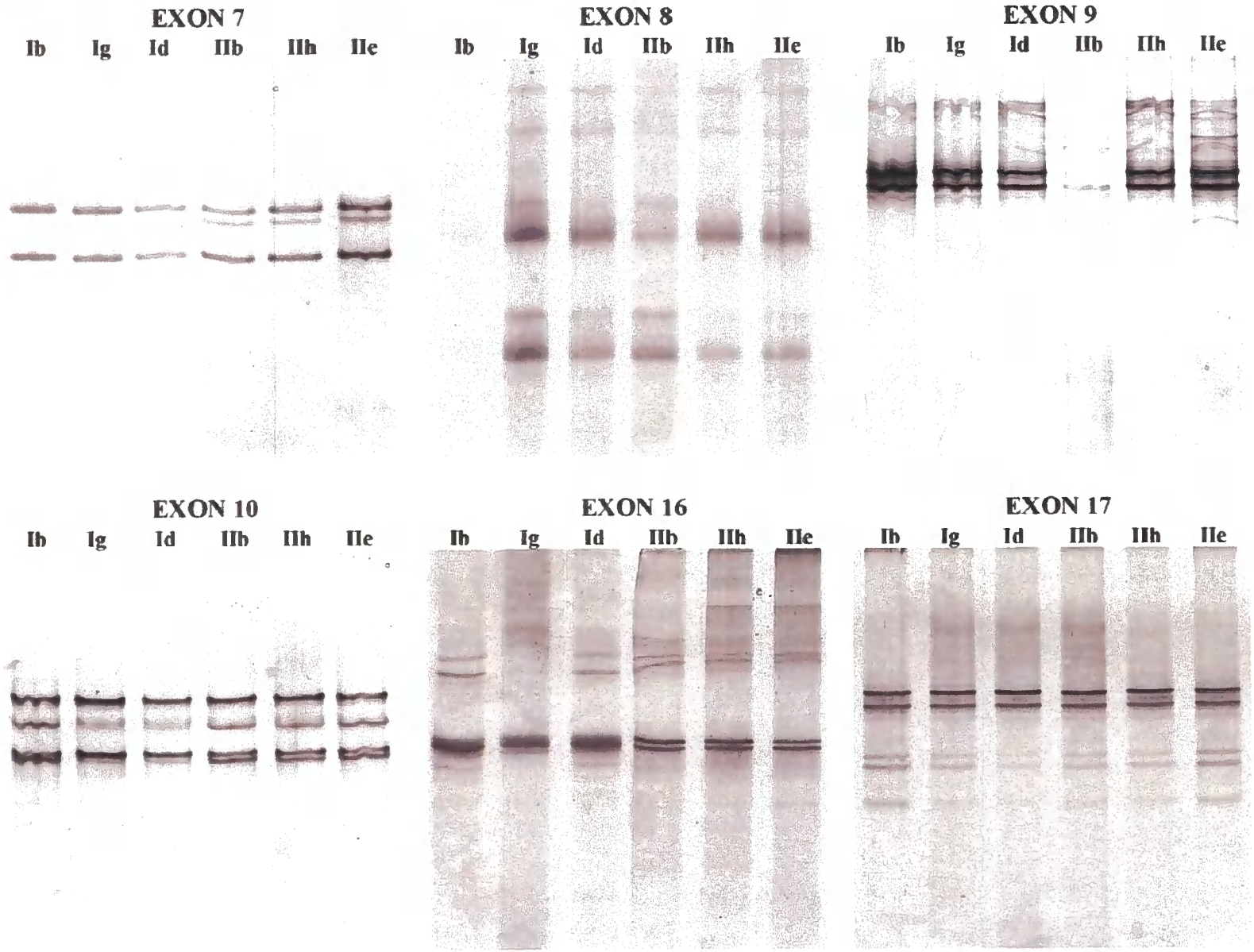
EXON 7
Ib Ig Id IIb IIh IIe
EXON 8
Ib Ig Id IIb IIh IIe
EXON 9
Ib Ig Id IIb IIh IIe
EXON 10
Ib Ig Id IIb IIh IIe
EXON 16
Ib Ig Id IIb IIh IIe
EXON 17
Ib Ig Id IIb IIh IIe

ANKRD26

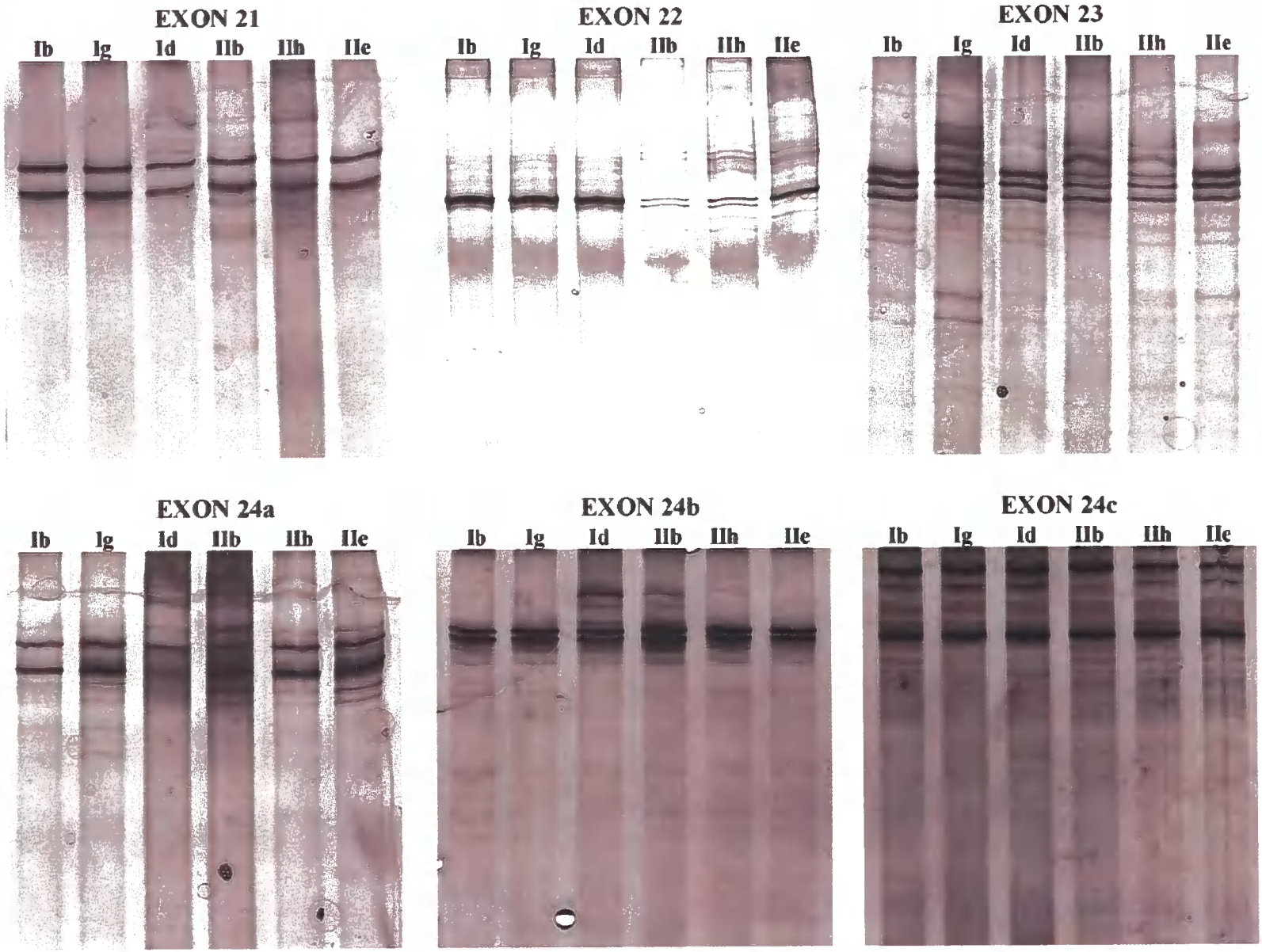
EXON 21
Ib Ig Id IIb IIh IIe
EXON 22
Ib Ig Id IIb IIh IIe
EXON 23
Ib Ig Id IIb IIh IIe
EXON 24a
Ib Ig Id IIb IIh IIe
EXON 24b
Ib Ig Id IIb IIh IIe
EXON 24c
Ib Ig Id IIb IIh IIe

ANKRD26

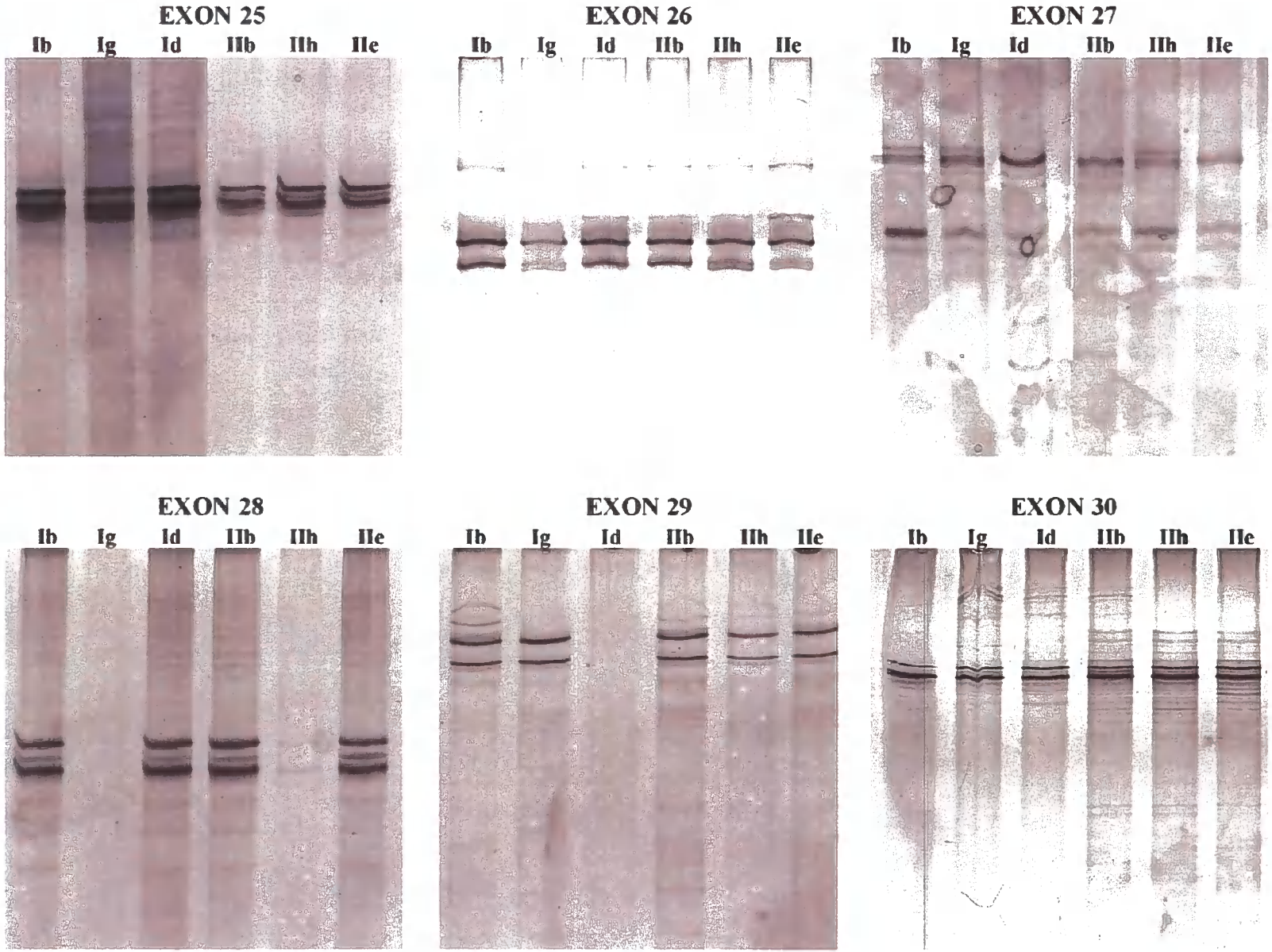
EXON 25
Ib Ig Id IIb IIh IIe
EXON 26
Ib Ig Id IIb IIh IIe
EXON 27
Ib Ig Id IIb IIh IIe
EXON 28
Ib Ig Id IIb IIh IIe
EXON 29
Ib Ig Id IIb IIh IIe
EXON 30
Ib Ig Id IIb IIh IIe

6.2.6 FLJ14813

MASTL (microtubule associated serine/threonine kinase-like) or FLJ14813 maps to the human chromosome 10p12.1 and consists of 12 exons. Since this work was performed mutations in this gene have been shown to cause autosomal dominant thrombocytopenia in humans (Gandhi et al., 2003). The function of the protein product of the FLJ14813 gene is still unknown. It belongs to the Serine/Threonine protein kinase family which contain the protein kinase C (PKC) enzymes and since the expression of nearly all PKC isoforms is known in human muscle (Itani et al., 2000) this made it a candidate for the SSCP screening in this project.

All PCR amplifications of this gene were done successfully. However, when analysed by SSCP few exons (1, 3, 4, 5,8a, 8c, 10, 11) need to be repeated in order to obtain a full SSCP profile but SSCP data obtained from the rest of the exons suggest no evident polymorphism.

Figure 6.6 SSCP gel analysis of FLJ14813 gene

Gel scans of FLJ14813 exons analysed by SSCP are shown in this figure. From left to right of each gel are two affected individuals from family I (Ib and Ig) alongside one carrier from family one (Id), followed by two affected individuals from family II (IIb and IIh) alongside one carrier from the same family (IIe). In some exons a control sample was added. As explained previously both families have been excluded from chromosome 2-linked- MM.

FLJ14813

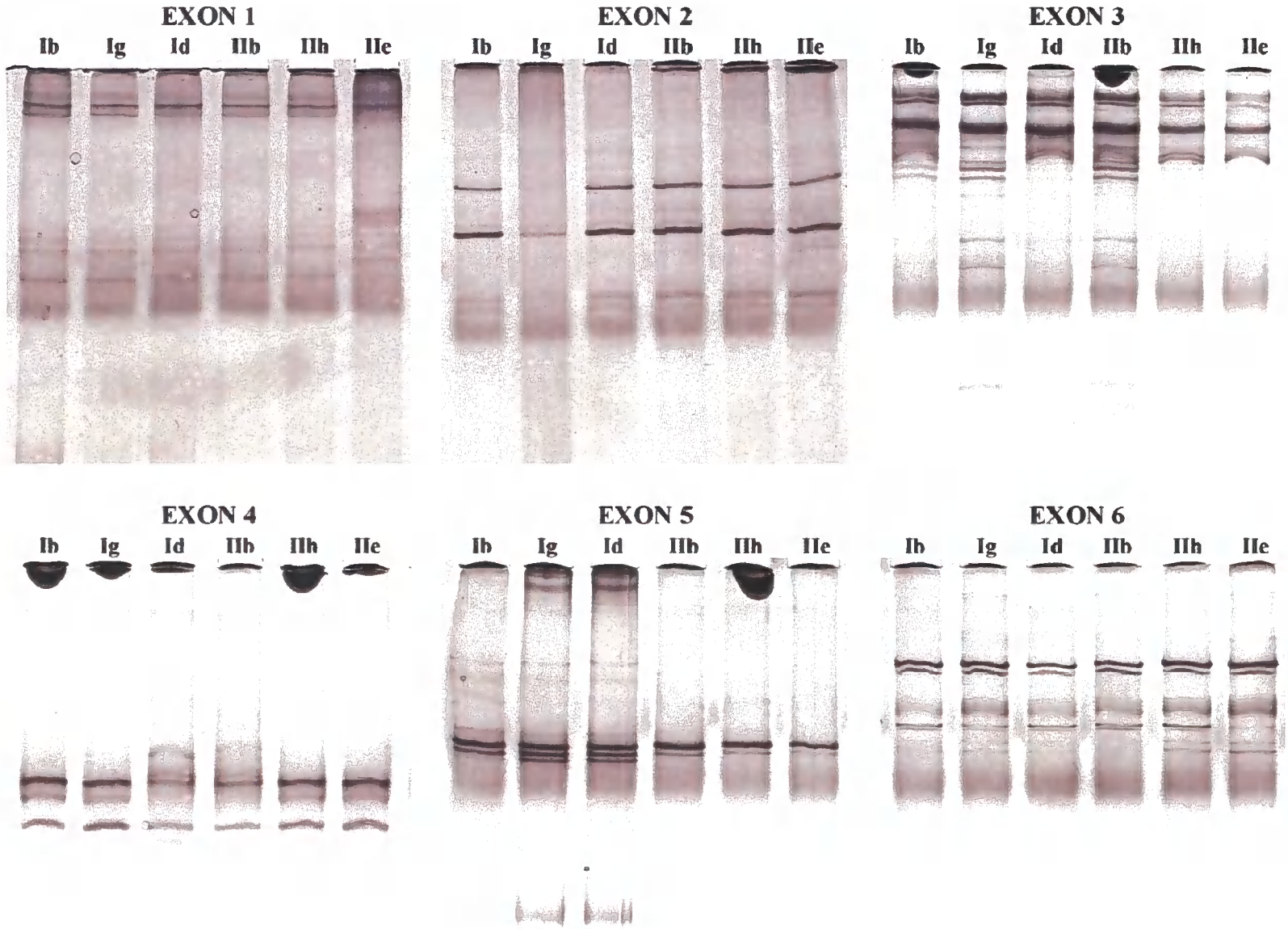
EXON 1
Ib Ig Id IIb IIh IIe
EXON 2
Ib Ig Id IIb IIh IIe
EXON 3
Ib Ig Id IIb IIh IIe
EXON 4
Ib Ig Id IIb IIh IIe
EXON 5
Ib Ig Id IIb IIh IIe
EXON 6
Ib Ig Id IIb IIh IIe

FLJ14813

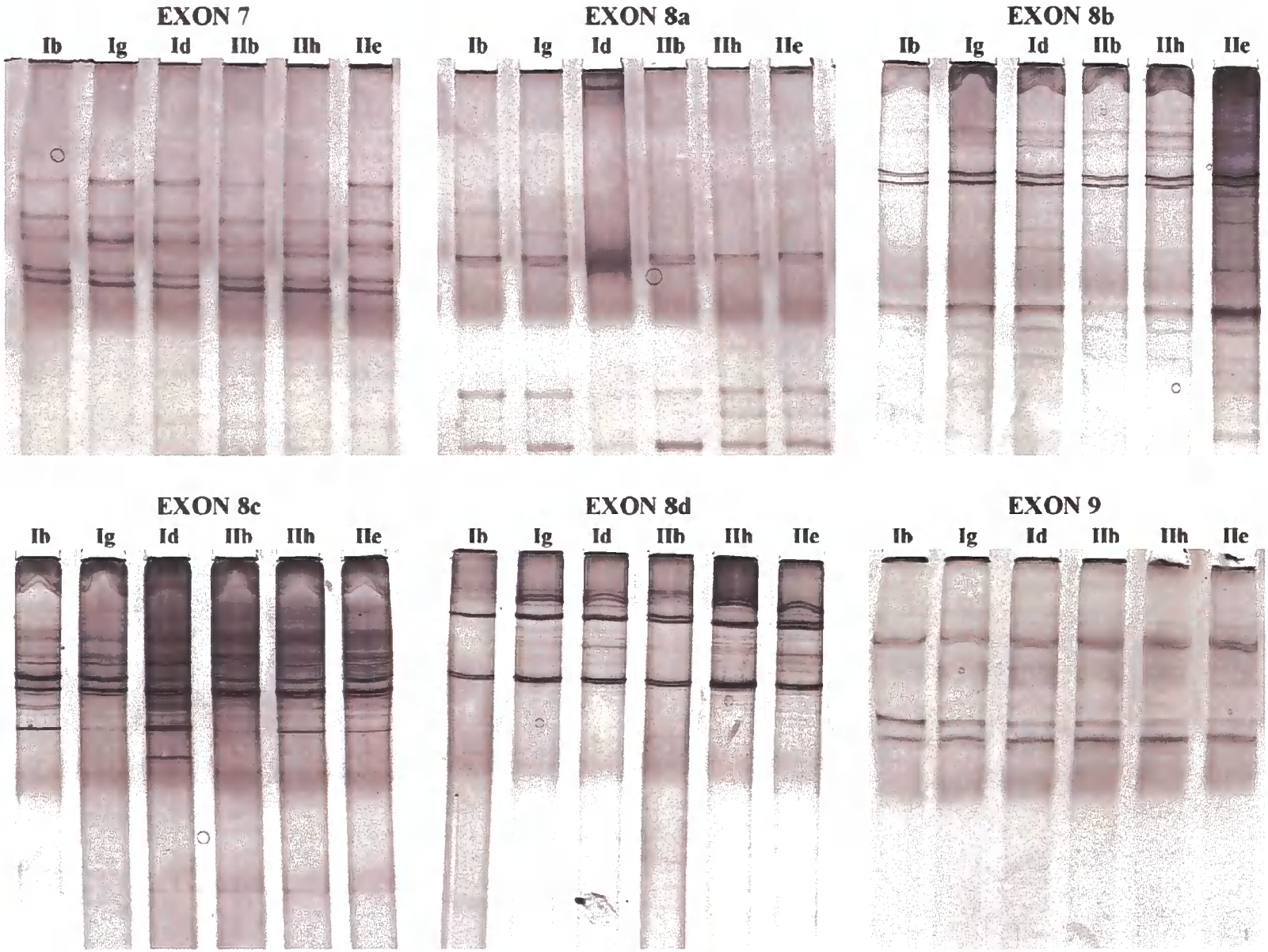
EXON 7
Ib Ig Id IIb IIh IIe
EXON 8a
Ib Ig Id IIb IIh IIe
EXON 8b
Ib Ig Id IIb IIh IIe
EXON 8c
Ib Ig Id IIb IIh IIe
EXON 8d
Ib Ig Id IIb IIh IIe
EXON 9
Ib Ig Id IIb IIh IIe

FLJ14813

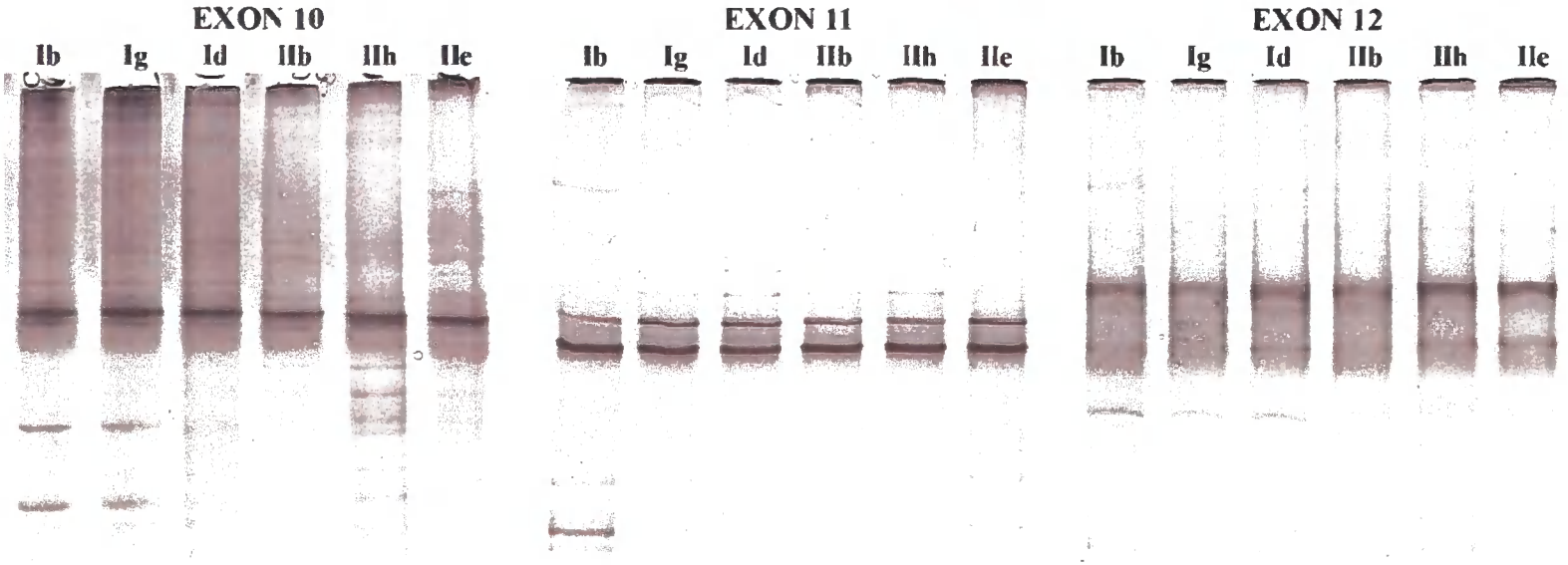
EXON 10
Ib
Ig
Id
IIb
IIh
IIe
EXON 11
Ib
Ig
Id
IIb
IIh
IIe
EXON 12
Ib
Ig
Id
IIb
IIh
IIe

6.2.7 Caveolin 3

As detailed in chapter 1 of this thesis, caveolin 3 is characteristically expressed in sarcolemma of muscle cells of all types and its expression is elevated during myoblast fusion (Tang et al., 1996). Caveolin 3 is also concentrated in developing T-tubule system of developing muscle but expressed at lower levels in the T-tubules of mature muscle (Parton et al., 1997). Caveolin 3 null mice are deficient in sarcolemmal caveolae but do not show evident clinical symptoms of LGMD1C even at old age as seen in humans as a result of caveolin 3 mutation, but they reveal variably sized muscle fibres, necrotic fibres and myopathic changes, indicating that caveolin 3 is needed in skeletal muscle cells for caveolar biogenesis (Razani & Lisanti, 2001) therefore making it a strong candidate for SSCP screening in non-dysferlin linked MM patients. Caveolin 3 was screened on a panel of 19 MM patients that were previously excluded by Dr. R. Bashir's group for mutations on chromosome 2 and 10.

Exon 1 sample panel gave a variable banding pattern which needs to be further investigated to exclude polymorphism while samples 4 and 5 from exon 2a need to be repeated. All samples from exons 2b showed a consistent banding pattern although in some lanes the bands were not reproducible when scanned. In exon 3, samples 1-9 PCR amplifications failed to work and again samples 15, 16 and 17 were not reproducible when gels were scanned

As explained earlier for reasons of resources and time it was only possible to conduct SSCP analysis once for each exon studied but in exons where PCR amplifications were not possible, redesign of primers combined with more time to optimise the PCR conditions could lead to successful amplification of these

exons in the future. However, in few other exons that were successfully amplified by PCR and analysed by SSCP, one or more of the samples need to be repeated either because their banding pattern was detectable by eye but have not been reproduced when the gels were scanned or because some lanes appeared to show differences in banding patterns when compared to the rest of the samples from the same exon. Although these samples need to be repeated because of apparent banding differences but the banding pattern in general obtained at the level of analysis adopted seem to be consistent with affected and carrier subjects suggesting no evident polymorphism.

Figure 6.7 SSCP gel analysis of Caveolin 3 gene

Caveolin 3 SSCP analysis was carried out on 19 MM patients that were excluded for chromosome 2 and 10 mutations. Exon 1 resulted in variable banding pattern which needs to be further investigated while samples 4 and 5 from exon 2a need to be repeated. All samples from exons 2b showed a consistent banding pattern although in some lanes the bands were not reproducible when scanned. In exon 3, samples 1-9 PCR amplifications failed to work and again samples 15, 16 and 17 were not reproducible when gels were scanned.

CAV3, EXON 1

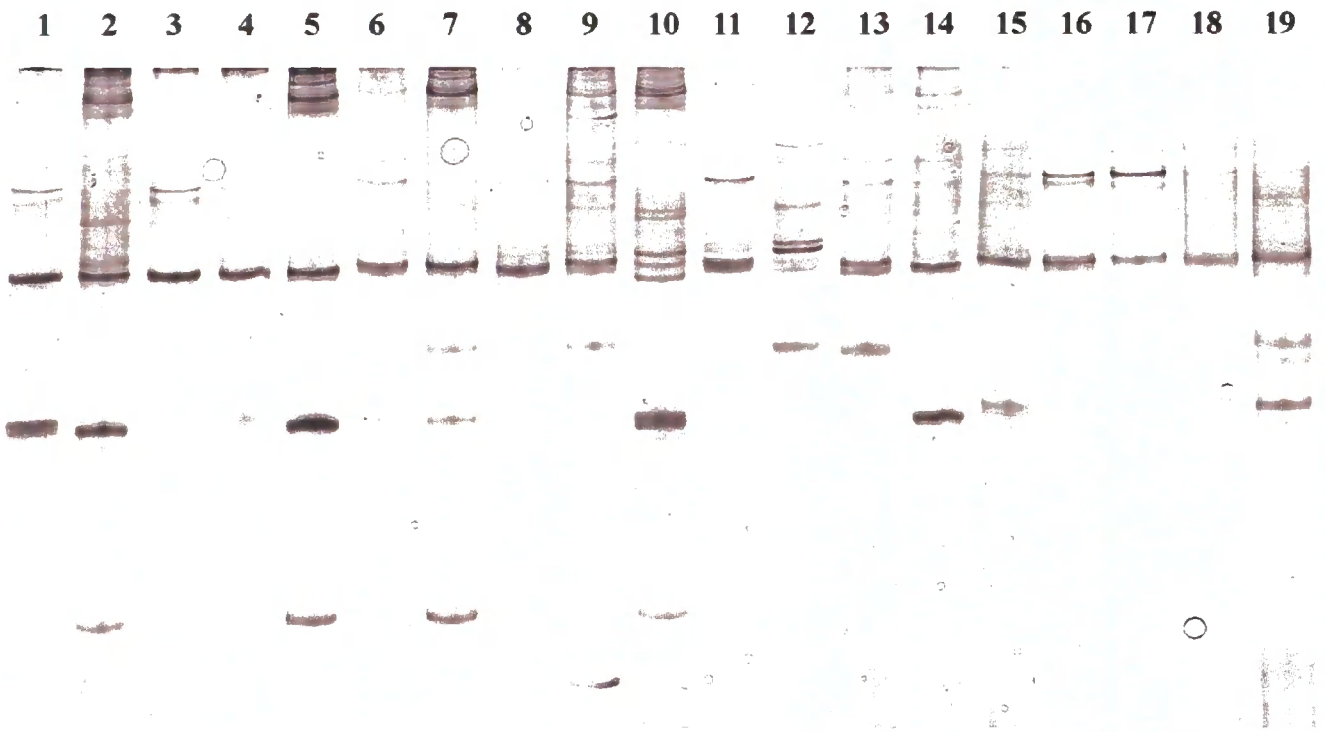

CAV3, EXON 2a

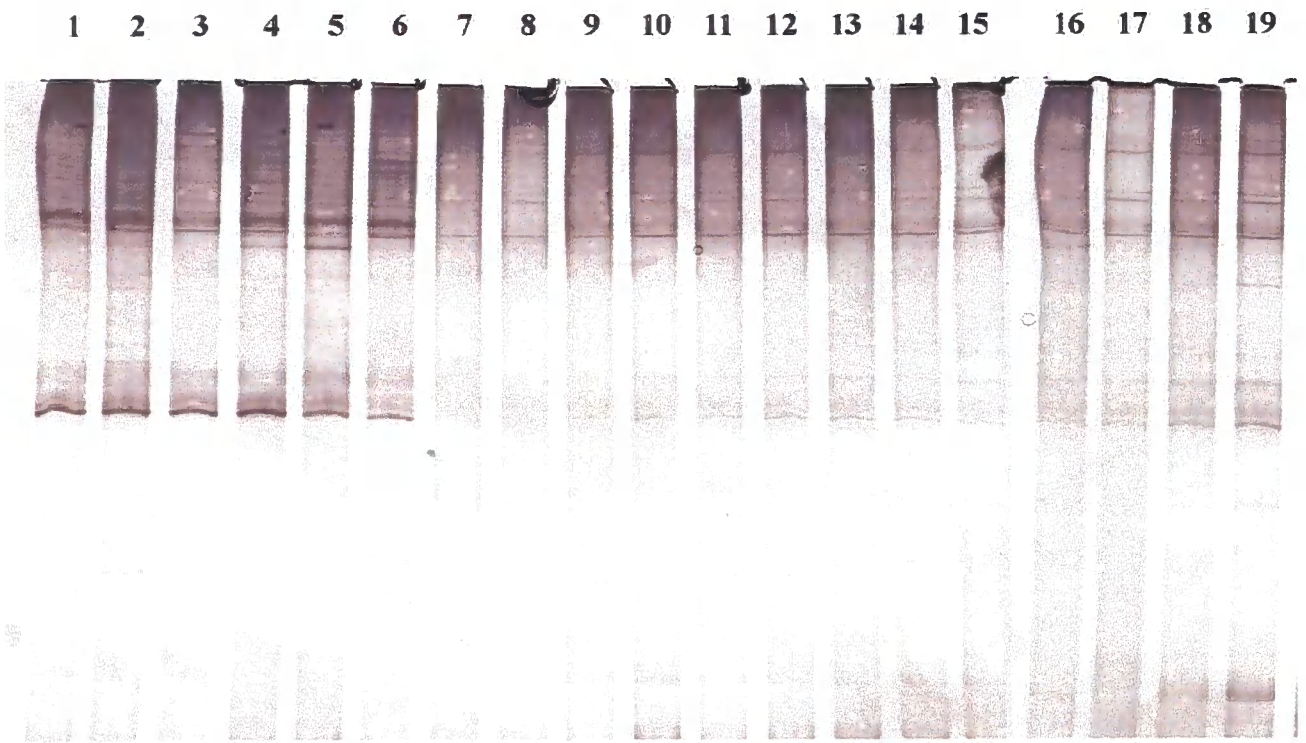

CAV3, EXON 2b

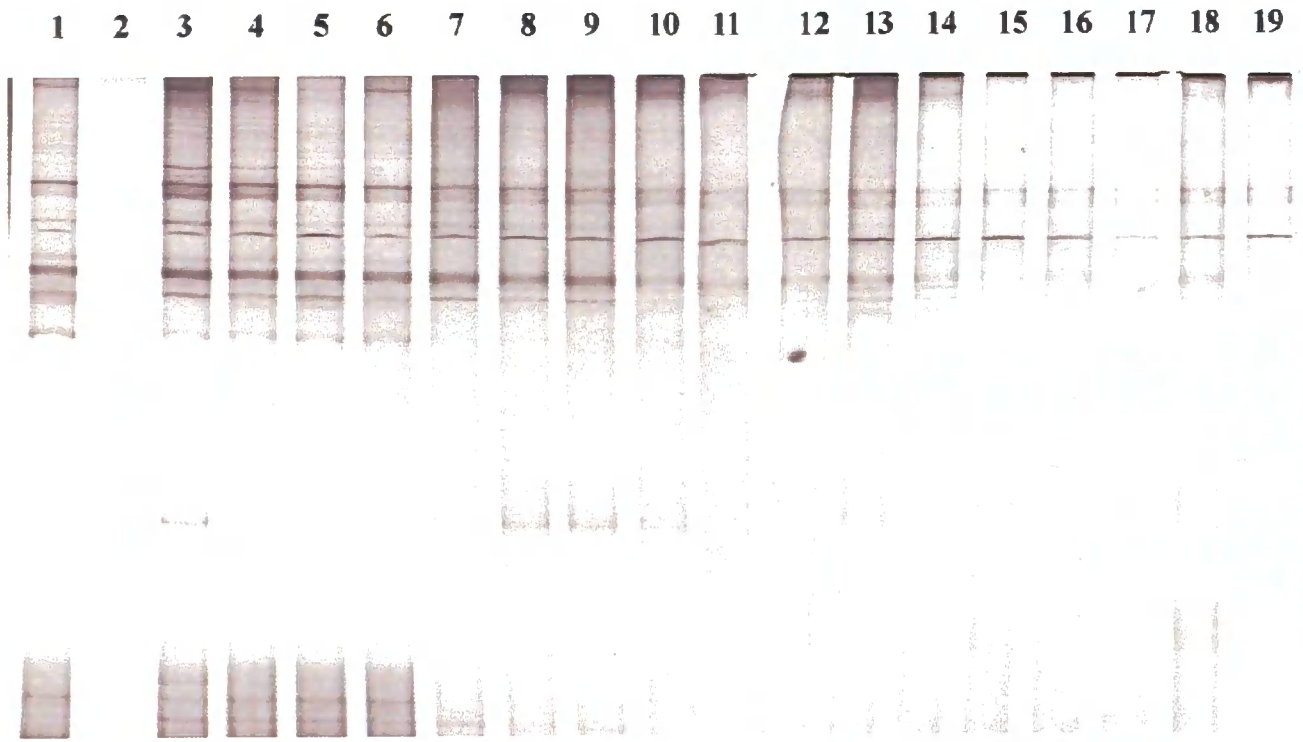

CAV3, EXON 3

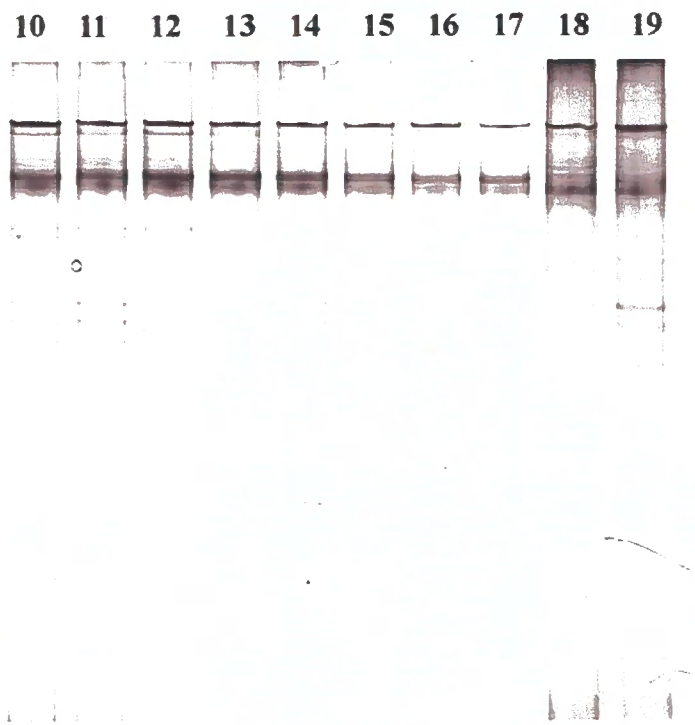

6.3 Summary

The experiments carried out in this chapter aimed to take a further insight to previous evidence that suggested the existence of a second gene responsible for MM, since not all MM patients showed linkage to chromosome 2.

In brief six genes located in or near the candidate region on chromosome 10 where chosen on the basis of their structure or function to be analysed by SSCP on affected and carrier individuals from two Dutch families excluded from linkage to chromosome 2.

In addition, 19 patients excluded from linkage to chromosome 2 and 10 were screened by SSCP on the caveolin 3 gene.

At the level of analysis adopted, there was no clear disease associated with polymorphism in these genetic loci. There are limitations in this data which preclude a definitive conclusion. Our approach was to examine polymorphism in the coding regions of the gene, as our hypothesis for disease associated mutation would be one of a change in structure of the gene product, but one possibility is that mutations in non-coding regions, potentially associated with changes in levels of expression or alternative splicing could still be present. In addition, although the vast majority of the coding regions of the six genes were analysed, there remains a possibility that mutations in those exons which could not be amplified remain to be detected. If further time and resource were available, the analysis of these exons would be completed. Finally, although the rationale for selecting the six candidate genes makes it more likely that they would contain the genetic mutations if present, there remain >100 other genes in this region of the chromosome, and these await further study.

7 Chapter Seven, Discussion

The objectives of this project were to conduct studies on muscular dystrophy associated genes. As explained in hypothesis section of chapter one of this thesis, one of these genes is myoferlin. Therefore one objective of this study was to investigate whether myoferlin might have a role in vesicle fusion similar to that of dysferlin and therefore be an essential component in membrane repair and other cellular functions of muscle cells such as differentiation. Other objectives of this study were to identify the genes that are thought to be responsible for MM genetic heterogeneity (i.e. in non-dysferlin-linked MM) such as that reported by Linssen et al (Linssen et al., 1998).

The results in the first part of this thesis have strongly suggested that FER1L3 is a myoferlin specific antibody and that myoferlin like dysferlin (Bansal et al., 2003) is enriched at plasma membrane disruption sites. However, further future experiments can be performed to enforce these findings. Although silencing mRNA, for example, to generate myoferlin-null cells is an arduous and time consuming method but generating myoferlin-null cells in the future and comparing FER1L3 antibody signal in these cells to wild type to see whether a total abolishment of signal from FER1L3 is observed or not would confirm the specificity of FER1L3 antibody.

In this project manual cell wounding combined with immunocytochemistry and confocal analysis were used to demonstrate myoferlin's enrichment at

plasma membrane disruption sites. However, another way to confirm that myoferlin's enrichment at the wound site is a specific response is to generate a GFP-myoferlin construct. Although GFP tagging has some disadvantages including the rate of successful transfection, the issue of GFP fusion proteins being generally over-expressed relative to endogenous proteins, or that the GFP tag might affect protein function but generating a GFP-myoferlin combined with live cell imaging and laser induced wounding could shed more light into myoferlin's localisation and mobilisation inside the cell and paint a clearer picture of what happens to myoferlin when plasma membrane disruptions are induced. A GFP-myoferlin construct was provided through collaborations but achieving a successful transfection level during the limited time of this project was not possible.

Another way of monitoring myoferlin's mobilisation during and after the induction of plasma membrane disruptions would be live cell imaging combined with laser induced wounding (Bansal et al., 2003) which can be used in studying plasma membrane repair or vesicle fusion at the site of plasma membrane disruption in cells lacking myoferlin or cells lacking both dysferlin and myoferlin.

As explained earlier in this project cell wounding was induced using a needle or glass beads. Therefore, most of the time only wounded cells could be distinguished from others rather than the specific site of injury in an individual cell. However, laser induced wounding similar to that used in confirming dysferlin's localisation to the injury site (Bansal et al., 2003) can give a more accurate answer to myoferlin's response to plasma membrane disruptions.

This method was successfully used in dysferlin-deficient and wild type muscle fibres where individual muscle fibres were injured using a multi-photon laser and imaged consecutively to show dysferlin enrichment at plasma membrane disruption sites (Bansal et al., 2003).

Immunogold labelling of myoferlin can also be a valuable tool in studying myoferlin's localisation and mobilisation, giving a very high resolution and accuracy especially compared to immunoflorescence. This method was used successfully in localisation of caveolin 1 in vascular smooth muscle cells (Robenek et al., 2003). Since it is known that perfecting the method for a specific antigen may need considerable time and resources immunogold labelling was not an option during this project. However, investing time and resources into this method can lead to a better understanding of myoferlin.

Laser capture micro-dissection in single cells (Benoyahu et al., 2005) or Real Time PCR in a group of cells (Sanchez et al., 2006) is another approach for future work since in requires a vast amount of time to set up in addition to resources. Laser capture micro-dissection has been used to successfully used to examine gene expression profiling in individual skeletal muscle cells (Benoyahu et al., 2005) suggesting that it could also be applied in future work in relation to myoferlin expression. This method will determine if even a sudden and one-off cell membrane injury induces the immediate transcription and translation of myoferlin therefore resulting in the enrichment seen at the site of plasma membrane disruption or if this enrichment is only the result of redistribution of the already expressed myoferlin inside the cell since it has

been shown that cells that undergo repeated cycles of plasma membrane disruption such as cells of *mdx* mice have upregulated myoferlin expression (Davis et al., 2000).

In a very recent study, Myof2 antibody was used to demonstrate that immunoreactivity of this anti-myoferlin antibody in dysferlin deficient muscles was only slightly weaker in intensity compared to controls. In addition, immunoblot analysis showed that myoferlin expression was similar in dysferlin-deficient muscle when compared to normal muscle. These results suggest that although myoferlin is upregulated in dystrophin-deficient muscle, the compensatory over-expression of myoferlin is not detected in dysferlin-deficient muscle (Inoue et al., 2006).

In the second part of this research the addition of a new member of the DysF ferlin protein family, named FER1L5 was reported as a part of this study's objective of studying muscular dystrophy associated genes. Although the results strongly suggested that FER1L5 is not a pseudogene and that like the other two members of the DysF ferlins its expression is elevated during myoblast differentiation, its involvement in muscular dystrophy is unknown and needs further investigation. The FER1L5 antibody used in this study did not give positive results by immunocytochemistry at the time these experiments were conducted and the results obtained could not be confirmed by confocal microscopy analysis.

Generating another FER1L5 antibody or the use of *in situ hybridization* can be the first steps in a better understanding of FER1L5 and to confirm the results reported in this project. In addition to similar experiments to those of

myoferlin can be carried out to study FER1L5 s cellular localisation and response to plasma membrane disruptions. *In situ hybridisation* has been successfully used in human skeletal muscle fibres to detect myosin heavy chain expression at the protein and mRNA level and could have similar implications in myoferlin's study (Serrano et al., 2001).

Generating a GFP-FER1L5 construct like that of myoferlin can provide a useful tool in understanding the role of FER1L5. Generating FER1L5-null mice can be problematic in terms of time needed or for example if the absence of the FER1L5 gene proves to lack a phenotype or is lethal, but either method, if successful, can clarify the role of FER1L5 at cellular and muscular function in general and help us understand the need for three highly similar proteins and their possible compensatory role in each others absence.

Recently a new sequence, also named FER1L5 was submitted on the National Centre for Biotechnology Information website. It is located on the human chromosome 8q24.13 and so far nothing is known about its function. This opens the possibility to the addition of a sixth member to the ferlin protein family and as research continues on this field the addition of more members is likely.

In the third section of this project, myoferlin's possible colocalisation with other cellular structures was investigated. Myoferlin was found to be partially colocalising with vesicles from the ER. This could not be further investigated at the time of this project but future work by immunogold labelling or live cell

imaging can help in understanding myoferlin's vesicle circulation inside the cell. These techniques can also be used to study what happens to myoferlin which is found at the site of plasma membrane disruption post recovery, whether these vesicles are degraded, recycled or simply redistributed into the cell is still unclear.

Another experiment for future work would be high resolution fractionation. Although density gradient fractionation on cellular membranes was performed early in this project, the results did not give conclusive results to where exactly myoferlin would be found. A high resolution fractionation combined with the use of a cell cracker (Rooney & Meldolesi, 1996) instead of homogenising cells using a hand-held homogeniser, such as the one used earlier in this project could clarify any possible colocalisation with other cellular compartments and confirm the partial colocalisation reported here with the ER.

High resolution fractionation could also be performed on cells pre-treated with LA-B and compared to untreated cells to confirm the change in distribution of myoferlin seen by immunocytochemistry in cells treated with LA-B.

And finally, the SSCP analysis performed in the last section of this thesis in search of MMD2 could benefit from future work. Revisionary work could lead to excluding some genes from the MMD2 candidate list and take us a step closer to identifying the MMD2 gene. However, a very recent study reported the identification and characterisation of a novel dysferlin transcript named *DYSF_v1*. This transcript differs from the currently known dysferlin transcript

in the sequence of the entire first exon which spans 232 bases. The first exons of *DYSF_v1,* is 85% homologous with the first exon of the mouse dysferlin and is derived from a region within intron 1 of the human dysferlin gene, driven by a distinct promoter and therefore has significantly closer homology to mouse dysferlin than the currently known human dysferlin. The expression of *DYSF_v1* transcript appears to be lower than that of the currently known transcript of dysferlin in both skeletal muscle (23%) and blood (12.6%) (Pramono et al., 2006). The identification of the new dysferlin transcript may hold the key to those non-dysferlin MM cases, as all previous screenings and genetic analysis focused on the currently known transcript. It may be that these non-dysferlin MM patients have a mutation in the new dysferlin transcript DYSF_*v1.*

Dysferlin associated proteins such as AHNAK and annexins A1 and A2 could be strong candidates for SSCP screening in MM patients excluded for chromosome 2 linkages. AHNAK is thought to be a candidate for SSCP screening because of its predominant expression in muscle and contractile cells (Gentil et al., 2003) and expression at the plasma membrane and its suggested regulatory role in Ca^{2+} homeostasis. Although AHNAK-null mice and ES cells showed no difference to wild type mice and cells, leading to the conclusion that AHNAK by itself had minimal or no affect on cell adhesion, tumorigenisis, proliferation and differentiation or overall mouse development (Kouno et al., 2004) but the possibility that this gene could have a role as a modifier gene in non-dysferlin MM has not been eliminated yet.

Annexins A1 and A2 are predicted to have a role in fusion and aggregation of intracellular vesicles in response to plasma membrane disruptions, and a role

in membrane trafficking and transmembrane channel activity (Lennon et al., 2003) and are therefore candidates for SSCP screening in non-dysferlin MM patients. Indeed, a very recent study showed that using an inhibitory antibody, a dominant negative mutant protein or a peptide competitor disrupt the function of annexin A1, resulting in defective membrane repair. In addition annexin A1 was found to be upregulated in LGMD2B and MM patients. These results suggest that annexin A1 is a requirement for successful plasma membrane repair by initiating homotypic and exocytotic membrane fusion events of resealing (McNeil et al., 2006).

Overall this project was aimed at studying genes and their proteins that might have a role or associated with muscular dystrophy or in specific MM.

Although the major bulk of this project was focused on myoferlin, its expression and role in membrane repair as a consequence of the curiosity raised by the attention given to its highly homologous protein, dysferlin which had left us with little information about myoferlin, but future work could shed more light on the third member of the DysF ferlin, FER1L5.

Identifying the complete set of genes involved in phenotypic variability of MM and understanding their role and their protein products in disease progression could have future therapeutic implications such as gene therapy for MM sufferers.

8 Abbreviations

2-DG	2-deoxyglucose
2-ME	2- Mercaptoethanol
AB	Antibody
APS	Ammonium persulfate
BFA	Brefeldin A
cDNA	Complementary deoxyribonucleic acid
CHO	Chinese Hamster Ovary
CK	Creatine Kinase
CREB	cAMP response element binding protein
DAPI	4', 6-Diamidino-2-phenylindole Dihydrochloride
DEPC	Diethyl pyrocarbonate
DGC	Dystroglycan Complex
dH_2O	Distilled water
DMD	Duchenne Muscular Dystrophy
D-MEM	Dulbecco's Modified Eagles Medium
DMSO	Dimethyl sulfoxide
DNA	Deoxyribonucleic acid
DNase	Deoxyribonuclease
EDTA	Ethylenediaminetetraacetic acid
EGTA	Ethylene-bis(oxyethylenenitrilo)tetraacetic acid
ER	Endoplasmic Reticulum
F-actin	Filamentous actin
FBS	Foetal Bovine Serum
GAPDH	Glyceraldehyde-3-phosphate dehydrogenase

GFP	Green Flourescent Protein
HDF	Human Dermal Fibroblasts
HEPES	N-(2-hydroxyethyl)piperazine-N'-(2-ethanesulfonic acid)
HMEM	HEPES-buffered minimal essential medium
HRP	Horseradish peroxidase
Kb	Kilobase
KDa	KiloDalton
LA-B	Latrunculin B
LGMD	Limb Girdle Muscular Dystrophy
LGMD2B	Limb Gridle muscular dystrophy type 2B
MM	Miyoshi Myopathy
MP	Milk Powder
mRNA	Messenger RiboNucleic Acid
MW	Molecular weight
NaN_3	Sodium azide
NRK	Normal Rat Kidney
oilgo(dT)	Oligodeoxythymidylic acid.
PAC	P1 derived Artificial Chromosome
PBS	Phosphate buffer saline
PKA	protein Kinase A
PKC	protein Kinase C
RIPA	RadioImmunoPrecipitation Assay Buffer
RNA	Ribonucleic acid
RT	Room Temperature
RT-PCR	Reverse Transcriptase Polymerase Chain Reaction

SDS	Sodium dodecyl sulfate
SDS-PAGE	Sodium dodecyl sulfate polyacrylamide gel electrophoresis
SLO	Streptolysin O
SNARE	Soluble N-ethylmaleimide-sensitive fusion (SNF) attachment protein (SNAP) receptors
SR101	Sulforhodamine 101
SSCP	Single strand conformational polymorphism
TBS	Tris Buffer Saline
TEMED	N,N,N′,N′-Tetramethylethylenediamine
Tween 20	Polyoxyethylene(20) sorbitan monolaurate

9 Appendix 1

Mowial	2.4 g Mowial 4.88, 6 g glycerol, 6 ml H2O, 12 ml 0.2 M tris base pH8.5, 10 µl 2 mg/ml DAPI
HES buffer	255 mM sucrose, 20 mM HEPES, 1 mM EDTA, pH 7.4.
5x sample buffer	1.5 g SDS, 3.75 ml 1 M tris pH6.8, 0.015 g DTT, 7.5 ml glycerol, 3.75 ml H2O
Transfer buffer	23.93 mM Tris, 193.15 mM glycine, 20% Methanol, pH 9.25.
Wash buffer	1% powdered milk, 0.2% Tween-20 in PBS.
Blocking buffer	5% fat free powdered milk (Tesco), 0.2% Tween-20 (sigma) in PBS
RIPA buffer	50 mM Tris HCl pH 8, 150 mM NaCl, 1% NP40, 0.5% sodium deoxycholate , 0.1% SDS
SSCP gel	30 ml Hydrolink-MDE (AT Biochem, USA), 3.6 ml 10x TBE, 6 ml 50% glycerol, 360 µl 10% APS, 55 µl TEMED, 20.4 ml H_2O
SSCP loading	95% v/v formaldehyde, 5% v/v 20 mM EDTA, 0.05% xylene, 0.05% bromophenol blue
Tank buffer	3.03 g Tris base, 14.41 g glycine, 1 g SDS in 1 L H_2O
10x TBE	108 g Tris base, 55 g Boric acid, 40 ml of 0.5M EDTA in 1L H_2O
SSCP solution1	10% ethanol v/v, 0.5% acetic acid v/v in 1L H_2O
SSCP solution2	0.1% w/v silver nitrate in H_2O

SSCP solution3	1.5% w/v sodium hydroxide, 0.15% v/v formaldehyde in H_2O

10 Appendix 2

Showing primer sequences of GAPDH, dysferlin, myoferlin, Otoferlin and FER1L5 sequences used in PCR of cDNA extracted from different stage of myoblast differentiation.

Primer	Sequence	Product
GAPDH _F	5 -AAG GTC ATC CCA GAG CTG AAC GG-3	190bp
GAPDH _R	5 -ACA ACC TGG TCC TCA GTG TAG CC-3	
Dysferlin_F	5 -CTG GAG AAG GGG GTG CAG -3	150
Dysferlin_R	5 -TGA AAA TAA CGT GAT TCC CAA G -3	
Myoferlin_F	5 -CAA AGC CAT GGA CCC TCT TA -3	200
Myoferlin_R	5 -GTC AAG CTT GGG GTT CAT GT -3	
Otoferlin_F	5 -TCT GGT TCC TGA ACC CAC TC -3	130
Otoferlin_R	5 - AGG CAA AAT ACG CAG CAG-3	
FER1L5_F	5 -ATG ACC CCG AGC TAC CTC CT -3	157
FER1L5_R	5 - TAG GCC CCA AAT GCT TGT AG -3	

11 Appendix 3

List of primers used in SSCP screening

This table shows the list of primers used in PCR amplifications in the seven genes screened by SSCP in this study. The primers were designed closely flanking each exon using the Primer 3 programme.

GENE: ARHGAP21		
EXON	PRIMER	5 -SEQUENCE-3
1	F	GAG GCG AGG GGA GAG TCC
1	R	TGA GAC GGA AAA GAA ACC AGA
2	F	TATTCCCTGGCACGTTGTCT
2	R	GGTAACCCCCAACTTGCAG
3	F	TATCTTTTCACTTTAGGTCTCAAAAA
3	R	GGAATGGCCTTGTGGTTT
4	F	ATCTGGGGAGGTCGATTTG
4	R	AAAGAAATGGGTAGAAAAACATTCA
5	F	AAAGAAATGGGTAGAAAAACATTCA
5	R	TTTAAAGAAGAATATCAGCACCT
6	F	TAACTTCTCTTTGAAGGTGACCGAAT
6	R	TGCTCTATTGATCTATAAAACCCATC
7	F	ACTTCTGAGTTAACTGTTTTTCCATT
7	R	AAATAAAACTTACCACTTGGAGAATGT
8	F	TTTTAGCTTGCCGTTTCCAG
8	R	AGCAAGGAAATGGCTACTGTG
9a	F	CCA GTG ACA CCT TCC TCT CA
9a	R	TAG GCC CTA CCA GGT TGT GT
9b	F	AGC AAA CAG CAA ACC AGT ACA
9b	R	TCT GCT CAC TCA CGC CAT AC
9c	F	GTA TGG CGT GAG TGA GCA GA

9c	R	GGG AAT TTG GCG AAT AGT GA
9d	F	CAG CAG ATC TCA AGC TGT GG
9d	R	TCT GTC GTG CTT TGA GAT GC
9e	F	GCA TCT CAA AGC ACG ACA GA
9e	R	ATG GAG ACG TCA GTG CTC CT
9f	F	AGG AGC ACT GAC GTC TCC AT
9f	R	ACG CTT GGA GCC ACA GTA AA
9g	F	TGG CTC CAA GCG TTG TTA AT
9g	R	CGT GGA AGG AGC TTT CAG AG
9h	F	TTC CAC GCA TGT CAC AAA AC
9h	R	TAG CAG CGT TTT CAC TCG AC
9i	F	AGT CGA GTG AAA ACG CTG GT
9i	R	TAG TGT CTG ACC CGG TCT CC
9j	F	AAG GCA TCA GTC TTA CAT CTT GG
9j	R	TGG CAT ATT AGC CAA TGA CTC T
10	F	GGTCATTGAACATTCTGATTTTCC
10	R	CCTTTAGACGTACCGTGGTCA
11	F	AATCTGTTGGCCCTCCTAGC
11	R	TCAAGGTCATGCTGAACACC
12	F	TTTTTCCCCAACAGGTCCTT
12	R	TCAGAAAAATCAGCACAATGTGTA
13	F	GATCGCAGACAGCCAAAAGT
13	R	CTGACACTCAGGGTGGCTTA
14	F	CGAGTTGGTGGAAGTATTCG

14	R	TGAACACCCACCTCTTCGTT
15	F	GGACACTGGAGTCACTAACAGG
15	R	TCTTGGAATGTATCCTTGCAAAT
16	F	TTTCCTTCAACAGCAAAGCA
16	R	ACCTCAACGATGCCAATTTT
17	F	TGATACCAGTCCCCCAAAAG
17	R	CTGGTGTCTCCTACCCGATT
18	F	TGTTGCAAATTAGTTGAAGAAAGA
18	R	CATATCCAGTTCCACCAAAGG
19	F	CCCTTTGGTGGAACTGGATA
19	R	TCTGGTATCTTTCACGGGAGTT
20	F	TGTTGTGGTTTAAAATTGATCCT
20	R	TTTTCACAATGGATTCAGAGG
21	F	CAGATTCACGATTTGCCTGA
21	R	CTTTTATTGACTATTTGGCATGAA
22	F	GGCAATTTCAGCCTACTTCC
22	R	TGCTGGATGAGCGTTTCTAC
23	F	AATTTTAGCATGACTGGTTTTTCA
23	R	AGCGGACAATAGCAAAGCAG
24	F	TAGACAACAGTGCAGGAGGAAA
24	R	GCTTTCAGCCTAGAGGTCAAGA
25	F	TTCAGCTACTAGTGACTCAACAAAA
25	R	GGAATGCATTTGTGTATCAACC
26a	F	CTC TTG CTT CCC AGG GTT CT

26a	R	CTG TTT TCT GCC CAG TGT CTC
26b	F	AAA GCA CAG CCT AGC AGC TC
26b	R	CTC TTT CAG GAT GGC AAA GC
26c	F	TCA CCA ACT CTC AGC TGT CG
26c	R	TCT GAG GTG ATG GTG CTG AC
26d	F	TTC CAC CAC ATC GTC TGC TA
26d	R	CTC CGG CTG CTC TTA GTC AC
26e	F	AGC CGG AGA AAT TCT GAA GG
26e	R	GGG TTC CTG TTT TTC GGA TT
26f	F	CCC ACA TGG AAA ACG AAA AT
26f	R	CTC TGC TCA TGC ACT TTC CA
26g	F	TTT GGA AAG TGC ATG AGC AG
26g	R	TGG AAG AAC TGC CTG TGT TG
26h	F	TGC AAC ACA GGC AGT TCT TC
26h	R	GAG TGG ACA TAG CCC CAG TTT

GENE: PRKCQ		
EXON	PRIMER	5 -SEQUENCE-3
1	F	CCCAAACAGCGTTTGTCTTT
1	R	CCTGGAAGACCTTGCTTCAT
2	F	TCCTAGAGAACGGGCAGATG
2	R	TGCAACGTTACCCATATTTCTG
3	F	TTCTCTCCTTCTCCCAACCA
3	R	GGTAAAATAAGCTGCATTTGAGG
4	F	TTCTTCCCCTCTCTCTTCCTG
4	R	CAGACAAACTCGTGGCAGAC
5/6	F	AGGGGCCTGAACAAACAGG
5/6	R	TGCACGTCAAAGAGGAGTGTA
7	F	TGCAAGAACATCCAAAGTCG
7	R	CCACTGGACTCACCATCACA
8	F	ATCCGCAAGGCTCTGTCTTA
8	R	GGCACATGCTCCTACCTGTT
9	F	GGTGGGTGGTCTGACTCTCT
9	R	TGCTGATCAGGACAGCTACC
10	F	CACCAGCTTGCATTTTCAGA
10	R	CTCCCGTGCATTAGCTTACC
11	F	TCTTCCTGGCAGAATTCAAGA
11	R	GAGCAGAAGCCATACCTTGG
12/13	F	CAGAGTGAGACCCTGTCTTGG
12/13	R	AAGCCTCTTACGTCGCTCTG

14	F	CTTCCCCCAGGTTTTATGCT
14	R	AGCACTCGGTGCAATGATTA
15	F	CTCAGGCTGCAATGAGACAA
15	R	TACCTCTGGGGCGATGTAGT
16	F	TTCCTGTCTGCCTTTTGGTT
16	R	GCTCTTGGCTTCGCTTCTTA
17	F	CTCCCTTTCAGCTCTTCGTG
17	R	GCGAGTCCTTACCACTTTCG
18	F	TGGCTGATTTTTCTTCTCTTTC
18	R	GTCTCTGGAGGGGCAAGATT

GENE: PTPLA		
EXON	PRIMER	5 -SEQUENCE-3
1a	F	GGT CCT GGA TCC CCA GTG
1a	R	ATG GCG ATG TCG TAG AAG G
1b	F	CCT GGC TCA CCT TCT ACG AC
1b	R	GTG CAC CGT ATT AGG CAA TG
2	F	TGG CAT TCA GCA AAT CCA TA
2	R	AAC GCT GCT GTA AAC ACA AA
3/4	F	CCT GCA GGC TCA AGT AGA CA
3/4	R	TGC TGA ATG CCA ATG TTG A
5	F	GTA AAG TAA GTA CCT TCA CTG
5	R	TAA GCA TGC ACA GGA CAA G
6	F	TAG CAA TAG ACC TGC AAT GT
6	R	CTA TCT CCC TTC ACT TTT CC
7	F	GGT TAT TCT GGA AAA AGC ACC TT
7	R	TGC CAC ATT TAA CAG GTT TCA A

GENE: RAB18		
EXON	PRIMER	5 -SEQUENCE-3
1	F	AGG AAG GTG GCA GAG GTG
1	R	CCG CTG CAG TTT ACA GTT CC
2	F	TTC AAG TTC CCA ACC TGT CTT T
2	R	AAG GCC AAA GGC AAG AAA AT
3	F	TCT GGT TTT CTT GGT AAT GGA
3	R	CAA ATT GTT CAT TCA CCA CCT C
4	F	ACT GCT GGT CAA GAG AGG TTT
4	R	TTT CAC AGA CTA GGA CAA TCA GAA A
5	F	TTA ATG CTT ATT TAA CAA ATG ACT CC
5	R	ATG CCA AGT GTC TGC CTT CT
6	F	ACA CTT GGC ATT TTG GTT CT
6	R	TTG GCA AAA ACT CCA TTC AA
7	F	TGA ATG ACC TTT TTC CTT GAA
7	R	TGC AAG GTC CCT AAA ATA GCA

GENE: ANKRD26		
EXON	PRIMER	5 -SEQUENCE-3
1	F	GATTTTTAGTAAGAAGGGCGAGTC
1	R	TGCGACGCCTATTACCTG
2	F	CCA TCT GAT GCT GAA AGA GC
2	R	GT TTT GAG ACA GTG CAC TAC AG
3	F	AAA GTT GGT TGA TCT ATA CCT TGT TTT
3	R	ACT CCC AGG CTG TAC AAT GC
4	F	CAG CTA CTG TAC CTT TCC AA
4	R	TTC AGC CGA GAATTA TGT A
5	F	ACC AAG AGA AAT TCA CTA TTG GAA G
5	R	ACA TTT TTC TAT ACA TAG CAG TCA
6	F	GGG ACG ACT ATA TGG AGA AGC A
6	R	TTA ATA GTG GAT GAA AGC TCT GAA
7	F	TTC ATG AGA GAG CAC TTT ACC TTA GT
7	R	TTC TAA AGG CTT TCT GGC AAA
8	F	AGT GAA TAA CAC AAG AAT AAG CAG TTT
8	R	GTT TTC TAG AAT GTC CCA AAA CCA A
9	F	AAA AAC AAC TTA CCT TCA TAA GAC CA
9	R	GTA GTA GAA GCA ACA TAT GGC ACT G
10	F	TTT TTG TGC ACT TCA TCA ACA T
10	R	TTT TAA TAG GAA GAA CCA ACA AAG C
11	F	AAG TCA AAG CAT CTC TTT ATG TTT TA
11	R	ATT TGA TAG ATA TGA TGT CCG CAT T

12	F	AAA ATG AAA TAT AGC TCT TAC CTT CTG
12	R	AGA AAA TCT TTA GCA ATT CAT TCT TT
13	F	GTG TTC TGA ATT GAT CAG CTT GG
13	R	AGA TGT GTT TTA TAT ACC TTC TTG C
14/15	F	TCA AAA ATT TTA ACG TAC TTC CTT CC
14/15	R	CCC TTT TGG TTT TTA GAG TCT CC
16	F	TGG ACT ATG TTA CAT CAT TAA AGC
16	R	GAC TAT ACC TTT TAC CTA ACT GTT CT
17	F	TCA GCT TAC CTA GCA TAC TCT TTA TTT
17	R	TCA TTA AAG GTT GAA GAA GAA AGG A
18	F	GAT TTT ACC TTC CTT CAT CCT CA
18	R	TGT CAT TTC CCA TGG ATT TTT
19	F	ACT GTG CCC AGC CCA CTT TA
19	R	CAT GTT TAC TAT TTG CCT GAA AGG
20	F	TGC AAT GGT CCT ACC TTT ACA C
20	R	ATT TAT TTC ATA GGT CAA AAA CCA A
21	F	AAA ACT AGG CTATAC CTC AAA GA
21	R	TCT TGT TTT CTT CCT GAT ACA GAT TC
22	F	ACA AAG CGG CAT ATC ACA CA
22	R	CAA AAG GAT GTG ATA ATA GTG ATG AA
23	F	AAG GAA ATA GAA ATA CCT CAG AA
23	R	TGT TTT AAA ATT CTG CTC TTG T
24A	F	TTT CTT GAT ACT TAC TTC TCT TTC TGC
24A	R	GTA TCA AAA TGA ACA AGT TAA AGT GAA

24B	F	TTA TTC ACT TTA ACT TGT TCA TTT T
24B	R	CGT GAT CAA AGT GAG ACA TCA
24C	F	ACT TTG ATC ACG ATC ATG TAT AGC
24C	R	TTA CTT AGA ATT CTC ATA GTC ATG AAG
25	F	ACA TAC TTG ATT TCT GAT TTG AC
25	R	TAT CAG GTT GTT GTG AGA CA
26	F	TGA CTG TGT TCC GAT AAG GTT
26	R	TGT TTT TCT GTG TGC TGC TTT
27	F	TTA TGC CTT CAG GTG TTT GC
27	R	CGA CAG AAA AGT GGC TGA
28	F	ATG AAT GGT TAA AAT GAT CTG AAA T
28	R	TTT TGT TTC AAA GTC TGA AGA TGA
29	F	CTT TAT TTC ACT GTT CAA AGC A
29	R	TGT TTG CCT TTT TAA AAC TTG
30	F	GCT AAC CTG TAA AAA TAG ATT GAC TTC
30	R	TCA TTC AGA TTG ATG ATC TTA CAG C
31	F	TGA CTT ACT TGG TTA GTT TAC TTG ACA
31	R	TGT TTT AGG CAC AAG CAG CA
32	F	AAC CTT GCT CAA GTA GTT CTC CA
32	R	CTT CTG CAA TCT TCA CAG AAC TAA
33	F	TCA TGA AGT TTG GCA ACA TAC C
33	R	ACA TCA TTT CTA TGT TAA TGT CTC TTG
34	F	AAC AAA ATG TCA CAT AAA CAG C
34	R	TAG CTG CTG CTG AAT TGG

GENE: FLJ14813		
EXON	PRIMER	5 -SEQUENCE-3
1	F	GCC GCT GTA TGC TGT CCA
1	R	CCC TTC CTT GCT ACT CGT TG
2	F	CCT GGG CAA GAG AAT GAG AC
2	R	TTT ACT CAC CAA GTA GAC ATT GTT TG
3	F	TGC CAA ATA TTG TAA CTG TAA TGC
3	R	AAG TGG TTA CTG TGA ATA TCT GAG AC
4	F	TGG TTA TCT AAT ATT TGC CTT TTG T
4	R	CTG GCC TGT TGG ATG TTT TA
5	F	TTT TTA GTC AAT GGG AGG TAA AGG
5	R	TGG TGA TCA TGA AGG GGT ATG
6	F	TGG GGA AGG TAA ACC TGT TG
6	R	GCC TGG CCT ACC TTT TCT TTT
7	F	CAT GGA ATT CAA TAT TGT CTC TTC TC
7	R	CCC TCA AAC CTG GCA ATC TT
8a	F	AGG AAA GTG ATG AAG CAT TGG
8a	R	CTG CTT CCC AAG AAA CTT CC
8b	F	GGA ACT TTC TTG GGA AGC AG
8b	R	TTT CTG GTG TTT GTT GTT TAT CAG
8c	F	AAG GAG AAC ATT GTC AAT TCT TTT A
8c	R	TCG ACA CCT TTT GGT GAG GT
8d	F	CCT CAC CAA AAG GTG TCG AG
8d	R	GCT TAG AGG CAA ATG TCT GTC TT

9	F	TTT CAC CAT TTT CTA TTC GGT GT
9	R	CAC TTC AAA AAC TCA AGA CAT GC
10	F	TGC TTG CAA CTT TAG CTG TTT C
10	R	CCA CTA TGC CCA GCC AGT AA
11	F	TTT AGA TAT CCC TTG GCC AGA A
11	R	CCC AGC CAG AAC TTG CTA TT
12	F	AAA ACG TCA TCC TCT CTT CAG TG
12	R	TGC AAG TTC ATT CTA TAA CAC AAG G

GENE: CAVEOLIN 3		
EXON	PRIMER	5 -SEQUENCE-3
1	F	CTC GGA TCT CCT CCT GTG G
1	R	CTC GCA AAC CTG ACA CTC TC
2a	F	CCT GCA GGT GGA TTT TGA AG
2a	R	CTC TTA ATG CAT GGC ACC AC
2b	F	GGT GGT GCC ATG CAT TAA G
2b	R	AGC AGC CCC TGT GAA GAA GT

References

Achanzar, W., and Ward, S. (1997), A nematode gene required for sperm vesicle fusion. *J. Cell Sci.* **110**, 1073-1081.

Ahnert-Hilger, G., Mach, W., Fohr, K., and Gratzl, M. (1989), Poration by alpha-toxin and streptolysin O: an approach to analyze intracellular processes. *Methods Cell Biol.* **31**, 63-90.

Allamand, V., and Campbell, K. P. (2000), Animal models for muscular dystrophy: valuable tools for the development of therapies. *Hum. Mol. Genet.* **9**, 2459-2467.

Amagai, M. (2004), A Mystery of AHNAK/Desmoyokin Still Goes On. *J. Invest. Dermatol.* **123**, 14-15.

Anderson, L., Davison, K., Moss, J., Young, C., Cullen, M., Walsh, J., Johnson, M., Bashir, R., Britton, S., Keers, S., Argov, Z., Mahjneh, I., Fougerousse, F., Beckmann, J., and Bushby, K. (1999), Dysferlin is a plasma membrane protein and is expressed early in human development [published erratum appears in Hum Mol Genet 1999 Jun;8(6):1141]. *Hum. Mol. Genet.* **8**, 855-861.

Anderson, L., Harrison, R., Pogue, R., Vafiadaki, E., Pollitt, C., Davison, K., Moss, J., Keers, S., Pyle, A., Shaw, P., Mahjneh, I., Argov, Z., Greenberg, C., Wrogemann, K., Bertorini, T., Goebel, H., Beckmann, J., Bashir, R., and Bushby, K. (2000), Secondary reduction in calpain 3 expression in patients with limb girdle muscular dystrophy type 2B and Miyoshi myopathy (primary dysferlinopathies). *Neuromuscul Disord.* **10**, 553-559.

Andrews, N. (2000), Regulated secretion of conventional lysosomes. *Trends Cell Biol.* **10**, 316-321.

Andrews, N. W. (2002), Lysosomes and the plasma membrane: trypanosomes reveal a secret relationship. *J. Cell Biol.* **158**, 389-394.

Andrews, N. W. (2005), Membrane Resealing: Synaptotagmin VII Keeps Running the Show. *Science's STKE.* **2005**, 19-21.

Aoki, M., Liu, J., Richard, I., Bashir, R., Britton, S., Keers, S. M., Oeltjen, J., V. Brown, H. E., Marchand, S., Bourg, N., Beley, C., McKenna-Yasek, D., Arahata, K., Bohlega, S., Cupler, E., Illa, I., Majneh, I., Barohn, R. J., Urtizberea, J. A., Fardeau, M., Amato, A., Angelini, C., Bushby, K., Beckmann, J. S., and Brown, R. H., Jr. (2001), Genomic organization of the dysferlin gene and novel mutations in Miyoshi myopathy. *Neurology.* **57**, 271-278.

Argov, Z., Sadeh, M., Mazor, K., Soffer, D., Kahana, E., Eisenberg, I., Mitrani-Rosenbaum, S., Richard, I., Beckmann, J., Keers, S., Bashir, R., Bushby, K., and Rosenmann, H. (2000), Muscular dystrophy due to dysferlin deficiency in Libyan Jews: Clinical and genetic features. *Brain.* **123**, 1229-1237.

Augustine, G., and Charlton, M. (1986), Calcium dependence of presynaptic calcium current and post-synaptic response at the squid giant synapse. *J. Physiol.* **381**, 619-640.

Augustine, G. J., Burns, M. E., DeBello, W. M., Hilfiker, S., Morgan, J. R., Schweizer, F. E., Tokumaru, H., and Umayahara, K. (1999), Proteins involved in synaptic vesicle trafficking. *J. Physiol.* **520**, 33-41.

Bakker, A., Webster, P., Jacob, W., and Andrews, N. (1997), Homotypic fusion between aggregated lysosomes triggered by elevated [Ca2+]i in fibroblasts. *J. Cell Sci.* **110**, 2227-2238.

Bannykh, S. I., and Balch, W. E. (1997), Membrane Dynamics at the Endoplasmic Reticulum-Golgi Interface. *J. Cell Biol.* **138**, 1-4.

Bansal, D., Miyake, K., Vogel, S., Groh, S., Chen, C., Williamson, R., McNeil, P., and Campbell, K. (2003), Defective membrane repair in dysferlin-deficient muscular dystrophy. *Nature.* **423**, 168-172.

Bansal, D., and Campbell, K. (2004), Dysferlin and the plasma membrane repair in muscular dystrophy. *Trends Cell Biol.* **14**, 206-213.

Barohn, R., Miller, R., and Griggs, R. (1991), Autosomal recessive distal dystrophy. *Neurology.* **41**, 1365-1370.

Bashir, R., Britton, S., Strachan, T., Keers, S., Vafiadaki, E., Lako, M., Richard, I., Marchand, S., Bourg, N., Argov, Z., Sadeh, M., Mahjneh, I., Marconi, G., Passos-Bueno, M., Moreira, E. S., Zatz, M., Beckmann, J., and Bushby, K. (1998), A gene related to Caenorhabditis elegans spermatogenesis factor fer-1 is mutated in limb-girdle muscular dystrophy type 2B. *Nat Genet.* **20**, 37-42.

Basseres, D., Tizzei, E., Duarte, A., Costa, F., and Saad, S. (2002), ARHGAP10, a novel human gene coding for a potentially cytoskeletal Rho-GTPase activating protein. *Biochem Biophys Res Commun.* **294**, 579-585.

Bejaoui, K., Liu, J., McKenna-Yasek, D., Le Paslier, D., Bossie, K., Gilligan, D., and Brown, R. (1998), Genetic fine mapping of the Miyoshi myopathy locus and exclusion of eight candidate genes. *Neurogenetics.* **1**, 189-196.

Bement, W., Mandato, C., and Kirsch, M. (1999), Wound-induced assembly and closure of an actomyosin purse string in Xenopus oocytes. *Curr Biol.* **9**, 579-587.

Benaud, C., Gentil, B. J., Assard, N., Court, M., Garin, J., Delphin, C., and Baudier, J. (2004), AHNAK interaction with the annexin 2/S100A10 complex regulates cell membrane cytoarchitecture. *J. Cell Biol.* **164**, 133-144.

Benoyahu, D., Akavia, U., Socher, R., and Shur, I. (2005), Gene expression in skeletal tissues: application of laser capture microdissection. *J Microsc.* **220**, 1-8.

Bernard, C., and Carnegie, P. (1975), Experimental autoimmune encephalomyelitis in mice: immunologic response to mouse spinal cord and myelin basic proteins. *J. Immunol.* **114**, 1537-1540.

Bi, G.-Q., Morris, R. L., Liao, G., Alderton, J. M., Scholey, J. M., and Steinhardt, R. A. (1997), Kinesin- and Myosin-driven Steps of Vesicle Recruitment for Ca2+-regulated Exocytosis. *J. Cell Biol.* **138**, 999-1008.

Bittner, R., Anderson, L., Burkhardt, E., Bashir, R., Vafiadaki, E., Ivanova, S., Raffelsberger, T., Maerk, I., Hoger, H., Jung, M., Karbasiyan, M., Storch, M., Lassmann, H., Moss, J., Davison, K., Harrison, R., Bushby, K., and Reis, A. (1999), Dysferlin deletion in SJL mice (SJL-Dysf) defines a natural model for limb girdle muscular dystrophy 2B. *Nat Genet.* **23**, 141-142.

Borgonovo, B., Cocucci, E., Racchetti, G., Podini, P., Bachi, A., and Meldolesi, J. (2002), Regulated exocytosis: a novel, widely expressed system. *Nat Cell Biol.* **4**, 955-962.

Bork, P. (1993), Hundreds of ankyrin-like repeats in functionally diverse proteins: mobile modules that cross phyla horizontally? *Proteins.* **17**, 363-374.

Bradford, M. (1976), A rapid and sensitive method for the quantitation of microgram quantities of protein utilizing the principle of protein-dye binding. *Anal Biochem.* **72**, 248-254.

Britton, S., Freeman, T., Vafiadaki, E., Keers, S., Harrison, R., Bushby, K., and Bashir, R. (2000), The third human FER-1-like protein is highly similar to dysferlin. *Genomics*. **68**, 313-321.

Brockway, B., Forster, S., and Freedman, R. (1980), Protein disulphide-isomerase activity in chick-embryo tissues. Correlation with the biosynthesis of procollagen. *Biochem J.* **191**, 873-876.

Brown, D. A., and London, E. (2000), Structure and Function of Sphingolipid- and Cholesterol-rich Membrane Rafts. *J. Biol. Chem.* **275**, 17221-17224.

Brown, T. W., Titorenko, V. I., and Rachubinski, R. A. (2000), Mutants of the Yarrowia lipolytica PEX23 Gene Encoding an Integral Peroxisomal Membrane Peroxin Mislocalize Matrix Proteins and Accumulate Vesicles Containing Peroxisomal Matrix and Membrane Proteins. *Mol. Biol. Cell.* **11**, 141-152.

Buchner, J., and Rudolph, R. (1991), Routes to active proteins from transformed microorganisms. *Curr Opin Biotechnol.* **2**, 532-538.

Bugnard, E., Zaal, K., and Ralston, E. (2005), Reorganization of microtubule nucleation during muscle differentiation. *Cell Motil Cytoskeleton.* **60**, 1-13.

Bulleid, N., and Freedman, R. (1988), Defective co-translational formation of disulphide bonds in protein disulphide-isomerase-deficient microsomes. *Nature*. **335**, 649-651.

Bushby, K. M. D. (1999), Making sense of the limb-girdle muscular dystrophies. *Brain*. **122**, 1403-1420.

Cagliani, R., Fortunato, F., Giorda, R., Rodolico, C., Bonaglia, M., Sironi, M., D'Angelo, M., Prelle, A., Locatelli, F., Toscano, A., Bresolin, N., and Comi, G. (2003), Molecular analysis of LGMD-2B and MM patients: identification of novel DYSF mutations and possible founder effect in the Italian population. *Neuromuscul Disord.* **13**, 788-795.

Campanaro, S., Romualdi, C., Fanin, M., Celegato, B., Pacchioni, B., Trevisan, S., Laveder, P., De Pitta, C., Pegoraro, E., Hayashi, Y. K., Valle, G., Angelini, C., and Lanfranchi, G. (2002), Gene expression profiling in dysferlinopathies using a dedicated muscle microarray. *Hum. Mol. Genet.* **11**, 3283-3298.

Casademont, J., Carpenter, S., and Karpati, G. (1988), Vacuolation of muscle fibers near sarcolemmal breaks represents T-tubule dilatation secondary to enhanced sodium pump activity. *J Neuropathol Exp Neurol.* **47**, 618-628.

Cassimeris, L. (1993), Regulation of microtubule dynamic instability. *Cell Motil Cytoskeleton.* **26**, 275-281.

Cenacchi, G., Fanin, M., De Giorgi, L. B., and Angelini, C. (2005), Ultrastructural changes in dysferlinopathy support defective membrane repair mechanism. *J. Clin. Pathol.* **58**, 190-195.

Cerny, J., Feng, Y., Yu, A., Miyake, K., Borgonovo, B., Klumperman, J., Meldolesi, J., McNeil, P. L., and Kirchhausen, T. (2004), The small chemical vacuolin-1 inhibits Ca2+-dependent lysosomal exocytosis but not cell resealing. *EMBO Rep.* **5**, 883-888.

Chakrabarti, S., Kobayashi, K. S., Flavell, R. A., Marks, C. B., Miyake, K., Liston, D. R., Fowler, K. T., Gorelick, F. S., and Andrews, N. W. (2003), Impaired membrane resealing and autoimmune myositis in synaptotagmin VII-deficient mice. *J. Cell Biol.* **162**, 543-549.

Chalfant, C. E., Ciaraldi, T. P., Watson, J. E., Nikoulina, S., Henry, R. R., and Cooper, D. R. (2000), Protein Kinase C{theta} Expression Is Increased upon Differentiation of Human Skeletal Muscle Cells: Dysregulation in Type 2

Diabetic Patients and a Possible Role for Protein Kinase C{theta} in Insulin-Stimulated Glycogen Synthase Activity. *Endocrinology*. **141**, 2773-2778.

Clarke, M., Khakee, R., and McNeil, P. (1993), Loss of cytoplasmic basic fibroblast growth factor from physiologically wounded myofibers of normal and dystrophic muscle. *J. Cell Sci.* **106**, 121-133.

Clarke, M. S. F., Caldwell, R. W., Chiao, H., Miyake, K., and McNeil, P. L. (1995), Contraction-Induced Cell Wounding and Release of Fibroblast Growth Factor in Heart. *Circ. Res.* **76**, 927-934.

Cocucci, E., Racchetti, G., Podini, P., Rupnik, M., and Meldolesi, J. (2004), Enlargeosome, an Exocytic Vesicle Resistant to Nonionic Detergents, Undergoes Endocytosis via a Nonacidic Route. *Mol. Biol. Cell.* **15**, 5356-5368.

Cohen, A. W., Hnasko, R., Schubert, W., and Lisanti, M. P. (2004), Role of Caveolae and Caveolins in Health and Disease. *Physiol Rev.* **84**, 1341-1379.

Cohn, R., and Campbell, K. (2000), Molecular basis of muscular dystrophies. *Muscle Nerve*. **23**, 1456-1471.

Cole, N., and Lippincott-Schwar, J. (1995), Organization of organelles and membrane traffic by microtubules. *Curr Opin Cell Biol.* **7**, 55-64.

Confalonieri, P., Oliva, L., Andreetta, F., Lorenzoni, R., Dassi, P., Mariani, E., Morandi, L., Mora, M., Cornelio, F., and Mantegazza, R. (2003), Muscle inflammation and MHC class I up-regulation in muscular dystrophy with lack of dysferlin: an immunopathological study. *J Neuroimmunol.* **142**, 130-136.

Craxton, M., and Goedert, M. (1999), Alternative splicing of synaptotagmins involving transmembrane exon skipping. *FEBS Lett.* **460**, 417-422.

Davis, D. B., Delmonte, A. J., Ly, C. T., and McNally, E. M. (2000), Myoferlin, a candidate gene and potential modifier of muscular dystrophy. *Hum. Mol. Genet.* **9**, 217-226.

Davis, D. B., Doherty, K. R., Delmonte, A. J., and McNally, E. M. (2002), Calcium-sensitive Phospholipid Binding Properties of Normal and Mutant Ferlin C2 Domains. *J. Biol. Chem.* **277**, 22883-22888.

Dell'Angelica, E. C., Mullins, C., Caplan, S., and Bonifacino, J. S. (2000), Lysosome-related organelles. *FASEB J.* **14**, 1265-1278.

Doherty, K., and McNally, E. (2003), Repairing the tears: dysferlin in muscle membrane repair. *Trends Mol Med.* **9**, 327-330.

Doherty, K. R., Cave, A., Davis, D. B., Delmonte, A. J., Posey, A., Earley, J. U., Hadhazy, M., and McNally, E. M. (2005), Normal myoblast fusion requires myoferlin. *Development*. **132**, 5565-5575.

Dou, T., Ji, C., Gu, S., Chen, F., Xu, J., Ye, X., Ying, K., Xie, Y., and Mao, Y. (2005), Cloning and characterization of a novel splice variant of human Rab18 gene (RAB18)dagger. *DNA Seq.* **16**, 230-234.

Duc-Nguyen, H. R., EN.; Zeigel, RF. (1966), Persistent infection of a rat kidney cell line with Rauscher murine leukemia virus. *J. Bacteriol.* **92**, 1133-1140.

Durbeej, M., and Campbell, K. (2002), Muscular dystrophies involving the dystrophin-glycoprotein complex: an overview of current mouse models. *Curr Opin Genet Dev.* **12**, 349-361.

Dyer, J., Kill, I., Pugh, G., Quinlan, R., Lane, E., and Hutchison, C. (1997), Cell cycle changes in A-type lamin associations detected in human dermal fibroblasts using monoclonal antibodies. *Chromosome Res.* **5**, 383-394.

Fanin, M., Pegoraro, E., Matsuda-Asada, C., Brown, R. H., Jr., and Angelini, C. (2001), Calpain-3 and dysferlin protein screening in patients with limb-girdle dystrophy and myopathy. *Neurology*. **56**, 660-665.

Festing, M. (1969), Inbred mice in research. *Nature*. **221**, 716.

Fielding, C., and Fielding, P. (2003), Relationship between cholesterol trafficking and signaling in rafts and caveolae. *Biochim Biophys Acta*. **1610**, 219-228.

Fletcher, L., Welsh, G., Oatey, P., and Tavare, J. (2000), Role for the microtubule cytoskeleton in GLUT4 vesicle trafficking and in the regulation of insulin-stimulated glucose uptake. *Biochem J*. **352 Pt 2**, 267-276.

Foxton, R., Laval, S., and Bushby, K. (2004), Characterisation of the dysferlin skeletal muscle promoter. *Eur J Hum Genet*. **12**, 127-131.

Galbiati, F., Volonte, D., Minetti, C., Chu, J. B., and Lisanti, M. P. (1999), Phenotypic Behavior of Caveolin-3 Mutations That Cause Autosomal Dominant Limb Girdle Muscular Dystrophy (LGMD-1C). Retention of LGMD-1C Caveolin-3 mutants within the Golgi complex. *J. Biol. Chem.* **274**, 25632-25641.

Gallardo, E., Rojas-Garcia, R., de Luna, N., Pou, A., Brown, R. H., Jr., and Illa, I. (2001), Inflammation in dysferlin myopathy: Immunohistochemical characterization of 13 patients. *Neurology*. **57**, 2136-2138.

Gandhi, M., Cummings, C., and Drachman, J. (2003), FLJ14813 missense mutation: a candidate for autosomal dominant thrombocytopenia on human chromosome 10. *Hum Hered*. **55**, 66-70.

Gentil, B. J., Delphin, C., Mbele, G. O., Deloulme, J. C., Ferro, M., Garin, J., and Baudier, J. (2001), The Giant Protein AHNAK Is a Specific Target for the Calcium- and Zinc-binding S100B Protein. Potential implications for Ca2+ homeostasis regulation by S100B. *J. Biol. Chem.* **276**, 23253-23261.

Gentil, B. J., Delphin, C., Benaud, C., and Baudier, J. (2003), Expression of the Giant Protein AHNAK (Desmoyokin) in Muscle and Lining Epithelial Cells. *J. Histochem. Cytochem.* **51**, 339-348.

Gerasimenko, J., Tepikin, A., Petersen, O., and Gerasimenko, O. (1998), Calcium uptake via endocytosis with rapid release from acidifying endosomes. *Curr Biol*. **8**, 1335-1338.

Gerasimenko, J. V., Gerasimenko, O. V., and Petersen, O. H. (2001), Membrane repair: Ca2+-elicited lysosomal exocytosis. *Current Biology*. **11**, R971-R974.

Gorter, E., and Grendel, F. (1925), on bimolecular layers of lipoids on the chromocytes of the blood. *J. Exp. Med*. **41**, 439-443.

Greengard, P., Valtorta, F., Czernik, A., and Benfenati, F. (1993), Synaptic vesicle phosphoproteins and regulation of synaptic function. *Science*. **259**, 780-785.

Gronewold, T., Sasse, F., Lunsdorf, H., and Reichenbach, H. (1999), Effects of rhizopodin and latrunculin B on the morphology and on the actin cytoskeleton of mammalian cells. *Cell Tissue Res*. **295**, 121-129.

Haase, H., Podzuweit, T., Lutsch, G., Hohaus, A., Kostka, S., Lindschau, C., Kott, M., Kraft, R., and Morano, I. (1999), Signaling from {beta}-adrenoceptor to L-type calcium channel: identification of a novel cardiac protein kinase A target possessing similarities to AHNAK. *FASEB J*. **13**, 2161-2172.

Harder, T., Kellner, R., Parton, R., and Gruenberg, J. (1997), Specific release of membrane-bound annexin II and cortical cytoskeletal elements by sequestration of membrane cholesterol. *Mol. Biol. Cell*. **8**, 533-545.

Hashimoto, T., Gamou, S., Shimizu, N., Kitajima, Y., and Nishikawa, T. (1995), Regulation of translocation of the desmoyokin/AHNAK protein to the

plasma membrane in keratinocytes by protein kinase C. *Exp Cell Res.* **217**, 258-266.

Hayashi, Y. K. (2003), Membrane-repair machinery and muscular dystrophy. *The Lancet.* **362**, 843-844.

Heilbrunn, L. (1958), The Dynamics of Living Cytoplasm. *New York: Academic Press.* 164.

Heilbrunn, L. V. (1930), The action of various salts on the first stage of the surface precipitation reaction in Arbacia egg protoplasm. *Protoplasma.* **11**, 558-573.

Hernandez-Deviez, D. M., S.; Laval, SH.; Lo, HP.;Cooper, ST.; North, KN.; Bushby, K.;Parton, RG. (2006), Aberrant dysferlin trafficking in cells lacking caveolin or expressing dystrophy mutants of caveolin-3. *Hum. Mol. Genet.,.* **15**, 129-142.

Heydemann, A., and McNally, E. M. (2004), Regenerating More Than Muscle in Muscular Dystrophy. *Circulation.* **110**, 3290-3292.

Hieda, Y., and Tsukita, S. (1989), A new high molecular mass protein showing unique localization in desmosomal plaque. *J. Cell Biol.* **109**, 1511-1518.

Ho, M., Gallardo, E., McKenna-Yasek, D., De Luna, N., Illa, I., and Brown Jr, R. (2002), A novel, blood-based diagnostic assay for limb girdle muscular dystrophy 2B and Miyoshi myopathy. *Ann Neurol.* **51**, 129-133.

Ho, M., Post, C. M., Donahue, L. R., Lidov, H. G. W., Bronson, R. T., Goolsby, H., Watkins, S. C., Cox, G. A., and Brown, R. H., Jr. (2004), Disruption of muscle membrane and phenotype divergence in two novel mouse models of dysferlin deficiency. *Hum. Mol. Genet.* **13**, 1999-2010.

Hoffman, E., and Kunkel, L. (1989), Dystrophin abnormalities in Duchenne/Becker muscular dystrophy. *Neuron.* **2**, 1019-1029.

Hohaus, A., Person, V., Behlke, J., Schaper, J., Morano, I., and Haase, H. (2002), The carboxyl-terminal region of ahnak provides a link between cardiac L-type Ca2+ channels and the actin-based cytoskeleton. *FASEB J.* **16**, 1205-1216.

Howland, J. L. (1973), Cell Physiology. *The Mcmillan Company, New York.* 461.

Humphrey, J., Peters, P., Yuan, L., and Bonifacino, J. (1993), Localization of TGN38 to the trans-Golgi network: involvement of a cytoplasmic tyrosine-containing sequence. *J. Cell Biol.* **120**, 1123-1135.

Hurtley, S., and Helenius, A. (1989), Protein oligomerization in the endoplasmic reticulum. *Annu Rev Cell Biol.* **5**, 277-307.

Huynh, C., Roth, D., Ward, D. M., Kaplan, J., and Andrews, N. W. (2004), From the Cover: Defective lysosomal exocytosis and plasma membrane repair in Chediak-Higashi/beige cells. *PNAS.* **101**, 16795-16800.

Huynh, C., and Andrews, N. (2005), The small chemical vacuolin-1 alters the morphology of lysosomes without inhibiting Ca2+-regulated exocytosis. *EMBO Rep.* **6**, 843-847.

Ikezoe, K., Furuya, H., Ohyagi, Y., Osoegawa, M., Nishino, I., Nonaka, I., and Kira, J. (2003), Dysferlin expression in tubular aggregates: their possible relationship to endoplasmic reticulum stress. *Acta Neuropathol (Berl).* **105**, 603-609.

Illa, I., Serrano-Munuera, C., Gallardo, E., Lasa, A., Rojas-Garcia, R., Palmer, J., Gallano, P., Baiget, M., Matsuda, C., and Brown, R. (2001), Distal anterior compartment myopathy: a dysferlin mutation causing a new muscular dystrophy phenotype. *Ann Neurol.* **49**, 130-134.

Illarioshkin, S. N., Ivanova-Smolenskaya, I. A., Greenberg, C. R., Nylen, E., Sukhorukov, V. S., Poleshchuk, V. V., Markova, E. D., and Wrogemann, K. (2000), Identical dysferlin mutation in limb-girdle muscular dystrophy type 2B and distal myopathy. *Neurology*. **55**, 1931-1933.

Inoue, M., Wakayama, Y., Kojima, H., Shibuya, S., Jimi, T., Oniki, H., Nishino, I., and Nonaka, I. (2006), Expression of myoferlin in skeletal muscles of patients with dysferlinopathy. *Tohoku J Exp Med*. **209**, 109-116.

Itani, S., Zhou, Q., Pories, W., MacDonald, K., and Dohm, G. (2000), Involvement of protein kinase C in human skeletal muscle insulin resistance and obesity. *Diabetes*. **49**, 1353-1358.

Jackman, R. W., and Kandarian, S. C. (2004), The molecular basis of skeletal muscle atrophy. *Am J Physiol Cell Physiol*. **287**, C834-843.

Jaiswal, J., Chakrabarti, S., Andrews, N., and Simon, S. (2004), Synaptotagmin VII restricts fusion pore expansion during lysosomal exocytosis. *PLoS Biol*. **2**, E233.

Jaiswal, J. K., Andrews, N. W., and Simon, S. M. (2002), Membrane proximal lysosomes are the major vesicles responsible for calcium-dependent exocytosis in nonsecretory cells. *J. Cell Biol*. **159**, 625-635.

Jones, S., Crosby, J., Salamero, J., and Howell, K. (1993), A cytosolic complex of p62 and rab6 associates with TGN38/41 and is involved in budding of exocytic vesicles from the trans-Golgi network. *J. Cell Biol*. **122**, 775-788.

Katz, J., Rando, T., Barohn, R., Saperstein, D., Jackson, C., Wicklund, M., and Amato, A. (2003), Late-onset distal muscular dystrophy affecting the posterior calves. *Muscle Nerve*. **28**, 443-448.

Khyrul, W. A. K. M., LaLonde, D. P., Brown, M. C., Levinson, H., and Turner, C. E. (2004), The Integrin-linked Kinase Regulates Cell Morphology and Motility in a Rho-associated Kinase-dependent Manner. *J. Biol. Chem*. **279**, 54131-54139.

Kima, P., Burleigh, B., and Andrews, N. (2000), Surface-targeted lysosomal membrane glycoprotein-1 (Lamp-1) enhances lysosome exocytosis and cell invasion by Trypanosoma cruzi. *Cell Microbiol*. **2**, 477-486.

Kofler, K., Kochl, S., Parson, W., Erdel, M., Utermann, G., and Baier, G. (1998), Molecular characterization of the human protein kinase C theta gene locus (PRKCQ). *Mol Gen Genet*. **259**, 398-403.

Komada, M., Masaki, R., Yamamoto, A., and Kitamura, N. (1997), Hrs, a Tyrosine Kinase Substrate with a Conserved Double Zinc Finger Domain, Is Localized to the Cytoplasmic Surface of Early Endosomes. *J. Biol. Chem*. **272**, 20538-20544.

Komnick, H., Stockem, W., and Wohlfarth-Botterm..., K. (1970), [Extensive fibrillar protoplasmic differentiations and their significance for protoplasmic streaming. VII. Experimental induction, contraction and extraction of the protoplasmic fibrils of Physarum polycephalum]. *Z Zellforsch Mikrosk Anat*. **109**, 420-430.

Komuro, A., Masuda, Y., Kobayashi, K., Babbitt, R., Gunel, M., Flavell, R. A., and Marchesi, V. T. (2004), The AHNAKs are a class of giant propeller-like proteins that associate with calcium channel proteins of cardiomyocytes and other cells. *PNAS*. **101**, 4053-4058.

Kong, K. Y., Ren, J., Kraus, M., Finklestein, S. P., and Brown, R. H., Jr. (2004), Human Umbilical Cord Blood Cells Differentiate into Muscle in sjl Muscular Dystrophy Mice. *Stem Cells*. **22**, 981-993.

Kostek, C. A., Dominov, J. A., and Miller, J. B. (2002), Up-Regulation of MHC Class I Expression Accompanies but Is Not Required for Spontaneous Myopathy in Dysferlin-Deficient SJL/J Mice. *Am. J. Pathol.* **160**, 833-839.

Kouno, M., Kondoh, G., Horie, K., Komazawa, N., Ishii, N., Takahashi, Y., Takeda, J., and Hashimoto, T. (2004), Ahnak/Desmoyokin Is Dispensable for Proliferation, Differentiation, and Maintenance of Integrity in Mouse Epidermis. *J. Invest. Dermatol.* **123**, 700-707.

Lassar, A., Skapek, S., and Novitch, B. (1994), Regulatory mechanisms that coordinate skeletal muscle differentiation and cell cycle withdrawal. *Curr Opin Cell Biol.* **6**, 788-794.

Lee, E., and Knecht, D. (2002), Visualization of actin dynamics during macropinocytosis and exocytosis. *Traffic.* **3**, 186-192.

Lemasters, J., DiGuiseppi, J., Nieminen, A., and Herman, B. (1987), Blebbing, free Ca2+ and mitochondrial membrane potential preceding cell death in hepatocytes. *Nature.* **325**, 78-81.

Lennon, N. J., Kho, A., Bacskai, B. J., Perlmutter, S. L., Hyman, B. T., and Brown ., R. H., Jr. (2003), Dysferlin interacts with annexins A1 and A2 and mediates sarcolemmal wound-healing. *J. Biol. Chem.*, 50466 - 50473.

Leriche-Guerin, K., Anderson, L., Wrogemann, K., Roy, B., Goulet, M., and Tremblay, J. (2002), Dysferlin expression after normal myoblast transplantation in SCID and in SJL mice. *Neuromuscul Disord.* **12**, 167-173.

Li, C., Ullrich, B., Zhang, J., Anderson, R., Brose, N., and Sudhof, T. (1995), Ca(2+)-dependent and -independent activities of neural and non-neural synaptotagmins. *Nature.* **375**, 594-599.

Li, H., Choudhary, S., Milner, D., Munir, M., Kuisk, I., and Capetanaki, Y. (1994), Inhibition of desmin expression blocks myoblast fusion and interferes with the myogenic regulators MyoD and myogenin. *J. Cell Biol.* **124**, 827-841.

Linssen, W., Notermans, N., Van der Graaf, Y., Wokke, J., Van Doorn, P., Howeler, C., Busch, H., De Jager, A., and De Visser, M. (1997), Miyoshi-type distal muscular dystrophy. Clinical spectrum in 24 Dutch patients. *Brain.* **120**, 1989-1996.

Linssen, W., de Visser, M., Notermans, N., Vreyling, J., Van Doorn, P., Wokke, J., Baas, F., and Bolhuis, P. (1998), Genetic heterogeneity in Miyoshi-type distal muscular dystrophy. *Neuromuscul Disord.* **8**, 317-320.

Liu, J., Aoki, M., Illa, I., Wu, C., Fardeau, M., Angelini, C., Serrano, C., Urtizberea, J., Hentati, F., Hamida, M., Bohlega, S., Culper, E., Amato, A., Bossie, K., Oeltjen, J., Bejaoui, K., McKenna-Yasek, D., Hosler, B., Schurr, E., Arahata, K., de Jong, P., and Brown, R. (1998), Dysferlin, a novel skeletal muscle gene, is mutated in Miyoshi myopathy and limb girdle muscular dystrophy. *Nat Genet.* **20**, 31-36.

Mahjneh, I., Marconi, G., Bushby, K., Anderson, L., Tolvanen-Mahjneh, H., and Somer, H. (2001), Dysferlinopathy (LGMD2B): a 23-year follow-up study of 10 patients homozygous for the same frameshifting dysferlin mutations. *Neuromuscul Disord.* **11**, 20-26.

Marchler-Bauer, A., Anderson, J. B., Cherukuri, P. F., DeWeese-Scott, C., Geer, L. Y., Gwadz, M., He, S., Hurwitz, D. I., Jackson, J. D., Ke, Z., Lanczycki, C. J., Liebert, C. A., Liu, C., Lu, F., Marchler, G. H., Mullokandov, M., Shoemaker, B. A., Simonyan, V., Song, J. S., Thiessen, P. A., Yamashita, R. A., Yin, J. J., Zhang, D., and Bryant,

S. H. (2005), CDD: a Conserved Domain Database for protein classification. *Nucleic Acids Res.* **33**, D192-196.

Markiewicz, E., Dechat, T., Foisner, R., Quinlan, R. A., and Hutchison, C. J. (2002), Lamin A/C Binding Protein LAP2alpha Is Required for Nuclear Anchorage of Retinoblastoma Protein. *Mol. Biol. Cell.* **13**, 4401-4413.

Martin, T. F. J., and Kowalchyk, J. A. (1997), Docked Secretory Vesicles Undergo Ca2+-activated Exocytosis in a Cell-free System. *J. Biol. Chem.* **272**, 14447-14453.

Martinez, I., Chakrabarti, S., Hellevik, T., Morehead, J., Fowler, K., and Andrews, N. W. (2000), Synaptotagmin VII Regulates Ca2+-dependent Exocytosis of Lysosomes in Fibroblasts. *J. Cell Biol.* **148**, 1141-1150.

Masunaga, T., Shimizu, H., Ishiko, A., Fujiwara, T., Hashimoto, T., and Nishikawa, T. (1995), Desmoyokin/AHNAK protein localizes to the non-desmosomal keratinocyte cell surface of human epidermis. *J Invest Dermatol.* **104**, 941-945.

Matsuda, C., Aoki, M., Hayashi, Y. K., Ho, M. F., Arahata, K., and Brown, R. H., Jr. (1999), Dysferlin is a surface membrane-associated protein that is absent in Miyoshi myopathy. *Neurology.* **53**, 1119.

Matsuda, C., Hayashi, Y. K., Ogawa, M., Aoki, M., Murayama, K., Nishino, I., Nonaka, I., Arahata, K., and Jr, R. H. B. (2001), The sarcolemmal proteins dysferlin and caveolin-3 interact in skeletal muscle. *Hum. Mol. Genet.* **10**, 1761-1766.

Matsuda, C., Kameyama, K., Tagawa, K., Ogawa, M., Suzuki, A., Yamaji, S., Okamoto, H., Nishino, I., and Hayashi, Y. (2005), Dysferlin interacts with affixin (beta-parvin) at the sarcolemma. *J Neuropathol Exp Neurol.* **64**, 334-340.

Mauro, A. (1961), Satellite cell of skeletal muscle fibers. *J. Cell Biol.* **9**, 493-495.

McNally, E., Ly, C., Rosenmann, H., Mitrani Rosenbaum, S., Jiang, W., Anderson, L., Soffer, D., and Argov, Z. (2000), Splicing mutation in dysferlin produces limb-girdle muscular dystrophy with inflammation. *Am J Med Genet.* **91**, 305-312.

McNeil, A. K., Rescher, U., Gerke, V., and McNeil, P. L. (2006), Requirement for Annexin A1 in Plasma Membrane Repair. *J. Biol. Chem.* **281**, 35202-35207.

McNeil, P., McKenna, M., and Taylor, D. (1985), A transient rise in cytosolic calcium follows stimulation of quiescent cells with growth factors and is inhibitable with phorbol myristate acetate. *J. Cell Biol.* **101**, 372-379.

McNeil, P., and Warder, E. (1987), Glass beads load macromolecules into living cells. *J. Cell Sci.* **88**, 669-678.

McNeil, P., and Khakee, R. (1992), Disruptions of muscle fiber plasma membranes. Role in exercise-induced damage. *Am. J. Pathol.* **140**, 1097-1109.

McNeil, P. (1993), Cellular and molecular adaptations to injurious mechanical stress. *Trends Cell Biol.* **3**, 302-307.

McNeil, P., Vogel, S., Miyake, K., and Terasaki, M. (2000), Patching plasma membrane disruptions with cytoplasmic membrane. *J. Cell Sci.* **113**, 1891-1902.

McNeil, P., and Terasaki, M. (2001), Coping with the inevitable: how cells repair a torn surface membrane. *Nat Cell Biol.* **3**, E124-129.

McNeil, P., and Kirchhausen, T. (2005), An emergency response team for membrane repair. *Nat Rev Mol Cell Biol.* **6**, 499-505.
McNeil, P. L., and Steinhardt, R. A. (1997), Loss, Restoration, and Maintenance of Plasma Membrane Integrity. *J. Cell Biol.* **137**, 1-4.
McNeil, P. L. (2002), Repairing a torn cell surface: make way, lysosomes to the rescue. *J Cell Sci.* **115**, 873-879.
McNeil, P. L., Miyake, K., and Vogel, S. S. (2003), The endomembrane requirement for cell surface repair. *PNAS.* **100**, 4592-4597.
McNeil, P. L. (2005), Yolk granule tethering: a role in cell resealing and identification of several protein components. *J. Cell Sci.* **118**, 4701-4708.
Megha, and London, E. (2004), Ceramide Selectively Displaces Cholesterol from Ordered Lipid Domains (Rafts):Implications for lipid raft structure and function. *J. Biol. Chem.* **279**, 9997-10004.
Meldolesi, J. (2003), Surface wound healing: a new, general function of eukaryotic cells. *J Cell Mol Med.* **7**, 197-203.
Meldolesi, J., and Chieregatti, E. (2004), Fusion has found its calcium sensor. *Nat Cell Biol.* **6**, 476-478.
Metzelaar, M., Wijngaard, P., Peters, P., Sixma, J., Nieuwenhuis, H., and Clevers, H. (1991), CD63 antigen. A novel lysosomal membrane glycoprotein, cloned by a screening procedure for intracellular antigens in eukaryotic cells. *J. Biol. Chem.* **266**, 3239-3245.
Mezghrani, A., Courageot, J., Mani, J. C., Pugniere, M., Bastiani, P., and Miquelis, R. (2000), Protein-disulfide Isomerase (PDI) in FRTL5 Cells. pH-dependent thyroglobulin/PDI interactions determine a novel PDI function in the post-ER of thyrocytes. *J. Biol. Chem.* **275**, 1920-1929.
Miller, M., Bang, M., Witt, C., Labeit, D., Trombitas, C., Watanabe, K., Granzier, H., McElhinny, A., Gregorio, C., and Labeit, S. (2003), The muscle ankyrin repeat proteins: CARP, ankrd2/Arpp and DARP as a family of titin filament-based stress response molecules. *J Mol Biol.* **333**, 951-964.
Minetti, C., Sotgia, F., Bruno, C., Scartezzini, P., Broda, P., Bado, M., Masetti, E., Mazzocco, M., Egeo, A., Donati, M., Volonte, D., Galbiati, F., Cordone, G., Bricarelli, F., Lisanti, M., and Zara, F. (1998), Mutations in the caveolin-3 gene cause autosomal dominant limb-girdle muscular dystrophy. *Nat Genet.* **18**, 365-368.
Miyake, K., and McNeil, P. (1995), Vesicle accumulation and exocytosis at sites of plasma membrane disruption. *J. Cell Biol.* **131**, 1737-1745.
Miyake, K., McNeil, P. L., Suzuki, K., Tsunoda, R., and Sugai, N. (2001), An actin barrier to resealing. *J. Cell Sci.* **114**, 3487-3494.
Miyoshi, K., Kawai, H., Iwasa, M., Kusaka, K., and Nishino, H. (1986), Autosomal recessive distal muscular dystrophy as a new type of progressive muscular dystrophy. *Brain.* **109**, 31-54.
Mullins, C., and Bonifacino, J. (2001), The molecular machinery for lysosome biogenesis. *Bioessays.* **23**, 333-343.
Nakagawa, M., Matsuzaki, T., Suehara, M., Kanzato, N., Takashima, H., Higuchi, I., Matsumura, T., Goto, K., Arahata, K., and Osame, M. (2001), Phenotypic variation in a large Japanese family with Miyoshi myopathy with nonsense mutation in exon 19 of dysferlin gene. *J Neurol Sci.* **184**, 15-19.

Nie, Z., Ning, W., Amagai, M., and Hashimoto, T. (2000), C-Terminus of desmoyokin/AHNAK protein is responsible for its translocation between the nucleus and cytoplasm. *J Invest Dermatol.* **114**, 1044-1049.

Olby, N., Sharp, N., Anderson, L., Kunkel, L., and Bonnemann, C. (2001), Evaluation of the dystrophin-glycoprotein complex, alpha-actinin, dysferlin and calpain 3 in an autosomal recessive muscular dystrophy in Labrador retrievers. *Neuromuscul Disord.* **11**, 41-49.

Ontell, M., Hughes, D., and Bourke, D. (1988), Morphometric analysis of the developing mouse soleus muscle. *Am J Anat.* **181**, 279-288.

Osada, S., Mizuno, K., Saido, T. C., Suzuki, K., Kuroki, T., and Ohno, S. (1992), A new member of the protein kinase C family, nPKC theta, predominantly expressed in skeletal muscle. *Mol. Cell. Biol.* **12**, 3930-3938.

Ozeki, S., Cheng, J., Tauchi-Sato, K., Hatano, N., Taniguchi, H., and Fujimoto, T. (2005), Rab18 localizes to lipid droplets and induces their close apposition to the endoplasmic reticulum-derived membrane. *J Cell Sci.* **118**, 2601-2611.

Parsegian, V., Rand, R., and Gingell, D. (1984), Lessons for the study of membrane fusion from membrane interactions in phospholipid systems. *Ciba Found Symp.* **103**, 9-27.

Parton, R., and Hancock, J. (2004), Lipid rafts and plasma membrane microorganization: insights from Ras. *Trends Cell Biol.* **14**, 141-147.

Parton, R. G., Way, M., Zorzi, N., and Stang, E. (1997), Caveolin-3 Associates with Developing T-tubules during Muscle Differentiation. *J. Cell Biol.* **136**, 137-154.

Passos-Bueno, M., Bashir, R., Moreira, E., Vainzof, M., Marie, S., Vasquez, L., Iughetti, P., Bakker, E., Keers, S., and Stephenson, A. (1995), Confirmation of the 2p locus for the mild autosomal recessive limb-girdle muscular dystrophy gene (LGMD2B) in three families allows refinement of the candidate region. *Genomics.* **27**, 192-195.

Passos-Bueno, M., Vainzof, M., Moreira, E., and Zatz, M. (1999), Seven autosomal recessive limb-girdle muscular dystrophies in the Brazilian population: from LGMD2A to LGMD2G. *Am J Med Genet.* **82**, 392-398.

Pele, M., Tiret, L., Kessler, J.-L., Blot, S., and Panthier, J.-J. (2005), SINE exonic insertion in the PTPLA gene leads to multiple splicing defects and segregates with the autosomal recessive centronuclear myopathy in dogs. *Hum. Mol. Genet.* **14**, 1417-1427.

Pena, J., Jimena, I., Luque, E., and Vaamonde, R. (1995), New fiber formation in rat soleus muscle following administration of denervated muscle extract. *J Neurol Sci.* **128**, 14-21.

Pessin, J. E., Thurmond, D. C., Elmendorf, J. S., Coker, K. J., and Okada, S. (1999), Molecular Basis of Insulin-stimulated GLUT4 Vesicle Trafficking. *J. Biol. Chem.* **274**, 2593-2596.

Piccolo, F., Moore, S., Ford, G., and Campbell, K. (2000), Intracellular accumulation and reduced sarcolemmal expression of dysferlin in limb--girdle muscular dystrophies. *Ann Neurol.* **48**, 902-912.

Pieribone, V., Shupliakov, O., Brodin, L., Hilfiker-Rothenfl, S., Czernik, A., and Greengard, P. (1995), Distinct pools of synaptic vesicles in neurotransmitter release. *Nature.* **375**, 493-497.

Ponnambalam, S., Rabouille, C., Luzio, J., Nilsson, T., and Warren, G. (1994), The TGN38 glycoprotein contains two non-overlapping signals that mediate localization to the trans-Golgi network. *J. Cell Biol.* **125**, 253-268.

Ponting, C. P., Mott, R., Bork, P., and Copley, R. R. (2001), Novel Protein Domains and Repeats in Drosophila melanogaster: Insights into Structure, Function, and Evolution. *Genome Res.* **11**, 1996-2008.

Pramono, Z., Lai, P., Tan, C., Takeda, S., and Yee, W. (2006), Identification and characterization of a novel human dysferlin transcript: dysferlin_v1. *Hum Genet.* **120**, 410-419.

Prelle, A., Sciacco, M., Tancredi, L., Fagiolari, G., Comi, G., Ciscato, P., Serafini, M., Fortunato, F., Zecca, C., Gallanti, A., Chiveri, L., Bresolin, N., Scarlato, G., and Moggio, M. (2003), Clinical, morphological and immunological evaluation of six patients with dysferlin deficiency. *Acta Neuropathol (Berl).* **105**, 537-542.

Rao, S. K., Huynh, C., Proux-Gillardeaux, V., Galli, T., and Andrews, N. W. (2004), Identification of SNAREs involved in synaptotagmin VII-regulated lysosomal exocytosis. *J. Biol. Chem.*, 20471-20479.

Razani, B., and Lisanti, M. P. (2001), Caveolin-deficient mice: insights into caveolar function and human disease. *J. Clin. Invest.* **108**, 1553-1561.

Reddy, A., Caler, E., and Andrews, N. (2001), Plasma membrane repair is mediated by Ca(2+)-regulated exocytosis of lysosomes. *Cell.* **106**, 157-169.

Reits, E., Benham, A., Plougastel, B., Neefjes, J., and Trowsdale, J. (1997), Dynamics of proteasome distribution in living cells. *EMBO J.* **16**, 6087-6094.

Rescher, U., and Gerke, V. (2004), Annexins - unique membrane binding proteins with diverse functions. *J. Cell Sci.* **117**, 2631-2639.

Rizo, J., and Sudhof, T. C. (1998), C2-domains, Structure and Function of a Universal Ca2+-binding Domain. *J. Biol. Chem.* **273**, 15879-15882.

Robenek, M. J., Schlattmann, K., Zimmer, K.-P., Plenz, G., Troyer, D., and Robenek, H. (2003), Cholesterol transporter caveolin-1 transits the lipid bilayer during intracellular cycling. *FASEB J.* 3-8.

Rodal, S. K., Skretting, G., Garred, O., Vilhardt, F., van Deurs, B., and Sandvig, K. (1999), Extraction of Cholesterol with Methyl-beta -Cyclodextrin Perturbs Formation of Clathrin-coated Endocytic Vesicles. *Mol. Biol. Cell.* **10**, 961-974.

Rodriguez, A., Rioult, M., Ora, A., and Andrews, N. (1995), A trypanosome-soluble factor induces IP3 formation, intracellular Ca2+ mobilization and microfilament rearrangement in host cells. *J. Cell Biol.* **129**, 1263-1273.

Rodriguez, A., Samoff, E., Rioult, M., Chung, A., and Andrews, N. (1996), Host cell invasion by trypanosomes requires lysosomes and microtubule/kinesin-mediated transport. *J. Cell Biol.* **134**, 349-362.

Rodriguez, A., Webster, P., Ortego, J., and Andrews, N. W. (1997), Lysosomes Behave as Ca2+-regulated Exocytic Vesicles in Fibroblasts and Epithelial Cells. *J. Cell Biol.* **137**, 93-104.

Rodriguez, A., Martinez, I., Chung, A., Berlot, C. H., and Andrews, N. W. (1999), cAMP Regulates Ca2+-dependent Exocytosis of Lysosomes and Lysosome-mediated Cell Invasion by Trypanosomes. *J. Biol. Chem.* **274**, 16754-16759.

Rooney, E., and Meldolesi, J. (1996), The Endoplasmic Reticulum in PC12 Cells. Evidence for a mosaic of domains differently specialized in Ca2+ handling. *J. Biol. Chem.* **271**, 29304-29311.

Roquemore, E. P., and Banting, G. (1998), Efficient Trafficking of TGN38 from the Endosome to the trans-Golgi Network Requires a Free Hydroxyl Group at Position 331 in the Cytosolic Domain. *Mol. Biol. Cell.* **9**, 2125-2144.

Rosenberg, N., Ringel, S., and Kotzin, B. (1987), Experimental autoimmune myositis in SJL/J mice. *Clin Exp Immunol.* **68**, 117-129.

Rowin, J., Meriggioli, M., Cochran, E., and Sanders, D. (1999), Prominent inflammatory changes on muscle biopsy in patients with Miyoshi myopathy. *Neuromuscul Disord.* **9**, 417-420.

Saito, A., Higuchi, I., Nakagawa, M., Saito, M., Hirata, K., Suehara, M., Yoshida, Y., Takahashi, T., Aoki, M., and Osame, M. (2002), Miyoshi myopathy patients with novel 5' splicing donor site mutations showed different dysferlin immunostaining at the sarcolemma. *Acta Neuropathol (Berl).* **104**, 615-620.

Salani, S., Lucchiari, S., Fortunato, F., Crimi, M., Corti, S., Locatelli, F., Bossolasco, P., Bresolin, N., and Comi, G. (2004), Developmental and tissue-specific regulation of a novel dysferlin isoform. *Muscle Nerve.* **30**, 366-374.

Sanchez, H., Chapot, R., Banzet, S., Koulmann, N., Birot, O., Bigard, A., and Peinnequin, A. (2006), Quantification by real-time PCR of developmental and adult myosin mRNA in rat muscles. *Biochem Biophys Res Commun.* **340**, 165-174.

Schafer, U., Seibold, S., Schneider, A., and Neugebauer, E. (2000), Isolation and characterisation of the human rab18 gene after stimulation of endothelial cells with histamine. *FEBS Lett.* **466**, 148-154.

Schiavo, G., Osborne, S., and Sgouros, J. (1998), Synaptotagmins: more isoforms than functions? *Biochem Biophys Res Commun.* **248**, 1-8.

Schmalbruch, H., and Lewis, D. (2000), Dynamics of nuclei of muscle fibers and connective tissue cells in normal and denervated rat muscles. *Muscle Nerve.* **23**, 617-626.

Schmoranzer, J., Kreitzer, G., and Simon, S. M. (2003), Migrating fibroblasts perform polarized, microtubule-dependent exocytosis towards the leading edge. *J. Cell Sci.* **116**, 4513-4519.

Selcen, D., Stilling, G., and Engel, A. G. (2001), The earliest pathologic alterations in dysferlinopathy. *Neurology.* **56**, 1472-1481.

Serrano, A., Perez, M., Lucia, A., Chicharro, J., Quiroz-Rothe, E., and Rivero, J. (2001), Immunolabelling, histochemistry and in situ hybridisation in human skeletal muscle fibres to detect myosin heavy chain expression at the protein and mRNA level. *J Anat.* **199**, 329-337.

Shen, S. S., Tucker, W. C., Chapman, E. R., and Steinhardt, R. A. (2005), Molecular regulation of membrane resealing in 3T3 fibroblasts. *J. Biol. Chem.*, 1652 - 1660.

Shtivelman, E., Cohen, F., and Bishop, J. (1992), A Human Gene (AHNAK) Encoding an Unusually Large Protein with a 1.2-{micro}m Polyionic Rod Structure. *PNAS.* **89**, 5472-5476.

Spector, I., Shochet, N., Blasberger, D., and Kashman, Y. (1989), Latrunculins--novel marine macrolides that disrupt microfilament organization and affect cell growth: I. Comparison with cytochalasin D. *Cell Motil Cytoskeleton.* **13**, 127-144.

Spence, H., Chen, Y., and Winder, S. (2002), Muscular dystrophies, the cytoskeleton and cell adhesion. *Bioessays.* **24**, 542-552.

Steinhardt, R. (1994), Cell Membrane Resealing by a Vesicular Mechanism Similar to Neurotransmitter Release. *Science's STKE.* **263**, 390-393.

Sudhof, T., and Rizo, J. (1996), Synaptotagmins: C2-domain proteins that regulate membrane traffic. *Neuron.* **17**, 379-388.

Sugita, S., Hata, Y., and Südhof, T. C. (1996), Distinct Ca2+-dependent Properties of the First and Second C(2)-domains of Synaptotagmin I. *J. Biol. Chem.* **271**, 1262-1265.

Sussman, J., Stokoe, D., Ossina, N., and Shtivelman, E. (2001), Protein kinase B phosphorylates AHNAK and regulates its subcellular localization. *J. Cell Biol.* **154**, 1019-1030.

Suzuki, N., Aoki, M., Hinuma, Y., Takahashi, T., Onodera, Y., Ishigaki, A., Kato, M., Warita, H., Tateyama, M., and Itoyama, Y. (2005), Expression profiling with progression of dystrophic change in dysferlin-deficient mice (SJL). *Neurosci Res.* **52**, 47-60.

Swanson, J. M., PL. (1987), Nuclear reassembly excludes large macromolecules. *Science.* **238**, 548-550.

Tagawa, K., Ogawa, M., Kawabe, K., Yamanaka, G., Matsumura, T., Goto, K., Nonaka, I., Nishino, I., and Hayashi, Y. (2003), Protein and gene analyses of dysferlinopathy in a large group of Japanese muscular dystrophy patients. *J Neurol Sci.* **211**, 23-28.

Takahashi, T., Aoki, M., Tateyama, M., Kondo, E., Mizuno, T., Onodera, Y., Takano, R., Kawai, H., Kamakura, K., Mochizuki, H., Shizuka-Ikeda, M., Nakagawa, M., Yoshida, Y., Akanuma, J., Hoshino, K., Saito, H., Nishizawa, M., Kato, S., Saito, K., Miyachi, T., Yamashita, H., Kawai, M., Matsumura, T., Kuzuhara, S., Ibi, T., Sahashi, K., Nakai, H., Kohnosu, T., Nonaka, I., Arahata, K., Brown, R. H., Jr., and Itoyama, Y. (2003), Dysferlin mutations in Japanese Miyoshi myopathy: Relationship to phenotype. *Neurology.* **60**, 1799-1804.

Tanford, C. (1973), The Hydrophobic Effect: Formation of Micelles and Biological Membranes. *Wiley and Sons, New York.* 16-23.

Tang, Z., Scherer, P. E., Okamoto, T., Song, K., Chu, C., Kohtz, D. S., Nishimoto, I., Lodish, H. F., and Lisanti, M. P. (1996), Molecular Cloning of Caveolin-3, a Novel Member of the Caveolin Gene Family Expressed Predominantly in Muscle. *J. Biol. Chem.* **271**, 2255-2261.

Tassin, A., Maro, B., and Bornens, M. (1985), Fate of microtubule-organizing centers during myogenesis in vitro. *J. Cell Biol.* **100**, 35-46.

Terasaki, M., Miyake, K., and McNeil, P. L. (1997), Large Plasma Membrane Disruptions Are Rapidly Resealed by Ca2+-dependent Vesicle-Vesicle Fusion Events. *J. Cell Biol.* **139**, 63-74.

Tjelle, T., Brech, A., Juvet, L., Griffiths, G., and Berg, T. (1996), Isolation and characterization of early endosomes, late endosomes and terminal lysosomes: their role in protein degradation. *J. Cell Sci.* **109**, 2905-2914.

Togo, T., Alderton, J., Bi, G., and Steinhardt, R. (1999), The mechanism of facilitated cell membrane resealing. *J. Cell Sci.* **112**, 719-731.

Togo, T., Krasieva, T. B., and Steinhardt, R. A. (2000), A Decrease in Membrane Tension Precedes Successful Cell-Membrane Repair. *Mol. Biol. Cell.* **11**, 4339-4346.

Togo, T., Alderton, J. M., and Steinhardt, R. A. (2003), Long-Term Potentiation of Exocytosis and Cell Membrane Repair in Fibroblasts. *Mol. Biol. Cell.* **14**, 93-106.

Togo, T. (2004), Long-term Potentiation of Wound-induced Exocytosis and Plasma Membrane Repair Is Dependant on cAMP-response Element-mediated

Transcription via a Protein Kinase C- and p38 MAPK-dependent Pathway. *J. Biol. Chem.* **279**, 44996-45003.

Ueyama, H., Kumamoto, T., Nagao, S., Masuda, T., Horinouchi, H., Fujimoto, S., and Tsuda, T. (2001), A new dysferlin gene mutation in two Japanese families with limb-girdle muscular dystrophy 2B and Miyoshi myopathy. *Neuromuscul Disord.* **11**, 139-145.

Ueyama, H., Kumamoto, T., Horinouchi, H., Fujimoto, S., Aono, H., and Tsuda, T. (2002), Clinical heterogeneity in dysferlinopathy. *Intern Med.* **41**, 532-536.

Ungermann, C., Sato, K., and Wickner, W. (1998), Defining the functions of trans-SNARE pairs. *Nature.* **396**, 543-548.

Uwanogho, D., Hardcastle, Z., Balogh, P., Mirza, G., Thornburg, K., Ragoussis, J., and Sharpe, P. (1999), Molecular cloning, chromosomal mapping, and developmental expression of a novel protein tyrosine phosphatase-like gene. *Genomics.* **62**, 406-416.

Vafiadaki, E., Reis, A., Keers, S., Harrison, R., Anderson, L., Raffelsberger, T., Ivanova, S., Hoger, H., Bittner, R., Bushby, K., and Bashir, R. (2001), Cloning of the mouse dysferlin gene and genomic characterization of the SJL-Dysf mutation. *Neuroreport.* **12**, 625-629.

Vainzof, M., Anderson, L., McNally, E., Davis, D., Faulkner, G., Valle, G., Moreira, E., Pavanello, R., Passos-Bueno, M., and Zatz, M. (2001), Dysferlin protein analysis in limb-girdle muscular dystrophies. *J Mol Neurosci.* **17**, 71-80.

Vasquez, R., Howell, B., Yvon, A., Wadsworth, P., and Cassimeris, L. (1997), Nanomolar concentrations of nocodazole alter microtubule dynamic instability in vivo and in vitro. *Mol. Biol. Cell.* **8**, 973-985.

Vaughan, O. A., Alvarez-Reyes, M., Bridger, J. M., Broers, J. L. V., Ramaekers, F. C. S., Wehnert, M., Morris, G. E., Whitfield, W. G. F., and Hutchison, C. J. (2001), Both emerin and lamin C depend on lamin A for localization at the nuclear envelope. *J Cell Sci.* **114**, 2577-2590.

von Tell, D., Bruder, C., Anderson, L., Anvret, M., and Ahlberg, G. (2003), Refined mapping of the Welander distal myopathy region on chromosome 2p13 positions the new candidate region telomeric of the DYSF locus. *Neurogenetics.* **4**, 173-177.

Wakatsuki, T., Schwab, B., Thompson, N., and Elson, E. (2001), Effects of cytochalasin D and latrunculin B on mechanical properties of cells. *J. Cell Sci.* **114**, 1025-1036.

Walker, R., O'Brien, E., Pryer, N., Soboeiro, M., Voter, W., Erickson, H., and Salmon, E. (1988), Dynamic instability of individual microtubules analyzed by video light microscopy: rate constants and transition frequencies. *J. Cell Biol.* **107**, 1437-1448.

Walter, M., Braun, C., Vorgerd, M., Poppe, M., Thirion, C., Schmidt, C., Schreiber, H., Knirsch, U., Brummer, D., Muller-Felber, W., Pongratz, D., Muller-Hocker, J., Huebner, A., and Lochmuller, H. (2003), Variable reduction of caveolin-3 in patients with LGMD2B/MM. *J Neurol.* **250**, 1431-1438.

Weiler, T., Greenberg, C., Nylen, E., Halliday, W., Morgan, K., Eggertson, D., and Wrogemann, K. (1996), Limb-girdle muscular dystrophy and Miyoshi myopathy in an aboriginal Canadian kindred map to LGMD2B and segregate with the same haplotype. *Am J Hum Genet.* **59**, 872-878.

Weiler, T., Bashir, R., Anderson, L., Davison, K., Moss, J., Britton, S., Nylen, E., Keers, S., Vafiadaki, E., Greenberg, C., Bushby, C., and Wrogemann, K. (1999), Identical mutation in patients with limb girdle muscular dystrophy type 2B or Miyoshi myopathy suggests a role for modifier gene(s). *Hum. Mol. Genet.* **8**, 871-877.

Weller, A., Magliato, S., Bell, K., and Rosenberg, N. (1997), Spontaneous myopathy in the SJL/J mouse: pathology and strength loss. *Muscle Nerve.* **20**, 72-82.

Woodman, S. E., Sotgia, F., Galbiati, F., Minetti, C., and Lisanti, M. P. (2004), Caveolinopathies: Mutations in caveolin-3 cause four distinct autosomal dominant muscle diseases. *Neurology.* **62**, 538-543.

Wubbolts, R., Fernandez-Borja, M., Oomen, L., Verwoerd, D., Janssen, H., Calafat, J., Tulp, A., Dusseljee, S., and Neefjes, J. (1996), Direct vesicular transport of MHC class II molecules from lysosomal structures to the cell surface. *J. Cell Biol.* **135**, 611-622.

Xue, M., and Zhang, B. (2002), Do SNARE proteins confer specificity for vesicle fusion? *PNAS.* **99**, 13359-13361.

Yaffe, D., and Saxel, O. (1977), Serial passaging and differentiation of myogenic cells isolated from dystrophic mouse muscle. *Nature.* **270**, 725-727.

Yasunaga, S., Grati, M., Cohen-Salmon, M., El-Amraoui, A., Mustapha, M., Salem, N., El-Zir, E., Loiselet, J., and Petit, C. (1999), A mutation in OTOF, encoding otoferlin, a FER-1-like protein, causes DFNB9, a nonsyndromic form of deafness. *Nat Genet.* **21**, 363-369.

Yasunaga, S., Grati, M., Chardenoux, S., Smith, T., Friedman, T., Lalwani, A., Wilcox, E., and Petit, C. (2000), OTOF encodes multiple long and short isoforms: genetic evidence that the long ones underlie recessive deafness DFNB9. *Am J Hum Genet.* **67**, 591-600.

Yawo, H., and Kuno, M. (1985), Calcium dependence of membrane sealing at the cut end of the cockroach giant axon. *J. Neurosci.* **5**, 1626-1632.

Yeagle, P. (1985), Cholesterol and the cell membrane. *Biochim Biophys Acta.* **822**, 267-287.

Yeung, E. W., Whitehead, N. P., Suchyna, T. M., Gottleib, P. A., Sachs, F., and Allen, D. G. (2004), Effects of stretch-activated channel blockers on [Ca2+]i and muscle damage in the mdx mouse. *J. Physiol.*, 551-556.

Yildiz, H., Emre, U., Coskun, O., Ergun, U., Atasoy, H., and Inan, L. (2003), Distal muscular dystrophy of the Miyoshi type. *Clin Neuropathol.* **22**, 204-208.

Zajchowski, L. D., and Robbins, S. M. (2002), Lipid rafts and little caves: Compartmentalized signalling in membrane microdomains. *Eur. J. Biochem.* **269**, 737-752.